SOME PROPERTIES OF

SILICA-SUPPORTED NICKEL CATALYSTS

A thesis submitted to

THE UNIVERSITY OF CAPE TOWN

in fulfilment of the requirements for the degree of

DOCTOR OF PHILOSOPHY

by

COLIN FIRER B.Sc. Hons. (Rand).

Department of Chemistry,
University of Cape Town,
Rondebosch, Cape,
South Africa.

March 1970.

ACKNOWLEDGMENTS

I would like to express my deep and sincere appreciation to Dr. P.W. Linder, Senior Lecturer in the Department of Chemistry, University of Cape Town, for the invaluable advice and guidance always freely given and for the interest shown throughout the period of the research.

I would also like to thank Professor E.C. Leisegang, Head of the Department of Chemistry, University of Cape Town, and his staff for the assistance they rendered at all times, and in particular Messrs. S.G. Harris and W. Lewis for the construction and maintenance of the high vacuum apparatus. Thanks are also due to Mr, A. Rodgers for his assistance with the proof-reading of this thesis.

I am indebted to the South African Council for Scientific and Industrial Research for the provision of financial assistance during the course of the research.

Finally I would like to thank my wife for all the years of support and encouragement she has given me.

SUMMARY

A literature survey has been made of earlier work on factors which have been found to influence the catalytic activity of supported metal catalysts. In particular an interaction has been shown to exist between the metal and its support in these catalysts. Two of the important factors which were shown to affect activity are the average metal crystallite size and the fraction of the metal present in a non-metallic form (for example as metal ions) in the catalyst. The earlier work consists almost exclusively of kinetic studies of heterogeneously catalyzed reactions. It is suggested that the conclusions are of a limited value owing to the widespread existence of the compensation effect, the fact that different test reactions may give contrasting results as to the relative activities of a series of catalysts and the belief that only a small fraction of the surface sites of a catalyst is generally involved in a given heterogeneous reaction.

The work described in this thesis consists of an investigation of the effects of various factors on the isosteric heat of adsorption of an adsorbate per unit metal area on supported metal catalysts. The heat of adsorption per unit metal area provides a measure of the strength of the bond between the adsorbate and the surface atoms of the adsorbent. It was felt that this approach would give further insight into the factors affecting catalytic activity because the disadvantages, mentioned above, of kinetic studies would be eliminated.

The majority of the catalysts studied were impregnation catalysts of nickel supported on a non-porous, low surface area, ground silica. These

were characterised by chemical analysis, optical and electron microscopy and X-ray diffraction line broadening. From the latter two techniques, estimates of the nickel crystallite size distribution and the average nickel crystallite size respectively were obtained. In addition, the fraction of the nickel present in the metallic state was determined by reaction with carbon monoxide to produce nickel carbonyl.

Isosteric heats of adsorption of hydrogen per unit metal area on a series of the catalysts indicated that the support interacted with the metal, thereby modifying the surface properties of the metal. The effects of the average nickel crystallite size, the nickel crystallite size distribution and the fraction of the nickel present in the metallic state in the catalysts, on the isosteric heat of adsorption of hydrogen per unit metal area were investigated. Below 5% metal concentration, the adsorbate-adsorbent bond strength was found to increase with decreasing average nickel crystallite size of the catalysts. The heat was found to become independent of the metal concentration above a value of about 5%. At these concentrations, evidently the nickel crystallite size becomes too large for the support to exert an influence on the surface properties of the metal.

Catalysts which were sintered in order to change the average nickel crystallite size at fixed metal concentrations did not give measurably different heats from those obtained with the corresponding unsintered catalysts. This was explained on the basis of a general change in the nickel crystallite size distribution which occurred on sintering such that the average crystallite size increased although there was no alteration of the distribution amongst the smaller

crystallites. No differences between the various catalysts were found in respect of the fraction of nickel present in the metallic state. In fact the metal component of every catalyst was found to consist exclusively of metallic nickel.

Two high surface area, non-porous silica-supported nickel catalysts were studied. Similar trends in the shapes of the heat curves to those obtained with the ground silica-supported catalysts were found. The heat curves for corresponding catalysts in the two classes did not coincide, however. No explanation could be put forward to account for this.

CONTENTS

Page

TABLE OF FIGURES

CHAPTER 1

INTRODUCTION

1.1 Historical Background.

In 1836 Berzelius first defined a catalyst as a substance that increases the rate at which a chemical reaction reaches equilibrium (Taylor, 1967). Today catalytic processes dominate the production of ammonia and sulphuric acid, the cracking of mineral oils, the hydrogenation and synthesis of hydrocarbons, the synthesis of plastics and many other chemicals and commodities.

In spite of the great success of catalytic methods, only moderate progress has been made in elucidating the mechanisms and basic nature of catalytic action. In the past catalysis was correctly designated as an art. Yet even today when a catalyst is needed to carry out a thermodynamically feasible reaction, the search is generally made mainly on an ad hoc basis. Thus a solution to the problem of understanding catalytic action will be of major benefit to industry and so it is not surprising that during the past fifty years all available scientific tools have been brought to bear on this problem.

By the end of the nineteen twenties several significant contributions had been made to the study of catalysis. Sabatier had suggested that metals such as nickel possessed their activity as a result of their ability to form an intermediate hydride. As a result of the work of Langmuir, Rideal, Hinshelwood and others, it became possible to formulate some generalised principles to account for the various rate-pressure relationships that had been observed experimentally in catalysed reactions. In 1925 the concept of active sites on catalyst surfaces, on which preferential adsorption took place, was introduced by H.S. Taylor, who also suggested that the process of chemisorption involves an activation energy. Baladin (1929) introduced his

hypothesis whereby catalytic activity was interpreted in terms of the arrangement of atoms at the catalyst surface. By 1945 the work of Beeck et al (1941) and Schwab et al (1943) had indicated a link between the electronic properties of catalysts and their activity. Since then enormous effort has been expended on studying the interaction of gas molecules and atoms at the catalyst surface and upon the structure of the surface itself.

To date the field of research consists largely of unconnected experimental results, in part due to the complex nature and enormous variability of catalytic phenomena. According to Bond (1962), inadequate and discordant results and inadequate or unusable theory has limited the advance in the field of catalysis, and he re-iterated a plea for high quality determinations of heats of adsorption and of the kinetics of simple catalysed processes.

Just as certain reaction mechanisms can be classified into two main groups, homogeneous and heterogeneous, so also is a distinction made between homogeneous and heterogeneous catalysis. In homogeneous catalysis, the catalyst forms a single phase with the reactants, whereas in heterogeneous catalysis the catalyst constitutes a separate phase. In this thesis only heterogeneous catalysis, and in particular the gas-solid interface will be discussed.

Heterogeneous catalysts can, according to the functions they best perform, be classified into 3 main groups: metals, metal oxides and sulphides, and salts and acids. Metal catalysts in turn can be sub-divided into 2 categories, forms containing no other component, such as colloidal metals, metal powders and evaporated metal films, and forms containing one or more other components, such as supported metals and promoted metals. Attention is directed towards

supported metal catalysts in this thesis.

A supported metal catalyst usually consists of two components, a metal and a support. The support itself frequently has no catalytic activity, but when a metal is supported on its surface, the physical and mechanical properties of the resulting catalyst are different from those of the unsupported metal. Usually less than twenty per cent by weight of the catalyst is metal.

Supported metal catalysts have been prepared in a variety of ways, individual researchers often using widely differing methods. However, all methods can broadly be classified into three main types, impregnation, co-precipitation, and deposition.

In the impregnation method, the support is usually added to a solution of a metal salt, such as the nitrate. The volume of solution is chosen so as just to wet the quantity of support being used. Thus a deposit of salt on the support is obtained. This product is dried and the salt is then reduced to the metal by flowing hydrogen over the material at a suitable temperature.

In co-precipitation, solutions of the metal salt are mixed with a second substance (waterglass, for example, if silica is to be the support). The two components of the catalyst are precipitated simultaneously by addition of a precipitating agent such as an alkali. This leads to a mixed precipitate of the metal hydroxide and the support which can then be dried and reduced to give the supported metal catalyst.

To prepare a deposition catalyst, the metal or one of its compounds is deposited from suspension onto a suspension of the support.

Catalysts prepared in these ways will obviously have very different

physical properties. Co-precipitation catalysts will possibly have some of the metal embedded within the support, and hence not accessible to the molecules of an adjacent fluid phase, whereas impregnation and deposition catalysts will have all the active component on the surface of the support. The particle size of the metal in the latter methods of preparation is usually influenced by the size of the pores in the support.

1.2 Factors Affecting the Catalytic Activity of Supported Metal Catalysts:

In the past it was thought that the only effect the support had on the metal was to increase its surface area to weight ratio, a purely physical action (Bond, 1962). Recent evidence suggests, however, that the catalytic properties of a metal may be noticeably affected by the support used.

For example Maxted and his co-workers (1960, 1961, 1962(a), 1962(b), 1964), studying the liquid phase hydrogenation of cyclohexene, ethyl crotonate and ethyl oleate, and the decomposition of hydrogen peroxide over metallic catalysts supported on a variety of metal oxides, found that the observed catalytic activity depended markedly on the support used. Sinfelt (1964) studied the kinetics of ethane hydrogenolysis over 0.6% platinum supported on both silica and alumina. He found a marked difference in the apparent activation energy for the hydrogenolysis over the two catalysts.

However, these, and other similar studies suffered from the disadvantage that metallic surface areas were not measured. It has subsequently been realized that it is necessary to express the results of such kinetic studies as "specific activities", i.e. activities per unit metal area per unit weight of catalyst, in order to ensure that the changes observed in catalytic activity are not simply due to differences in the surface area to weight ratio of the metal when supported on a series of supports. It should be noted that if heats of adsorption (section 1.4) are expressed as heats per unit metal area, the results obtained become in effect measures of adsorption bond strengths per surface metal atom.

In an attempt to investigate the nature of the effect the support had on

the catalytic properties of metals, Taylor, Yates and Sinfelt carried out a number of kinetic studies on supported metal catalysts. In all cases the metal surface areas of the catalysts were measured and specific activities quoted. Taylor et al (1964) investigated the kinetics of ethane hydrogenolysis over 10% nickel supported on silica, alumina and silica-alumina. The specific activities of the silica- and the silica-alumina-supported catalysts were found to differ by a factor of fifty. A similar, though smaller, effect was observed on comparing the silica and alumina supports. This study was extended by Taylor, Sinfelt and Yates (1965) to include catalysts containing lower concentrations of metal. Again the specific activity was found to vary with support type as well as with metal concentration, the differences in activity being greatest at the lowest metal concentration (1%). In 1967 Taylor confirmed these results using benzene hydrogenation as the test reaction.

The possibility that the activity differences noted above may have been the result of incomplete reduction was considered by Carter and Sinfelt (1966). However, by means of magnetic measurements they demonstrated that for all the catalysts used by themselves, Yates and Taylor, complete reduction had been effected.

Taylor, Yates and Sinfelt (1965) studying the reaction of cyclopropane and hydrogen found that the distribution of reaction products (methane, ethane and propane) was influenced by the nature of the support.

The results of this work showed conclusively that the nature of the support affects catalytic activity over and above any effects of changing the surface area of the metal. This effect is evident most strongly at low metal concentrations,

and can have an influence on the distribution of reaction products.

On changing the metal from nickel to cobalt, Yates et al (1965) observed similar effects on the specific activity of the series of catalysts towards the ethane hydrogenolysis reaction. Differences in specific activities between the various cobalt catalysts were not, however, found by Taylor (1967). Taylor investigated the benzene hydrogenation reaction over the same catalysts. In both the studies of Yates et al (1965) and Taylor (1967), however, cobalt supported on silica, silica-alumina and alumina catalysts gave rise to the same apparent activation energies. If the support was changed to carbon, in both studies a substantially different activation energy was obtained, thus leading one to the conclusion that the above-mentioned oxides and carbon differ markedly in their functioning as supports.

Whether, then, this support effect is observed with supported cobalt catalysts, appears to depend on the test reaction chosen. In the case of silica-, alumina- and silica-alumina-supported platinum, Cusumano, Dembinski and Sinfelt (1966) found no difference in specific activity for cyclohexane dehydrogenation among the three catalysts.

It should be noted here that different metals catalyse a particular reaction to differing extents. In order to be able to predict the probable effectiveness of a catalyst, correlations between both the electronic and the geometric properties of various catalytically active metals with catalytic activity have been attempted. However, no single property of the metal has been successfully correlated with the available information on catalytic behaviour (Bond, 1962), and thus detailed predictions of a metal's catalytic behaviour

cannot as yet be made with confidence.

Having established the existence of a support effect, particularly in the case of supported nickel catalysts, the question to be posed is how does the support influence the catalytic properties of the metal? Taylor, Sinfelt and Yates (1965) suggested that the effect the support had on the metal was one of changing the electron density in the metal. Evidence for this has come from infra-red studies of adsorbed molecules on catalyst surfaces. When carbon monoxide is adsorbed on the surface of a supported metal catalyst, two distinct bands in the infra-red spectrum are observed. The interpretation of the causes of these bands has been the subject of a controversy in the literature. This controversy is discussed in appendix 1. In the appendix the conclusion is drawn that the bands can be attributed to two distinct types of bonding between the carbon monoxide molecules and the metal surface. One band is ascribed to an adsorbate molecule bound to one metal atom (the so-called linear form) and the other to a carbon monoxide molecule bound to two metal atoms (the bridged form) (Eischens, Pliskin and Francis, 1954; O'Neill and Yates, 1961; Yates and Garland, 1961). The existence of these two bands has been used to interpret the nature of the interaction between metal and support. O'Neill and Yates (1961), using nickel supported on silica and on alumina, and Eischens and Pliskin (1958), using platinum supported on the same supports, both observed that the ratio of the amounts of linear and bridged adsorbed carbon monoxide varied as the support was changed. The ratio was approximately two for silica-supported nickel and about one for the alumina-supported nickel. Similar ratios were observed for

the platinum catalysts. Eischens and Pliskin also found differences in the chemical behaviour of their two catalysts. For example, the initial reduction of the chloroplatinic acid on the silica support began at 35°C, but temperatures in excess of 200°C were required when the support was alumina. Since a higher electron density at a metal surface favours the bridged rather than the linear structure (Eischens and Pliskin, 1958), it appears that the alumina in some way increases the electron density of the metal supported upon it to a level greater than that found in the silica-supported metal.

Confirmation of this change in metal electron density by the support emerges from a study by Brownlie, Fryer and Webb (1969). They studied the hydroisomerisation of 1-butene over graphite-supported palladium catalysts. Both impregnated catalysts and catalysts prepared by the vapour phase deposition of the metal were studied. In both cases elecron microscopy showed the palladium crystallites to be randomly dispersed on the surface of the graphite. The catalysts were heated to 300° - 500°C and this caused the palladium to migrate over the surface of the graphite and form large (>1000 Å) crystallites, nucleation occurring preferentially at defects and surface steps on the graphite. This so-called decoration of the catalyst caused an increase in the observed catalytic activity, from which the authors conclude that, since decoration sites are favourable for the formation of metal-substrate interfaces (Sears and Hudson, 1963) across which electrons may flow, it appears that one of the main functions of a support for enhancing catalytic activity would be the ability to change the electron content of the metallic bonding orbitals of surface atoms in such a way as to favour formation of the reaction intermediates.

Metal surface areas were not reported by the authors and thus it is to be concluded that the published rates are not rates per unit metal area. However, the observed increases in rate took place as the metal particle size was increased, and thus could not have been due to an increase in the metallic surface area.

Assuming then, on the basis of this evidence, that the factor which is affecting the catalytic activity of the metal may be a change in the electron density within the metal crystallites, a number of possible hypotheses can be put forward to explain how this electron transfer between support and metal may be enhanced. The presence of unreducible metal ions combined with the support is a possible means. Selwood first reported the existence of such ions. In the late nineteen forties, he began a series of magnetic studies on supported metal catalysts (Selwood et al, 1946; Eischens and Selwood, 1947(a); Selwood and Dallas 1948; Eischens and Selwood, 1948) which led him to propose a principle which he called "Valence Inductivity" (Selwood, 1948). This he described as "an induced change of valence brought about when a transition group ion is supported on a high area surface with which it may become isomorphous, and in which the ions may become isometric". His later work (Selwood, Moore, Ellis and Wethington, 1949; Selwood, Ellis and Wethington, 1949) provided examples of this principle. For example, an impregnation catalyst of nickel on magnesium II oxide displayed a nickel valence of +2, nickel II oxide being isomorphous with magnesium oxide. But if the support is changed to gamma-alumina, and the concentration of the nickel is not greater than 10%, a valence of +3 is displayed by the nickel. It is assumed that the alumina exerts an inductive action on the nickel and influences its radius and oxidation state such

that it is able easily to fit into the alumina lattice. This principle implies that there exists a definite electronic interaction between the metal ion and its support. If as a result of the impregnation, drying and decomposition stages, the support exerts an inductive action on the metal ions, some of these ions may be incorporated into the support lattice, thus rendering their reduction very difficult, if not impossible.

Swift, Lutinski and Kehl (1965) showed that when a supported metal catalyst is prepared, not all of the metal exists in the form of crystallites or atoms, but some if it can be held in the lattice of the support in the form of metal ions. Using silica-alumina as their support they found that the amount of nickel chemically associated with the support decreased as the silica content of the support increased. The metallic nickel was determined by removal of the metal atoms from the catalysts by flowing carbon monoxide over the reduced samples and decomposing the resulting nickel tetracarbonyl. A parallel study by Swift, Lutinski and Tobin (1966) on silica-, silica-alumina- and alumina-supported nickel confirmed this observation. From 6% metal catalysts, all the nickel could be removed from the silica-supported sample, but only 78% and 47% from the silica-alumina- and alumina-supported samples respectively. Using two nickel-alumina catalysts, they observed that the amounts of metallic nickel present in the catalysts were related to the BET surface areas (section 2.2) of the supports. The lower the BET area, the less alumina is available for combination with the metal, and hence the more metal could be removed by carbonyl formation. In contrast to this work, however, Yoshimoti, Morita and Yamomoto (1963) found evidence for the existence of a nickel aluminate

spinel in nickel alumina catalysts. However the existence of the spinel compound in Swift, Lutinski and Tobin's catalysts cannot be disproved on the basis of the lack of observable X-ray diffraction pattern, for the spinel may exist as a non-crystalline phase. The metallic phase in supported metal catalysts may thus be dispersed not only on the surface of the support, but also on an ionic metal phase, and the presence of this phase may alter the catalytic properties of the metal covering it.

By means of infra-red studies Peri (1966) also pointed to the formation of such unreducible metal ions. Uchida and Imai (1962) thought that the acid sites created on the surface of silica impregnated with nickel were protonic. However the spectra of strongly adsorbed ammonia obtained by Peri indicated that this acidity of "dry" nickel-silica is due to incompletely coordinated nickel ions. He found that carbon monoxide is adsorbed on similar sites on the catalyst surface to those on which ammonia is most strongly adsorbed. Since ammonia cannot be strongly held by oxide ions alone, as both are strong Lewis bases, incompletely coordinated nickel ions must also be present on these sites. He suggested that the carbon monoxide could be held by a weak sigma bond, the nickel being tetrahedrally coordinated.

Hydrogen chloride chemisorption prior to carbon monoxide adsorption may modify the coordination of the nickel and thus change the manner in which the carbon monoxide is subsequently held. Here the adsorption of carbon monoxide may complete the octahedral coordination of the nickel. Evidence for this is found in a lowering of the C=O stretching frequency which comes about as a result of back bonding of d-electrons from the metal as the coordination shell fills.

Some infra-red bands suggest that surface carbonyl structures are formed by interaction of carbon monoxide with reduced nickel atoms, small clusters of atoms or small nickel crystallites. Evidence points to at least three ionic and four metallic types of sites, but detailed characterisation is not possible at present, according to Peri.

These conclusions cannot be looked upon as final, however, for the spectroscopic data are difficult to interpret unambiguously. It has not been established whether any of these adsorbed complexes take an active role in catalysis, no spectra having been obtained which cannot be attributed to reasonably stable surface species, and much work will have to be carried out before the complexity of the oxide surface can be adequately understood. It is very likely that only a small portion of all the metal present in these silica-supported catalysts is in the form of ions, unlike the silica-alumina-, and alumina-supported catalysts mentioned above. Thus although the abovementioned coordination effects appear to have some significance, the variations in catalytic activity with changes in the nature of the support may be due to the presence of substantial amounts of unreducible metal ions in silica-alumina- and alumina-supported catalysts.

Taylor, Sinfelt and Yates (1965) ascribed the effect of the support on the catalytic activity of the metal supported upon it to an unknown interaction between metal and support. They felt it was reasonable to expect that the metal interacts electronically with the support, for "in general electron transfer occurs at the junction between a metal and a semiconductor". Now when a metal and a semiconductor are brought into intimate contact with one another, electrons flow

either from the semiconductor to the metal or vice versa, depending on the relative Fermi energy levels, until at equilibrium the Fermi energy in the metal and the semiconductor is at the same energy level. This mechanism, then, may well provide an answer to the question of how the support can alter the electronic properties of the metal, for in many supported metal catalysts, the metal crystallites are small (of the order of 100 Å) and thus their electronic properties can be drastically altered by a relatively small absolute change in their electron density. The validity of the mechanism, however, depends on whether or not the supports used by Taylor, Sinfelt and Yates, namely silica and silica-alumina, are semiconductors. Both silica and alumina are insulators, having resistivities of approximately 10^{10} and 10^{12} ohm cm at 25^{0}C respectively, and thus it appears unlikely that electron transfer could take place across the support metal interface by this mechanism. Graphite, however is a conductor, and thus it may be possible to explain the results of Brownlie, Fryer and Webb (page 9) on the basis of an electrical junction effect.

Although in general the effects of catalysts do not depend on the amount of catalyst present, the concentration of the metal in a supported metal catalyst appears to have an influence on the catalyst's activity. For example, Hill and Selwood (1949) found that nickel-alumina catalysts containing less than 3% nickel were virtually inactive for the benzene hydrogenation reaction, whilst catalysts containing more than 10% nickel were highly active. Taylor, Sinfelt and Yates (1965) too found that as the metal concentration was increased in the range 1% to 10%, the specific activity for ethane hydrogenolysis of both silica- and

silica-alumina-supported nickel catalysts increased by over two orders of magnitude. The work of Taylor (1967) on the benzene hydrogenation reaction confirmed Taylor, Sinfelt and Yates' observations.

Hill and Selwood's results suggest a geometric factor, that is, a minimum size of aggregate of nickel atoms is required to catalyse the hydrogenation of benzene. This was not the case with Taylor, Sinfelt and Yates' work however. They explained their results on the assumption that the first amounts of nickel are selectively impregnated on the most energetic sites of the support. On this basis a heterogeneity of nickel sites would be expected. When the metal concentration is low, the fraction of the metal in the catalyst on such favourable sites would be large, this fraction decreasing as the metal concentration is increased. The possibility also exists that nickel impregnated on such sites may be unreducible, and as such induce additional activity into the nickel crystallites which subsequently cover them.

Taylor and Staffin (1967), when studying the benzene hydrogenation reaction, found that the observed decrease in activity with decreasing metal concentration could be explained in terms of a decrease in metal surface area, for silica-supported nickel catalysts, but, with silica-alumina-supported nickel, the activity of the catalysts decreased to a greater extent than could be explained by the decrease in metal surface area. They suggested that this was caused by an interaction of the metal with the silica-alumina substrate. In this study, therefore, it appears that in the case of silica-supported catalysts, the effect of metal concentration is simply one of altering the metal particle size, whereas with silica-alumina-supported samples an additional effect exists. These results

can be contrasted with the observations of Taylor, Sinfelt and Yates (1965) and Taylor (1967) (page 14) who noted changes in the specific activity of both silica- and silica-alumina-supported catalysts as the metal concentration was changed.

This apparent metal concentration effect may be related to the state of subdivision of the metal in the catalysts. Before investigating this hypothesis, it is necessary to examine the properties of small crystallites. Magnetic measurements have shown that small metal crystallites differ from the bulk metal in their electronic behaviour. Kubicka (1966) found a decrease in the paramagnetism of palladium black, as compared to the bulk metal, with increasing dispersion of the palladium. These results suggested that the palladium atoms in small crystallites have an electronic structure intermediate between the $4d^{10}$ shells of isolated palladium atoms and the electronic state of metallic palladium, usually taken to be $4d^{9.4}\ 5s^{0.6}$, which is paramagnetic.

Carter and Sinfelt (1968) studied the paramagnetic susceptibility of supported nickel. Their results indicated a lower number of unpaired electrons in atomic d orbitals in silica-supported nickel as compared to bulk nickel. As the concentration of nickel in the supported catalysts was decreased, the difference from bulk nickel became even more pronounced. This difference could possibly arise from differences in the electronic structure of surface and bulk metal atoms, and would become more pronounced at low metal concentrations, where large proportions of the metal atoms are surface atoms.

Crystallographic differences, too, may exist between small crystallites

and larger crystals.

Thus it appears that the electronic properties of small metal crystallites vary according to the size of the crystallites, and this prompts one to ask whether a link can be found between catalytic activity and crystallite size. Margineanu and Olariu (1967) carried out a series of experiments in order to throw some light on this problem. They found that addition of chromia to pure nickel increased the available surface of the nickel by nearly one order of magnitude. The fraction of nickel atoms in the surface increased from 0.7% to 5% and the catalytic activity per unit metal area of the catalyst increased by more than two orders of magnitude. Both the structural effect and the increase in specific activity exhibited a saturation tendency after the chromia content of the samples reached about 10%. However further increase in chromia content resulted in a corresponding increase in the total surface area of the catalysts. In the concentration range where the activity was found to change, the catalysts exhibited metallic behaviour, but at 10% chromia, their electrical conductivity decreased by nearly ten orders of magnitude and they displayed semiconductor properties. The surface area of unreduced pure nickel oxide was 270 m^2/g and that of the reduced catalyst 4.3 m^2/g catalyst. Thus during the reduction process, a large amount of sintering took place. The addition of small amounts of chromia appear to inhibit this sintering, but as the chromia content was increased, the effect tailed off and the chromia induced only an increase in the total surface area, nickel dispersion remaining unchanged. (The chromia cannot be included in the lattice of the nickel on account of its relatively much larger size compared to the interatomic spacing of the nickel). Three

alternative explanations were put forward to account for the observed change in specific activity. Firstly, if it is assumed that all superficial nickel atoms are active centres, in the presence of small amounts of chromia, more nickel atoms are surface atoms and hence active centres. However after saturation of the surface with chromia, the activity per unit metal area becomes unaffected by chromia content. Secondly, the contact points between nickel and chromia crystallites may be active centres. A decrease in the nickel crystallite size due to the structural promoting effects of chromia induces an increase in the number of such active centres. However, the number of nickel-chromia contact points is generally not proportional to the surface area of nickel. Thirdly, the catalytic activity can increase simply as a result of the decrease in nickel crystallite size. Such a dependence has been found by Selwood, Adler and Phillips (1955) and by Carter, Cusumano and Sinfelt (1966). Thus the results of Margineanu and Olariu seem to be in agreement with the idea of a correlation between specific activity and crystallite size, but in order to state certainly what the correct explanation for the observed phenomena is, more information is required concerning the correlation between the specific activity and the active surface area for promoted metals.

Yates et al. (1964) on the other hand found that the specific catalytic activity of their silica-supported nickel catalysts (for ethane hydrogenolysis) was constant, although the metal surface area was changed by sintering at high temperature. This implied that for a fixed amount of metal on a support the specific catalytic activity did not depend on the state of subdivision of the metal, within the range studied.

The lack of sensitivity of specific activity to crystallite size found by Yates et al prompts one to ask whether in fact there exists an optimum metal crystallite size for maximum catalytic activity and how this activity varies with crystallite size.

Carter, Cusumano and Sinfelt (1966) studied the effect of varying the crystallite size of nickel supported on silica-alumina. They found that the catalytic activity per unit metal area decreased with increasing crystallite size. This indicated that a factor other than the change in metal surface area was responsible for the observed change in activity. However, the work of Taylor et al (1964), using nickel-silica catalysts, did not show an effect of comparable magnitude. The crystallite sizes of the metal in Taylor et al's study were very much smaller than those observed in Carter, Cusumano and Sinfelt's investigation. It is possible, therefore, that below a certain crystallite size, an increase in specific activity with decreasing crystallite size is not substantial, and that different supports may exert differing influences on the metallic crystallite size and size distribution of a catalyst.

Yates and Sinfelt (1967) studied the catalytic activity of rhodium for ethane hydrogenolysis in relation to its state of dispersion on a silica support. They found that the specific activity of supported rhodium in a highly dispersed state (crystallite size < 40 Å) declined by a factor of four as the metal concentration was reduced from 1% to 0.1%. Moving in the opposite direction, the specific activities of unsupported rhodium and of a 5% silica-supported rhodium catalyst sintered at 800 °C were 20 to 40 times lower than those of well dispersed catalysts in the concentration range 1% to 10% metal. Hence when the dispersion

is varied markedly in either direction from that encountered in the catalysts which are fairly typical of those used in practice (viz. well dispersed, 1% to 10% metal concentration) specific activity declines. This leads one to the conclusion that maximum specific activity occurs corresponding to an intermediate state of metal dispersion.

These results are consistent with the findings of Dorling and Moss (1966), who studied the hydrogenation of benzene over platinum-silica catalysts. For catalysts fired at temperatures below 400°C, which contained varying amounts of highly dispersed platinum, the specific activity for benzene hydrogenation was essentially constant, although large variations in crystallite size and size distribution existed. Catalysts fired at 400°C and 500°C showed smaller specific activity, and those fired at 600°C and 800°C were inactive. Dorling and Moss (1967), using the same catalysts, found that as they increased the platinum content, the surface area per gram of catalyst increased. They associated this area change with the growth of a fixed number of crystallites of regular shape and suggested that the number of crystallites is related to the pore structure of the silica support.

Recently Dorling, Eastlake and Moss (1969) reported an interesting series of experiments in which they measured the specific activity for ethylene hydrogenation over a series of platinum-silica catalysts in which the state of metal subdivision was varied by means of differing methods of preparation, temperatures of reduction, sintering in air and by using catalysts of different metal concentration. An analysis of the effects that the different metal

dispersions had on specific activity led them to the interesting conclusion that the parameters which are varied in order to induce a variation in crystallite size can themselves produce changes in the observed specific activity of the catalysts. For example, increasing the reduction temperature from 80°C to 500°C in a 10% catalyst caused the average crystallite size to increase from about 50 Å to 75 Å and this was accompanied by a ten-fold increase in specific activity. This ten-fold activity increase was also noted for a 3.4% catalyst, although the change in reduction temperature in this case caused almost no variation in the average crystallite size. Dorling, Eastlake and Moss put forward the suggestion that catalytic activity may well be determined by the efficiency with which the last traces of chlorine (from the chloroplatinic acid with which the catalysts were prepared) is removed. They found that exposure of a catalyst which had been reduced at 500°C to chlorine gas at 250°C for one hour followed by reduction at 80°C for 5 minutes increased the activity to a level comparable with that displayed by catalysts reduced at 50°C.

The specific activity of 1% to 4.5% catalysts reduced at 80°C increased by a factor of four as the metal concentration was increased. This, Dorling, Eastlake and Moss speculated, was the result of the more complete removal of chlorine (and hence lower activity) of catalysts with low metal content. In contrast, the specific activity of catalysts reduced at 210°C was found not to be a function of the crystallite size of the metal. Also, catalysts prepared in the absence of chlorine, and those prepared from chloroplatinic acid but reduced at 300°C and 500°C, had the same specific activity, although appreciable crystallite size differences existed among the catalysts. Thus Dorling, Eastlake and Moss

conclude that crystallite size in the range studied (13 Å to 75 Å) does not affect the specific activity of the platinum-silica catalysts for ethylene hydrogenation, provided the complicating effect of promotion of the reaction by chlorine is absent. Apparent effects can, however, be produced by methods usually adopted to vary crystallite size.

From the evidence discussed above, it appears that the factor of metal concentration can be linked to the size and hence the properties of the metal crystallites in the catalyst. Evidence exists that an optimum crystallite size for maximum catalytic activity exists, although great care must be exercised in the interpretation of crystallite size effects, for methods commonly used to vary crystallite size may, in themselves, change catalytic activity.

The effect a support has on the catalytic properties of a metal need not necessarily be one of altering the electronic properties of the metal through a particular support-metal interaction. The role of the support may be such as to determine the ultimate state of dispersion of the metal, the actual state of subdivision of the metal then determining its electronic, and hence catalytic, properties.

Reinen and Selwood (1963) carried out a study of nickel supported on silica and alumina in order to test the effects of the support on the degree of dispersion of the metal. They measured the surface areas of the supports before and after impregnating them with the metal. The alumina showed a much greater loss of specific surface area than the silica. This greater

decrease in the case of alumina could only be explained by assuming that the alumina surface itself is diminished by the impregnation process used in the preparation of the catalyst, with thin nickel layers or very small nickel particles filling the pores and surface defects of the support, whereas the authors explained the smaller decrease in the area of the silica by assuming that spherical particles of silica mixed with nickel particles of approximately the same size during the impregnation process.

Alder and Keavney (1960) suggested that platinum-alumina catalysts prepared via impregnation contained the platinum in very thin layers which cover large areas of the alumina surface, with much of the metal in the form of very small particles (i.e. an appreciable fraction of the metal having extremely small dimensions), whereas co-gelled preparations of platinum-alumina contain the platinum as almost spherical particles of more uniform size.

Kubicka (1968) studied the reaction of benzene and hydrogen over 1% alumina- and silica-supported technetium, rhenium, ruthenium, platinum and palladium, She found that agreement was obtained between the surface areas obtained from hydrogen chemisorption and X-ray line broadening data for silica-supported metals, indicating that substantial amounts of metal crystallites of uniform size, sufficiently large to be detected by the X-ray method, were present. This was not the case for the alumina-supported catalysts, however, and the experimental results suggested that an appreciable fraction of the metal existed in a highly dispersed form on the alumina-supported samples, thus not being included in the X-ray estimation of the average crystallite size.

Now it has been pointed out (Schuit and van Reijen, 1958; Dorling and

Moss, 1967) that the dispersion of supported metals in impregnation catalysts may be related to the pore structure of the support and that during the impregnation process all pores which contribute to the surface area of the support are filled with the impregnating solution.

Kubicka explained the differences in crystallite size distributions mentioned above by assuming that in alumina, unlike silica, both macro- and micropores significantly contribute to the surface area, and that the metal particles deposited in the micropores of the alumina cannot undergo extensive recrystallization, which would result in the formation of larger crystallites, during the reduction process.

Thus one can conclude that porous supports will inevitably affect, to a greater or less extent, the crystallite size distribution in supported metal catalysts. This limit is thus a function of the nature of the support, and thus the latter could introduce a confounding effect when such factors as metal concentration and average metal particle size are being considered. Separation of these factors from the effects observed as a result of the porous structure of the support may be an exceedingly complex problem.

Studies on reaction rates may also be affected by the size of the pores in a catalyst, for such rates may well be influenced by the rate of diffusion of reactants into the pores. Thus comparisons of rates amongst catalysts in which the supports have different pore structures may be of limited value unless the pore structures have been characterised.

Kubicka (1968) found that metals supported on alumina displayed a lower specific activity for benzene hydrogenation and hydrogenolysis as compared to that

of silica-supported metals. This fact was explained by suggesting that the metal particles in the very fine micropores of the alumina are inaccessible for the large hydrocarbon molecules. Thus it appears that in this case the nature of the support affects in the first place the degree of dispersion of the metal, and then also possibly the accessibility of the metal surface for reactant molecules.

Finally, in discussing the factors which influence catalytic activity, it is not unreasonable to suppose that the catalytic properties of a supported metal catalyst may well depend on the method of preparation of the catalyst or on such factors as the treatment to which the catalyst is subjected prior to use.

Taylor, Yates and Sinfelt (1965) found that for 10% nickel supported on silica and silica-alumina, the distribution of products of the reaction of cyclopropane and hydrogen (methane and ethane/propane) depended on the conditions of pretreatment of the catalyst prior to reaction. If, after reduction, the catalyst was cooled down in flowing hydrogen to the reaction temperature, the ratio of hydrogenation (forming propane) to hydrogenolysis (in which methane and ethane are formed) was about 1.4 whereas if the catalyst was purged with helium at the reduction temperature and then cooled to the reaction temperature in flowing helium, this ratio increased to about 5. The presence of an adsorbed layer of hydrogen incorporated during the catalyst pretreatment evidently markedly increases the selectivity of the catalyst in favour of the hydrogenolysis reaction.

In conclusion, it appears that a number of factors can influence the

catalytic activity of a supported metal catalyst. In some instances, the nature of the support may influence the activity to a greater extent than can be attributed to any changes in the metal surface area imposed by the support. Infra-red studies have indicated that the change in activity may be the result of changes in the electron density of the metal when supported on a series of supports. This change in electron density may come about either as a result of electron transfer across the metal-support interface if the support is a semiconductor, and/or could result from the presence of unreducible metal ions chemically combined with the support.

The metal concentration of a supported metal catalyst also affects activity. This appears to be a result of the change in metal crystallite size with changes in metal concentration. Evidence points to the requirement of a minimum crystallite size for measurable catalytic activity and an intermediate size for optimum activity. However the support can influence the ultimate crystallite size distribution as a result of its pore structure. An interrelationship between the factors of support type and metal concentration may thus exist in a catalyst. The pore structure of the support may also affect the measured reaction rate which may be controlled by the rate of diffusion of reactants in the pores. This could confound attempts at elucidating the factors affecting catalytic activity.

It has been shown that the conditions of catalyst pretreatment may affect catalytic activity and that in investigating factors such as metal crystallite size, observed changes in catalytic activity may result not only from any changes wrought in the factor being studied, but also from the treatment to which the catalyst is subjected in order to bring about these changes.

1.3 The Difficulties Involved in Using Kinetic Studies as a Tool for Elucidating the Factors Affecting Catalytic Activity.

Most of the studies reported in section 1.2 which aimed at the elucidation of factors which influence catalytic activity, had, as their basis, kinetic experiments. Three possible objections can however be raised to such an approach.

(a) In a catalysed chemical reaction, the catalyst serves the function of lowering the activation energy of the reaction. However, the magnitude of the value of the activation energy of a heterogeneously catalysed reaction cannot be taken as a quantitative measure of catalytic activity. This is mainly the result of the widespread occurrence of the compensation effect. It was Constable (1923) who first reported the existence of this effect. Using a series of copper catalysts he found that an increase in the activation energy of the dehydrogenation of ethanol did not always lead to the expected decrease in the rate constant because of concomitant increase in the pre-exponential term of the Arrhenius equation. This compensation effect has been observed to operate in a wide variety of systems (Thomas and Thomas, 1967). The relationship between these two parameters is usually of the form

$$\log A = mE + C_A \qquad 1.3.1.$$

(for meanings of symbols see Appendix 8).

The effect can be represented diagrammatically as shown in figure 1.1. From the figure it can be seen that there exists a characteristic temperature, T_s, where the activities of all catalysts in the series are

FIG. 1.1.

DIAGRAMMATIC REPRESENTATION OF THE COMPENSATION EFFECT

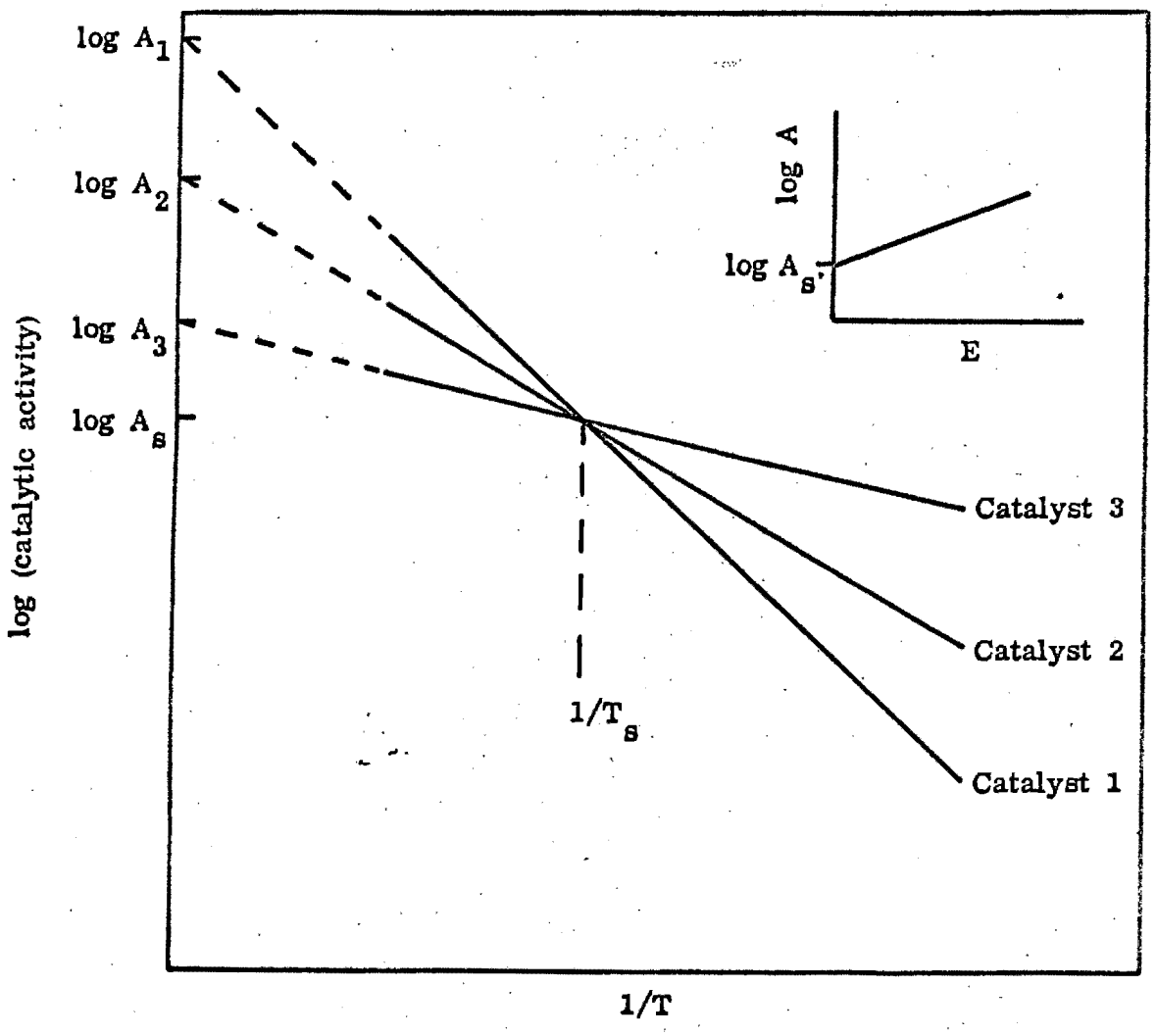

equal. If kinetic studies had been made at a temperature greater than T_s, a particular order of activity for the catalyst series would have been found, but if it so happened that a temperature lower than T_s had been chosen, it can be seen that the determined order of activity of the catalysts would have been reversed. It has been suggested by Cremer (1955) that this effect arises as a result of the effect of temperature on the distribution of active sites on the surfaces of the catalysts.

This effect can thus confound kinetic studies aimed at elucidating factors affecting catalytic activity. The variations in A and E should therefore be determined in any such study.

(b) The rates of an extremely large number of heterogeneously catalysed reactions can be expressed in terms of the Langmuir Hinshelwood kinetic laws which were derived on the basis of the Langmuir isotherm (section 2.2). For reaction between two species, A and B, the process may be formulated as

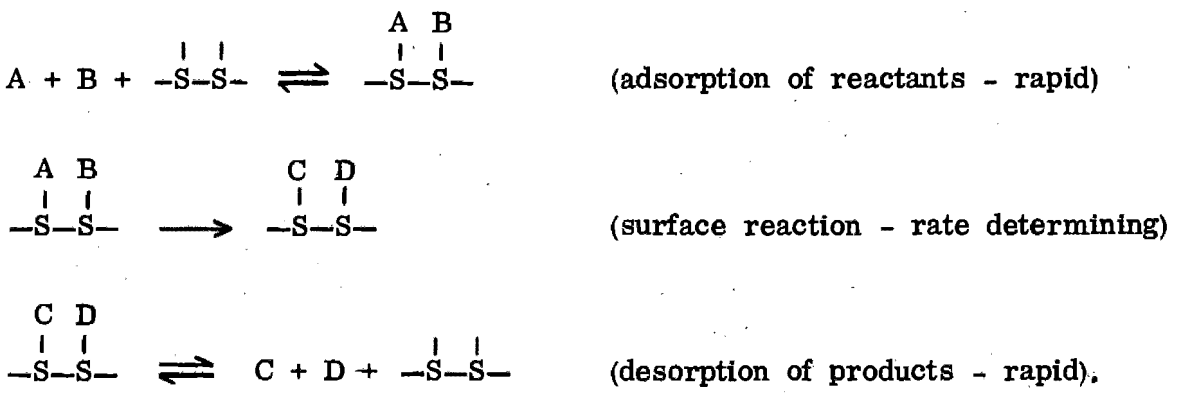

Inherent in the use of the Langmuir isotherm for the adsorption process is the assumption that the solid surface is homogeneous. This is very

rarely so (Laidler, 1954), surface heterogeneity manifesting itself in the variation of the heat of adsorption with coverage (section 1.4). Thus it is at first sight surprising that so many reactions obey the Langmuir Hinshelwood kinetic laws. The explanation of this paradox can be found in the fact that on a catalytic surface, one group of sites with lower activation energy than the other sites exists. Since relatively small increases in activation energy result in marked decreases in reaction rates (the rate varies exponentially with activation energy), it can be assumed that reaction will take place overwhelmingly on that group of sites with lowest activation energy. To a first approximation, these sites will have a constant activation energy, and so reaction can be regarded as taking place on an energetically homogeneous surface. Thus kinetic studies in which the reaction is found to follow Langmuir Hinshelwood kinetic laws essentially only study a very small fraction of the catalyst surface. (The fact that very small quantities of catalyst poison are effective in completely deactivating a catalyst indicates that reaction does in fact occur on only a few catalyst sites).

(c) The nature of the test reaction used to investigate the factors which affect catalytic activity may lead to contrasting conclusions as to the activity of a particular catalyst. By studying the hydrogenation of cyclopropane on platinum catalysts, Boudart et al (1966) found a lack of sensitivity of specific activity to crystallite size, nature of the support or details of catalyst preparation. However they point out that this

insensitivity would only be expected for what they termed "facile" reactions, i.e. those reactions for which the majority of catalyst sites possess ample activity under the conditions used. These reactions fail to sense the heterogeneity of the surface which becomes important with more "demanding" reactions, when, for example, stereospecificity is involved, or where, from a reactivity point of view, the reaction is difficult. Such a reaction is the interaction of p-xylene and deuterium, studied by Hightower and Kemball (1965). They found that the specific activity exhibited a dependence on the particular support used.

Yates et al (1965) found that the specific activity of cobalt catalysts supported on silica and on alumina was greater than that for silica-alumina-supported catalysts. Taylor (1967), however, found approximately the same activity for cobalt catalysts supported by silica, alumina and silica-alumina. Yates et al used ethane hydrogenolysis as a test reaction, and Taylor, benzene hydrogenolysis.

Taylor, Thompson and Webb (1968), studying the reactivity of adsorbed species on alumina-supported palladium, rhodium and platinum catalysts found that adsorbed ethylene is not present on the same surface sites as adsorbed acetylene. They concluded that for different hydrocarbons, the catalyst surface exhibited different types of heterogeneity.

Different test reactions may thus lead to contrasting conclusions as to the activity of a particular catalyst. Each test reaction may take place on only a small group of sites on the catalyst surface, and the

particular group of sites involved may change from one test reaction to another, possibly as a result of the actual mechanism of the reaction being studied.

As a result of these three complicating factors, kinetic studies, therefore, do not necessarily give a complete picture of the energetics of the entire catalyst surface.

Heats of adsorption per unit metal area are in effect measures of the bond strength of adsorbate-adsorbent bonds. Now, in a catalytic reaction, if the reactants are too strongly bound to the catalyst surface, desorption will not occur easily and the catalyst surface will effectively be poisoned by the reactants. On the other hand, if the adsorbate-adsorbent bond is too weak, insufficient activation of the reactants will occur. Thus a study of how this bond strength varies with those factors discussed above which affect catalytic activity may help to understand the mechanisms whereby such factors operate. Determining heats of adsorption per unit metal area as a function of the coverage of the catalyst surface will, in principle, enable one not only to map the energetics of the entire surface, but also to investigate how the energetics of the surface varies with changes in such factors as the average metal particle size and the fraction of metal present in the form of metal atoms in the catalysts.

Therefore, in the following section, the determination of heats of adsorption is discussed and the published literature dealing with heats of adsorption on supported metal catalysts is reviewed.

1.4 Heats of Adsorption.

All adsorptive processes are accompanied by the evolution of heat, the magnitude of the evolution depending on whether the adsorbate is held by van der Waals forces (physical adsorption) or forces resembling those in a chemical bond (chemisorption) (section 2.1).

The heat of physical adsorption invariably lies near the heat of liquefaction of the adsorbate and its magnitude is decided primarily by the nature of the adsorbate. Heats of physical adsorption are seldom greater than about 10 kcal/mole, but the range of heats of chemisorption that have been measured is much wider. In chemisorption, the heat evolved depends on the nature of both the adsorbate and the adsorbent. Heats as high as 194 kcal/mole (oxygen on tungsten) have been found (Brennan, Hayward and Trapnell, 1960).

For the vast majority of gas-solid systems, the heat of chemisorption is found to decrease as the surface coverage increases. Only in a few instances, for example hydrogen on iron films at -183^{0}C (Beeck, 1950a), nitrogen on tungsten filaments (Kisliuk, 1959), is the measured heat independent of coverage. Three possible reasons for this decrease have been recognised.

Constable (1925) and Taylor (1925) suggested that the fall is due to the heterogeneity of the solid surface. Adsorption on certain sites is energetically more favoured than on other sites of lower adsorption potential. The first addition of gas to such a surface will be adsorbed preferentially on the most "active" sites, either because the rate of adsorption is greatest on to such sites or, if the adsorbed layer is mobile, adsorbed species will migrate to these energetically favourable sites. Thus as surface coverage increases,

adsorption will take place on sites of lower and lower activities and thus the heat of adsorption will decrease. Such surface heterogeneity as lattice defects, crystal edges and corners and the exposure of different crystallographic planes may also contribute to the observed decrease in heat of adsorption (Brock, 1957).

Mutual interaction of adsorbed species is a second possible cause of the decrease (Roberts, 1935). This could be the result of either dipole-dipole interactions or the overlap of adsorbate electron shells. In practice this cause only makes a small contribution to the observed heat decrease (Bond, 1962).

A third possible cause (Eley, 1951) takes into account the progressive change in the work function of the surface as the coverage increases. If, for example in the hydrogen-metal system, the electron contributed by the adsorbent comes from the top of the conductivity band, as adsorption proceeds, the Fermi surface's energy will fall, thus increasing the work function of the metal. At higher coverage, more energy is required to excite an electron in the conductivity band to the surface orbitals of the metal, and thus the heat of adsorption will be smaller.

It seems likely that a combination of all three effects, and possibly other, as yet undiscovered, factors causes the observed decrease in heats of adsorption. However, it has not been possible to describe theoretically the variety of shapes of heat of adsorption with coverage curves on the basis of the above models (Bond, 1962).

Although the measurement of the heat of physical adsorption can be reproduced within experimental error by different workers, this is not always the case with the heat of chemisorption (Hayward and Trapnell, 1964). With

metals in particular, the heat varies from sample to sample and the heats obtained with powdered metals have lower values and show greater discordance than those obtained on evaporated films. For example, hydrogen chemisorption on nickel powder at low coverages yields values of -21 to -24 kcal/mole (Shield and Russell, 1960) whereas on nickel films, a value of -30 kcal/mole has been obtained (Beeck, 1950b; Wahba and Kemball, 1953). Powders are likely to be contaminated to an unknown and variable extent, and thus measurements are made on an already partly covered surface.

Initial heats of chemisorption (i.e. at zero coverage) may vary with the temperature at which the measurements are made, either because different mechanisms are operative at the different temperatures or because the adsorbed layer may be immobile at one temperature but not at the other. For example Beeck (1950a) found that the initial heat of chemisorption of nitrogen on iron was -10 kcal/mole when measured at -196^{0}C, but -40 kcal/mole when measured at room temperature.

Heats of adsorption can be expressed in two different ways, either as an integral heat, which represents the total amount of heat evolved for adsorption up to a given coverage, or as a differential heat, which measures the increase in heat content for the adsorption of an infinitesimal quantity of gas at a particular surface coverage. These heats may be determined either calorimetrically or by means of adsorption isosteres,

$$p = f(T)_n \qquad 1.4.1,$$

which may be constructed from a family of adsorption isotherms at different temperatures.

The isosteric heat of adsorption (a differential heat) may be determined by applying the integrated form of the Clausius-Clapeyron equation,

$$\ell n\, p = \frac{q_{st}}{RT} + \text{constant} \qquad 1.4.2.$$

Since this equation is thermodynamic in origin, it is valid only for thermodynamically reversible processes. The method normally used in the evaluation of isosteric heats of adsorption is applied by plotting the isotherms as "semi-log" isotherms, i.e. as curves of amount of gas adsorbed versus the logarithm of the equilibrium pressure. This is done for two or more temperatures not too widely separated. For a fixed amount of gas adsorbed, log p values are read off the isotherms. A plot of log p against the reciprocal of the absolute temperature should give a straight line of slope $q_{st}/2.303R$. Thermodynamic reversibility must be checked by (say) raising the temperature of the adsorbent and then lowering it to its original value in a closed system. The equilibrium pressure should return to the original value if the system is thermodynamically reversible. It is also essential to ensure that the isotherms are reproducible within experimental error, since many adsorbents change slightly from one isotherm to the next (Gregg, 1961).

If true thermodynamic equilibrium is not attained during the adsorption process, the measurement of the evolution of heat can be made using a calorimeter. Most adsorption calorimeters are designed in such a way that the

heat evolved is retained in the adsorbent, whose temperature rise is measured with a resistance thermometer or a thermocouple (Ward, 1931; Beebe and Wildner, 1934; Garner and Veal, 1935; Klemperer and Stone, 1958).

The heats of adsorption of hydrogen on evaporated nickel films have been measured by several workers (Beeck, 1950b; Wahba and Kemball, 1953; Klemperer and Stone, 1958 and Rideal and Sweet, 1960). Although similar values for the heat were obtained by all these workers at high coverages, the heats of adsorption obtained by Klemperer and Stone at low coverages were substantially higher than those of the other workers. They explained this phenomenon as follows: in a small calorimeter, the hot wire from which the film is evaporated, is relatively close to the film, and the heat generated by the wire could cause the film to sinter during its deposition. Sintering will tend to remove many crystal imperfections. In an unsintered film these defects will tend to be removed under the influence of the emitted heat of adsorption, the strain energy so released giving rise to an increased heat emission. The initial heats measured by Klemperer and Stone were higher because they used a larger calorimeter than the other workers, and so their film was less likely to be sintered by the hot wire. This release of stored energy is probably complete at coverages of the order of 20% (Bond, 1962), and thus comparisons of heats of adsorption on evaporated metal films are probably best done at such a coverage and not at $\theta = 0$.

Klemperer and Stone also found that very thick nickel films tend to give a higher initial heat of hydrogen adsorption than thinner ones.

Eucken (1949) and Shield and Russell (1960) determined the heats of adsorption of hydrogen on nickel powders calorimetrically and Kwan (1949) and Roberts and Sykes (1958) determined the heats isosterically. The heats obtained vary considerably, the calorimetric determinations being somewhat lower than the heats obtained isosterically. Published values of the heat of adsorption of hydrogen on various forms of nickel are summarised in table 1.1 below.

TABLE 1.1.

Form of Metal	$-q_{st}(\theta = 0)$ (kcal/mole)	$-q_{st}(\theta = 0.2)$ (kcal/mole)	Method Used	Reference
Nickel film	43	34	Calorimetric	Klemperer and Stone, 1957.
	32	26	Isosteric	Rideal and Sweet, 1960.
	31	29	Calorimetric	Beeck, 1950b.
	29	27	Calorimetric	Wahba and Kemball, 1953.
Nickel powder	27		Isosteric	Rideal and Sweet, 1960.
	26		Isosteric	Kwan, 1949.
	24		Calorimetric	Shield and Russell, 1960.
	21		Calorimetric	Eucken, 1949.
Silica-supported nickel	26		Isosteric	Schuit and de Boer, 1953.
	25.5		Calorimetric	Schuit and de Boer, 1953.

The only published values of isosterically determined heats of adsorption on supported metal catalysts which was found in the literature is that by Schuit and de Boer, (1953) who only measured the heat of adsorption of hydrogen on a single impregnated silica-supported nickel catalyst of 9.7% metal concentration.

distribution although no differences in average metal crystallite size may be found.

Nickel was chosen as the metal component of the catalysts since it is relatively easy to reduce as compared say to iron or cobalt, it has been extensively used in catalytic studies in the past and, unlike platinum, for example, the fraction of the metal present in the metallic state in the catalysts may be determined using carbon monoxide if the metal is nickel, as described in section 4.5.

Silica was used as the support for the following reason. A non-porous support was required in order to eliminate confounding effects of pores and it was felt that it would be easier to obtain silica in a non-porous form than some of the other commonly used supports.

The two most frequently used methods of preparation of supported metal catalysts are impregnation and co-precipitation. Since co-precipitation catalysts may have a substantantial fraction of the metal embedded within the support, and hence not accessible to the adsorbate molecules, it was decided to use the impregnation method in which all the metal is situated on the surface of the support.

The objectives of the research project can now be summarised:

1. To determine whether a support-metal interaction in non-porous silica-supported nickel catalysts can be detected using isosteric heats of adsorption of hydrogen per unit metal area.

CHAPTER 2

THE MEASUREMENT OF THE SURFACE AREA OF SOLIDS

2.1 The Adsorption of a Gas by a Solid.

When a gas and a solid are brought into contact with one another, the concentration of the gas phase is almost always found to be greater at the interface than in the bulk of the gas. This tendency for one phase to accumulate at the interface is called adsorption. The phenomenon arises because atoms in any surface are subject to unbalanced forces of attraction. The balance of these forces can be partially restored by the adsorption of molecules of the second phase.

Adsorption is a dynamical process: gas molecules continuously strike the surface and either rebound or remain on the surface for a finite period of time, after which they leave in a direction and with a velocity independent of their original direction of approach and velocity. Temperature, pressure and the molar mass of the gas determine the rate of collision with the surface. Equilibrium is attained when the rates of adsorption and desorption of the gas molecules are equal.

Adsorption is accompanied by a decrease in the free energy of the system, since the process is spontaneous. The entropy of the system also decreases, for adsorption involves the loss of degrees of freedom of the gas when the latter passes from the gaseous to the adsorbed state.

It follows from the thermodynamic relationship,

$$\Delta G_a = \Delta H_a - T\Delta S_a \qquad 2.1.1,$$

that the adsorption process is exothermic. The heat, ΔH_a, that is evolved when

adsorption occurs is known as the heat of adsorption.

Adsorption processes can be classified as physical or chemical depending on the nature of the forces holding the adsorbed molecules to the surface of the solid. Physical adsorption is caused by intermolecular forces. Chemical adsorption or chemisorption involves the transfer of electrons between the solid (called the adsorbent) and the gas (called the adsorbate). The latter process involves the formation of a type of chemical compound between the adsorbate and the outermost layer of atoms of the adsorbent.

Some of the criteria by means of which distinction between the two types of processes can be made are listed below:

(a) The best single criterion is the magnitude of the heat of adsorption. Heats of chemisorption are usually large and have values in the range of heats of ordinary chemical reactions whereas heats of physical adsorption are low and in the neighbourhood of heats of liquefaction.

(b) As physical adsorption and liquefaction are related, physical adsorption tends to take place only at temperatures lower than the critical point of the adsorbate. Although chemisorption often takes place at temperatures well in excess of the critical point of the adsorbate, instances of chemisorption at temperatures as low as $-196^{0}C$ have been reported.

(c) Chemisorption, being a chemical reaction, may require an appreciable activation energy and in this case it will proceed at a

reasonable rate only above a certain minimum temperature. Physical adsorption, however, requires little or no activation energy and should therefore be rapid at all temperatures.

Experimental measurements of the amount of gas adsorbed, n, as a function of the temperature and the pressure, may be conveniently represented by adsorption isotherms,

$$n = f(p)_T \qquad 2.1.2,$$

the form of which can yield qualitative information about the adsorptive process.

Although many different shapes have been reported for such isotherms, Brunauer et al (1940) introduced a system of classification for all isotherms at temperatures below the critical temperature of the adsorbate and this classification has proved to be of great value in adsorption studies. The five basic types of isotherms they proposed are shown in figure 2.1. Type I isotherms are usually associated with systems where adsorption does not proceed beyond a unimolecular layer. The remainder are associated with multilayer formation, isotherms IV and V being characteristic of porous adsorbents.

FIG. 2.1.

THE FIVE BASIC ISOTHERM SHAPES

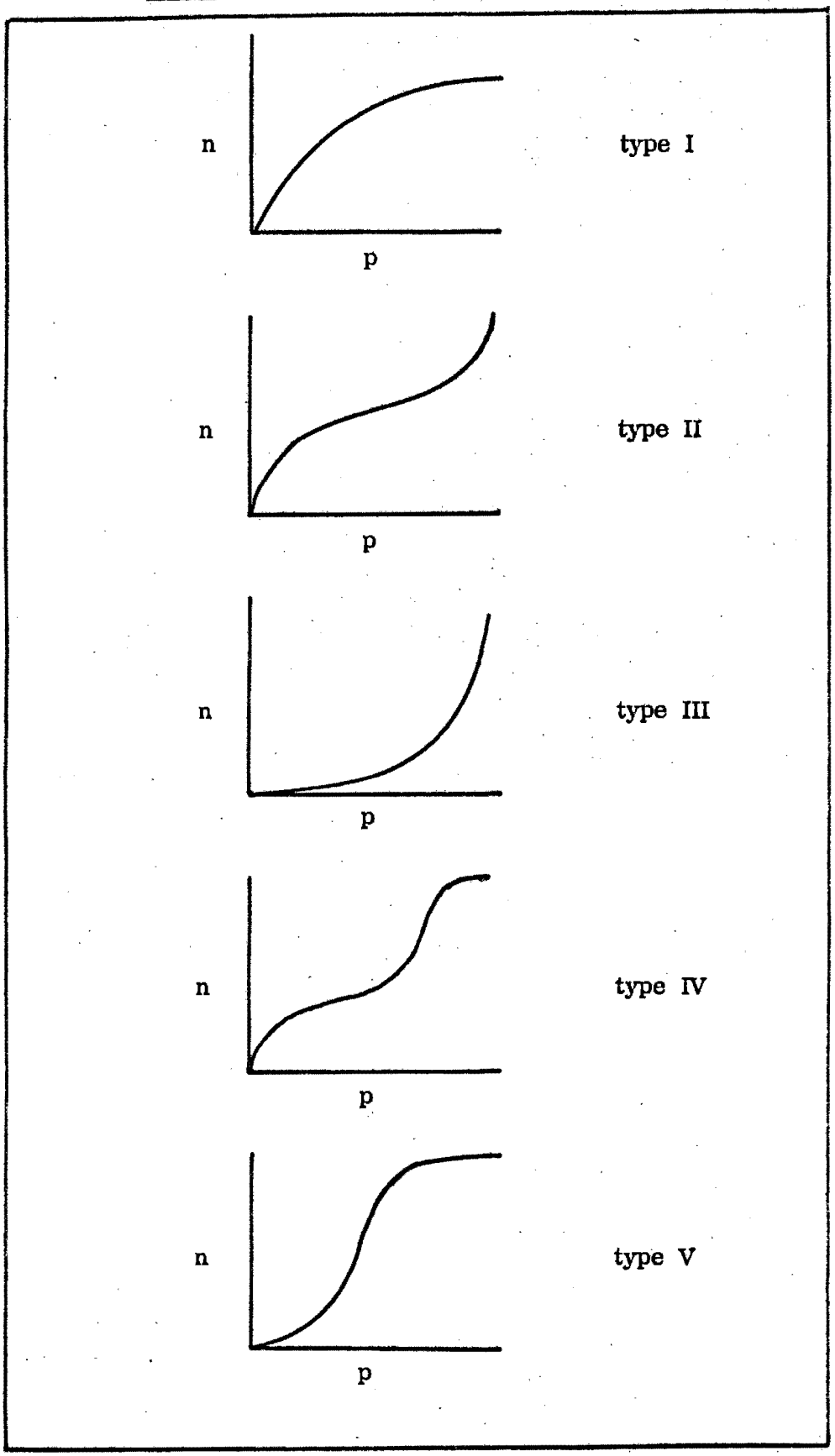

2.2 Physical Adsorption and the Measurement of Surface Area.

The relatively weak physical adsorption provides a method for estimating the surface area of an adsorbent for, if one could determine the number of adsorbed molecules which cover the adsorbent with a unimolecular layer, and if the area occupied by a single adsorbate molecule were known, the surface area accessible to the adsorbate molecules could easily be calculated.

The first useful theory of adsorption which enabled a value for the monolayer capacity of a solid to be determined was developed by Langmuir (1915, 1916, 1918) who assumed that the adsorbed entities are attached on the surface of the adsorbent at definite, localized sites, that each site can accomodate only one adsorbed entity, and that the energy of the adsorbed entity is the same at all sites on the surface and is independent of the presence or absence of other adsorbed entities at neighbouring sites. He visualized the sorption equilibrium to be a dynamical process, the rate of condensation of molecules on a surface exactly balancing their rate of evaporation. On the basis of these assumptions he derived the equation,

$$\frac{n}{n_m} = \frac{kp}{1 + kp} \qquad 2.2.1.$$

However this equation failed to describe the large majority of experimentally determined isotherms, due to the oversimplified assumptions made in its derivation. In particular the assumptions about surface homogeneity, the absence of lateral interactions and the limitation of monolayer adsorption are unrealistic for the vast majority of gas-solid systems. No solid surface is

ideally uniform, for example, and in the absence of other factors, edges, dislocations and other imperfections always introduce a measure of heterogeneity in all solid surfaces.

In 1938, Brunauer, Emmett and Teller developed their theory of multimolecular adsorption in which Langmuir's concept of unimolecularity was discarded. They assumed that the same forces that produce condensation are also responsible for multilayer adsorption, and that an infinite number of layers can form. They ignored lateral interactions between adsorbed molecules and assumed that the differential heat of adsorption falls discontinuously from a relatively large value for molecules comprising the first layer to the normal heat of liquefaction of the adsorbate for the second and successive layers. Despite the assumptions which they made, the equation they derived (called the BET equation) remains one of the most widely used today. It can be derived kinetically, thermodynamically and statistically and may be written in the linear form

$$p/n(p_o - p) = 1/n_m c + (c - 1)/n_m c \cdot p/p_o \qquad 2.2.2.$$

The constant c is related to the heats of adsorption and liquefaction of the adsorbate and can be represented (Brunauer, 1943) by the expression,

$$c = \exp\left[(\Delta H_a - \Delta H_L)/RT\right] \qquad 2.2.3.$$

When the derivation is carried out on the assumption that only a unimolecular layer of adsorbate will be adsorbed, the equation reduces to the Langmuir

equation (equation 2.2.1).

If $p/n(p_o - p)$ is plotted against p/p_o, provided c is constant, a straight line is obtained. Although c is rarely constant from $p = 0$ to $p = p_o$, for a large number of type II isotherms (figure 2.1), c is found to be constant between relative pressures of about 0.05 and 0.35. When this is the case, the slope and intercept of the $p/n(p_o - p)$ against p/p_o plot yield values for n_m and c, and in such cases the BET equation can be used to evaluate the amount of adsorbate, n_m, necessary to form a monolayer on the surface of an adsorbent.

For non-porous solids, areas obtained by using nitrogen adsorption isotherms at liquid nitrogen temperatures in conjunction with the BET equation are usually in good agreement with areas obtained by such independent means as electron microscopy, direct microscopic examinations of suitably sized solids, permeability measurements, heats of immersion and the adsorption of stearic acid and other molecules from solution (Emmett, 1948).

For porous solids, although there exist fewer methods for obtaining independent estimates of the areas, some published results of such comparisons indicate that for porous solids, too, the nitrogen adsorption method gives reliable results (e.g. Elkin et al, 1945).

Emmett and Brunauer (1937b) suggested that the cross-sectional area of an adsorbate molecule could be calculated on using the assumption that the density of the adsorbate monolayer is the same as the density of either the liquified or solidified adsorbate at the temperature of the adsorption. Thus

the area per adsorbed molecule,

$$A_m = 1.091 \left(\frac{M}{N\rho}\right)^{2/3} \qquad 2.2.4$$

This derivation was based on the assumption that the adsorbate molecules are held in a two dimensional close packed structure on the surface, the area occupied by each molecule being the projected cross sections of the molecular volumes calculated from the density of the solidified or liquified adsorbate.

Unless the adsorbed molecule is spherically symmetrical, the area occupied by the molecule on the surface of the adsorbent will depend on the way the molecule is orientated towards the surface. However the value of 16.2 $Å^2$ for the area occupied by a nitrogen molecule at -196^0 C, obtained by Emmett and Brunauer using equation 2.2.4 (which was also obtained by Harkins and Jura (1944) using an independent method, although Livingstone (1949), using a two-dimensional analogue of the van der Waals' equation, calculated a value of 15.4 $Å^2$), is now generally accepted (Young and Crowell, 1962; Dubinin, 1960). The values for other molecules are usually obtained by comparison of the adsorption isotherms on a standard solid.

The specific surface area, Σ, of a solid may thus be calculated from the relationship:

$$\Sigma = 10^{-26} N A_m n_m \qquad 2.2.5.$$

In the widely used volumetric method of obtaining Σ, a dose of adsorbate is admitted to the adsorption cell and the amount of gas adsorbed

calculated by subtracting the amount of gas unadsorbed from the amount of gas added to the cell. Now the higher the adsorbate pressure, the greater is the amount of gas remaining unadsorbed in the adsorption cell. For solids having relatively high specific surface areas, nitrogen adsorption is generally used to measure their surface areas. However, because of the high saturation vapour pressure of nitrogen at liquid nitrogen temperatures (of the order of 760 torr), if the amount of gas adsorbed by the solid is small (i.e. the solid has a small surface area), the errors involved in measuring the amount unadsorbed are of approximately the same magnitude as the amount of nitrogen adsorbed, and so the method becomes unreliable.

Following the work of Beebe, Beckwith and Honig (1945), krypton adsorption has been employed for determining the specific surface area of a wide range of finely divided and porous solids. The method is particularly useful with solids having relatively small areas (less than $1\,m^2/g$) on which nitrogen adsorption is difficult to measure. The low saturation pressure of krypton (about 2 torr) at liquid nitrogen temperatures means that over the usual working range of relative pressure (i.e. 0.05 - 0.35), the correction term for the amount of unabsorbed gas is much less important than it is with nitrogen at the same temperature.

One difficulty in using krypton adsorption to determine surface areas comes in the choice of an appropriate value of p_o at -196^0C. Although this temperature is well below the triple point of krypton (-157^0C), Beebe et al (1945) adopted a suggestion made by Emmett, that the saturation vapour pressure is related not to p_o (solid) but to p_o (liquid). The procedure of using p_o (liquid) for the BET plot has been followed by most other researchers. However the

BET isotherm is not very sensitive to a change in p_o (Gregg and Jacobs, 1948), a 40% difference in p_o leading to an uncertainty of only about 10% in n_m (Sing and Swallow, 1965).

The second problem in the use of krypton for the determination of surface areas lies in the choice of A_m, the area occupied by a krypton atom on the surface of the solid. Using the density of the bulk phase, calculation of A_m for a close packed liquid or solid monolayer yields values of 15.2 $Å^2$ and 14.0 $Å^2$ respectively. Beebe et al (1945) obtained a value of 19.5 $Å^2$ for A_m (krypton), using a "standard" sample of anatase which had been characterised by nitrogen adsorption, electron microscopy and the heat of immersion method of Harkins and Jura (1943, 1944). Wheatley (1959) confirmed this value, measuring surface areas by electron microscopy and nitrogen adsorption, and the value of 19.5 $Å^2$ for A_m has come to be generally accepted. Haul (1956) found that using this value for A_m and p_o for liquid krypton leads to the same BET surface area as using a value of 21.5 $Å^2$ for A_m and p_o for solid krypton. Sing and Swallow (1960) confirmed Haul's observations.

In recent years xenon has also been used for the measurement of the surface areas of low area solids (Thomas and Thomas, 1967). The advantage of using xenon over krypton is that xenon has a lower p_o value, so that in a volumetric apparatus, dead space corrections will be even smaller than for krypton.

The total surface area of a solid can thus be determined by means of the well established techniques discussed above. Because physical adsorption is used, no differentiation can be made between various parts of the surface: for

example the metal and the support in a supported metal catalyst. It is necessary to look to chemisorption techniques in order to measure the metal surface areas of supported metal catalysts.

2.3 The Determination of Metal Surface Areas by Gas Chemisorption.

In a supported metal catalyst, the surface consists of two components, the metal and the support. In order to calculate specific catalytic activities (section 1.2) it is necessary to have a method of measuring the surface area of the metal.

Emmett and his co-workers (1937a, 1943), studying iron catalysts used in the synthesis of ammonia, developed a low temperature chemisorption method to determine the surface concentration of the different catalyst components. Anderson et al (1948) and D'or and Orzechowski (1954) applied the method to other catalysts. However the method was only applicable to catalysts in which the metal concentration was high enough to represent a substantial part of the surface. With the increasing importance to industry of catalysts having a low metal concentration, and with the inapplicability of X-ray techniques to the study of the surface physical properties of such catalysts because of the small size of the metal crystallites on the support surface, a resurgence of interest in gas chemisorption as a technique for such studies occurred during the past two decades. Boreskov and Karnaukhov (1952) were the first to use the principle of selecting adsorption and adsorbate conditions in such a way as to minimise adsorption on the support and maximise adsorption on the metal. Since then much work has been carried out on the estimation of metal surface areas of supported metal catalysts, individual researchers adopting quite different conditions in their determinations (Gruber, 1962; Nikolajenko, Bosacek and Danes, 1963; Yates, Taylor and Sinfelt, 1964; Carter, Cusumano and Sinfelt, 1966; Geus and Nobel, 1966; Swift, Lutinski and Tobin, 1966;

Rostrup-Nielson, 1968; Brooks and Christopher, 1968).

The following eight features were regarded by the author as essential in the precise determination of the metal surface areas of supported metal catalysts and the literature published on such determinations is thus reviewed below in terms of these features.

(i) The gas should chemisorb with a high degree of specificity on the metal but not on the support.

(ii) The gas must cover all available surface sites on the metal.

(iii) Adsorption conditions must be chosen such that physical adsorption does not occur as a variable and indeterminate component in addition to chemisorption.

(iv) The catalyst pretreatment should not significantly alter the state of metal dispersion. If it does, the effect should be reproducible.

(v) The chemisorption isotherm should, above a particular pressure, become independent of the pressure so that an estimate of the number of sites on the surface of the metal available for chemisorption can be made.

(vi) The number of surface sites available for adsorption should be independent of temperature.

(vii) The isotherms must be reproducible within experimental error.

(viii) An estimate must be made of the area occupied by an adsorbate molecule on the surface of the adsorbent.

(i) The gas should chemisorb with a high degree of specificity on the metal but not on the support.

Both hydrogen and carbon monoxide have been used in the determination of metal surface areas of supported metal catalysts. When the metal is nickel, hydrogen is preferred because of the possibility of nickel tetracarbonyl formation (Hughes et al, 1962). No uniformity exists in the literature as to the extent, if any, of the adsorption of hydrogen on the support in a supported metal catalyst. According to Adler and Keavney (1960) hydrogen does not chemisorb on γ-alumina. However Cusumano, Dembinski and Sinfelt (1966) found a measurable adsorption of hydrogen on both alumina and silica-alumina, as did Gruber (1962) on alumina. Yates et al (1964) apparently found no adsorption of hydrogen on silica for they did not report any correction to the amount of gas adsorbed on their catalysts resulting from adsorption on the support. On the other hand Dorling, Burlace and Moss (1968) found that small amounts of hydrogen are adsorbed at 20^0C and a few torr pressure on the support of their platinum-silica catalysts. Even when such adsorption does occur, it is usually very small in comparison to the adsorption on the metal component of the catalyst. In practice, therefore, selective adsorption of hydrogen on supported nickel catalysts does occur, but the actual extent, if any, of adsorption on the support should be determined for each catalyst studied.

(ii) The gas should cover all surface sites on the metal.

Brooks and Christopher (1968) showed that on nickel-alumina catalysts the mole ratios of the amounts of carbon monoxide to hydrogen adsorbed remain about the same over a range of vapour pressures, thus providing strong evidence that both gases "see" essentially the same adsorption sites, even considering the difference in temperatures at which the studies were carried out (250^{0}C for hydrogen, 23^{0}C for carbon monoxide). The fact that metal areas calculated from X-ray line broadening and hydrogen chemisorption agreed well showed that the adsorption was occurring primarily on the same metal crystallites that were measured by X-ray techniques, namely those greater than about 50 Å in diameter. Brooks and Christopher suggested that this was due either to the fact that dissociative hydrogen chemisorption occurred only on crystallites of sufficient size to afford adjacent hydrogen adsorption sites or that some labile hydrogen remained on the surface of the "degassed" sample and this led to a reduced amount of hydrogen that could be adsorbed.

Sadek and Taylor (1950) showed that the amount of hydrogen adsorbed by a supported nickel catalyst at a particular pressure decreases as the temperature is increased. Because of the relatively high temperature (250^{0}C) used by Brooks and Christopher, the conclusions they drew from their results are open to question. At lower temperatures more hydrogen may have been adsorbed, leading to a larger metal area than estimated using X-ray techniques.

The fact that dissociative hydrogen chemisorption does occur on very small crystallites (about 15 Å diameter) was shown by Benesi et al (1968). Studying highly dispersed platinum supported on silica gel they found that each atom of metal adsorbs one atom of hydrogen.

(iii) Adsorption conditions must be chosen so that physical adsorption does not occur as a variable and indeterminate component in addition to chemisorption.

The amount of physical adsorption on a given adsorbent decreases with decreasing boiling point of the adsorbate, with decreasing pressure and with increasing temperature. Thus it is desirable to work at as high a temperature as possible and as low a pressure as possible, using an adsorbate readily chemisorbed by the metal but not by the support. Of the gases, hydrogen, oxygen and carbon monoxide, oxygen can be discarded because it forms a surface film of oxide on the metal.

Benton and White (1930) found that below -100^0 C physical adsorption of hydrogen on nickel occurs. Between -100^0C and 0^0C, the 600 torr isobar was flat, suggestive of a nickel surface entirely saturated with a single layer of adsorbed atoms. Although all the earlier estimations of metal surface areas of supported nickel catalysts were made by Sinfelt and his co-workers using hydrogen at room temperature or 0^0C, in 1966, Carter, Cusumano and Sinfelt used -78^0 C; no reason being given for the change. Brooks and Christopher (1968) found that the adsorption of carbon monoxide and hydrogen on nickel zeolites shows an appreciable pressure dependence. The amount changes by a factor of 2

or more for pressure changes from 10 torr to several hundred torr, indicating that at least part of the gas forms a relatively weak adsorption bond. However their nickel-alumina catalyst showed a negligible pressure dependence above 50 torr for carbon monoxide adsorption, indicating that this adsorbate is held, in the main, by chemisorption bonds.

The adsorption isobar of hydrogen on nickel appears to reach a maximum in the temperature range -100^{0}C to 0^{0}C. In order to determine the position of a maximum amount of adsorption on a particular catalyst, it would be necessary to determine isobars for the system.

(iv) The catalyst pretreatment should not significantly alter the state of metal dispersion. If it does, the effect should be reproducible.

In discussing catalyst pretreatment, the temperature necessary for complete reduction of the catalysts must be investigated. Measuring the extent of reduction of nickel catalysts on a vacuum microbalance, Taylor, Yates and Sinfelt (1964) showed that reduction took place at temperatures as low as 250^{0}C and that at 370^{0}C essentially complete reduction took place. On increasing the reduction temperature to 450^{0}C, Carter, Cusumano and Sinfelt (1966) found no decrease in the adsorptive capacity of their supported nickel catalysts, but did observe a decrease when reduction was carried out at 500^{0}C and 580^{0}C.

Heating supported metal catalysts in air prior to reduction causes a decrease in the adsorptive capacity of the catalyst (Yates, Taylor and Sinfelt, 1964). Benesi et al (1968) noted that the magnetisation of platinum-silica catalysts increased with increasing reduction temperature.

They considered the possibility that the increase was due to better reduction of the metal at the higher reduction temperature. This was disproved by heating a catalyst, reduced at the usual temperature of 370°C, to 800°C in vacuo. This resulted in the previously observed increase in magnetisation which could then be said to be due to the sintering at the elevated reduction temperatures and not to more complete reduction taking place at the higher temperatures.

In a similar study Carter and Sinfelt (1968) found that reduction for an additional hour at 500°C after an initial overnight reduction at 370°C prior to degassing at 500°C had no significant effect on the magnetisation properties of the metal in their catalysts. However increasing the degassing temperature resulted in an increase in the magnetic susceptibility of the catalysts.

In general, Schuit and de Boer (1953) claim that the metal surface of nickel-silica catalysts is extremely heat stable and can be cleaned effectively by re-reduction and evacuation at high temperatures.

For nickel catalysts, therefore reduction and degassing temperatures of the order of 370°C appear not to alter the degree of metal dispersion in the catalysts.

(v) The chemisorption isotherm should, above a particular pressure, become independent of the pressure so that an estimate of the number of sites on the surface of the metal available for chemisorption can be made.

Sinfelt, Taylor and Yates' isotherms (1965) indicated that saturation of the surface is approached at hydrogen pressures above

30 torr at 18°C on silica-supported nickel catalysts. They chose the amount of hydrogen adsorbed at a pressure of 100 torr as representing complete coverage of the surface of the metal.

Carter, Cusumano and Sinfelt (1966) found that, at -78°C, at pressures above 100 torr no further adsorption of hydrogen on silica-alumina-supported catalysts took place. They chose the amount of hydrogen adsorbed at 250 torr and -78°C as representing full metal surface coverage.

Adams et al (1962) found that in the pressure range 0.5 torr to 2.5 torr hydrogen adsorption isotherms on platinum-silica gel catalysts appear to flatten out (about 5% more hydrogen is adsorbed at 2.5 torr than 0.5 torr on the -78°C isotherm). This is in agreement with the work of Beeck (1950b) on metal films. Beeck found that metal films were saturated with hydrogen at 1 torr pressure.

Schuit and van Reijen (1958) concluded from a study of isobars of hydrogen adsorbed on a nickel-silica catalyst that even at -78°C and 100 torr pressure incomplete coverage exists, but that the amounts adsorbed reasonably approximate to complete coverage.

Dorling, Burlace and Moss (1968) found that the hydrogen adsorption isotherms on platinum-silica catalysts flattened out at a pressure of a few torr. They extrapolated the linear portion of the isotherm back to the ordinate (amount of gas adsorbed) axis, in order to obtain an estimate of "apparent hydrogen monolayer volume".

Although generalisations cannot be made, it appears that at -78°C

and at pressures in the region of 25 to 100 torr reasonably complete coverage by hydrogen of the surface of supported nickel and platinum catalysts exists.

(vi) The number of surface sites available for adsorption should be independent of temperature.

Beeck (1950a) has shown that adsorption of hydrogen on nickel films shows a marked temperature dependence, the isobar having a minimum at about -196^{0}C and a maximum at approximately -90^{0}C. Reduced nickel oxide shows an even greater heterogeneity (Benton and White, 1930), and Sadek and Taylor (1950) have observed the same effect for a supported nickel catalyst.

Brooks and Christopher (1968) found that the hydrogen adsorptive capacity of nickel powder at 100 torr was unchanged between room temperature and 150^{0}C. On the other hand the carbon monoxide capacity decreased when the temperature was increased from -196^{0}C to 25^{0}C.

Adams et al (1962) chose the 0^{0}C isotherm in order to compute the "available metal surface area" of their catalyst (silica-supported platinum) although they demonstrated that this "available surface area" was not temperature independent. They gave no reason for their choice of temperature, but from their results at -78^{0}C, it can be shown that the difference in estimates of metal surface area would have changed by only 2.5% if the -78^{0}C isotherm had been used.

Poltorak and Boronin (1965) found that hydrogen adsorption on

highly dispersed platinum supported on silica was practically the same at -196°C as at 20°C. Adsorption at -78°C was greater, but variable. Dorling, Burlace and Moss (1968), in a study on similar catalysts, measured the amounts of hydrogen necessary to form a monolayer on their catalyst surfaces at 20°C, preferring the higher temperature because of the more rapid attainment of equilibrium.

As discussed in section 5.7, isobars of the adsorption of hydrogen on a catalyst, whilst showing the adsorption to be temperature dependent, do give a guide as to the best temperature to use in order to attain maximum chemisorption on the catalyst surface. Any breaks or sharp changes of slope of the isobar may give clues as to a possible change in mechanism of adsorption taking place.

(vii) The isotherms must be reproducible within experimental error.

Brooks and Christopher (1968) found that the initial hydrogen uptake on a catalyst exceeded all subsequent uptakes. This, they showed, could not be due to solubility of hydrogen in the nickel, but they speculated that it may possibly be due to residual reduction of oxides of the metal. They also observed a decrease in adsorption between the second and third isotherms on a particular sample which, they felt, indicated some sintering during the intervening evacuation between isotherms. They observed greater reproducibility for hydrogen isotherms at 150°C than for carbon monoxide isotherms at 23°C.

If adsorption of the adsorbate on the support occurs, care must be

taken to ensure that this adsorption is reproducible. The surface properties of some supports, such as alumina, depend not only on the type of alumina used, but also on the previous history of the support. The work of Russell and Stokes (1947) and Guenther (1955) indicate that even with identical samples of alumina, the adsorption of hydrogen is difficult to reproduce precisely.

(viii) An estimate must be made of the area occupied by an adsorbate molecule on the surface of the adsorbent.

If metal surface areas are to be computed from adsorption data, it is necessary to obtain an estimate of the area effectively occupied by an adsorbate atom or molecule on the surface of the adsorbent. Yates, Taylor and Sinfelt (1964) assumed that one nickel atom in the surface of a supported nickel catalyst adsorbs one hydrogen atom. From the assumption that one third of the surface nickel atoms were atoms in a (100) crystallographic plane, one third in a (110), and the remaining third in a (111) crystallographic plane, they calculated a value of 6.5 $Å^2$ as the average area effectively occupied by a hydrogen atom on the surface of nickel. O'Neill (1961) showed that the surface area of reduced nickel powder obtained by the physical adsorption of argon agreed very well with the hydrogen area computed using the value of 6.5 $Å^2$.

Brooks and Christopher (1968) used a value of 6.0 $Å^2$ for the area effectively occupied by a hydrogen atom on a nickel surface. This area was chosen because it approximated to that for the normal liquid

packing density configuration for hydrogen. This does not appear to be a reasonable deduction on the part of Brooks and Christopher, for the area per adsorbed atom in site adsorption ought to be determined, not by the packing density of the adsorbate, but by the surface crystallography of the adsorbent. The value of 6.0 $Å^2$ was also computed by Beeck (1950b) who obtained it by dividing the specific surface area of a nickel film (obtained by krypton adsorption) by the number of hydrogen atoms adsorbed by one gram of the film. This method of calculation is also open to question, for Beeck used a computed value of 14.6 $Å^2$ for the area per adsorbed krypton atom in contrast to the generally accepted area of 19.5 $Å^2$ (section 2.2).

If a sample of a metal having a known surface area is available, the area occupied by a hydrogen atom on the surface of the metal may be estimated from gas chemisorption measurements on the metal, assuming that a reasonable estimate of the amount of gas covering the surface of the metal in a unimolecular layer can be made. Adams et al (1962) used a sample of platinum black of known surface area in order to derive a value of 11.2 $Å^2$ for the area effectively occupied by a hydrogen atom on the surface of platinum. (They do not, however, state by what independent method the surface area of the platinum black was obtained). Comparing this value with the area per platinum atom in the (100), (110), (111) crystallographic planes (7.68, 10.85, 6.65 $Å^2$ respectively) indicated that the (110) plane predominates in the surface of platinum. The area of 11.2 $Å^2$ was then used to estimate metal

surface areas of silica-supported platinum. Good agreement was obtained between the gas adsorption and X-ray methods.

Thus, from a study of the literature, it can be seen that no general agreement exists as to which are the "correct" parameters to use in order to evaluate metal surface areas of supported metal catalyst by gas chemisorption. What does emerge, however, is the fact that each individual adsorbate-adsorbent system must be investigated in order to determine which parameters and conditions will lead to an estimate of the amount of gas adsorbed which most closely approximates to "complete surface coverage". However the following conclusions on the nickel-silica system can be drawn.

A temperature in the region of 370^0C appears to be suitable for catalyst pretreatment. Hydrogen appears to be the most suitable adsorbate to use, the formation of nickel tetracarbonyl and the fact that carbon monoxide may be bound to the surface in a number of different ways (appendix 1) ruling out the use of carbon monoxide. Hydrogen does not appear to adsorb on silica at temperatures above -78^0C. This, of course, would require verification.

On the basis of the work carried out on nickel, it is not possible at this stage to say with complete certainty whether hydrogen chemisorption occurs on single metal atoms on the surface of a support or not.

The hydrogen chemisorption isotherms on various nickel-support systems do not appear to become temperature independent at similar pressures. The pressure at which the isotherm becomes temperature independent would have to be determined experimentally in a study on any particular series of catalysts.

Evaluation of the adsorption isobar appears to be essential in deciding on the temperature at which adsorption is to be studied. (If no adsorption on the support is evident, temperatures in the region of -78°C appear to be suitable).

The area occupied by an adsorbate atom or molecule on the metal surface remains a highly speculative quantity. Confounding factors, such as preferred orientation of particular crystallographic planes could significantly affect this parameter. However, if metal areas are to be used only for comparison purposes between catalysts, the magnitude of the problem is considerably reduced. The value of 6.5 $\AA^2$ for a hydrogen atom, used by Yates, Taylor and Sinfelt (1964), appears to be not unreasonable.

CHAPTER 3

APPARATUS AND EXPERIMENTAL TECHNIQUES

3.1 Requirements in the Design of the Apparatus.

In the design of the apparatus used for measuring adsorption isotherms, certain general requirements had to be fulfilled:

(a) A high vacuum apparatus was required so that adsorbed gases could be removed as completely as possible from the adsorbents.

(b) It was desirable to keep the apparatus as simple as possible.

(c) The gases used in the experiments had to be of high purity and a simple gas purification train was desirable. In order to permit evacuation of the gas train, solid, as opposed to liquid, absorbents were necessary.

(d) It was essential to keep the adsorbent sample at a constant temperature during the measurement of the isotherms.

(e) In order to be able to estimate the amount of gas adsorbed by an adsorbent, all pressure, volume and temperature measurements should be as precise as possible.

(f) It was desirable to incorporate certain safety devices into the apparatus in order to switch off furnaces and the diffusion pump in the event of either a failure in the water supply or breakage of the apparatus.

3.2 The Design, Construction and Calibration of the Apparatus.

3.2.1 General.

Figure 3.1 shows the general layout of the apparatus which was constructed throughout from pyrex glass. A mercury diffusion pump (D) was used to produce the high vacuum. It was backed by a rotary oil pump (R). Liquid nitrogen traps (T) were situated, one between the pumps, and a second between the diffusion pump and the rest of the apparatus. Gases introduced into the apparatus were purified in the gas purification train (G) and stored in the gas storage bulbs (S). The section of the apparatus in which measurements of the pressure and the volume of adsorbate gas were made consisted of a gas burette (B), a constant volume manometer (M) and two McLeod gauges (M_L and M_H). A second constant volume manometer, not shown in figure 3.1, was connected to the adsorption cell (C). This manometer was only used in preliminary experiments in which nitrogen was used as adsorbate, and was removed when no longer required. The temperature of the liquid nitrogen bath surrounding the adsorption cell during the determination of krypton isotherms was measured by means of the gas thermometer (W).

The various components of the apparatus are now described in greater detail.

3.2.2 Pumps.

The two-stage mercury diffusion pump (D) was charged with triple distilled mercury. It was heated electrically by a 150 watt spiral heater encased in the bottom of an asbestos box into which the reservoir of the pump

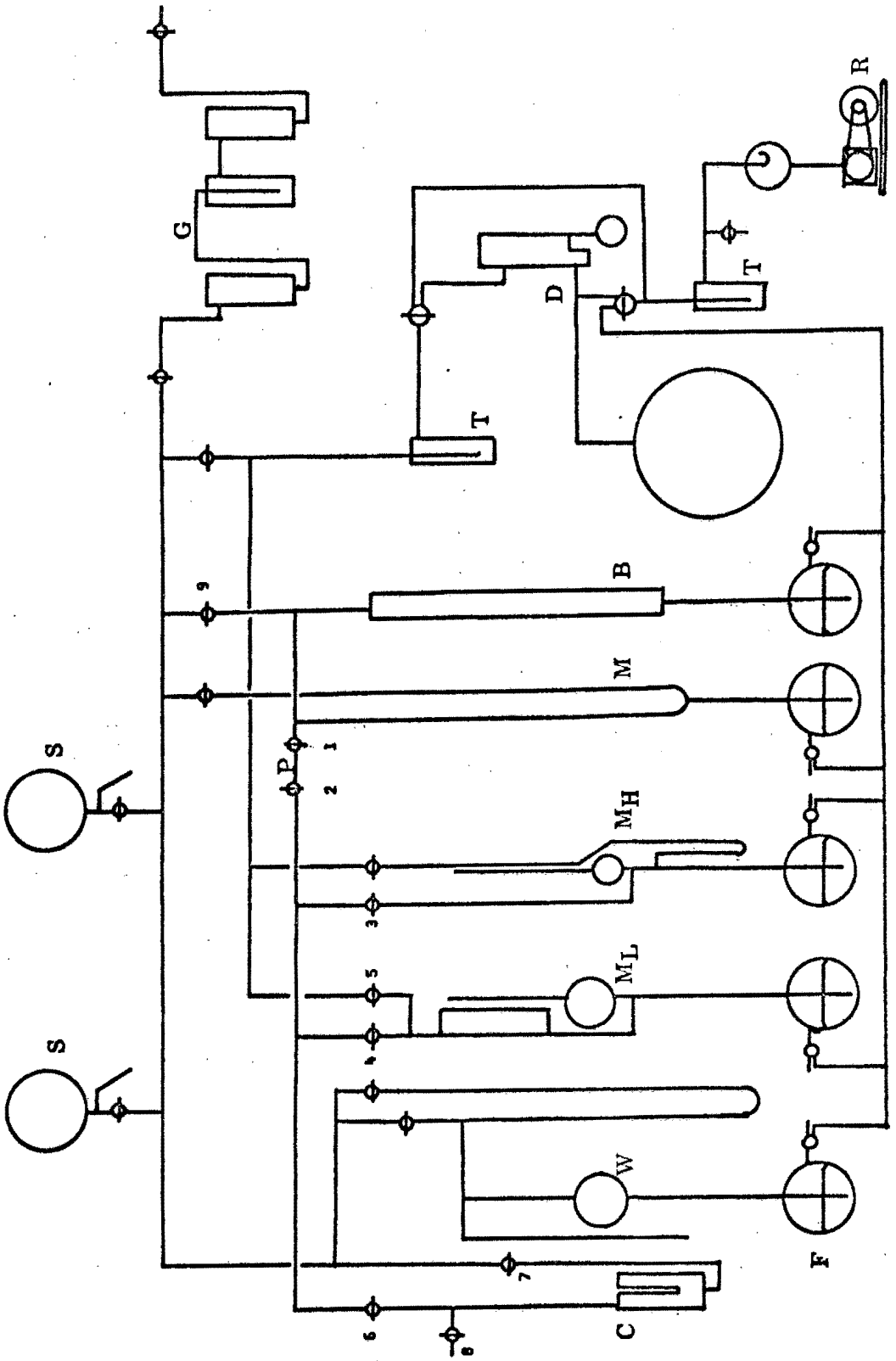

FIG. 3.1. THE HIGH VACUUM APPARATUS

fitted snugly. When backed by a pressure of approximately 10^{-2} torr the pump was capable of producing a vacuum of 1×10^{-5} torr within 15 minutes in a well outgassed apparatus. Pressures in the region of 10^{-6} torr could be obtained by pumping for longer periods. The diffusion pump was backed by a two-stage Speedivac rotary oil pump (R), type 2SC20A, manufactured by Edwards and Co., London. The rotary pump was capable of providing a backing pressure of 10^{-3} torr. The liquid nitrogen traps (T) protected the rotary pump from condensible vapours and prevented mercury vapour, escaping from the diffusion pump, from diffusing back into the apparatus.

3.2.3 Mercury Reservoirs.

The gas thermometer (W), the McLeod gauges (M_L and M_H), the manometer (M) and the gas burette (B) were each connected to a mercury reservoir (F) (figure 3.1). Attached to each reservoir was a double-oblique stopcock. The mercury level in each of the devices mentioned above could be raised by connecting the space above the mercury in the reservoir to the atmosphere, or returned to the reservoir by evacuating the space above the mercury in the reservoir using the rotary pump (R).

3.2.4 The Gas Burette and Constant Volume Manometer.

The gas burette (B) was constructed from a length of graduated pyrex glass tubing. It was surrounded by a water jacket. Water from a thermostat bath could be passed through the jacket in order to thermostat the burette and its contents. The bottom of the burette led into a mercury reservoir (section 3.2.3).

A constant volume manometer (M) was used for measuring the pressure of the gas in the gas burette. The manometer was also connected to a mercury reservoir. Because of the necessity of keeping the volume of the apparatus constant, the mercury in the pressure limb of the manometer was always adjusted to a reference point (a piece of tungsten wire sealed into the glass of the manometer) before reading pressures. In order to minimise capillary effects, the diameter of the glass tubing at the reference point was the same as that of the opposite leg. Tubing of internal diameter 6 mm was used. Above the reference point in the pressure limb, the manometer was constructed from capillary tubing. The manometer extended for several centimetres below the reference point so as to avoid the danger of mercury being forced around the U bend in the event of a rapid increase in pressure. The right hand limb of the manometer could be evacuated through the stopcock at the top of the limb.

Aliquots of gas could be admitted to that section of the apparatus consisting of the adsorption cell (C) and the McLeod gauges (M_L and M_H) from the gas burette (B) through a pipette (P) consisting of two stopcocks joined by a short length of capillary tubing. Before the pipette was sealed onto the apparatus, its volume was measured by weighing the quantity of mercury which filled the pipette.

3.2.5 Calibration of the Gas Burette Dead Space.

In order to estimate the amount of gas present in the gas burette system, the volume of the apparatus between stopcocks 2 and 9, the constant level mark

on the manometer (M) and the zero mark on the gas burette, K_g, had first to be calibrated. Helium was used as the calibrating gas for calibrating all sections of the apparatus as it is chemically inert and is not adsorbed appreciably, even at liquid nitrogen temperatures (Homfray, 1910).

Ross and Olivier (1964) describe a method whereby the error made in measuring an unknown volume, V_u, by expansion of gas from a known volume, V_c, can be minimised. Their argument is as follows. If p_1 is the pressure of the gas in V_c and p_2 the pressure in $(V_u + V_c)$ then, using Boyle's Law, it follows that

$$\frac{V_u}{V_c} = \frac{p_2}{p_1 - p_2} \qquad 3.2.1.$$

To ensure that the relative error in V_u is no greater than the relative error in p_2, the difference, $(p_1 - p_2)$, must be equal to p_2 and thus it follows from equation 3.2.1 that V_c should be approximately equal to V_u. In addition, the pressures p_1 and p_2 should both lie in the range of greatest precision of the pressure measuring device being used. Figure 3.2, which shows how the relative error in the measurement of $(V_u + V_c)$ varies with the ratio V_u/V_c, assuming a relative error of 0.1% in the measurement of V_c, is reproduced from Ross and Olivier's book. It can be seen that the error is a minimum when V_u equals V_c.

Now the smaller the actual value of any pressure and volume readings, the higher the error will be in the estimation of the amount of gas in a particular volume. A series of error curves were computed in order to

FIG. 3.2.

VARIATION IN THE ERROR OF A CALIBRATED VOLUME AS A FUNCTION OF (CALIBRATED VOLUME/REFERENCE VOLUME)

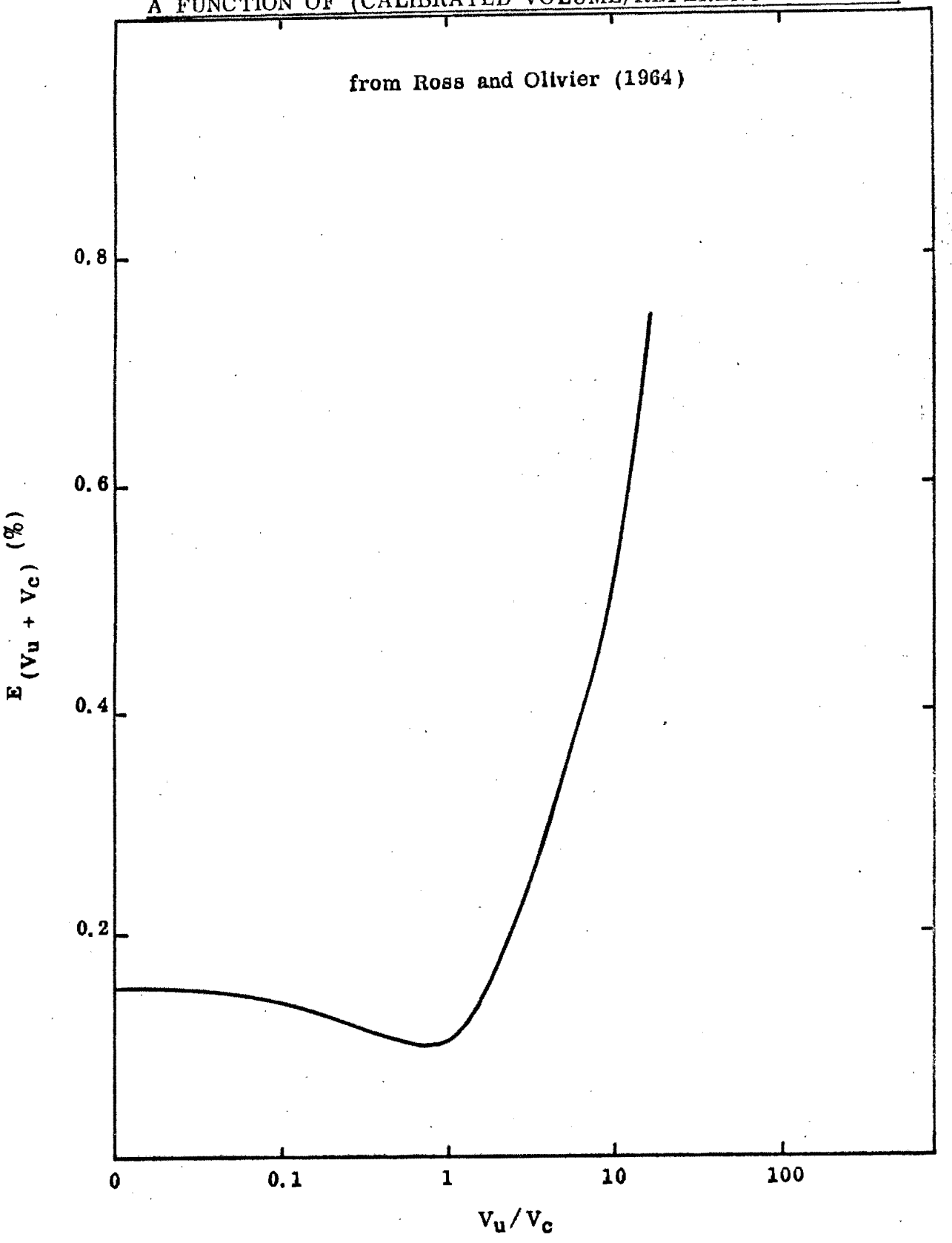

determine the smallest values of pressure and volume which could be used on the apparatus without drastically increasing the relative error in pV/760RT, These curves are shown in figures 3.3 and 3.4. The estimated errors in pressure, volume and temperature were:

$$e_p = \pm 0.1 \text{ torr}, \quad e_V = \pm 0.5 \text{ ml}, \quad e_T = \pm 0.3^0\text{K}.$$

From the curves it can be seen that the relative error in pV/760RT rises fairly sharply at pressures below 200 torr and volumes below 30 ml. Thus, where possible, aliquots of gas should be taken such that measurement of the amount of gas present does not require use of pressures and volumes read below these minimum values.

The volume K_g was calibrated as follows. An aliquot of helium was admitted to the gas burette through stopcock 9, stopcock 2 being closed and stopcock 1 open. The mercury level in the gas burette was adjusted to approximately the 40 ml mark. The pressure and volume of the gas in the gas burette were noted and the mercury level in the burette lowered to a point such that the increase in volume in the gas burette system was approximately equal to the sum of the first volume noted plus K_g. Care was taken to ensure that a sufficiently large aliquot of gas was admitted to the gas burette so that on expansion, the gas pressure was greater than 200 torr. Nine such sets of readings were taken. From each set of readings, a value for K_g can be computed using Boyle's Law, from which it follows that,

FIG. 3.3.

RELATIVE ERROR IN pV/760RT AS A FUNCTION OF PRESSURE AT CONSTANT VOLUME

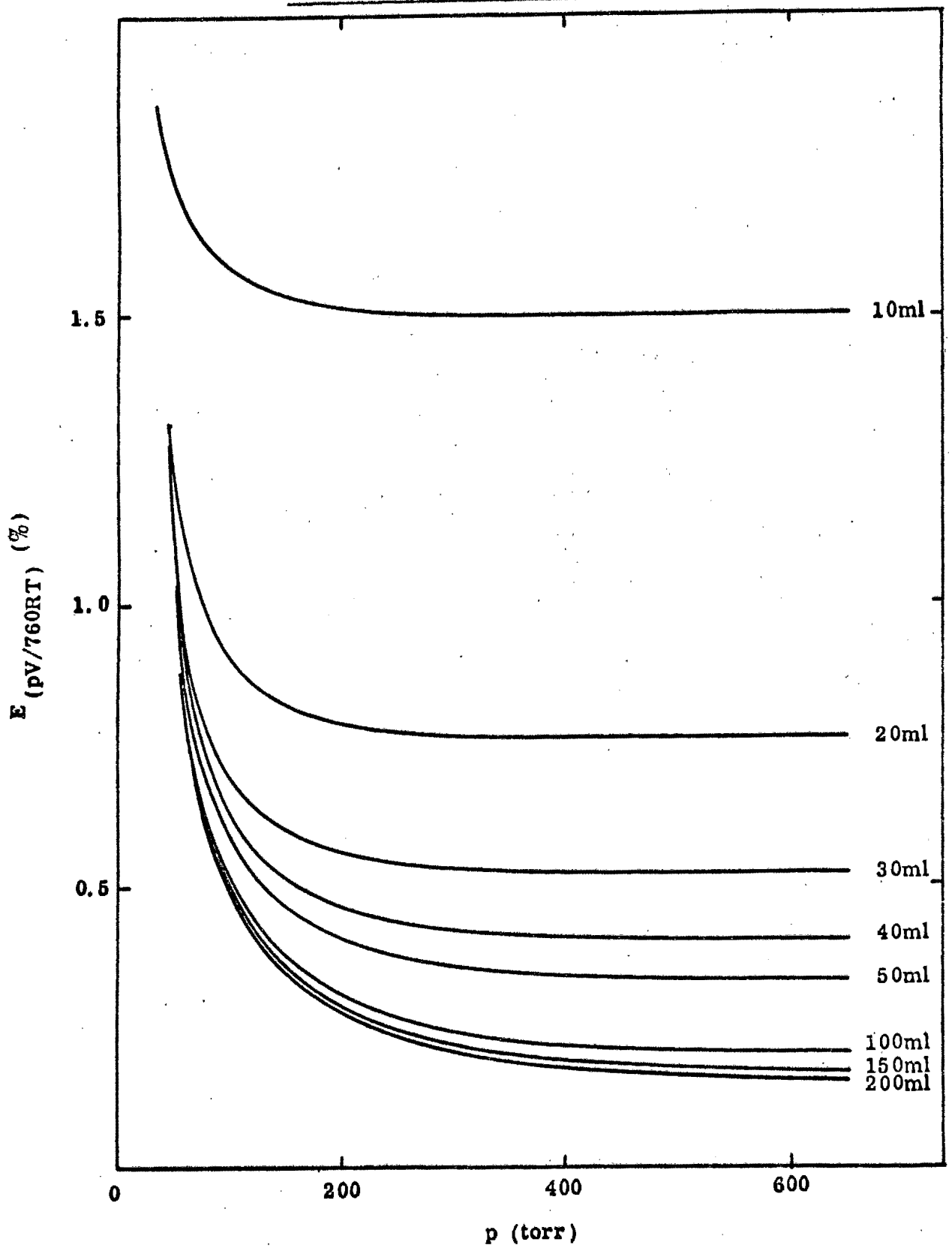

FIG. 3.4.

RELATIVE ERROR IN pV/760RT AS A FUNCTION OF VOLUME AT CONSTANT PRESSURE

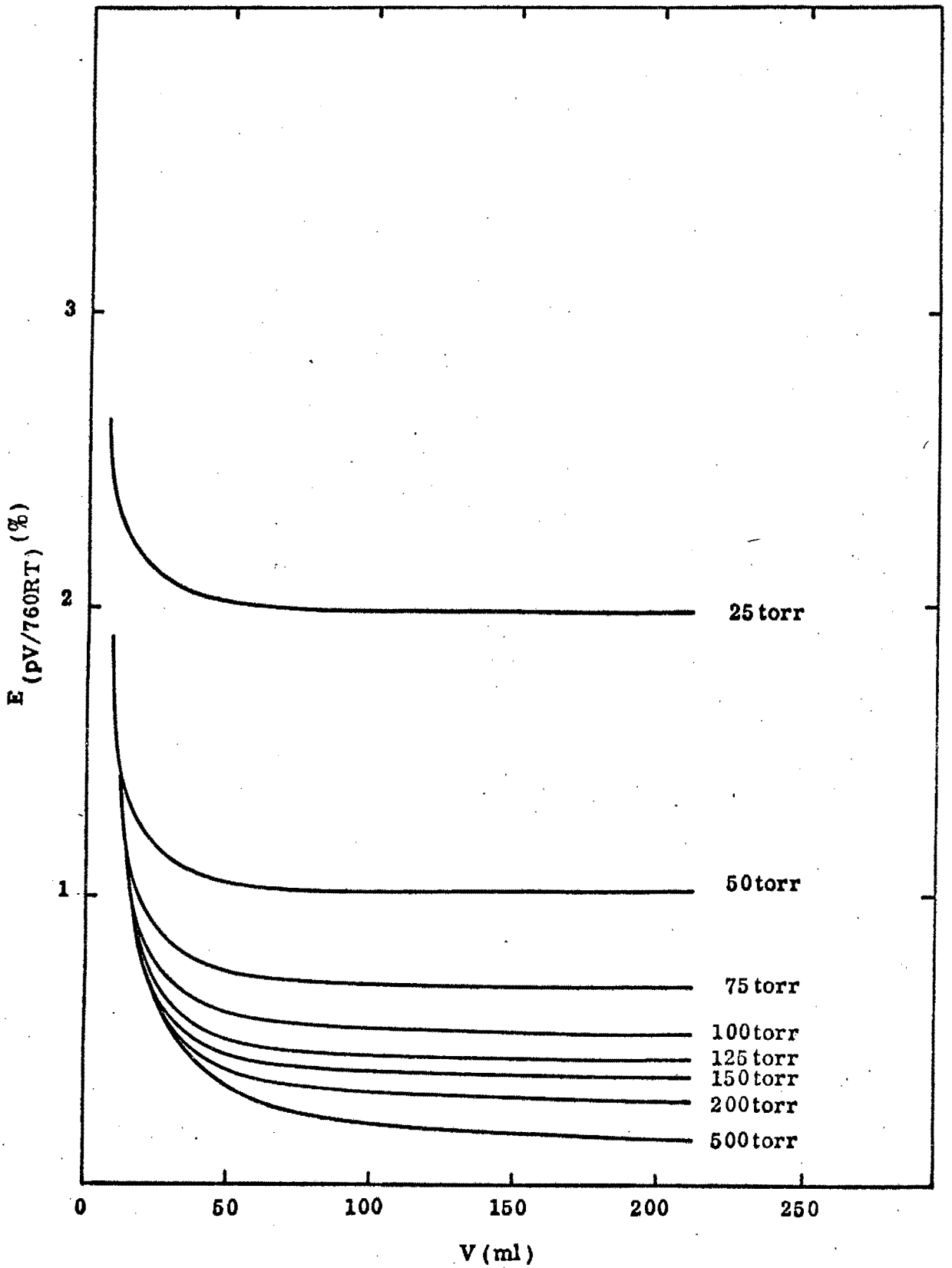

$$K_g = \frac{p_2V_2 - p_1V_1}{p_1 - p_2} \qquad 3.2.2.$$

The mean value of K_g obtained was 5.24 ml. The standard error was ±0.05 ml.

3.2.6 The McLeod Gauges.

McLeod gauges were chosen to measure pressures in the range 10^{-4} torr to 50 torr since they are absolute pressure gauges and could be constructed and calibrated in the department. The principle on which the gauge operates is that of compression of a known volume of gas at an unknown pressure to a smaller volume. The pressure at the smaller volume is determined by the difference in the heights of mercury columns. Thus the original pressure can be calculated using Boyle's Law. The range 10^{-4} torr to 2 torr was covered by a conventional McLeod gauge (M_L) designated the "low pressure McLeod". A somewhat different design was used for the gauge reading in the range 1 torr to 50 torr (Barr and Anhorn, 1949, page 204), designated the "high pressure McLeod" (M_H). The gauges are depicted in figures 3.5 and 3.6. The gauges are operated by causing mercury to rise and enter the bulb of the gauge. The gas in the bulb and capillary which is sealed to the bulb is cut off from the rest of the system. The gas is further compressed by the mercury until the mercury column in the outer capillary is approximately level with the end of the closed capillary. If the volume of the bulb plus capillary of the gauge is V_g, the height of the gas column in the closed capillary is ℓ and the difference in heights of the mercury in the open and closed capillaries, $\Delta\ell$, by Boyle's Law, the initial pressure in the gauge is given by,

LOW PRESSURE McLEOD GAUGE

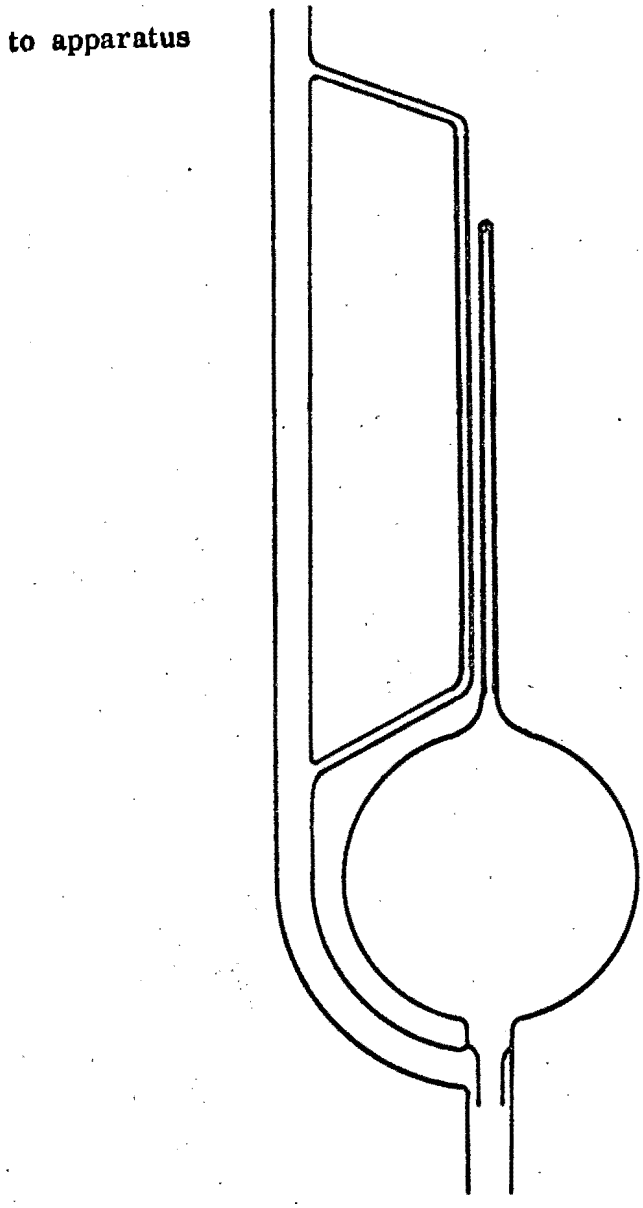

FIG. 3.5.

HIGH PRESSURE McLEOD GAUGE

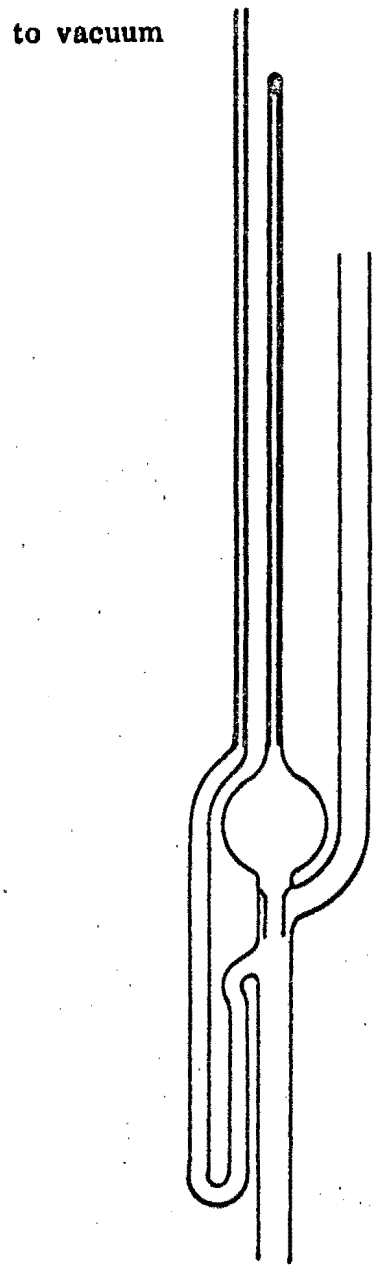

FIG. 3.6.

$$p = \frac{\pi r^2 \ell \, \Delta\ell}{V_g} \qquad 3.2.3.$$

In the high pressure range (1 torr to 50 torr) the pressure of the gas in the open capillary capillary arm cannot be neglected and thus the difference in heights of the mercury columns is not a measure of the pressure of the gas in the closed capillary. The design shown in figure 3.6 overcomes this problem, for the space above the mercury in the open capillary is evacuated. The U-tube below the open capillary serves as a mercury seal to prevent the escape of the gas in the gauge.

3.2.7 Calibration of the McLeod Gauges.

The capillaries of the gauges were made of precision bore "Veridia" tubing purchased from Chance Brothers, England. The tubing was of 2 mm bore and the tolerance quoted by the manufacturers was ±0.01 mm. The volume of the bulb plus capillary of the low pressure McLeod gauge was calibrated with water, since no balance which could weigh the requisite quantity of mercury was available. The volume, V_ℓ, was 133.1 ±0.2 ml (6 determinations), from which the McLeod gauge constant, $K_\ell = 10^{-3}\pi r^2/V_\ell$, was calculated and found to be 2.360×10^{-5} mm^{-1}. Because of its very much smaller volume, the high pressure McLeod gauge was calibrated using mercury. A value for V_h of 5.12 ±0.01 ml (8 determinations) was obtained, from which a value of $6.14 \times 10^{-4} mm^{-1}$ for K_h was calculated.

Once the McLeod gauges were sealed onto the apparatus, it was necessary to know the total volume of each gauge plus its connecting tubing up

to the adsorption cell stopcock (6).

(a) The volume of the low pressure McLeod gauge plus connecting tubing up to stopcocks 2, 3, 5 and 6 (V_L).

After evacuating the apparatus to a pressure of 10^{-6} torr, helium was introduced into the gas burette, stopcocks 2, 3, 5 and 6 being closed. Now, as can be seen in figure 3.2, expansion from a small known volume into a large unknown volume would lead to large relative errors. Although the ratio of V_u/V_c could not be brought down to the ideal value of unity, by the procedure outlined below, the ratio was of the order of 3. The mercury level in the gas burette was lowered to the 100 ml mark, the largest volume obtainable with the burette. The pressure and volume of the helium in the burette were noted, the aliquot being of such a size that after expansion, the pressure of the helium was greater than 200 torr. Stopcock 2 was opened and the gas expanded into the McLeod gauge and connecting tubing. The mercury level in the gas burette was set at the 30 ml mark, the mercury level in the McLeod gauge was set at the cut off point at the bottom of the bulb, and the pressure and volume of the helium noted on the constant volume manometer and gas burette respectively. Using Boyle's Law, V_L was calculated to be 233.9 $\pm$1.0 ml (10 determinations).

(b) The volume of the high pressure McLeod gauge plus connecting tubing up to stopcocks 2, 4, and 6 (V_H).

Using the same criterion (V_u/V_c as close to unity as possible), the volume V_H was found to be 29.9 $\pm$ 0.2 ml (10 determinations).

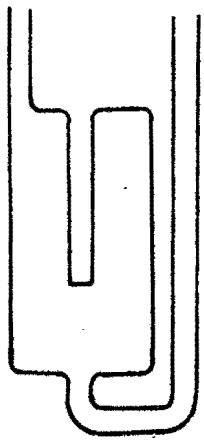

FIG. 3.7.

ADSORPTION CELL

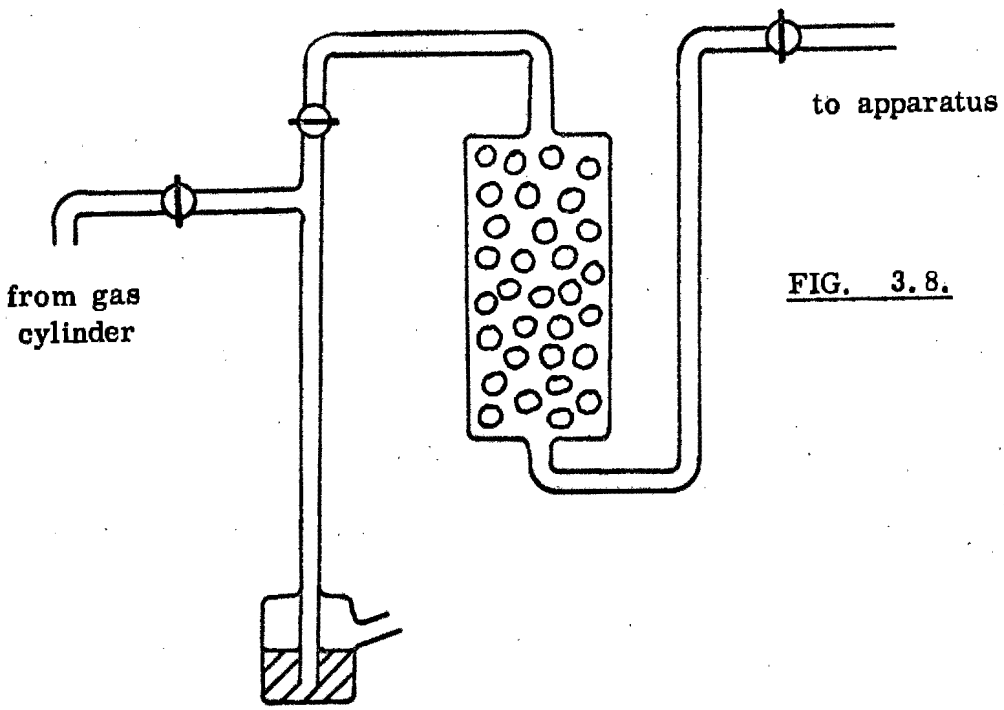

FIG. 3.8.

GAS FILLER

short length of capillary tubing, was used to measure the flow rate of hydrogen through the adsorption cell during the reduction process. It was situated downstream from the mercury valve and was calibrated with hydrogen prior to use.

3.2.9 Calibration of the Adsorption Cell Dead Space.

It was necessary to obtain a measure of the amount of gas present in the adsorption cell which remained unadsorbed in order to calculate the amount of gas adsorbed by an adsorbent. A series of isotherms was to be measured on each catalyst and thus the adsorption cell was calibrated at each of the isotherm temperatures to be used. Pressures more or less in the centre of the range of pressures to be employed in the determination of the isotherms were used in the calibrations.

After the adsorption cell was filled with the requisite amount of catalyst and sealed onto the vacuum line, and the catalyst reduced and degassed (section 3.3), the adsorption cell was thermostatted (section 3.2.10) at the required temperature. One hour was allowed for the attainment of thermal equilibrium. Thereafter stopcocks 2, 3, 5, 6 and 7 were closed and a suitable aliquot of helium was admitted to the low pressure McLeod gauge and tubing leading to the adsorption cell (V_L) through the gas pipette (P). The pressure, p_1, of the helium in the known volume, V_L, was measured using the McLeod gauge (M_L). Stopcock 6 was opened and the helium allowed to expand into the adsorption cell. After 5 minutes stopcock 6 was closed and the new pressure, p_2, measured. (Preliminary experiments showed that no change in the pressure

occurred after 5 minutes). The amount of gas in the adsorption cell at pressure p_2 is given by the expression,

$$n_c = \frac{10^{-3} p_1 V_L}{760RT} - \frac{10^{-3} p_2 V_L}{760RT} \qquad 3.2.4.$$

Successive aliquots of helium were added to the volume, V_L, in the same fashion and the above procedure repeated for each aliquot. A graph of the cumulative amount of helium, Σn_c, added to the adsorption cell against the corresponding equilibrium pressures was plotted. The slope, w, of the resulting straight line was computed using the method of least squares.

Thus in order to estimate the amount of adsorbate present in the adsorption cell but not adsorbed, it was simply necessary to multiply the equilibrium pressure of the adsorbate by w.

Between calibrations at one temperature and another, the adsorption cell was evacuated for 1 hour. At the end of this period pressures in the region of 10^{-6} torr were attained.

3.2.10 Thermostatting of the Adsorption Cell.

For all isotherms measured at temperatures above 150°C, the adsorption cell was thermostatted by means of a furnace. The furnace was constructed by winding 26 swg Nichrome wire (100 ohm total resistance at 25°C) around an asbestos-paper-covered silica tube. In order to ensure that no temperature gradients existed along the length of the furnace, the windings were spaced closer together at the ends of the furnace than in the middle. The wire was covered with a moist mixture of equal parts of powdered asbestos and magnesium

oxide. When the mixture was dry, the construction of the furnace was completed by covering its exterior with a layer of asbestos string. Power for the furnace was supplied through a Variac. Although fluctuations in mains voltage, especially at the start and the end of the University working day, did cause variations in the furnace temperature, with experience it was possible to minimise these fluctuations by careful adjustment of the Variac. Using this method, temperature fluctuations during the course of an isotherm could be kept down to $\pm 2^{0}C$. The furnace was also used for degassing the adsorbents prior to the determination of the isotherms.

For experiments conducted between room temperature and $50^{0}C$ a conventional water-bath thermostat was used, and in the range $50^{0}C$ to $150^{0}C$ the water was replaced by glycerine. In the temperature range $-60^{0}C$ to room temperature, the adsorbent was thermostatted using a specially designed cryostat. By means of this cryostat the temperature of the adsorption cell could be maintained within $\pm 0.2^{0}C$ for prolonged periods of time. Details of the design of the cryostat are given in appendix 5. The adsorption cell was thermostatted at $-78^{0}C$ by a dry ice-alcohol bath which was constantly stirred. When determining the isobars for the catalysts (section 5.7) it was felt desirable to extend the temperature range covered to below $-78^{0}C$. Because of the unavailability of a contact thermometer operative in the temperature range below $-60^{0}C$, for the points on the isobars measured at $-105^{0}C$, a Sirect Temperature Controller was borrowed. It consisted basically of a platinum resistance thermometer connected to a silicon controlled rectifier bridge and this unit was used in place of the contact thermometer in the cryostat (appendix 5). It was

only possible to obtain the controller for very short periods of time, and thus the contact thermometer was used in conjunction with the cryostat for all temperatures in the range -60°C to room temperature.

For isotherms carried out at liquid nitrogen temperature the following procedure was adopted. The adsorption cell was surrounded by a dewar containing freshly produced liquid nitrogen. Since on standing liquid nitrogen absorbs atmospheric oxygen, oxygen having a higher boiling point than nitrogen, the mouth of the dewar was covered and nitrogen was bubbled through the liquid nitrogen bath at a rate of about 60 bubbles per minute. This procedure resulted in the maintenance of a steady bath temperature.

3.2.11 Measurement of the Temperature of the Adsorbent.

The temperature of the liquid nitrogen bath was measured by means of a gas thermometer (W). The thermometer consisted of a mercury manometer, made from 5 mm i.d. glass tubing, connected to a condensation bulb and to a bulb of volume approximately 250 ml which was in turn connected to a mercury reservoir (section 3.2.3). The thermometer was filled to a pressure of 500 torr with nitrogen. When a liquid nitrogen bath was placed around the adsorption cell and condensation bulb, which were situated adjacent to one another, liquid-vapour equilibrium was produced in the condensation bulb by raising the mercury level in the 250 ml bulb until nitrogen condensed in the condensation bulb. The saturated vapour pressure of the liquid nitrogen in the latter bulb was read on the manometer. From a plot of the saturation vapour pressure of nitrogen against 1/T (Dodge and Davis, 1927) the temperature

of the liquid nitrogen bath was obtained.

Temperatures in the range 0°C to 400°C were measured by means of a platinum resistance thermometer. The thermometer had a resistance of 100 ohms at 0°C. It's shape was roughly cylindrical, being 5 mm in length and 3 mm in diameter. It fitted into the well in the adsorption cell (section 3.2.8). The thermometer was calibrated at the melting point of ice and the boiling points of water and sulphur.

Temperatures in the range -60°C to 0°C were measured by means of a conventional mercury in glass thermometer which was calibrated against a standard thermometer before use. The Sirect Temperature Controller had previously been calibrated by its owner.

3.2.12 Gas Purification Train (Barr and Anhorn, 1949, p. 273).

The gas purification train (G) used to purify tank hydrogen for the reduction of the catalysts consisted of a trap containing previously reduced copper turnings heated to 350°C followed by a trap cooled in liquid nitrogen and then by a trap containing activated charcoal, also cooled in liquid nitrogen. Prior to use the gas train was evacuated for 8 hours and the charcoal trap heated to 250°C in order to activate the charcoal. At the end of this time, pressures in the region of 10^{-5} torr were recorded.

3.2.13 The Adsorbates.

3.2.13.1 Hydrogen.

The hydrogen used in the determination of the adsorption isotherms was Mathieson prepurified grade of claimed purity greater than 99.95%.

It had a quoted oxygen content of less than twenty parts per million. A gas filler and trap (figure 3.8, page 83) was used to transfer the hydrogen from the cylinder in which it was obtained from the manufacturers to the storage bulb on the apparatus. The cylinder was connected to the inlet of the gas filler by means of copper tubing. The gas filler, trap and connecting copper tubing were evacuated, the stopcock above the gas filler was closed and hydrogen allowed to bubble through the mercury in the gas filler at the rate of about 2 bubbles per second for 5 minutes. The trap was then surrounded by a dewar containing liquid nitrogen and the stopcock between the gas filler and the trap opened. Gas then flowed into the gas storage bulb which had been previously evacuated to a pressure of less than 10^{-6} torr. When the bulb was filled to atmospheric pressure, the gas again bubbled through the mercury in the gas filler. The stopcock between the gas filler and the trap was closed and the storage bulb and trap re-evacuated. The bulb was then refilled in a similar fashion to the method outlined above.

3.2.13.2 Krypton.

Krypton was required for the determination of the total surface area of the catalysts. It was obtained from Air Products and Chemicals Incorporated, Allentown, Pennsylvania, U.S.A. in two litre sealed pyrex flasks. A stopcock was sealed onto the flask, and between the flask and stopcock a side arm was welded. A small glass encased iron bar was carefully placed in the assembly which was then sealed onto the apparatus. After the connecting tubing had been thoroughly degassed and evacuated to a pressure of less than

10^{-6} torr, the stopcock was closed and the seal on the flask was broken by hammering the glass-enclosed rod on the seal using a magnet. After an isotherm had been completed most of the krypton used could be recovered by placing a dewar containing liquid nitrogen around the side arm and solidifying the krypton. The vapour pressure of solid krypton at -195^{0}C is approximately 2 torr (Beebe et al, 1945).

3.2.13.3 Nitrogen.

Nitrogen was used in some of the earler isotherms. The storage bulb was filled with high purity grade nitrogen (99.9% purity) which was further purified by passing the gas over reduced copper turnings at 350^{0}C and then through a trap filled with glass beads and cooled to liquid nitrogen temperature in order to remove any oxygen present.

3.2.14 Safety Devices.

The following safety devices were incorporated into the apparatus:

(a) In the event of a water supply failure: A float switch was inserted in series on the water outlet pipe of the diffusion pump. When the water supply failed, the float dropped, closing a mercury switch attached to the float. This completed a circuit through a 'Sunvic' control relay (normally open type), breaking the circuit to the diffusion pump and the heaters.

(b) In the event of a breakage in the apparatus: An LKB Autovac Pirani-type gauge head was attached to the apparatus through a B14 cone and socket joint. This gauge operated an LKB 3294B Autovac

Vacuum gauge (Manufactured by LKB Produkter AB, Stockholm, Sweden). The scale of this instrument was divided into two ranges, 70 torr to 0.1 torr and 0.1 torr to 0.001 torr. A relay, which performs the automatic range switching is equipped with an extra pair of contacts. These contacts were utilized to switch off the diffusion pump and the furnaces in the event of a pressure rise in the system (i.e. above 0.1 torr).

3.3 Preparation and Pretreatment of the Catalysts.

The ground silica support (section 5.1) was prepared as follows. A large quantity of silica tubing, purchased from the British Thermal Syndicate Company Ltd., Wallsend, Northumberland, England, was broken by hand and then ground in a tungsten carbide ball mill for five minutes. The resulting powder was sieved to -120 +150 mesh.

Preliminary experiments showed that mixing a suitable aliquot of the ground silica with enough of a solution of nickel nitrate to just wet the silica and then drying the resulting mixture did not yield a catalyst of uniform impregnation. Although Yates, Taylor and Sinfelt (1964) reported using this method with success, as have other authors, because of the small surface areas of the ground silica-supported catalysts used in the present project, large quantities of catalyst were required. It was felt that the non-uniform impregnation was the result of there being such large quantities of support which were impregnated at once. The problem of non-uniform impregnation was solved by packing the silica in a length of glass tubing, placing enough nickel nitrate solution (of the correct metal ion concentration) in the tube to just wet the silica and allowing the solution to filter through the column. This process took about 2 days for 100 g of silica packed in a 10 mm i.d. column. After impregnation, the impregnated support was removed from the column and dried in an oven at 105 ^{0}C for 12 hours. It was then sieved to -120 +150 mesh.

Two batches, designated batch A and batch B, of each of the 0.25%, 0.51% and 2.20% nickel on ground silica catalysts were prepared. A single batch of the 5% and 20% nickel on ground silica catalysts was prepared. 100 g

of catalyst were prepared for each batch in order to have sufficient catalyst available in case of mishap or the need to repeat any experiments.

50 g of batch A of the 0.25%, 0.51% and 2.20% catalysts were sintered by heating the unreduced catalyst in a current of dry air to a temperature of 500^{0}C for 4 hours.

The sintered catalysts and 50 g each of the unsintered catalysts discussed above, were each reduced for 24 hours at 400^{0}C and a hydrogen flow rate of 200 ml per minute and then degassed for 48 hours at the same temperature. After cooling to room temperature, the 50 g of catalyst were exposed to the air and suitably sized aliquots were taken for the various experiments. The pretreatment to which each catalyst was subjected, therefore, exceeded both in terms of temperature and time the re-reduction and degassing conditions used prior to the determination of each isotherm (section 3.4).

The Cabosil support was obtained from the Cabot Corporation, Boston, U.S.A. It is claimed by the manufacturers to be a finely powdered, non-porous form of silica (340 m^2/g surface area). Because of its high surface area, small (1 g to 2 g) quantities were sufficient for the adsorption measurements. Thus only 10 g of the two Cabosil-supported nickel catalysts were prepared. Their method of preparation and the pretreatment they were subjected to was identical to that of the ground silica-supported catalysts discussed above. Cabosil-supported nickel catalysts of metal concentrations 1.9% and 5.5% were prepared.

3.4 Determination of the Isotherms.

Prior to the determination of each of the hydrogen and krypton isotherms the following standard procedure was adopted. The gas purification train was evacuated and the charcoal heated to 250^{0}C for eight hours. The adsorption cell was then evacuated for one hour at room temperature. Dewars containing liquid nitrogen were placed around the traps of the gas purification train, and hydrogen flowed through the gas train and over the adsorbent at a flow rate of 200 ml per minute. The adsorption cell furnace was switched on and after one hour the required reduction temperature (section 5.3) of 370^{0}C was reached. Hydrogen was flowed through the adsorbent for a further twelve hours, the temperature being held constant at 370^{0}C. Thereafter, the hydrogen flow was stopped and the adsorption cell was evacuated for 24 hours at the same temperature. At the end of this period of time, pressures of less than 10^{-6} torr were recorded in the tubing above the adsorption cell. The adsorption cell furnace was then allowed to cool to the required temperature.

Because of this lengthy preparative period and the fact that 1 to 2 days were required for the actual determination of the isotherm, 3 to 4 days were required for the complete determination of each isotherm.

3.4.1 Hydrogen Isotherms.

After the catalyst pretreatment procedure discussed in section 3.3, an aliquot of the batch reduced catalyst was placed in the adsorption cell, and re-reduced and degassed by the method described in section 3.4. In order to reduce the errors in the amounts of gas adsorbed (appendix 3), approximately

7 g of adsorbent were used. The adsorption cell was allowed to equilibrate for one hour at the isotherm temperature before the start of an isotherm. Thereafter stopcocks 2, 3, 5, 6 and 7 were closed. Adsorbate at a previously estimated pressure was admitted to the low pressure McLeod gauge through the gas pipette (P). With stopcock 2 closed, the pressure of the hydrogen was measured. The mercury level in the McLeod gauge was set just below the cut-off point. Stopcock 6 was opened and the adsorption of hydrogen began. It was determined in preliminary experiments that in 1.5 hours equilibrium was attained. Therefore, when 1.5 hours had elapsed stopcock 6 was closed, and the equilibrium pressure measured with the McLeod gauge. A second aliquot of gas was admitted to the McLeod gauge through the gas pipette and the new pressure read on the McLeod gauge. Stopcock 6 was opened and adsorption begun to give the second point on the isotherm. In the same way, aliquots of gas were added until the equilibrium pressure in the adsorption cell was approximately 1.5 torr, the largest pressure measurable on the low pressure McLeod gauge. Stopcock 4 was closed after the equilibrium pressure measurement had been made, and stopcock 3 was opened. An aliquot of gas was added to the high pressure McLeod gauge. The pressure of the gas was measured and the isotherm was continued as before.

When an aliquot of gas was added to a McLeod gauge, the pressure was read after one minute in order to allow the system to come to equilibrium. The mercury level in the gauges was always carefully set to the same position after each pressure reading in order to maintain constant volume conditions. This was particularly important in the case of the high pressure gauge, the total

volume of which was only about 30 ml.

Equilibrium pressures were corrected, where necessary, for thermal transpiration effects (appendix 2).

3.4.2 Krypton Isotherms.

Approximately two or three grams of catalyst were used in the determination of total surface area by the adsorption of krypton. The catalyst was re-reduced and degassed using the procedure outlined in section 3.4. Thereafter the adsorption cell was thermostatted with a dewar containing liquid nitrogen through which nitrogen gas was bubbled at the rate of approximately one bubble per second.

The method for the determination of the experimental data using krypton as adsorbate was similar to that outlined in section 3.4.1 for the determination of hydrogen isotherms. However, since equilibrium pressures of krypton were only required up to a partial pressure of about 0.35 (which was found to be the upper limit of linearity of the BET plot (section 2.2)), only the low pressure McLeod gauge was required for the determination. The estimation of p_o for krypton (section 2.2) was carried out as follows. Using the gas thermometer (W), the value of p_o for nitrogen at the temperature of the liquid nitrogen bath was determined (section 3.2.11). The value of p_o for krypton was then obtained indirectly using an extrapolated plot of log p of krypton versus 1/T (Meihuizen and Crommelin, 1937; Keeson et al, 1935), superimposed on a plot of log p of nitrogen versus 1/T (Dodge and Davis, 1927) over the temperature range -203°C to -188°C. To determine the p_o value for liquid krypton, the

value of 1/T for p_o (nitrogen) was located on the graph and a vertical line drawn to intersect the log p versus 1/T curve for liquid krypton. The ordinate of the point of intersection represented the value of p_o for liquid krypton at the thermostat bath temperature.

3.4.3 Nitrogen Isotherms.

Nitrogen was used as adsorbate in some of the earlier isotherms measured using various forms of silica as adsorbent (section 5.1). The determination of these isotherms was carried out as follows. The adsorption cell was charged with about 0.5 g of adsorbent and sealed onto the apparatus. The adsorbent was degassed by heating at 370^{0}C and evacuating for twelve hours. At the end of this period the residual pressure in the apparatus was of the order of 10^{-6} torr.

A suitable quantity of nitrogen was admitted to the gas burette from a storage bulb through stopcock 9, stopcocks 2, 3, 4, 7 and 8 being closed, and stopcocks 6 and 1 open. The stopcock to the adsorption cell manometer was also open (section 3.2.1). The mercury level in the gas burette manometer was adjusted to the reference mark and the pressure, volume and temperature of the gas in the gas burette noted. With a liquid nitrogen bath in place around the adsorption cell, stopcock 1 was closed and stopcock 2 was opened and then closed. The pressure, volume and temperature of the gas remaining in the gas burette was noted. The mercury level of the adsorption cell manometer was set on the reference mark, and when no further decrease in pressure was noted, the equilibrium pressure of the gas in the adsorption cell was measured

on the manometer. A second dose of gas was then admitted to the adsorption cell through stopcocks 1 and 2 and the above procedure repeated. Data were obtained in this fashion until a partial pressure of approximately 1.0 was obtained.

The desorption branch of the isotherm was determined in a similar fashion. Here, however, gas was removed from the adsorption cell by decreasing the pressure in the gas burette until it had a lower value than the gas in the adsorption cell and then opening stopcocks 1 and 2 and allowing some of the gas in the adsorption cell to expand into the gas burette. Because of the limited capacity of the gas burette it was necessary at some stage during the adsorption isotherm to refill the gas burette with nitrogen and during the measurement of the desorption isotherm it proved necessary to occasionally evacuate the gas burette in order to be able to decrease the pressure in the adsorption cell.

For these isotherms, the adsorption cell dead space was that volume bounded by stopcocks 2, 3, 4, 6, 7 and 8. It was calibrated with helium by expansion of the gas from the gas burette.

CHAPTER 4

TECHNIQUES FOR THE CHARACTERISATION OF THE CATALYSTS

4.1 Chemical Analysis of the Catalysts.

Initially an attempt was made to estimate the amount of nickel present in a catalyst by means of colorimetric analysis. The method used was that described by Belcher and Nutten (1960). Briefly the method consisted of adding bromine water to a nickel solution in which the nickel concentration was in the range 1 to 10 ppm. Ammonia solution (S.G. = 0.910) was added until the colour of the bromine water was discharged. A slight excess of ammonia was added, followed by 0.5 ml of a 1% ethanolic solution of dimethyl glyoxime. The resulting solution was diluted to 100 ml and the optical density measured on a Unicam SP600 spectrophotometer. Measurements were always made a fixed time after adding the dimethyl glyoxime. However, the nickel dimethyl glyoxime tended to precipitate out in the higher concentration solutions and reproducible results could not be obtained. Figure 4.1 shows the results of replicate determinations of the optical densities of a series of gravimetrically standardised nickel solutions. The optical density against nickel concentration curve could not be used to determine the nickel concentrations of unknown nickel solutions since the curve was not reproducible. The method advocated by Snell and Snell (1949) was then tried. It was substantially the same as that of Belcher and Nutten but experimental conditions and reagent concentrations differed slightly. Although no traces of a nickel dimethyl glyoxime precipitate were observed, reproducible optical densities of standard solutions were not obtained with this procedure (figure 4.2).

Because of the apparent unsuitability of these colorimetric methods, a volumetric method of analysis, using ethylenediaminetetraacetic acid (EDTA), was

IRREPRODUCIBILITY :

SPECTROPHOTOMETRIC DETERMINATION OF NICKEL

FIG. 4.1.

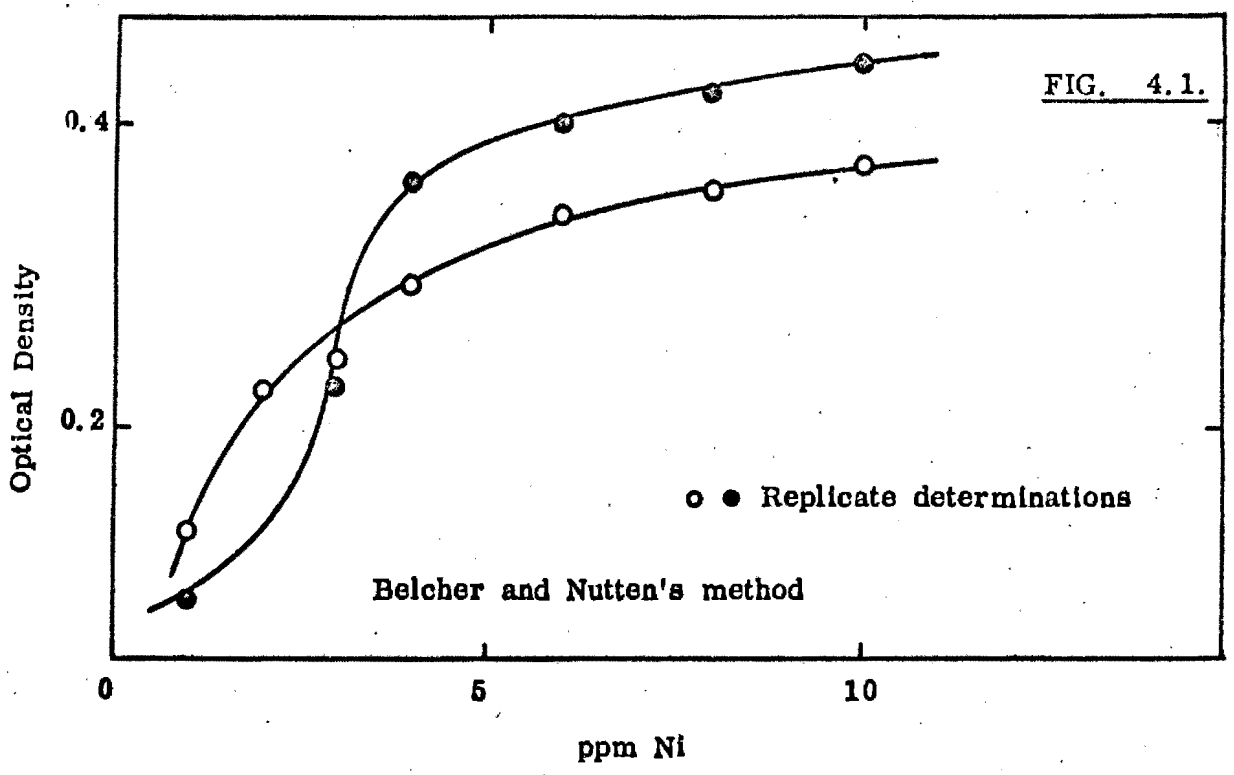

FIG. 4.2.

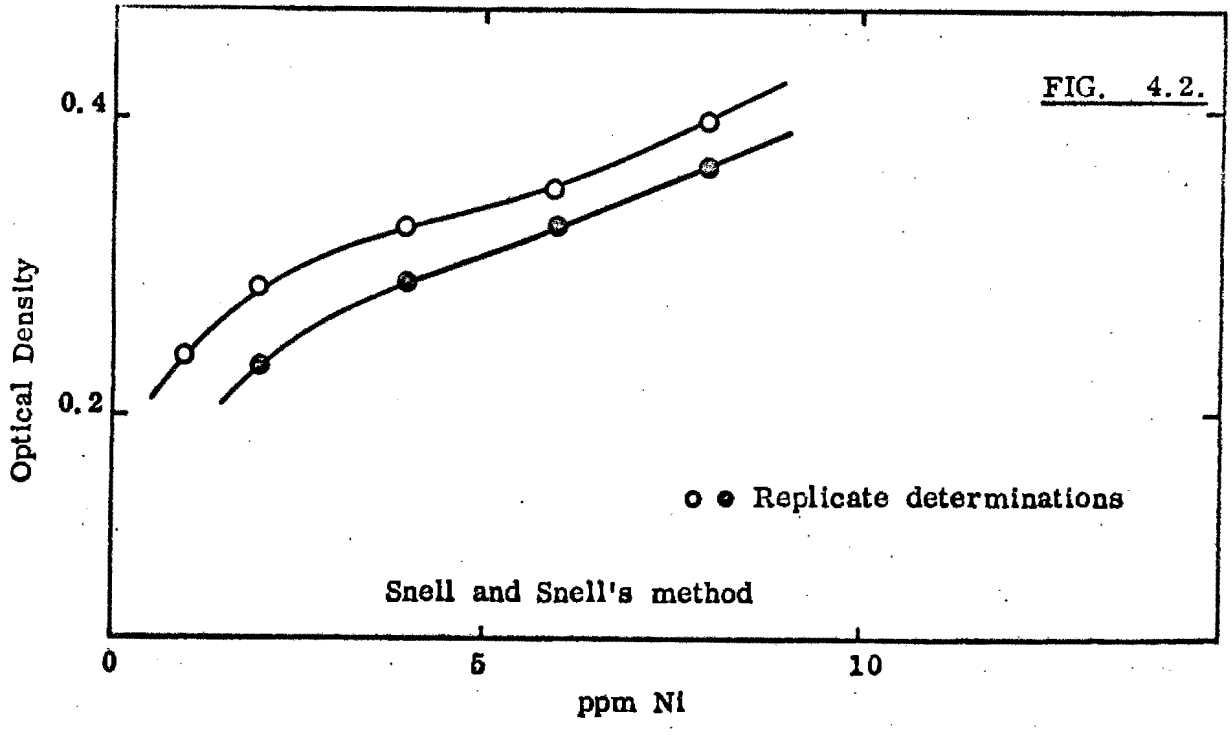

investigated. Outlined below is the method used, which is basically that described by Wilson and Wilson (1962). - To an acidic solution of nickel, 0.1 g of tartaric acid was added. The solution was made alkaline with an ammonia solution of S.G. 0.910, an excess of 5 ml being added. 0.2 g of murexide indicator, made by grinding together 0.2 g of murexide and 100 g of sodium chloride in a mortar, was added, and the resulting solution titrated against a previously standardised solution of EDTA. . . Heating the solution to 50^{0}C prior to titration and the use of a freshly prepared indicator markedly improved the detection of the end-point (Irving, 1967). Replicate determinations of the concentrations of nickel solutions which had been previously standardised gravimetrically using dimethyl glyoxime yielded results which differed from the concentration determined gravimetrically by less than 1%.

The catalysts were prepared for analysis as follows. Enough catalyst was weighed out to give an EDTA titre of about 20 ml. Duplicate samples were placed in platinum crucibles. Sufficient water was added to the samples just to wet them. 2 to 3 drops of concentrated sulphuric acid and 3 ml of concentrated hydrofluoric acid were added to the samples which were then heated on a hot plate. Addition of hydrofluoric acid was continued in small quantities until the sample had completely dissolved. The solution was then washed out of the crucible, made up to about 20 ml and titrated, as described above, against EDTA to a magenta end-point.

4.2 Optical Microscopy.

Catalysts were viewed using a Leitz Ortholux Optical Microscope fitted with an Ultropak incident light illuminator. Samples could be viewed either by reflected or by transmitted light. Two objectives were used: U.O. 6.5 and U.O. 11, with 10x and 25x eyepieces. Coupled with a magnification factor of 1.25x, visual observations under magnifications of 81, 138, 203 and 344 could be made.

The catalysts were viewed with the microscope in an attempt to ascertain whether or not impregnation had been uniform and to ensure that the catalysts did not consist of particles of nickel between silica particles. The maximum resolution obtainable with the objectives available was 2×10^{-3} mm. At this resolution all the catalyst particles appeared to be of uniform texture and no particles of a grossly different nature could be observed between the silica particles. In order to get an idea of what inter-silica-particle nickel might look like, some of the samples studied were doped with finely ground nickel particles, the concentration of such particles being of the same order as the metal concentration in the catalyst. In these cases the nickel particles, which were about 0.01 mm in diameter, were clearly visible. Thus it appeared that no inter-silica-particle nickel particles of a size greater than 2×10^{-3} mm, the maximum resolution of the microscope, were present. Care was taken to view a number of samples of each catalyst to ensure that the samples observed were representative of the catalyst.

4.3 Electron Microscopy.

4.3.1 The Use of the Electron Microscope in the Study of the Surfaces of Solids.

In the last 30 years, the electron microscope has become an important research tool in the investigation of the micro-structure of matter. The microscope itself follows the general lines of the optical microscope: a condensing system projects illumination onto the specimen which lies in the focal plane of the objective, and a subsequent lens provides additional enlargement. The differences of principle and construction follow from the essentially different nature of the illuminations used in optical and electron microscopy. Light, an electromagnetic wave motion, is focused by the fields within certain solid or liquid aggregations of particles (transparent media). Electrons, a particulate radiation, are focused by electromagnetic or electrostatic fields of appropriate distribution, and are scattered by other particles. Hence the electron beam suffers from the disadvantage that its path must be in high vacuum. As in the case of light, the phenomenon of scattering is the primary source of image contrast: various parts of the specimen will appear light or dark, depending on differential scattering of electrons. Micrographs of graded density are thus obtained, not merely silhouettes, provided that the specimen is below a thickness of about 3000 Å. Above this thickness most material becomes opaque to the electron beam.

The great value of the electron microscope is that a vastly superior resolution can be obtained with the instrument as compared to using an optical microscope. Resolving power, expressed say as the number of lines per cm

that can be observed as discreet lines, is inversely proportional to the wavelength of the illumination used (Shillaber, 1944). Because of the very much smaller wavelength associated with the electron beam as compared to that of light, superior resolution is achieved.

For materials which are impenetrable to the electron beam, replica techniques have been devised for studying surface structure. Plastic films, such as nitro-cellulose and Formvar, evaporated films of silica and, more recently, carbon have been used. Most replica methods are limited primarily by self-structure to resolutions of the order of 200 Å. However the carbon replica method devised by Bradley (1954) appears not to suffer from this defect right down to resolutions of about 10 Å. The carbon is usually evaporated from an arc and is deposited either directly onto the specimen or onto a thick primary replica of plastic. The carbon film, usually about 100 Å in thickness, is then floated off in a suitable solvent, and picked up on an electron microscope sample holder.

An alternative method of studying materials which are greater than 3000 Å in size is by cutting very thin sections of the sample (ultramicrotome sections). This is a well established technique, and the knife used for cutting is usually made either of specially cut glass or diamond.

The greatest appeal, therefore, of the electron microscope technique in the study of supported metal catalysts is that the investigator can, under favourable conditions, "see" the metal particles which are the seat of catalytic activity. Thus he can determine the distribution of metal particle sizes, calculate the average particle size, and can even discover whether these

particles are randomly distributed or whether they are concentrated in clusters or piles. If the particles are large enough, it may even be possible to determine their shape and crystalline form. The greatest danger, however, is that the sample being studied is not truly representative of the original sample under study, for the amount of sample examined in the microscope is very small. Thus pictures of several samples should be taken. The reproducibility among the pictures can then be used to gauge whether or not the samples are representative of the bulk material.

4.3.2 Examination of Catalysts under the Electron Microscope.

As outlined in section 4.3.1, for viewing by transmission electron microscopy, materials should not be thicker than about 3000 Å. Since the catalyst particles studied in this thesis had diameters at least a factor of 100 greater than this maximum value, alternate methods of studying the surfaces of the particles were investigated.

Because of the relative hardness of the silica particles (hardness 7 on the Mohs scale), the particles cannot be cut into ultramicrotome sections using a glass knife. To make such sections a diamond knife is necessary, but the unavailability of such a knife precluded the use of this method of preparing the catalysts for study using the electron microscope.

The next method tried was that of producing carbon replicas of the catalyst surfaces. Two major problems were encountered in the preparation of these replicas. Firstly the catalyst particles were so small that it was difficult to spread them out on a flat surface prior to evaporation of carbon to

form the film, for simply spreading them onto a glass slide and then tapping the excess solid off may well leave the smaller particles on the slide, thus leading to a non-representative sample. Secondly, after a layer of carbon had been evaporated over the particles of catalyst, it was necessary to dissolve away the particles using some suitable solvent. The only solvent which will dissolve silica at room temperature is hydrofluoric acid. This solvent, however, attacks most of the materials on which the catalyst could be supported during deposition of the carbon film. Polythene, polyvinyl chloride and similar materials are not attacked, and so supporting the catalyst on a piece of polyvinyl chloride during evaporation was tried. However the film of carbon could not be freed from the plastic, even after prolonged soaking in hydrofluoric acid. The very thin glass slides used as microscope slide cover slips (thickness about 0.1 mm) were then used as a support of the catalyst particles. When the glass slide, catalyst and carbon film were immersed in 40% hydrofluoric acid the glass slide dissolved completely in about two hours and the carbon film floated free. After allowing a further two hours for complete dissolution of the catalyst particles, the hydrofluoric acid was carefully replaced by water by pipetting out the acid and adding water until the pH of the liquid was 7. Sections of the carbon film were carefully lifted off the liquid by means of the grid used to support the sample in the electron microscope. The film and grid were then allowed to dry. Carbon replicas of both the catalyst and the pure support material were made. However no marked areas corresponding to positions occupied by nickel crystallites on the original catalyst could be discerned, and so, after a number of attempts at preparation of such replicas, this technique,

too, was abandoned.

It was then decided to try and find either catalyst particles small enough to transmit the electron beam or else to try and look at the edges of catalyst particles which may, for example, be wedge shaped, and thus the thin edges of the wedges would be thin enough to obtain a transmission electron micrograph. 0.1 grams of catalyst were suspended in a sample tube containing 10 ml of triple-distilled n-butyl alcohol. The tube was sealed with a polythene stopper and shaken. It was then allowed to stand for some hours. A drop of the liquid from the top of the tube was placed on an electron microscope grid and allowed to dry. It was then viewed in a Philips EM300 electron microscope.

Five or six electron micrographs of each catalyst were obtained. The metal crystallites were clearly visible as dark patches on a lighter background. In order to measure the particle sizes of the metal particles, the electron micrograph negatives were enlarged ten times and the dimensions of at least one hundred metal crystallites determined to the nearest millimeter using a pair of dividers and a steel rule. (The overall magnification of the enlarged negatives was of the order of 600,000 times). In the case of non-spherical crystallites, a mean value of the length and breadth of the crystallite was taken as its diameter. Histograms of the metal crystallite size distribution were plotted. The results are presented in section 5.12. An example of one of the micrographs is shown in figure 4.3.

FIG. 4.3

ELECTRON MICROGRAPH

0.25% NICKEL ON GROUND SILICA CATALYST (BATCH A)

MAGNIFICATION: ~200,000x

4.4 The Determination of Average Crystallite Size by X-ray Diffraction Line Broadening.

4.4.1 Theory.

If an extremely narrow X-ray beam is diffracted by a large, perfect crystal which is rotated, each diffracted beam will have a definite orientation with respect to the original X-ray beam (as predicted by the Bragg equation), and the diffracted beams will have widths only a few seconds of an arc in thickness. However a crystal smaller than 10^{-5} cm in diameter will not behave in this fashion toward the X-ray beam. Now an optical diffraction grating with comparatively few lines gives rise to a more diffuse diffracted beam than a grating with a large number of lines (Halliday and Resnick, 1960), and this same effect is observed with small crystals in their behaviour toward the X-ray beam, for in comparison to crystals of size greater than 10^{-5} cm, such crystals have relatively few lattice planes from which reflection of the X-ray beam occurs. The resulting broadened beam can be represented graphically as a plot of intensity against twice the Bragg angle (γ), as shown in figure 4.4.

Scherrer (1918) showed that the mean dimension, d, of the crystallites composing a powder is related to the pure X-ray diffraction line broadening, β, by the equation

$$\beta = \frac{C_s \lambda}{d \cos \gamma} \qquad 4.4.1$$

where C_s is a constant approximately equal to unity and related both to the shape of the crystallites and the way in which β and d are defined, β has

FIG. 4.4.

IDEAL X-RAY DIFFRACTION PROFILE

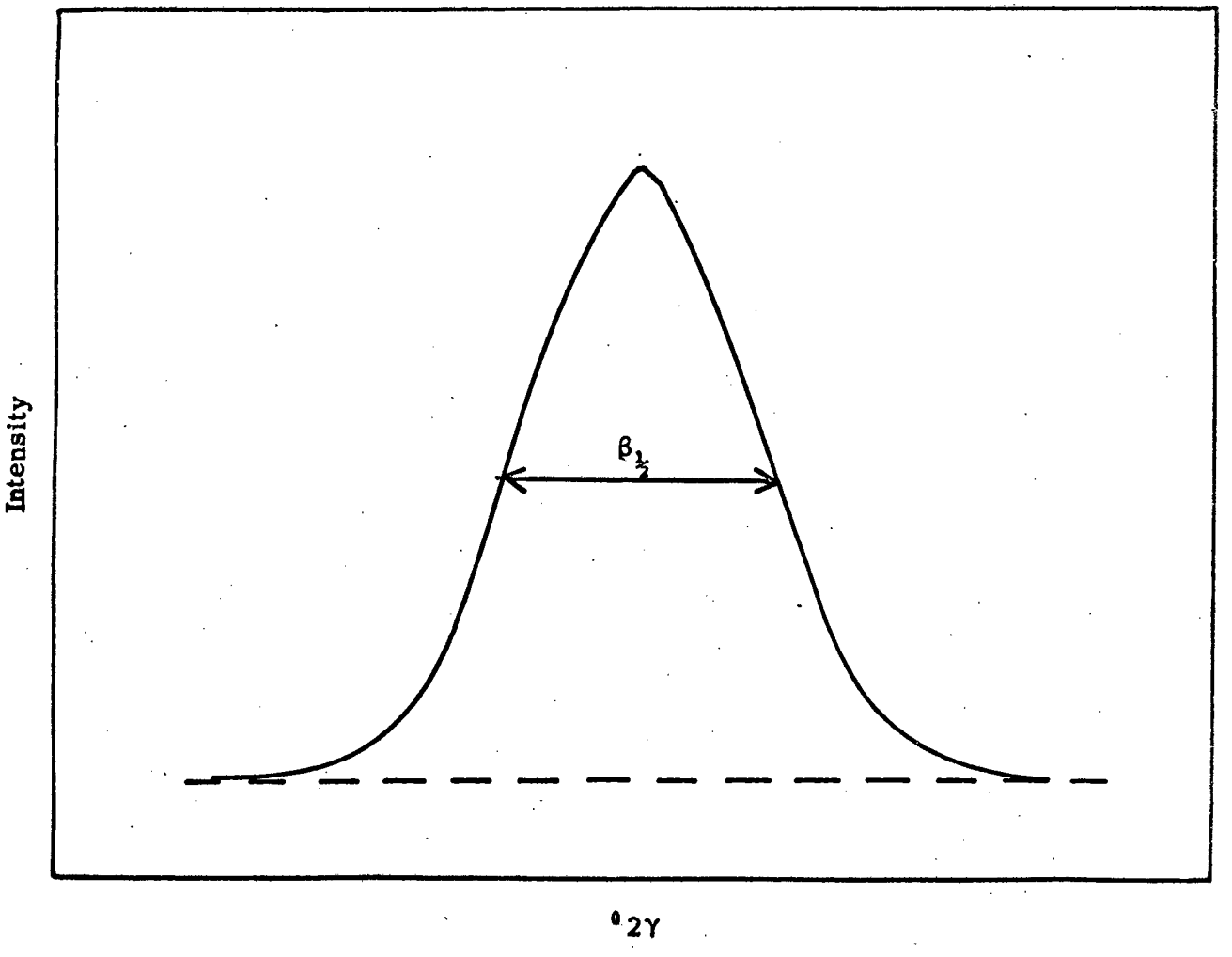

been defined in two ways. It can be defined as the angular width between the points at which the intensity of a line falls to one half of its maximum value ($\beta_{\frac{1}{2}}$, figure 4.4). Alternatively, after the manner of Laue (1926), it can be defined as the area of the angle-intensity curve (figure 4.4) divided by its height (β_I). $\beta_{\frac{1}{2}}$ is referred to as the half-height breadth and β_I as the integral breadth. When using the half-height breadth, the constant C_s is usually given the value 0.9. This is strictly only valid when the particles are spherical, belong to the cubic system, and are uniform in size. However, in any given specimen, the shape and size distributions of the particles are usually not known and so at best equation 4.4.1 yields only approximate crystallite sizes. In relation to experimental errors and other uncertainties, no serious error is incurred in accepting the value of 0.9 (Bunn, 1961) and in fact there is only a small dependence of C_s on the crystallite shape (Klug and Alexander, 1954). If β_I is used, the constant is somewhat larger. Work by Patterson (1939) and Stokes and Wilson (1942) point to a value of between 1.0 and 1.3 for various reflecting planes of differently shaped crystals. However when the shape is not known, a value of 1.15 is generally used (Bunn, 1961). Since $\beta_{\frac{1}{2}}$ can more easily, and usually more accurately, be measured in experimental work (Klug and Alexander, 1954), it is the definition commonly used.

When the profile of a diffracted beam from crystals of size greater than 10^{-5} cm is obtained, it is found to have a finite breadth, b, called the instrumental broadening. b results not only from the divergence of the X-ray beam after it leaves the collimating system of the X-ray generator, but also

from the absorption of the beam in the sample. Thus the breadth, B, of a profile as actually measured under a given set of experimental conditions is made up not only of the broadening, β , due to small size of crystallites in the sample, but also of a contribution due to the instrumental broadening, b. The magnitude of b is usually estimated by measuring the line breadths of one or more standard materials of particle size greater than 10^{-5} cm. Brooks and Christopher (1968), for example, determined the natural instrumental line breadths of their diffractometer by measuring the line breadths of two materials, namely the (111) peak of coarse nickel powder, and the (220) peak of sodium chloride. It is essential to ensure a uniform sample thickness for both the reference material and the sample giving the broadened profile so that absorption in the specimen will be the same in both cases.

Since instrumental broadening varies with the Bragg angle, it is necessary to choose a reference substance which yields a strong diffraction line at about the same Bragg angle as the material under investigation. If this is not possible, a curve of breadth, b, against γ must be plotted and by interpolation the value of b at the required Bragg angle read off.

Apart from the above considerations, line breadths may still be affected by one source of error, namely, neglect of the broadening due to separation of the $K\alpha_1\alpha_2$-doublet of the X-radiation. X-rays from a copper source consist of a single peak ($K\beta$) at a wavelength of 1.39217 Å, a doublet ($K\alpha_1\alpha_2$) at wavelengths 1.54051 Å and 1.54433 Å as well as a low energy continuous band of radiation covering the wavelength range from about 0.25 Å to 1.20 Å. The use of a nickel filter eliminates all the radiation bar the $K\alpha_1\alpha_2$-doublet (Bunn,

1961). At low Bragg angles, where the angular separation of α_1 and α_2 is small, the amount of broadening is inconsequential, but as the Bragg angle increases, the effect becomes progressively more important. If the angle is sufficiently large, the problem can be overcome by measuring the separate profile of either an α_1 or an α_2 maximum. However, in between these two extremes, $K\alpha_1\alpha_2$-doublet broadening should be taken into account in crystallite size measurements.

Jones (1938) derived a correction curve in which b/b_o is depicted as a function of D/b_o, where b_o is the measured breadth of an X-ray diffraction line, D, is the angular separation of the $K\alpha_1\alpha_2$-doublet in degrees 2γ for the particular value of 2γ at which the line has its maximum, and b is the corrected value of the line breadth. (Of course the curve applies equally well to breadths, B, of broadened profiles, furnishing B/B_o as a function of D/B_o). Obviously the narrower an X-ray line, the more important the $K\alpha_1\alpha_2$-doublet broadening will be.

In his original investigation, Scherrer (1918) proposed that the actual line broadening due to the small crystallite size was related to the observed line broadening and the instrumental broadening by the equation

$$\beta = B - b \qquad 4.4.2.$$

However this equation has been found to have no general validity (Klug and Alexander, 1954). Although the ideal method of obtaining β is by a Fourier analysis of the line shape (Stokes, 1948) it is common practice to use the relationship,

$$\beta^2 = B^2 - b^2 \qquad 4.4.3$$

proposed by Warren (1941) or the correction curves derived by Jones (1938). The latter two methods give very similar results (Klug and Alexander, 1954).

Thus it is possible to measure the average metal crystallite size in supported metal catalysts by means of X-ray diffraction line broadening. In general estimates to within about 10% can be made using this technique (Klug and Alexander, 1954) although in unfavourable situations (such as at low metal concentrations) the uncertainties in measuring the breadth of the X-ray line can cause larger errors.

4.4.2 Experimental Procedures.

Nickel powder sieved to -120 +150 mesh was chosen as the reference substance from which the natural instrumental line broadening of the diffractometer was determined. All samples used had approximately the same weight (1 g) and were pressed into a rectangular hole in the sample holder (a 3 mm thick piece of stainless steel) in such a way that the sample surface presented to the X-ray beam was smooth to the naked eye.

A 1 kilowatt Philips X-ray Diffractometer and a proportional counter with discriminator were used to obtain the X-ray peaks. Nickel-filtered copper radiation was used. The various instrumental settings were obtained by trial and error, emphasis being placed on a slow scanning rate for maximum precision. Scanning rates of 0.25^0 2γ per minute and a chart speed of 800 mm per hour were used throughout the work.

In common with the practice suggested by Klug and Alexander (1954), the

X-ray line broadening was measured as $\beta_{\frac{1}{2}}$, the half-height breadth. Warren's method of computation of $\beta_{\frac{1}{2}}$ from the measured line breadth and the breadth due to instrumental broadening was adopted.

Sample calculations were carried out on the catalysts giving the broadest and the narrowest profiles in order to determine the probable extent of error incurred by not applying a correction for the $K\alpha_1\alpha_2$-doublet separation. Using the correction curve of Jones (1938), the measured breadths of the diffraction lines of the catalysts (B_o) and the nickel standard (b_o) were converted into corrected breadths (B and b) (section 4.4.1). Using equation 4.4.3, $\beta_{\frac{1}{2}}$ for each catalyst was computed and the value obtained compared with the value obtained when the correction for $K\alpha_1\alpha_2$-doublet separation was neglected. In the case of the 0.25% nickel sample, the error was less than 1%, and in the case of the 2.2% nickel sample about 4%. Since these errors are well within the probable experimental error (Klug and Alexander, 1954), the results presented in this thesis are uncorrected for the doublet separation.

Because the X-ray diffractometer could only be used for limited periods, the diffraction profiles obtained were determined over the course of a number of widely separated days. In order to check the accuracy of reproduction, on each separate occasion the profile of the 0.25% nickel catalyst was determined. The instrumental broadening was determined using the pure nickel sample at the start and the end of each day's work. No significant variations in measured peak width were obtained in either case.

Each peak was determined at least twice and a mean value of the peak width was chosen for computation purposes. The peak widths at half peak height

were measured to 0.01 cm using a travelling microscope. The results obtained are presented in section 5.11.

4.5 Estimation of the Fraction of the Metal in the Form of Metal Atoms in the Catalysts.

Because of the possibility that a fraction of the metal in a supported metal catalyst may not be in the form of metal atoms (section 1.2), it is desirable to have a technique which enables one to determine this fraction of non-metallic nickel. Carbon monoxide reacts with metallic nickel to form nickel tetracarbonyl, and this reaction has been used to determine the fraction of nickel in the form of nickel atoms supported nickel catalysts.

Swift, Lutinski and Kehl (1965) claim that treatment of silica-supported nickel catalysts with carbon monoxide results in the complete removal of all the nickel present in the catalyst, provided treatment is continued for a sufficient period of time, thus implying that all the nickel is present in the form of metal atoms in silica-supported catalysts. However they published no experimental results to support this claim, nor did they quote a reference to any such work. Their own study indicated that as the fraction of alumina in a silica-alumina support was increased, the fraction of nickel that could be removed by carbon monoxide treatment decreased. They also found that after treating a sample of reduced nickel powder with carbon monoxide for six hours, only 5.5% of the metal could be removed. Swift, Lutinski and Tobin (1966) studied the removal of nickel from alumina-supported catalysts. The fraction of nickel which could be removed appeared to be related to the surface area of the particular alumina support used, suggesting that chemical association with the support was responsible for the non-reactivity of the remaining metal. They found that four hours sufficed for the removal of all metal that could be removed with

be correct. Reactor temperatures of about 80°C, in common with that used by Swift, Lutinski and Kehl (1965) had been used. Trout (1937) and other authors give the decomposition temperature of nickel carbonyl as between 50°C and 60°C, and it was thought that some of the carbonyl being formed may have been decomposed in the reactor, and hence was not being swept away by the carbon monoxide stream into the decomposition chamber, which was thermostatted at 300°C. Therefore reactor temperatures in the range 20°C to 80°C were tried, as well as temperatures above 80°C, but in all cases substantially less metal was removed than the amount removed at 80°C.

It is possible that impurities in the carbon monoxide were responsible for the failure to remove 100% of the nickel from the sample of nickel powder. However since Swift, Lutinski and Kehl (1965) had also found that 100% conversion of nickel powder to nickel carbonyl did not readily occur, and in view of their claim that this was possible using impregnated nickel-silica catalysts, it was decided to investigate the reaction over the catalysts studied in this thesis before looking for any further impurities in the carbon monoxide.

Carbon monoxide, purified by passage through a trap containing copper turnings at 350°C followed by a trap surrounded by a dry ice-alcohol mixture, was flowed over the catalyst sample for 48 hours. The reactor chamber was thermostatted at 80°C. The catalyst sample had previously been reduced in situ for 12 hours at a temperature of 370°C. The amount of nickel decomposed in the decomposition chamber was determined by weighing the chamber before and after deposition of the metal. Using this method approximately 100% of the nickel in ground silica-supported catalysts was found to be removable by carbon

monoxide. Determinations on each catalyst were carried out twice and the average values obtained are listed in table 5.2.

CHAPTER 5

EXPERIMENTAL RESULTS

5.1 Selection of a Suitable Support.

As discussed in section 1.2, the pores of a support may introduce a confounding effect when studying the effect of such factors as average metal crystallite size. Hence it was decided to prepare a non-porous silica for use as a support. The first attempt at preparation was carried out as follows: tetraethylorthosilicate was heated under reflux for 1 hour with a slight excess of dilute hydrochloric acid (one part acid to one part water). After cooling, the white precipitate which separated out was washed with distilled water until the washings were chloride free. The precipitate was then autoclaved for 4 hours at 4 atmospheres pressure. The solid was again washed first with water and then with methanol. The methanol was then removed by heating the sample in an oven at 100^0C. The resulting silica was sieved to -44 to +85 mesh.

Two aliquots were drawn from this batch of silica. The surface area of each aliquot was determined three times using nitrogen as adsorbate (sections 2.2 and 3.4.3). The areas obtained were:

Aliquot 1:	223.9 m^2/g	228.0 m^2/g	227.6 m^2/g
Aliquot 2:	191.4 m^2/g	195.7 m^2/g	192.7 m^2/g.

The good agreement obtained amongst the replicate determinations on each aliquot demonstrated that reproducible results could be obtained using the apparatus. A complete adsorption-desorption isotherm was determined on aliquot 2 of the silica (figure 5.1). It displayed a reversible hysteresis loop. According to Cohan (1938, 1944) and Foster (1932, 1948, 1951) such hysteresis can be attributed to an open pore structure of the adsorbate. It was thought that it

FIG. 5.1.

NITROGEN ISOTHERM : FIRST SILICA PREPARATION

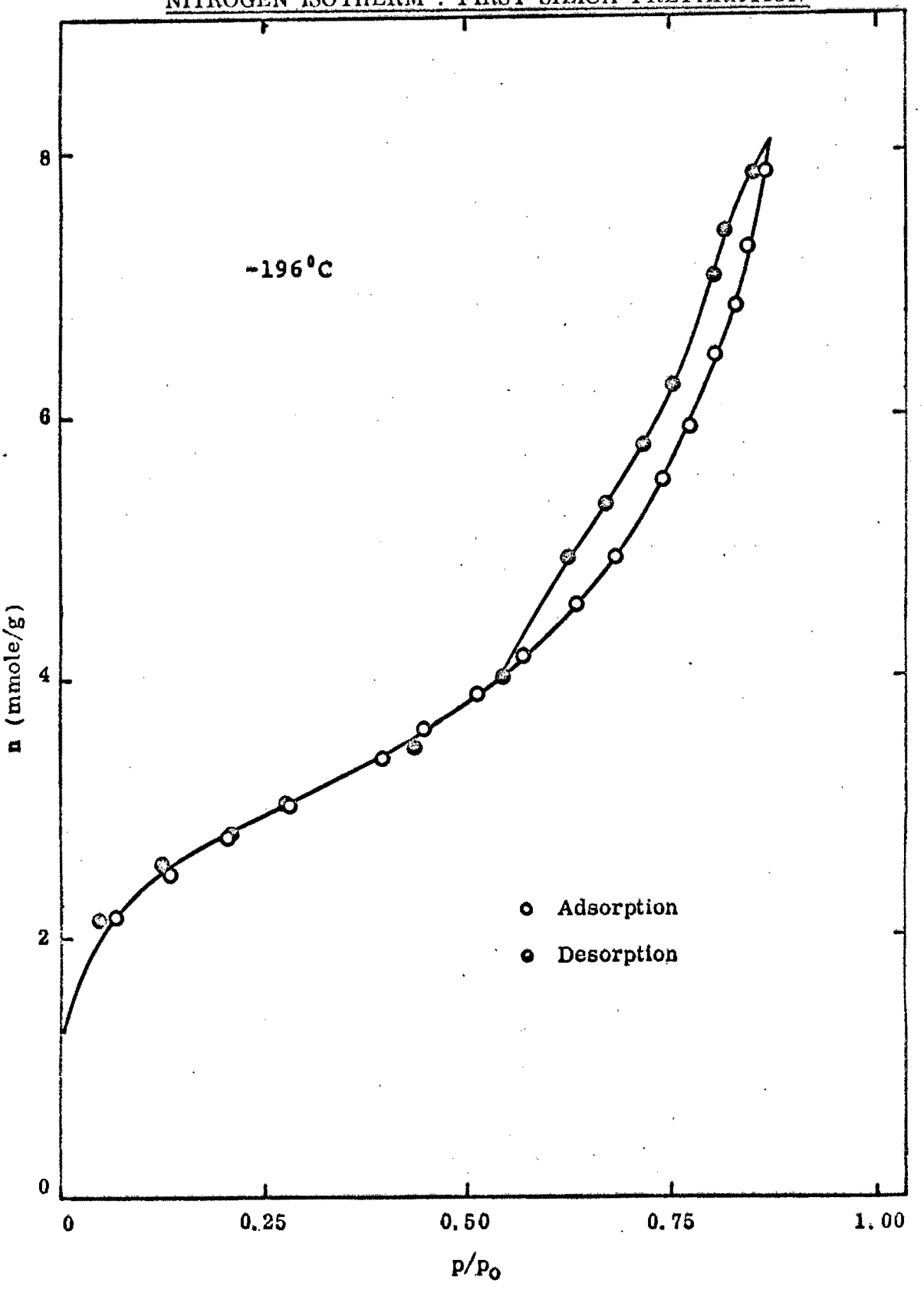

may be possible to collapse this pore structure by cycling several times through a temperature of 573°C, the temperature at which silica undergoes a phase change from alpha-quartz to beta-quartz. The surface areas measured after a variety of such heat cycles are presented in the table below:

TABLE 5.1.

Aliquot Number	Details of Cycling	Resultant Surface Area (m^2/g)
1	Heated for one hour at 600°C.	178.7
2	Heated for one hour at 600°C, cooled and the procedure repeated 5 times.	156.1
3	Heated for one hour at 600°C, cooled and the procedure repeated 10 times.	153.5
4	Same procedure as for aliquot 3.	165.2
5	Heated for 10 hours at 600°C.	166.7

The isotherms obtained on aliquots 2, 3 and 5 each contained an hysteresis loop, and, as before, were type II (figure 2.1) in shape. No marked decrease in surface area (which one would expect on collapse of a porous structure) was observed, and thus the method whereby the silica was prepared was discarded.

Dollimore and Heal (1963) published a method whereby they claim to have produced silica of very low porosity, the diameter of the pores being of the order of 5 Å. Briefly their method consisted of the following: powdered sodium metasilicate was added to a slurry of the cation exchange resin ZEOCARB 225 and water, the pH being adjusted to 2-3. The pH was read continuously on a direct reading pH meter, the addition of silicate being made slowly so that the pH

FIG. 5.2.

NITROGEN ISOTHERM : GROUND SILICA TUBING

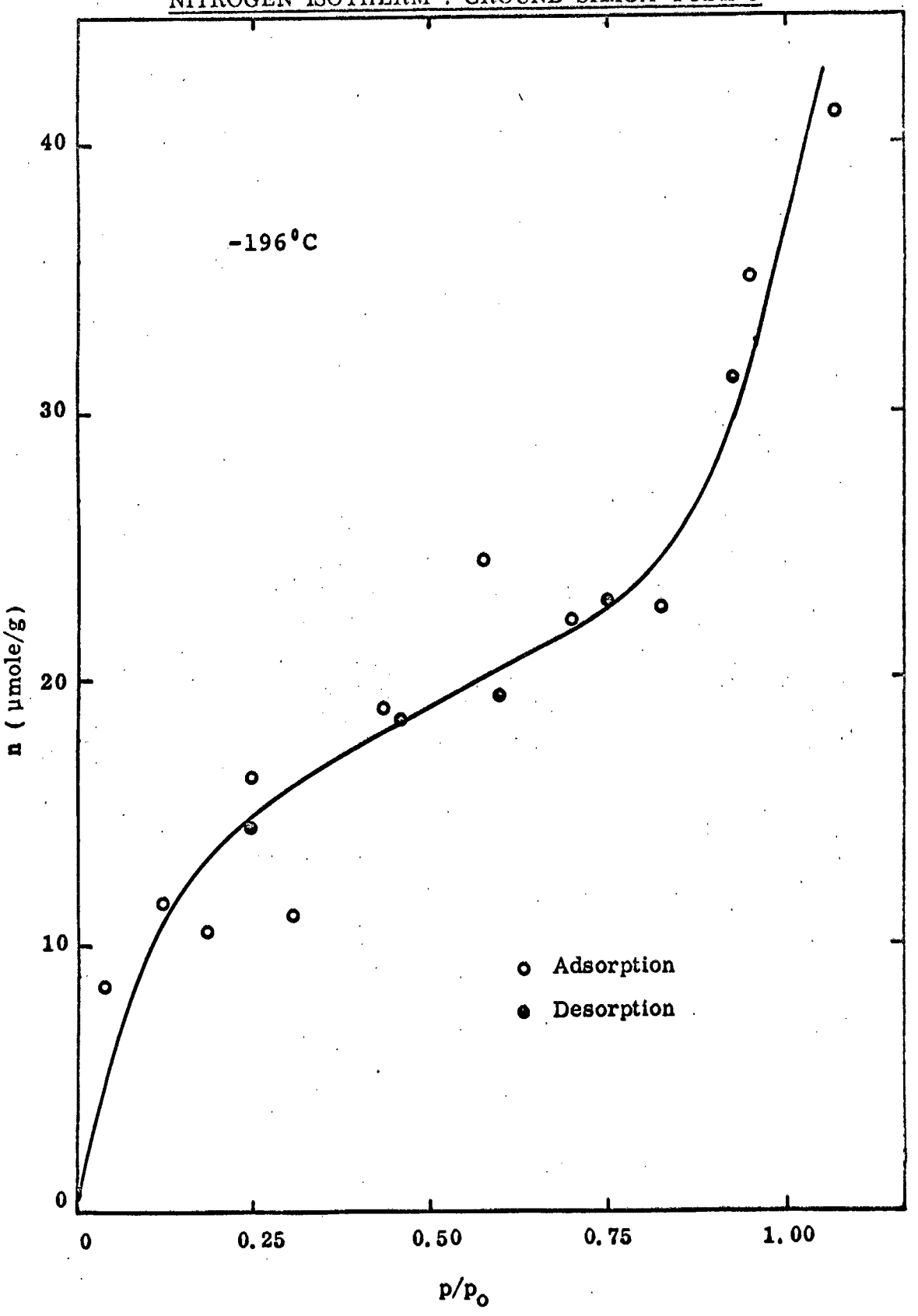

FIG. 5.3.

KRYPTON ISOTHERM : GROUND SILICA TUBING

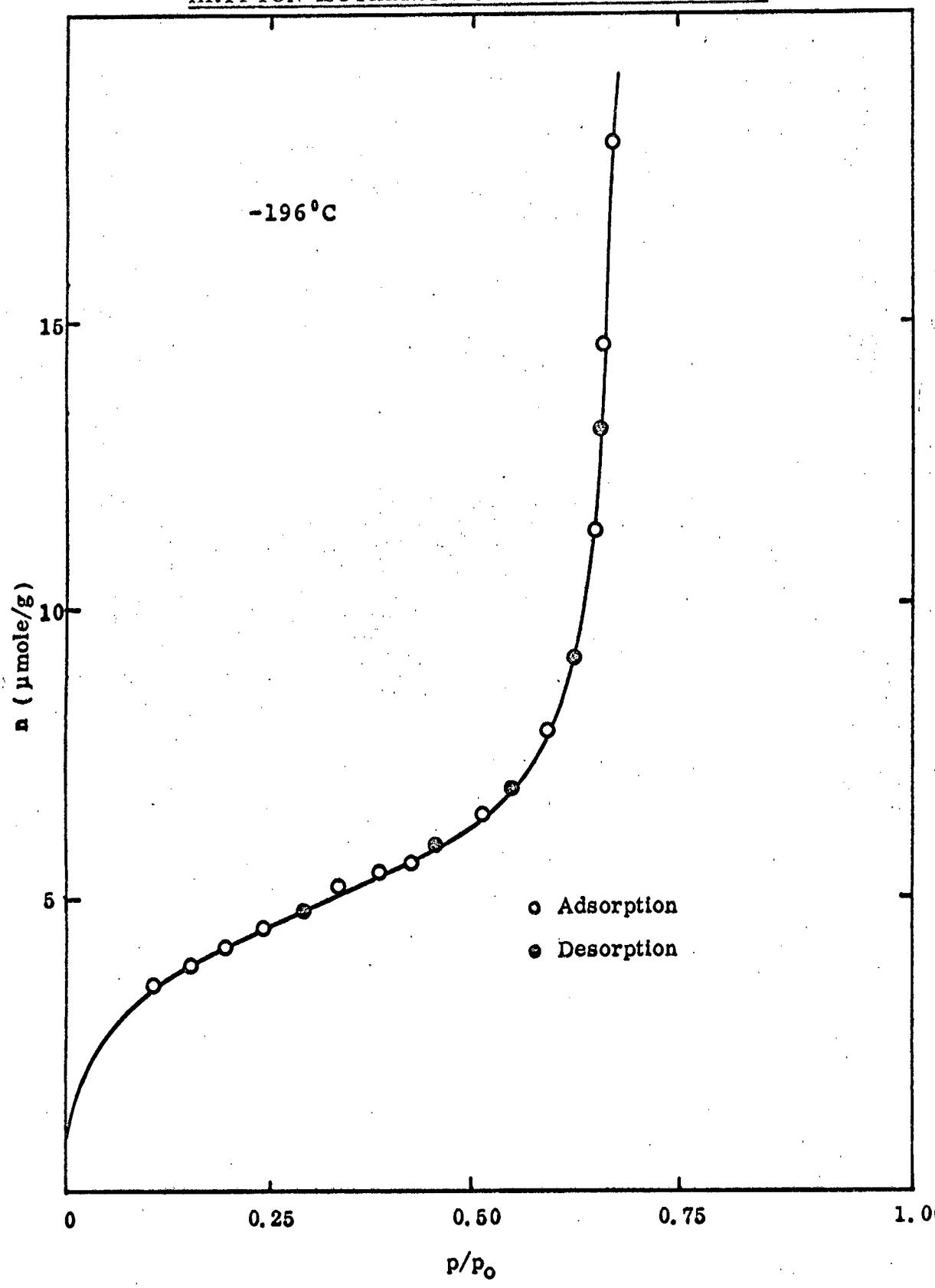

used. An investigation was carried out in order to determine how the equilibration time varied with the initial pressure of krypton for a sample of ground silica of -20 +40 mesh. Using an initial pressure of 0.2 torr, equilibrium was attained in 75 minutes. As the initial pressure was increased, so the time required for equilibration decreased. When an initial krypton pressure of 100.8 torr was used, equilibrium was attained in 6 minutes. As a check two equilibration time curves for the same sample of silica were obtained using nitrogen as adsorbate, one at 110 torr, the other at 0.698 torr initial pressure. In this case, too, the aliquot of adsorbate having the lower initial pressure gave rise to the longer equilibration time (15 minutes as opposed to 5). Because the nitrogen equilibration, especially for smaller initial pressures, was faster than that for krypton, it appeared that either the silica contained pores, the diameter of which approximated to that of the krypton atom, or the diffusion of the adsorbate molecules through the bulk of the powder was responsible for the equilibration times observed.

The following experiment was carried out in order to try and establish which effect was being observed. Samples of the silica were ground to different particle sizes (-20 + 40, -80 + 120, -120 + 150 mesh). Approximately equivalent aliquots of krypton were added to each sample. The results indicated that the coarser the silica, the faster equilibrium was attained. On the basis of this result it was thought that the long equilibration times which occurred when krypton was used as adsorbate could be attributed to an interparticle diffusion effect and not to pores in the silica.

On the strength of this evidence and the lack of hysteresis reported above, it was concluded that the silica was non-porous. Thus it was decided to use ground silica tubing as the support for the catalysts to be studied. No commercial non-porous silicas were available at the time that work on this project was commenced. Accordingly sufficient silica for the whole research programme (2 kg) was prepared by the method described in section 3.3.

Before any studies on supported metal catalysts were carried out, the extent of hydrogen adsorption on the silica was measured. It was shown that within the limits of experimental error, no measurable adsorption occurred in the temperature range $-78^{0}C$ to $300^{0}C$.

5.2 Selection of Catalysts of Suitable Metal Concentrations.

A number of catalysts of differing metal concentrations were prepared (section 3.3) in an attempt to find three catalysts having measurably different adsorptive capacities. 0.004% and 0.07% catalysts showed no measurable hydrogen adsorption at 1 torr pressure and temperatures as low as -78°C. However 0.25%, 0.51% and 2.20% nickel catalysts gave measurable hydrogen adsorption at 0°C in the pressure range 0.001 to 1 torr. As can be seen from the isobars in figure 5.10 the amounts adsorbed were substantially different amongst the three catalysts. These three catalysts were chosen for study. Later in the work it was found necessary to prepare two additional catalysts of 5% and 20% metal concentrations. Towards the end of the work a commercially prepared, high surface area, non-porous silica (Cabosil HS5) was obtained. Catalysts containing 1.9% and 5.5% nickel were prepared using the Cabosil support.

5.3 Investigation of the Conditions of Reduction of the Catalysts.

A wide variety of temperatures and reduction times have been used in the past in order to effect the reduction of the nickel in supported nickel catalysts (section 2.3). Temperatures of 300 ^{0}C to 400 ^{0}C in conjunction with hydrogen flow rates of 200 to 500 ml per minute for periods of time usually described as overnight are reported to have been used (Taylor, Yates and Sinfelt, 1964; Brooks and Christopher, 1968).

Nowak and Koros (1967) reported that nickel nitrate supported on silica and on alumina as well as pure nickel nitrate hexahydrate undergo abrupt decomposition both in vacuo and in an atmosphere of hydrogen at temperatures between 210 ^{0}C and 230 ^{0}C. They also observed that bulk nickel oxide was easier to reduce than supported nickel oxide. Benton and Emmett (1924) showed that bulk nickel oxide was almost completely reduced in one hour at 200 ^{0}C and Bandrowski et al (1962) found that 99% of a sample of bulk nickel oxide could be reduced in a few minutes at 295 ^{0}C. Hill and Selwood (1949), on the other hand, found that in order to effect complete reduction of nickel oxide supported on alumina, temperatures as high as 510 ^{0}C were necessary. Taylor, Yates and Sinfelt (1964) measured the extent of reduction of silica-, alumina- and silica-alumina- supported nickel oxide using a vacuum microbalance. They found that for a period of time which they described as "overnight", reduction was extensive at temperatures as low as 250 ^{0}C and was essentially complete in this period of time if a temperature of 370 ^{0}C was used.

Consideration of the equilibrium constant, K, for the reaction

$$NiO + H_2 \rightleftharpoons Ni + H_2O$$

shows that in the temperature range 300°C to 400°C, K has values of the order of 500 (Anderson, 1956). Thus substantial partial pressures of water are required to reverse the direction of the reduction reaction. Hence when using flow rates of hydrogen of the order of 200 ml per minute, the small quantities of water formed ought not to be sufficient to retard the reduction significantly.

From the information reported in the literature, therefore, it appeared that although temperatures of the order of 370°C and reduction times of about 12 hours with a hydrogen flow rate of 200 ml per minute might be sufficient to ensure complete reduction of supported nickel oxide, it nevertheless seemed essential to test each individual type of catalyst preparation to ensure that under the particular conditions of reduction chosen, the reduction was complete. Using samples of a 2.2% nickel-silica catalyst, reduction was carried out at hydrogen flow rates of 200 ml per minute and a temperature of 370°C for a number of different periods of time. The adsorptive capacities of the various reduced samples were measured at 1 torr pressure and 140°C. The results are shown in figure 5.4. From the figure it appeared that extending the reduction time from 8 to 16 hours did not lead to an increased adsorption by the sample at 1 torr pressure and 140°C. It was felt therefore that a reduction time of 12 hours ought to be sufficient for complete reduction of the nickel-silica catalysts described in this thesis. Samples of the catalyst were then reduced at 300°C, 350°C and 400°C for 12 hours at a hydrogen flow rate of 200 ml per minute. The amount of hydrogen adsorbed at 1 torr

FIG. 5.4.

HYDROGEN ADSORPTION AS A FUNCTION OF REDUCTION TIME

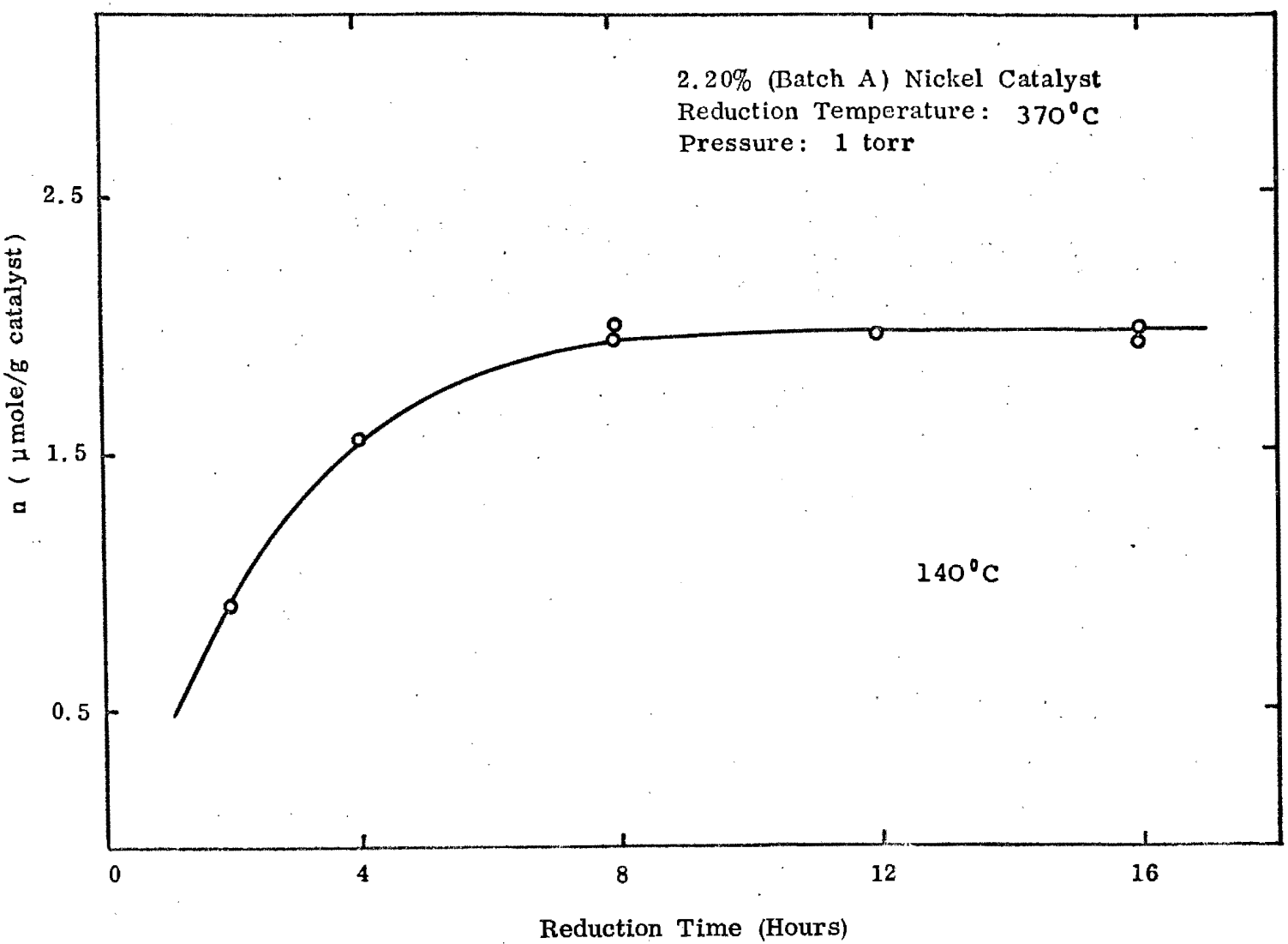

pressure and 140°C by the sample reduced at 300°C was 15% lower than the amount adsorbed under the same conditions by the samples reduced at 350°C and 400°C. The latter two samples had similar adsorptive capacities.

Thus the standard reduction conditions chosen for the catalysts studied in this thesis were a reduction temperature of 370°C, a hydrogen flow rate of 200 ml per minute and a reduction time of 12 hours plus 1 hour, the time necessary for the furnace to reach the required operating temperature.

5.4 Reproducibility of the Hydrogen Isotherms.

In the early stages of the work considerable difficulty was encountered in reproducing the hydrogen adsorption isotherms. Figure 5.5 depicts a typical set of replicate isotherms obtained on a single sample. The catalyst sample was degassed at 370 ^{0}C for 24 hours after the determination of each isotherm. Varying the degassing time and degassing temperature did not appear to improve the reproducibility of the isotherms.

The possibility that air, retained by the grease of a freshly greased stopcock and released on turning the stopcock key, may be oxidizing part of the metal surface, thus lowering the adsorptive capacity of the catalyst under a given set of conditions, was considered. Because of the relatively low surface areas of the catalysts, an appreciable fraction of the metal surface may thus be poisoned. Consequently stopcocks were regreased as infrequently as possible and usually after all the isotherms on a particular catalyst had been completed. After a stopcock had been regreased it was degassed as thoroughly as possible by warming the barrel and turning the key a number of times, simultaneously applying a vacuum to both sides of the stopcock. However this procedure was not effective in obtaining isotherm reproducibility.

Finally it was decided to reproduce in every detail the catalyst pre-treatment after each isotherm. This meant that between each pair of isotherms, not only was the sample degassed for 24 hours at 370 ^{0}C, but prior to the degassing, the sample was re-reduced with hydrogen (flow rate 200 ml per minute) for 12 hours at 370 ^{0}C. This procedure had the desired effect and with catalysts treated in this fashion reproducibility of the hydrogen

FIG. 5.6. REPRODUCIBILITY OF HYDROGEN ISOTHERMS

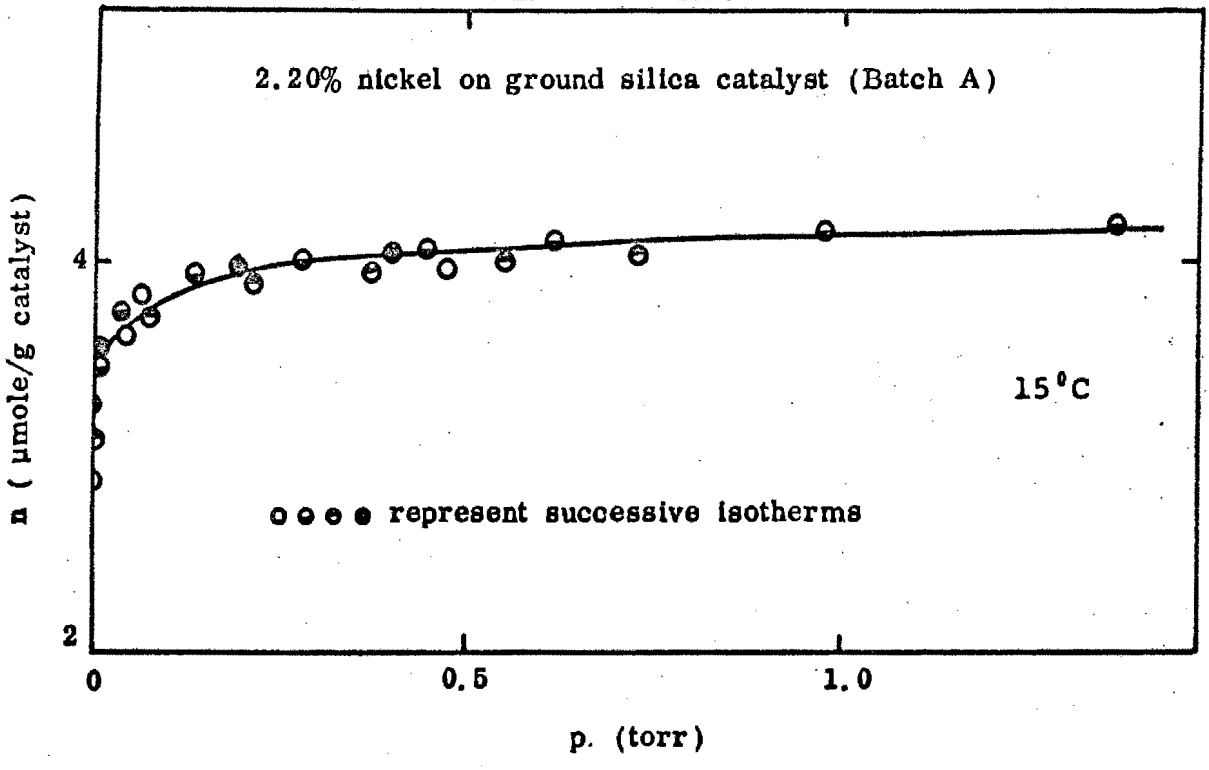

FIG. 5.5. IRREPRODUCIBILITY OF HYDROGEN ISOTHERMS

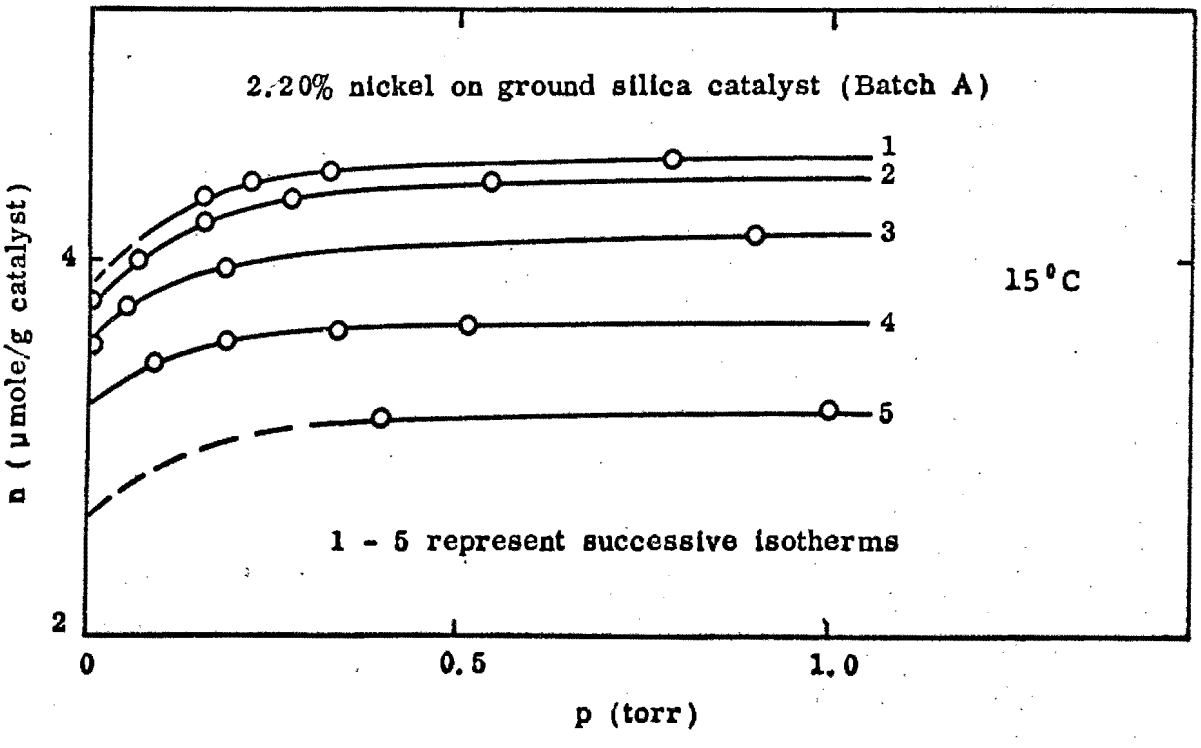

adsorption isotherms was attained (figure 5.6). The reduction and degassing conditions were rigidly adhered to throughout the project and as complete uniformity of procedure as possible was used for each sample studied.

5.5 Reproducibility of Krypton Isotherms.

Replicate determinations of the total surface area of a catalyst by krypton adsorption (section 2.2) produced surface area values which differed by less than 1%. Between replicate determinations, the adsorbents were degassed for 12 hours at 370^{0}C, since it was found that the introduction of a reduction step before degassing (as was done between successive hydrogen isotherms, section 5.4) did not materially affect the value obtained for the surface area of the sample. The BET isotherms were all linear in the range of relative pressures from 0.05 to 0.25. Figure 5.7 shows BET plots of two determinations of krypton adsorption isotherms on a 0.51% ground silica-supported nickel catalyst.

FIG. 5.7.

REPRODUCIBILITY OF KRYPTON ISOTHERMS
0.51% NICKEL ON GROUND SILICA CATALYST (BATCH A)

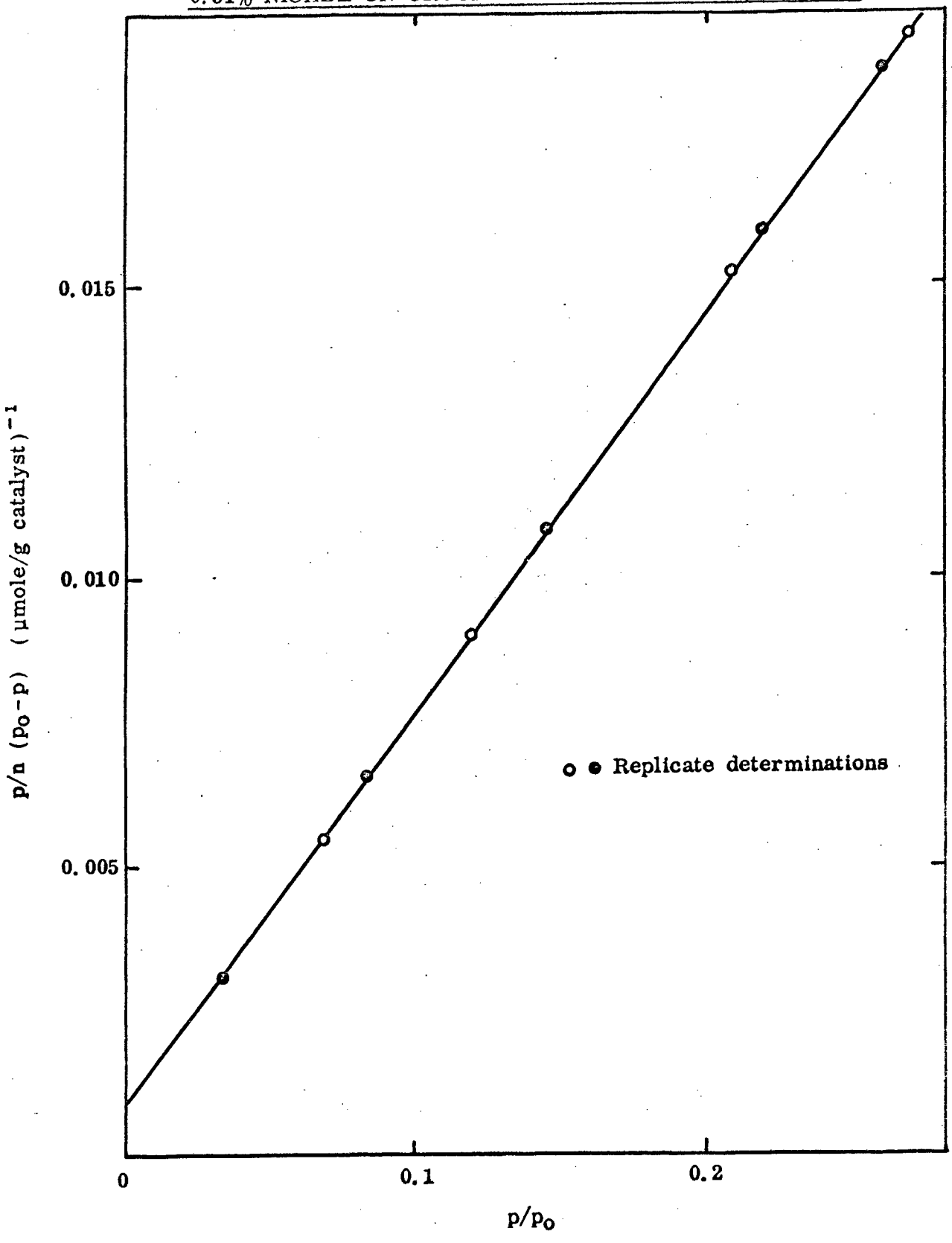

5.6 Thermodynamic Reversibility.

The system hydrogen/ground silica-supported nickel was tested for thermodynamic reversibility as follows. Hydrogen adsorption isotherms were measured at 180°C and 240°C on a 2.20% nickel catalyst. The isotherms are represented by the solid lines in figure 5.8. At the end of the 240°C isotherm (point 1) the temperature was lowered to 180°C (point 2), raised to 240°C (point 3), gas was desorbed at 240°C (point 4), the temperature lowered to 180°C (point 5), and the adsorption isotherm at 180°C continued (points 6, 7 and 8). From these results it was concluded that the hydrogen/ground silica-supported nickel system was thermodynamically reversible.

FIG. 5.8.

THERMODYNAMIC REVERSIBILITY TEST
2.20% NICKEL ON GROUND SILICA CATALYST (BATCH B)

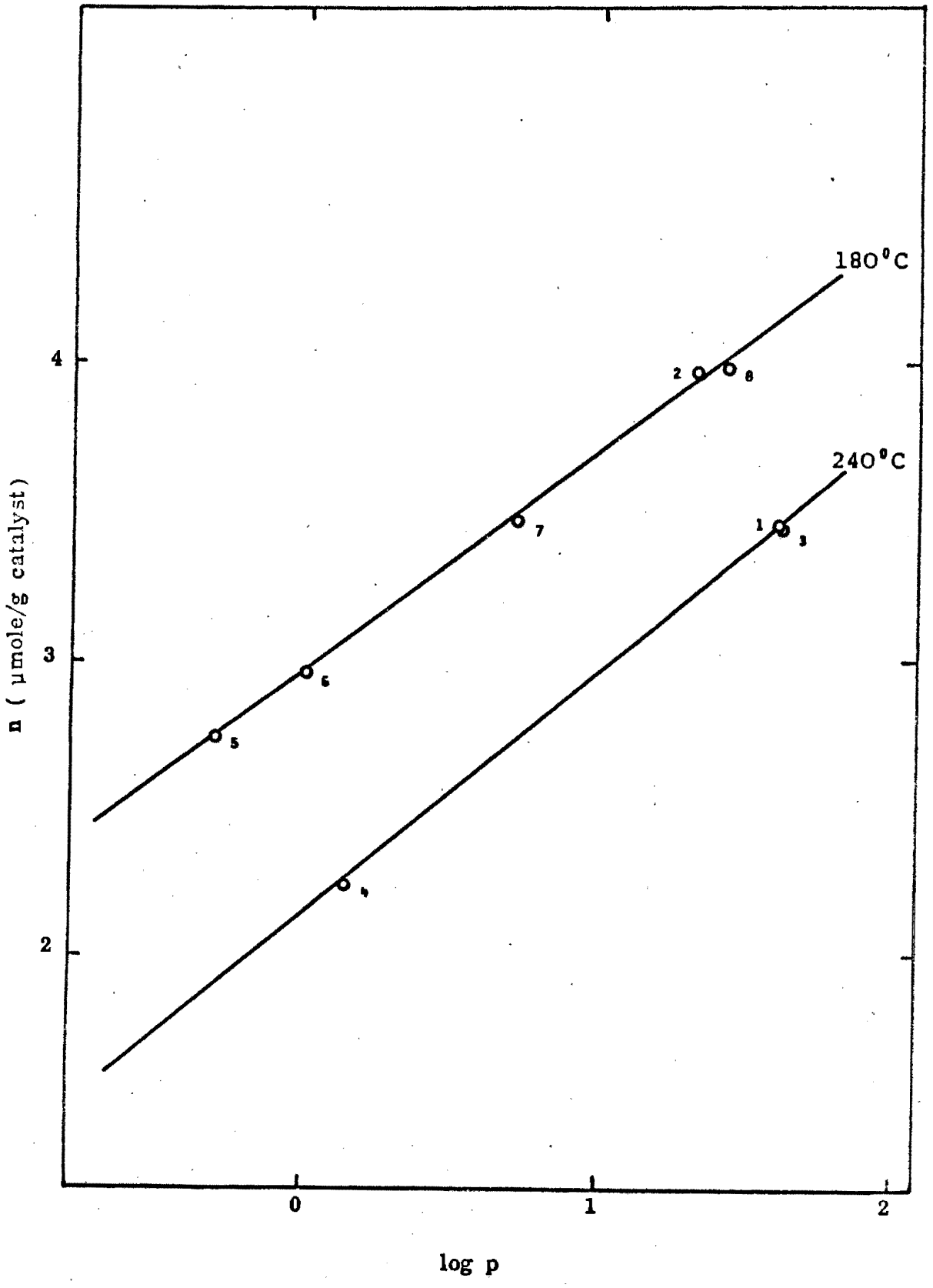

5.7 Estimation of the Amount of Hydrogen Required to Form a Monolayer on the Surface of the Catalysts.

In order to estimate the surface coverage, θ, at any particular set of experimental conditions it is necessary to obtain an estimate of the amount of gas required to form a monolayer on the surface of the metal (n_m). As discussed in section 2.3, it appears that the amount of gas adsorbed at -78^0C and 100 torr pressure gives a reasonable estimate of monolayer coverage on silica-supported nickel catalysts.

Now because of the small metal surface areas of the catalysts, their adsorptive capacity was low. Thus use of the gas burette and constant volume manometer in measuring the amount of gas adsorbed was ruled out, for the errors incurred in measuring the amount of gas admitted to the adsorption cell approximated to the actual amount of gas adsorbed by the catalyst. A similar lack of precision was encountered earlier on in the work, when points on a nitrogen isotherm, measured on the ground silica support, showed a wide scatter (figure 5.2).

The use of a McLeod gauge considerably increased the precision of the measurements. However the high pressure McLeod gauge could only measure pressures up to 50 torr. It was decided therefore to use a pressure of 40 torr to estimate the monolayer capacities of the catalysts and not 100 torr. Although the use of the lower pressure does introduce a source of error into the absolute value of n_m, since the present study is essentially a comparative one between catalysts of differing metal concentrations, this source of error was felt not to be a serious problem.

As stated above a temperature of -78°C has been commonly used to measure the value of n_m. However it is essential to check that the same type of adsorption is operative both at -78°C and at the temperatures at which the isotherms were measured.

Adsorption isobars are useful in ascertaining whether two or more types of adsorption are taking place over a temperature range studied (Thomas and Thomas, 1967). In general for a system in which an adsorbate M_2 is dissociatively adsorbed by an adsorbent, and only one type of chemisorption in addition to physical adsorption occurs, the isobar would have the shape shown in figure 5.9.

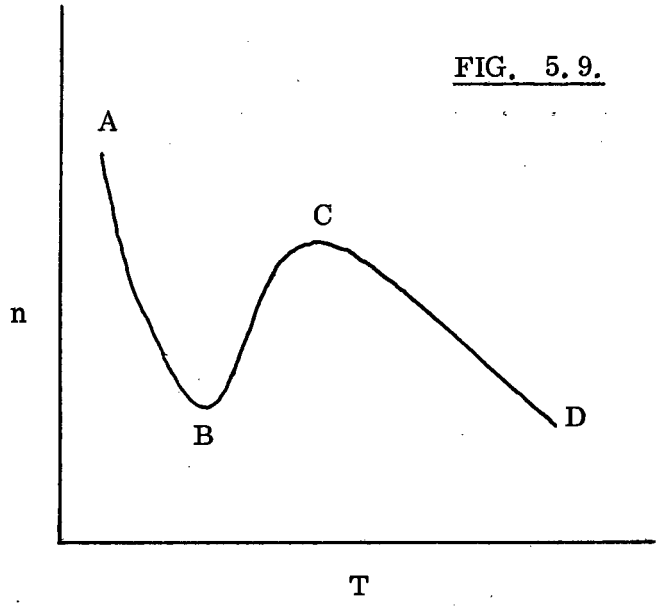

FIG. 5.9.

If the adsorbent is exposed to the adsorbate at temperatures near the boiling point of the latter (A), extensive adsorption would occur, consisting both of physical and chemisorption. Upon increasing the temperature the

amount of physically adsorbed gas would fall from A to B. A further increase in temperature provides the activation necessary for more gas to be chemisorbed. However as the temperature is increased, the tendency for the gas to be desorbed increases. Thus at C the adsorption reaches a maximum, and at higher temperatures the solid displays a lower adsorptive capacity. If two or more distinct types of chemisorption bonds form, their presence would show up on the isobar by additional maxima.

Isobars of the adsorption of hydrogen on the various catalysts are shown in figure 5.10. The temperature range covered was from -110^{0}C to 300^{0}C. Because the temperature in this range is well above the boiling point of hydrogen, it can be presumed that the adsorption taking place was chemisorption. The isobars flattened out at about -80^{0}C, an observation also recorded by Benton and White (1930) who studied the adsorption of hydrogen on nickel powder, and at temperatures between -80^{0}C and 300^{0}C a smooth curve containing no further maxima or minima was obtained. Hence it was concluded that only one type of chemisorption bond was being formed in the temperature range -80^{0}C to 300^{0}C.

Thus -78^{0}C was used in the determination of the values of n_m for the catalysts. The metal surface areas of the catalysts computed from estimates of n_m using equation 2.2.5 are listed in table 5.2.

HYDROGEN ADSORPTION ISOBARS
GROUND SILICA-SUPPORTED CATALYSTS

FIG. 5.10.

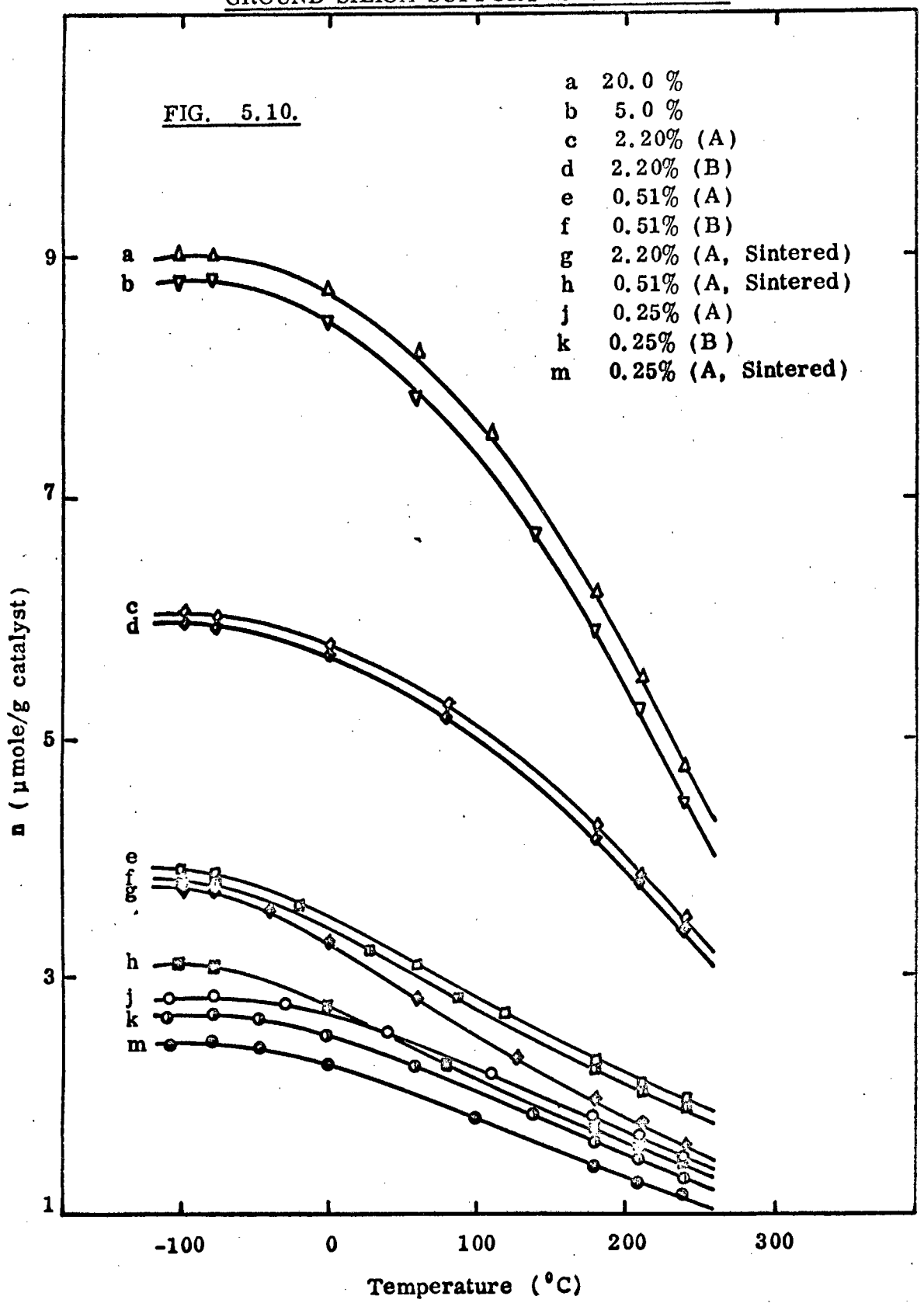

TABLE 5.2.

Catalyst / Technique			Hydrogen Chemisorption	Krypton Adsorption	X-rayLine Broadening	Electron Microscopy		Nickel Carbonyl Formation	Isosteric Heat of Adsorption Per Unit Metal Area
Support	Metal Concentration %	Batch	Metal surface area (m^2/g catalyst)	Total surface area (m^2/g catalyst)	Average crystallite size (Å)	Class interval in which mode of crystallite size distribution falls (Å)	Class interval in which median of crystallite size distribution falls (Å)	Amount of metal removable by $Ni(CO)_4$ formation %	Value of heat at $\theta = 0.2$ (kcal/mole)/ (m^2/g catalyst)
Ground Silica	0		0	1.32					
	0.25	A	0.222	1.55	146	107 - 120	107 - 120	100.1	96.0
	0.25	B	0.210	1.51	143	107 - 120	107 - 120		93.5
	0.25	A (S)	0.192	1.48	194	148 - 159	120 - 133	100.0	96.8
	0.51	A	0.298	1.69	232	177 - 194	177 - 194	99.7	68.0
	0.51	B	0.299	1.71	249	177 - 194	177 - 194		63.0
	0.51	A (S)	0.240	1.65	290	211 - 228	194 - 211		69.2
	2.20	A	0.471	1.92	503	400 - 450	400 - 450	100.3	45.1
	2.20	B	0.467	1.86	544	400 - 450	400 - 450		47.2
	2.20	A (S)	0.300	1.63	700	550 - 600	450 - 500	99.9	47.7
	5.0		0.690	2.31	>1,000	750 - 850	750 - 850		35.9
	20.0		0.705	2.40	>1,000	800 - 900	800 - 900		34.0
Cabosil	1.9		2.46		85				10.0
	5.5		6.52		136				3.75

S refers to catalysts which were sintered for 4 hours at 500°C (section 3.3).

5.8 Hydrogen Isotherms.

In order to obtain isosteric heats of adsorption it is first necessary to construct a family of adsorption isotherms in a temperature range in which the heat of adsorption is constant. Because of the latter requirement, it is usual to keep the temperature range covered by the family of isotherms as small as possible.

The hydrogen adsorption isobars (figure 5.10) were used in order to choose a temperature range in which to measure the isotherms. From the isobars it can be seen that the steepest portion of the isobars occurs at the high temperature region of between about 150°C and 250°C. It was decided to measure the isotherms at temperatures within this range in order that maximum differences in adsorption would be obtained for the minimum temperature differences between isotherms. The estimated experimental error in measuring the amount of gas adsorbed by the catalysts was of the order of 0.01 μmole per gram catalyst (appendix 2). In the temperature range 150°C to 250°C, temperature differences of 30°C between isotherms resulted in differences in the amounts of hydrogen adsorbed per gram of catalyst of approximately 0.20 μmole. Larger temperature differences would give errors less than the estimated 5% error for a 30°C temperature gap between isotherms. However, since isotherms at three temperatures were required for each catalyst, it was decided that a 60°C temperature range was already substantial and an increase in precision by using greater temperature differences would not compensate for the possibility of changes in heats of

adsorption with temperature.

The pressure range covered in the measurement of the isotherms (about four orders of magnitude) was too large to allow the isotherms to be plotted in the form of pressure against amount of gas adsorbed.

The ideal method of representing the experimental data would be in a linear form, and thus attempts were made to fit the data to one of the empirical isotherms: Langmuir, Freundlich or Temkin. However it was found that none of these empirical isotherms could suitably represent the complete range of data of the experimental isotherms.

Now, in common with many chemisorption isotherms, the hydrogen adsorption isotherms obtained in the present study rose very steeply at low pressures (figure 5.11) (Gregg, 1961). In order to transpose the isotherms to isosteres as precisely as possible, the experimental results were plotted as semi-logarithmic isotherms on large sheets of graph paper, log (pressure) being plotted as abscissa and the amount of hydrogen adsorbed per gram of catalyst as ordinate.

Figures 5.14 to 5.24 on pages 162 to 172 represent the hydrogen adsorption isotherms measured on the various ground silica-supported nickel catalysts (section 3.3). The experimental data for the isotherms are listed in appendix 6. From large scale drawings of the isotherms the corresponding plots of log p against 1/T (referred to hereafter as transformed isosteres) were mapped. An example of one such set of transformed isosteres is shown in figure 5.12. The estimation of the best straight lines through the

FIG. 5.11.

HYDROGEN ISOTHERMS

2.20% NICKEL ON GROUND SILICA CATALYST (BATCH A)

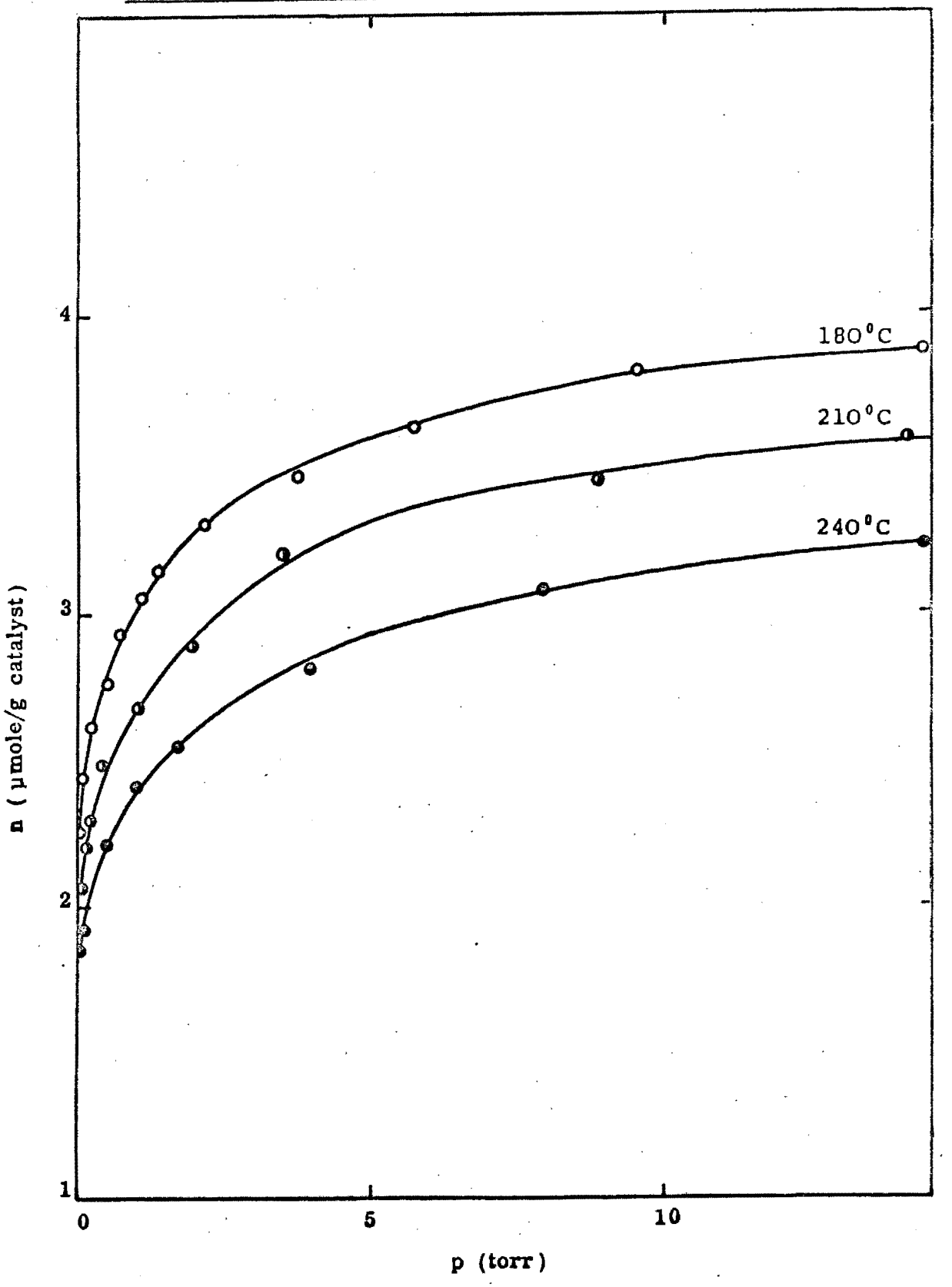

FIG. 5.12.

TRANSPOSED ISOSTERES : HYDROGEN ADSORPTION
0.25% NICKEL ON GROUND SILICA CATALYST (BATCH A)

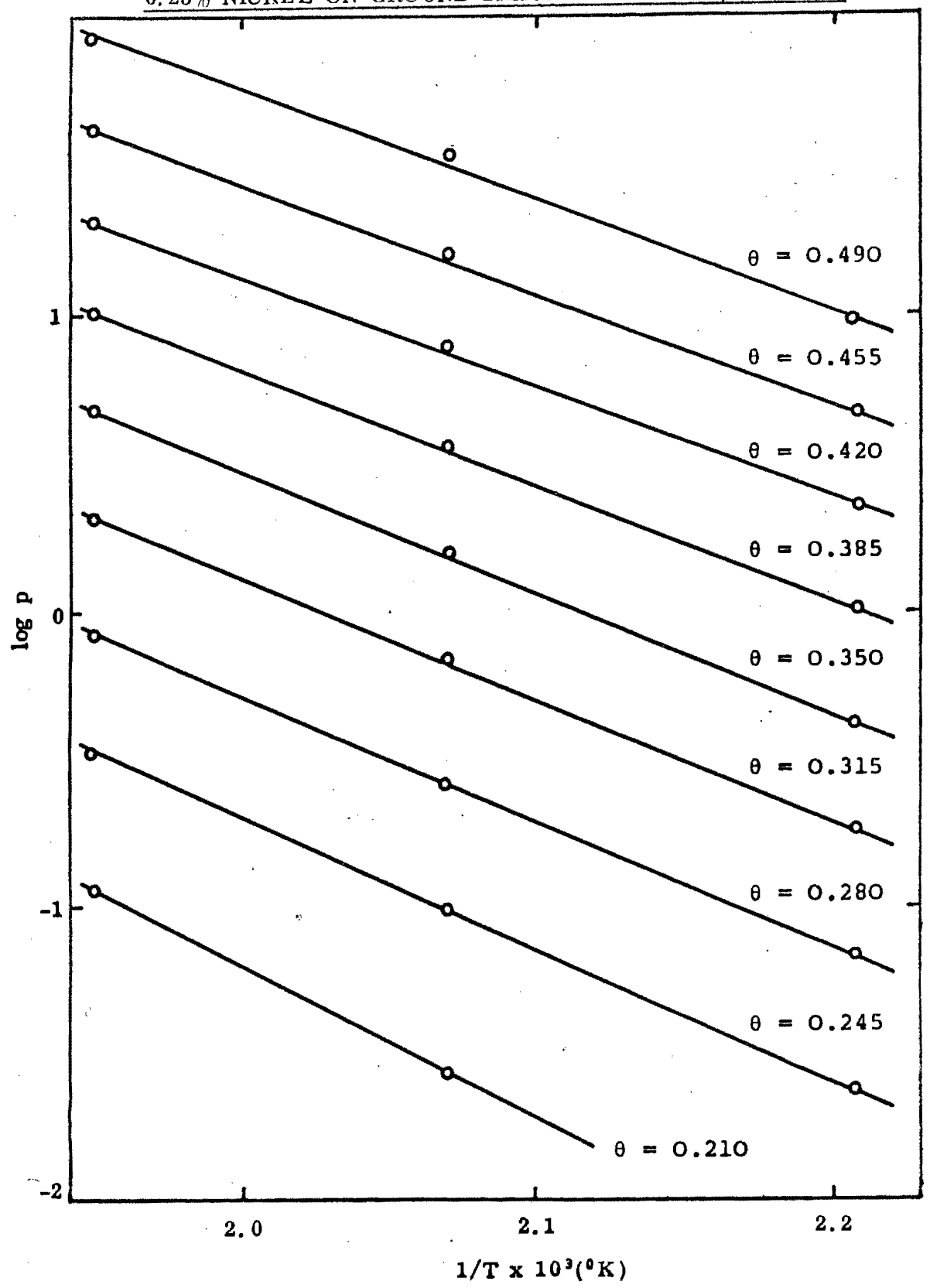

experimental points was made using the method of least squares. From the slopes of the transformed isosteres, isosteric heats of adsorption of hydrogen at the various coverages represented by the transformed isosteres were calculated using the Clausius-Clapeyron equation (equation 1.4.2). From the isosteric heats, isosteric heats of adsorption per unit metal area, Qst, were calculated. Plots of Q_{st} against coverage for all the ground silica-supported catalysts are shown in figure 5.13.

The apparatus was, of necessity, constructed using a relatively large number of greased stopcocks and joints. This created a problem in that each grease point was a potential source of leakage and throughout the course of the work, a substantial number of leaks were encountered. Apart from the inconvenience of the leak, the presence of oxygen in the adsorption cell at the elevated temperatures at which the isotherms were determined caused an unestimable amount of sintering of the catalyst surface.

Thus, if at any stage during the determination of a series of isotherms on a catalyst a leak occurred, the sample was discarded and a second sample, drawn from the same batch of initially reduced material (section 3.3), was used.

FIG. 5.13.

ISOSTERIC HEATS OF ADSORPTION OF HYDROGEN PER UNIT METAL AREA
GROUND SILICA-SUPPORTED CATALYSTS

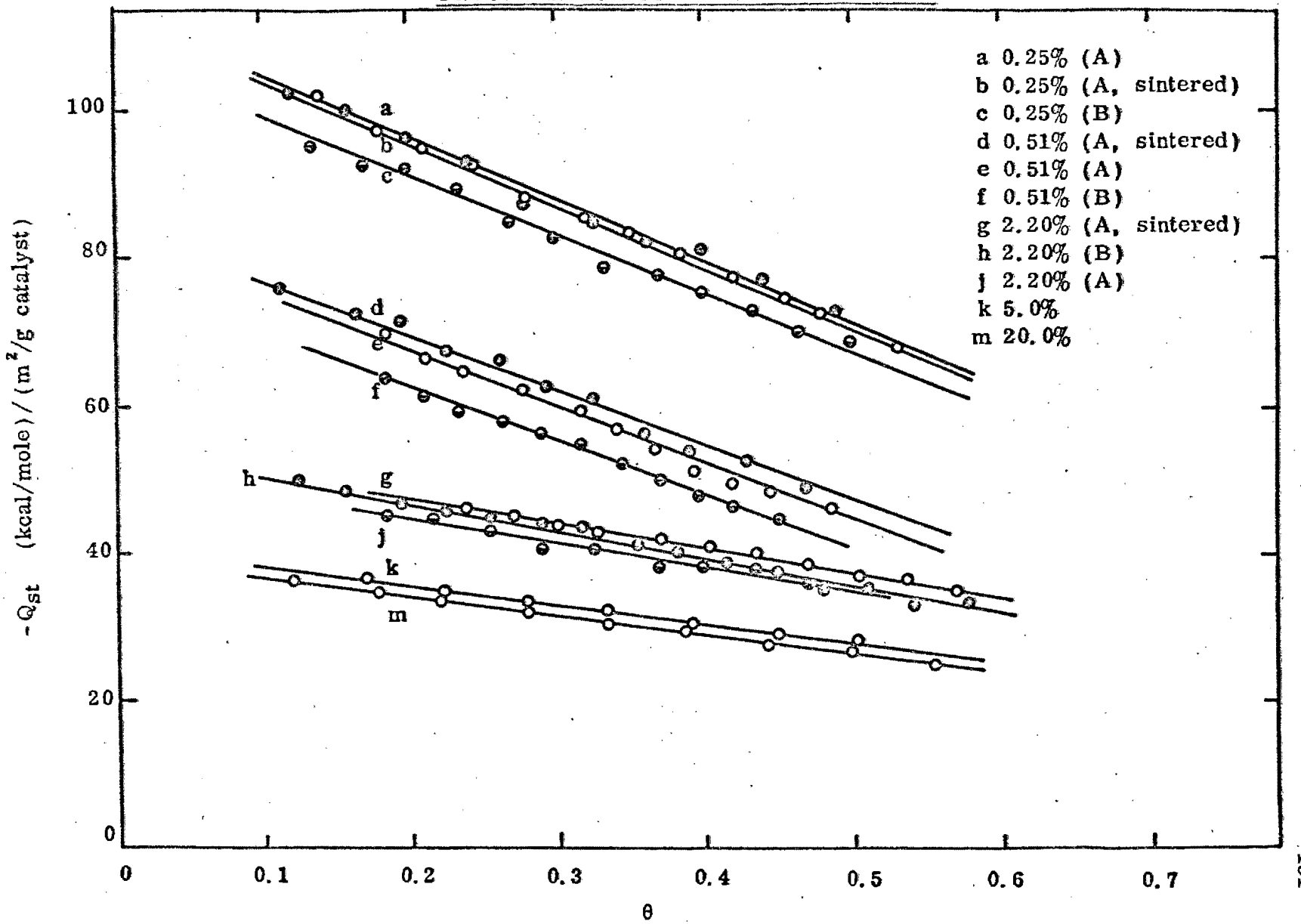

5.9 Total Surface Areas of the Catalysts.

The total surface areas of the ground silica-supported catalysts described in section 5.2 and of the ground silica support were determined using krypton as adsorbate (section 2.2). The co-ordinates of the BET isotherms together with the resultant slopes and intercepts of the isotherms are given in appendix 7. The total surface areas of the samples, calculated from the BET isotherms, are listed in table 5.2.

5.10 Hydrogen Isotherms on Cabosil- Supported Nickel Catalysts.

For the reasons discussed in chapter 6, isosteric heats of adsorption per unit metal area were determined on Cabosil-supported nickel catalysts of 1.9% and 5.5% metal concentrations. Isotherms on the catalysts were only determined at two temperatures because the results were just to be used to confirm trends in the heat curves noted for the ground silica-supported catalysts. The experimental data for the isotherms are listed in appendix 6. The isotherms are represented graphically in figures 5.25 and 5.26 on pages 173 and 174. The isosteric heats of adsorption per unit metal area derived from the isotherms are shown in figure 5.27.

Identical catalyst pretreatment conditions to those employed with the ground silica-supported catalysts were used and the catalysts were reduced and degassed between each isotherm according to the procedure laid down in section 5.4.

FIG. 5.27.

ISOSTERIC HEATS OF ADSORPTION OF HYDROGEN PER UNIT METAL AREA
CABOSIL-SUPPORTED CATALYSTS

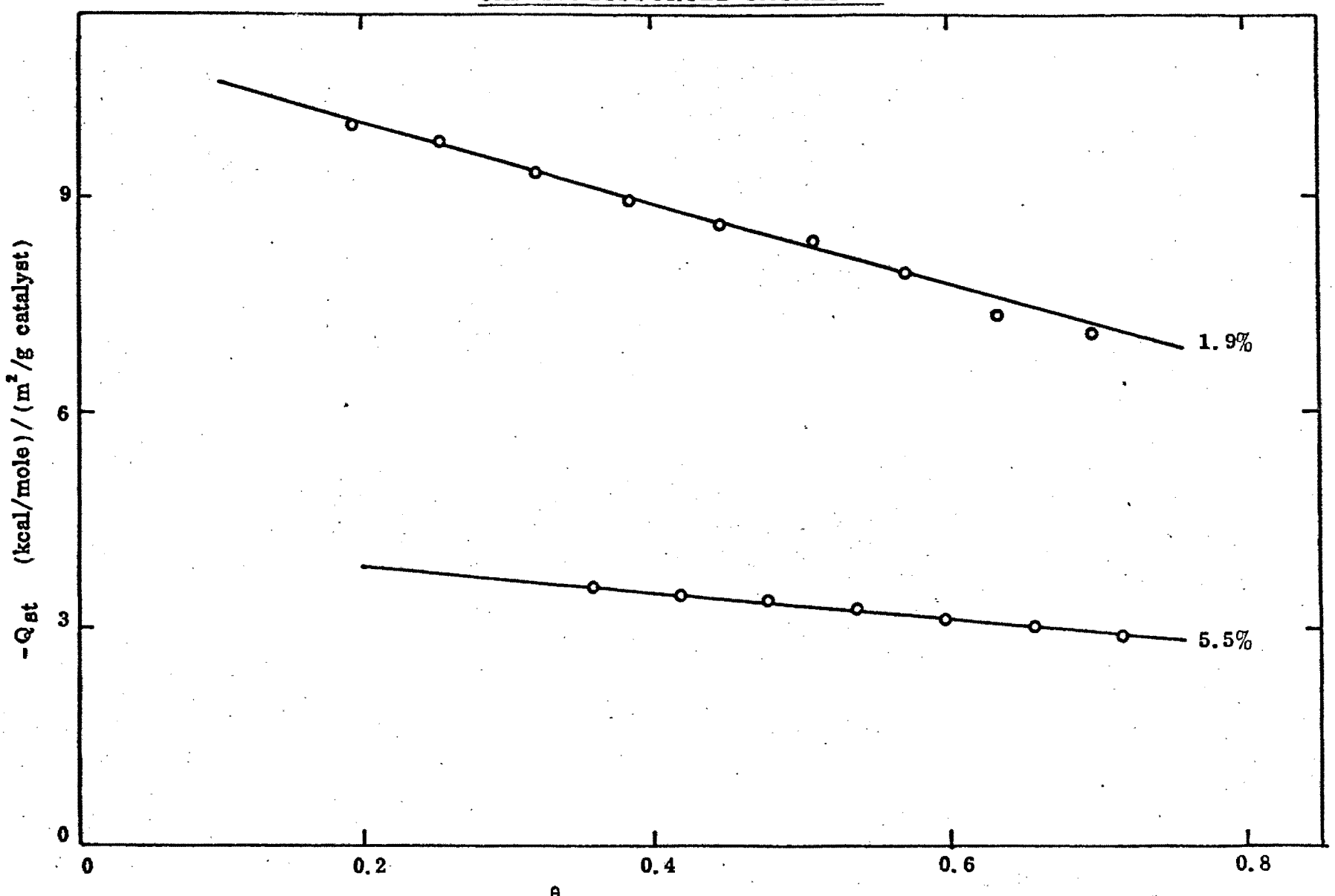

5.11 X-ray Line Broadening Results.

TABLE 5.3.

Sample	Measured profile widths at half peak heights (cm)	Mean Width (cm)	Mean Crystallite Size (Å)
Pure Nickel	1.73, 1.66, 1.70, 1.60, 1.72, 1.69, 1.70	1.69	-
0.25% (A)	3.60, 3.50, 3.55, 3.64, 3.47, 3.51, 3.59	3.55	146
0.25% (B)	3.60, 3.70, 3.51	3.60	143
0.25% (Sintered)	2.87, 2.90, 2.93	2.90	194
0.51% (A)	2.58, 2.61, 2.61	2.60	232
0.51% (B)	2.55, 2.47	2.51	249
0.51% (Sintered)	2.25, 2.38	2.31	290
2.20% (A)	1.96, 1.89	1.92	503
2.20% (B)	1.85, 1.94	1.89	544
2.20% (Sintered)	1.75, 1.89	1.82	700
5.0%	1.75, 1.69	1.73	>1,000
20.0%	1.63, 1.68	1.66	>1,000
1.9% (Cabosil support)	5.75, 5.54	5.65	85
5.5% (Cabosil support)	3.70, 3.80	3.75	136

The descriptions of the catalysts in the first column refer to the percentage of nickel in a nickel on ground silica catalyst. A and B refer to the batch of catalyst and sintered refers to catalysts of batch A which were sintered for 4 hours at 500°C (section 3.3). The last two figures in the column refer to Cabosil-supported nickel catalysts.

The mean crystallite sizes given in table 5.3 were calculated according to the method discussed in section 4.4.

5.12 Electron Microscopy Results.

Figures 5.28 to 5.38 (to be found on pages 175 to 181) are the histograms of the nickel crystallite size distributions found for the various ground silica-supported nickel catalysts. Values of the mean crystallite size of the nickel in the catalysts, as represented by both the mode and the median of the histograms, are listed in table 5.2, page 145 as the limits of the class intervals into which these values fell. It should be pointed out that because the micrographs obtained on the 5.0% and 20.0% catalysts contained only a small number of crystallites, the values for the mode and mean for these catalysts may not be very reliable.

5.13 Discussion.

The fact that reproducible heats of adsorption per unit metal area on two independently prepared catalysts were obtained (figure 5.13) gave confidence that the catalyst preparation procedures were reproducible. Under optical microscopic observation (section 4.2) the catalysts appeared to be of uniform composition. In particular, no metal particles between the silica particles could be detected.

As stated in section 5.4, hydrogen isotherm reproducibility could only be obtained if the catalysts were reduced prior to degassing between each isotherm. A possible explanation that may be considered for this phenomenon is that the catalyst surface may be poisoned by oxidation by traces of oxygen impurity during the course of an isotherm. Because of the relatively low surface area of the catalysts, a small amount of oxidation may effectively poison a substantial fraction of the metallic surface. This would account for the effects shown in figure 5.5. The hydrogen used had a quoted oxygen content of less than 20 ppm. It is doubtful that this oxygen content would be sufficient to cause reductions in the adsorptive capacity of the catalysts of up to the 5% obtained.

The possibility of the occurrence of a leak when the gas was transferred from the cylinder to the gas storage bulb was not discounted. However the section of the apparatus to be used in the transfer was always tested for vacuum tightness prior to use, thus minimising any possibility of contamination. Also, if at any stage the slightest doubt existed as to the vacuum tightness of the storage bulb stopcock, the gas in the bulb was discarded and, after attention to

the stopcock, the bulb was refilled with gas.

The phenomenon of deterioration of a catalyst with use is not unknown. For example, Dorling, Eastlake and Moss (1969), found that the activity of their silica-supported platinum catalysts decreased with time, particularly the low concentration 0.1% platinum catalyst which had a metal area of only 0.06 m^2/g catalyst. Although they suspected that the more rapid deterioration of the low concentration catalyst was the result of having to use a higher temperature in order to obtain a measurable rate of ethylene hydrogenation, they did find that re-reducing their catalysts for a short period of time did effectively restore much of the lost activity.

No tests were made in the present study to determine whether reduction for shorter periods of time could be used to effectively re-reduce the catalysts between the determinations of successive isotherms. The paper by Dorling, Eastlake and Moss was only published after most of the experimental work contained in this thesis was carried out, and since reproducibility had been attained by the procedures discussed in section 5.4, it was felt that no purpose would be served by investigating shorter re-reduction periods.

Schuit and van Reijen (1958), in discussing the advantages of supported metal catalysts over other types of metal catalysts, state that one advantage of supported metal catalysts is that they can be effectively cleaned by re-reduction and degassing at elevated temperature.

In judging the reliability of isosteric heats of adsorption, three requirements must be met. Firstly, the system under consideration should be thermo-

dynamically reversible. Secondly the heat of adsorption should be constant over the temperature range of the isotherms from which it is derived and thirdly the heats themselves should be reproducible, especially when measured on two supposedly identical catalysts, independently prepared.

The results in section 5.6 show that the adsorption of hydrogen by the catalyst samples of this project was thermodynamically reversible.

The constancy of the heat of adsorption over the temperature range used can be tested by inspection of the transposed isosteres. Deviation of the isosteres from linearity would indicate a variation in the heat with temperature. The transposed isosteres obtained were linear in the temperature range 180^{0}C to 240^{0}C (figure 5.12). Preliminary experiments showed that when this temperature range was extended by 30^{0}C to 60^{0}C, deviations from linearity did occur.

Figure 5.13 shows the results of repeating the determination of heats of adsorption per unit metal area on pairs of independently prepared catalysts. Differences in the pairs of heat curves were within the estimated experimental error (appendix 3).

On the basis of these considerations it was felt that the heats of adsorption per unit metal area obtained were reliable.

All crystallite sizes obtained by X-ray line broadening were some twenty to thirty per cent higher than those obtained from the electron micrographs. Any crystallites smaller than about 50 Å in diameter are not detected by X-ray line broadening, and so characterising catalysts with an appreciable

fraction of metal present in very small crystallites using this technique will lead to an average crystallite size larger than the actual average. This might well explain the discrepancy in results from the two methods for catalysts of small average crystallite size, but it is difficult to see how this could apply to catalysts with average crystallite sizes of the order of 250 to 500 Å. From the histograms (figures 5.31 to 5.38) it can be seen that no metal crystallites in the range below 50 Å were observed for these catalysts. There remains the possibility, of course, that one method may inherently give consistently high or low results. Lack of precision does not appear to afford the answer because of the consistent difference obtained with all catalysts. Jones (1938) states that a wide range of crystallite sizes in a particular sample will have the effect that the mean crystallite size observed by X-ray line broadening will be greater than the actual mean size, but that this difference is unlikely to be much greater than about 30%. Since the differences in average nickel crystallite size obtained by the author using the two methods were of the order of 20% to 30%, it appears that the effect suggested by Jones accounts fully for the observed discrepancies.

Symmetrical crystallite size distributions were obtained for the unsintered catalysts, the median and the mode of the distributions lying within the same class interval on the histograms. However in the case of the sintered catalysts (section 3.3) slightly asymmetrical distributions were obtained, the median of the distributions lying either one or two class intervals to the left (lower crystallite size) side of the mode.

In the experiments carried out in order to determine the fraction of nickel in the metallic state in the catalysts (section 4.5), the amount of catalyst used was estimated to be sufficient to produce about 50 mg of nickel in the decomposition chamber. It is estimated that the error in the determination of the amount of nickel was of the order of 0.75%, although improved precision may in principle be attainable by using larger catalyst samples. In practice, however, too large a sample becomes unwieldy to handle. Thus it can be seen that the results obtained by this method (table 5.2, page 145) cannot, within experimental error, be said to differ from 100% nickel in the metallic state. It is, however, possible that the catalysts did contain very small percentages of nickel not in the metallic state, but the method employed was not sensitive enough to detect these small percentages.

HYDROGEN ISOTHERMS

0.25% NICKEL ON GROUND SILICA CATALYST (BATCH A)

FIG. 5.14.

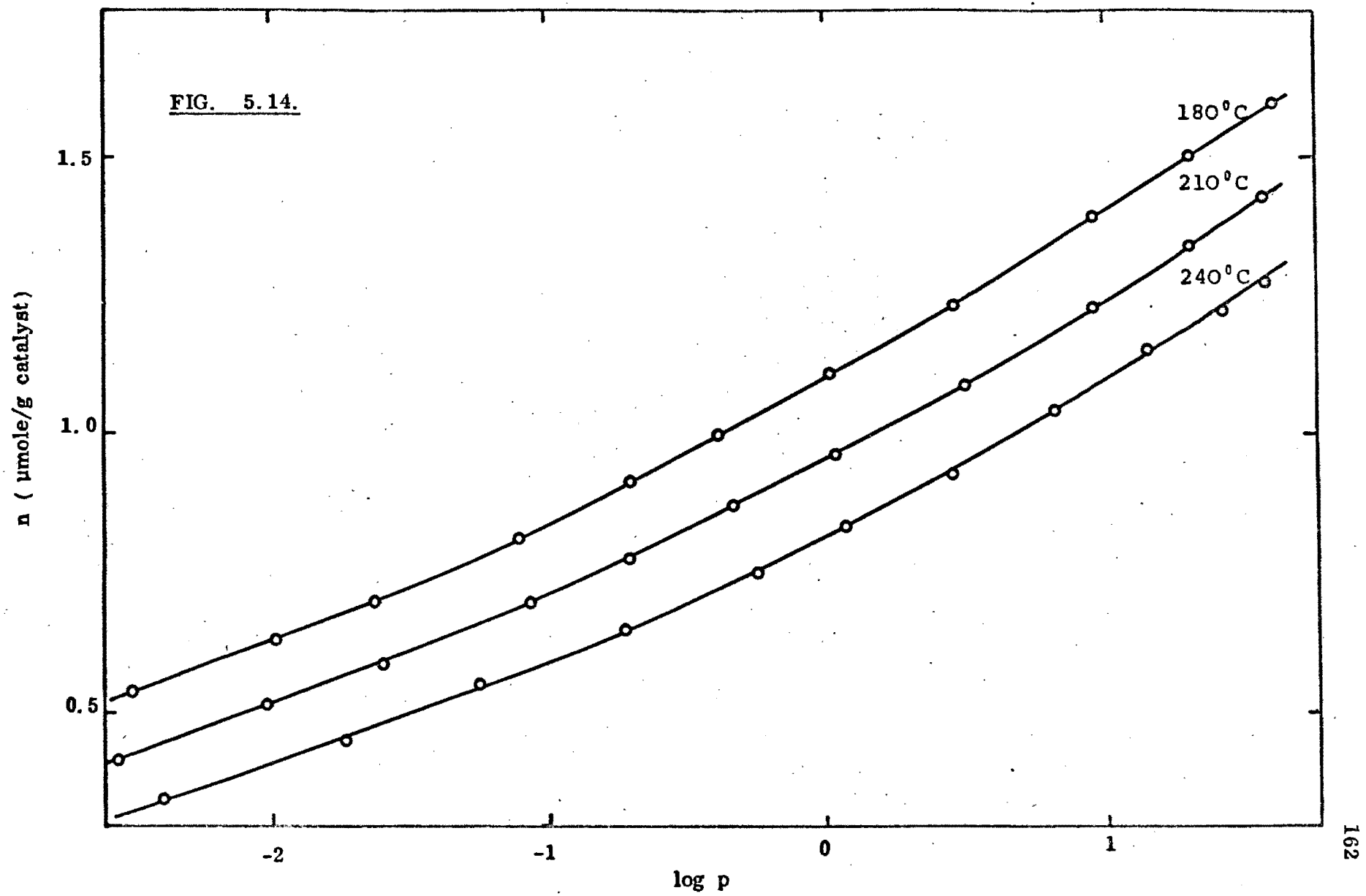

HYDROGEN ISOTHERMS

0.51% NICKEL ON GROUND SILICA CATALYST (BATCH A)

FIG. 5.15.

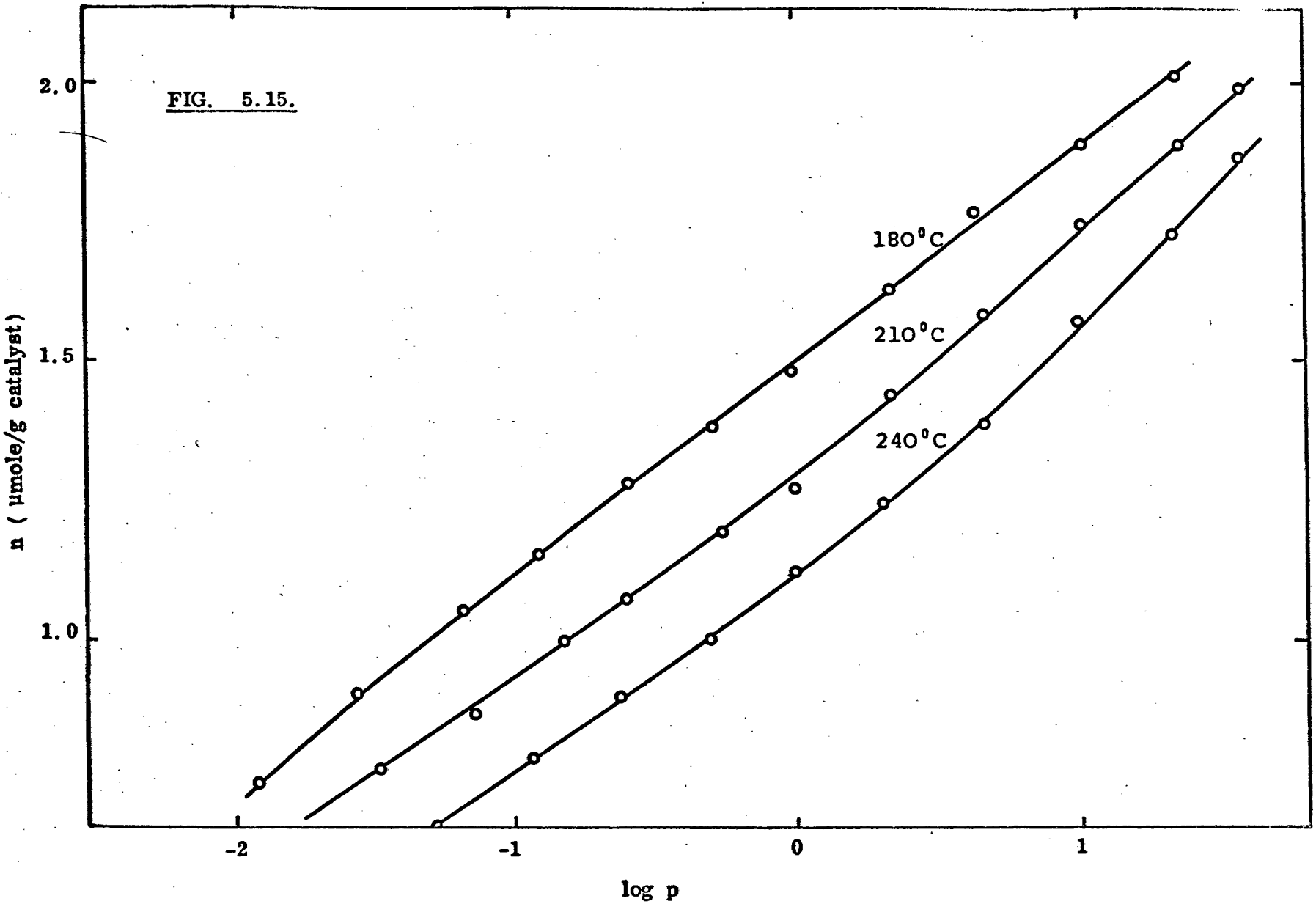

HYDROGEN ISOTHERMS

2.20% NICKEL ON GROUND SILICA CATALYST (BATCH A)

FIG. 5.16.

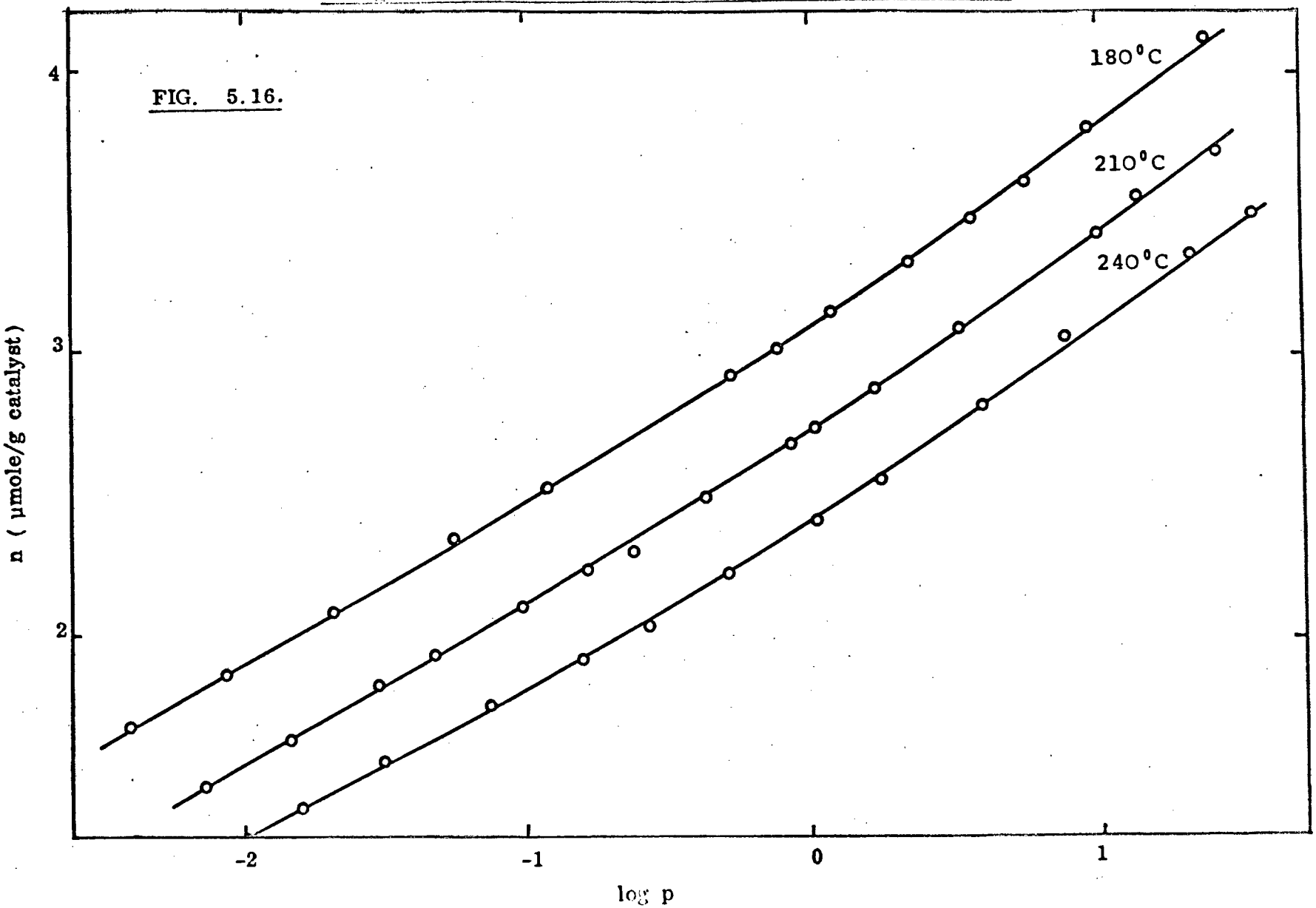

HYDROGEN ISOTHERMS

0.25% NICKEL ON GROUND SILICA CATALYST (BATCH B)

FIG. 5.17.

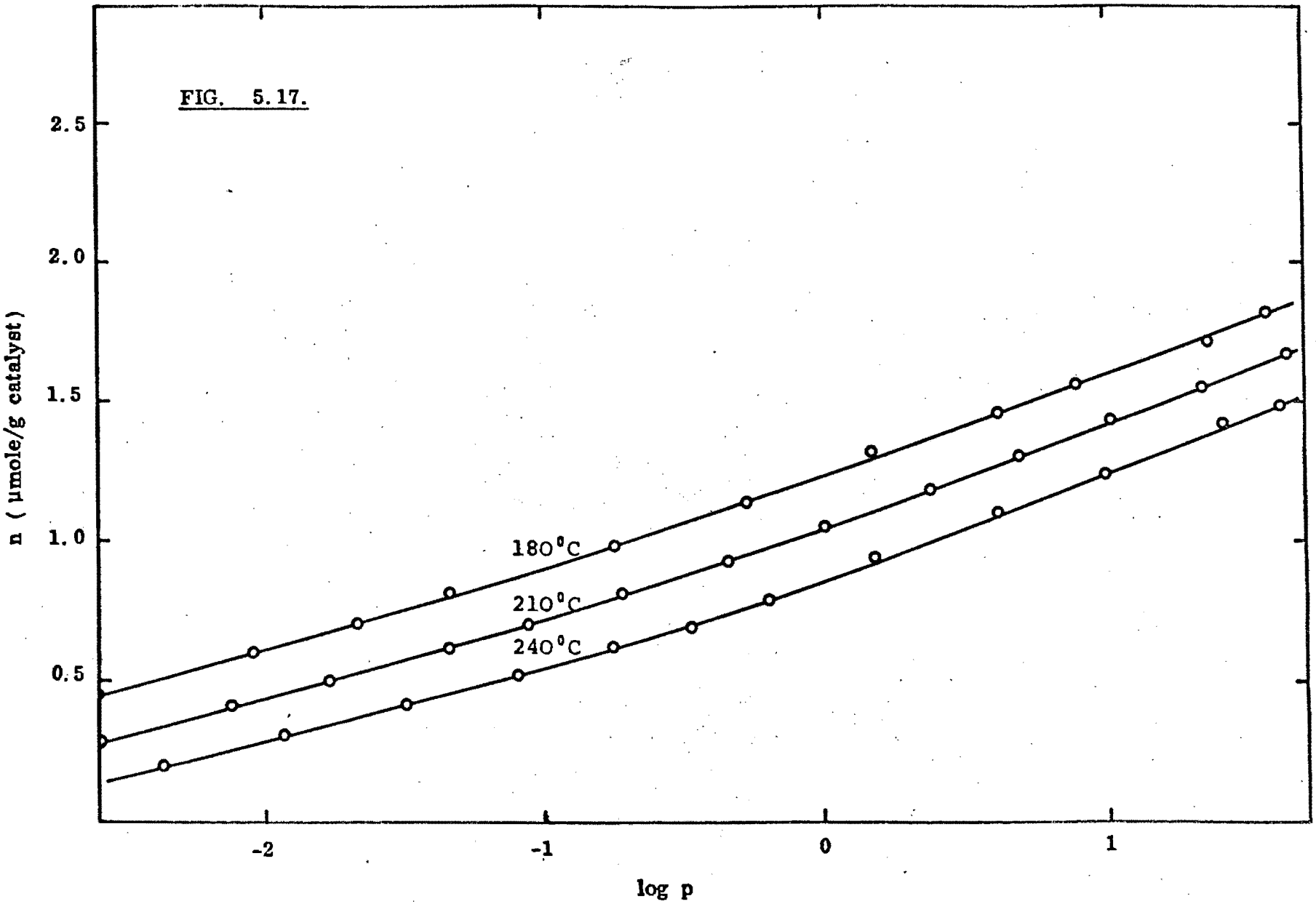

HYDROGEN ISOTHERMS

0.51% NICKEL ON GROUND SILICA CATALYST (BATCH B)

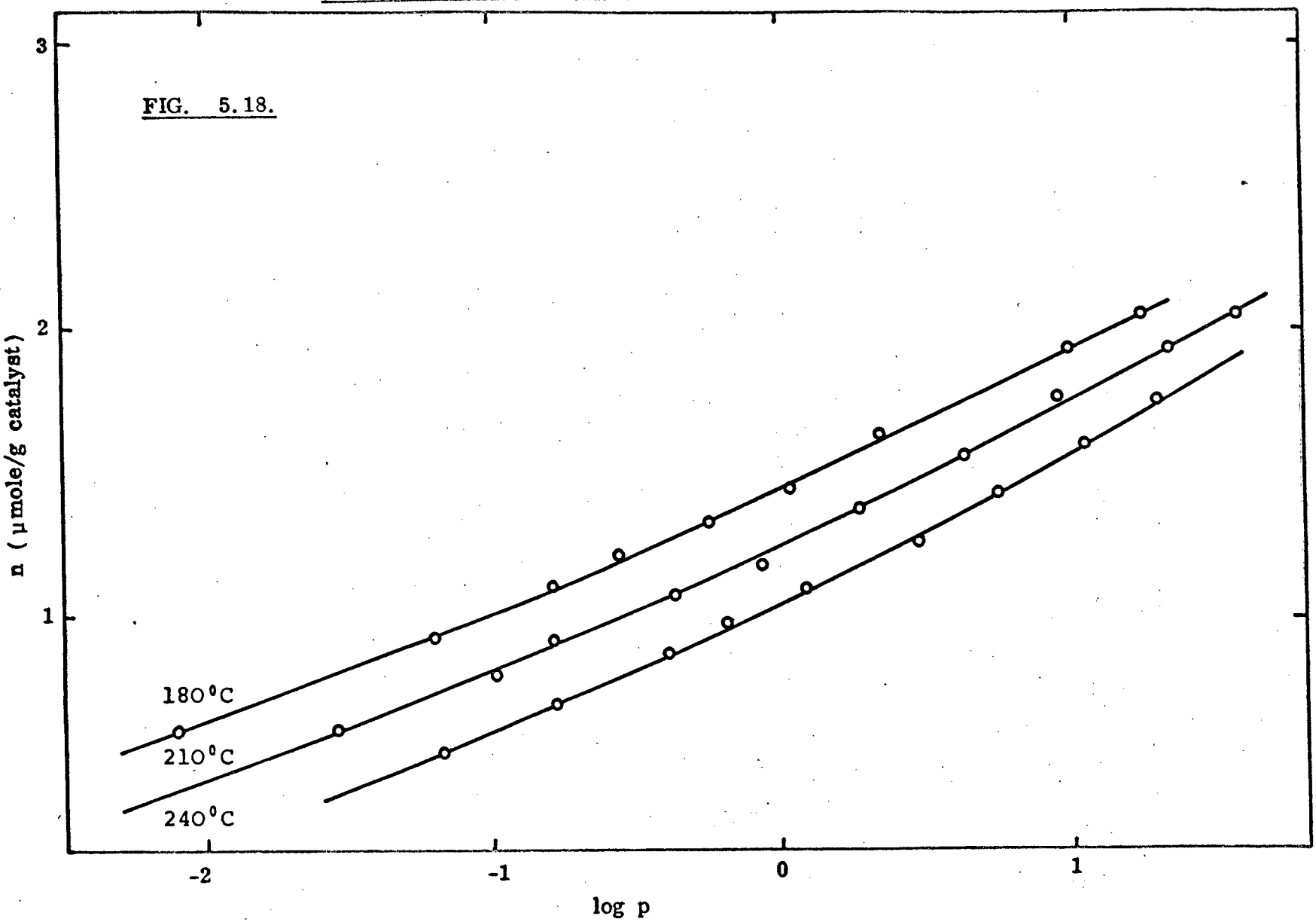

FIG. 5.18.

HYDROGEN ISOTHERMS

2.20% NICKEL ON GROUND SILICA CATALYST (BATCH B)

FIG. 5.19.

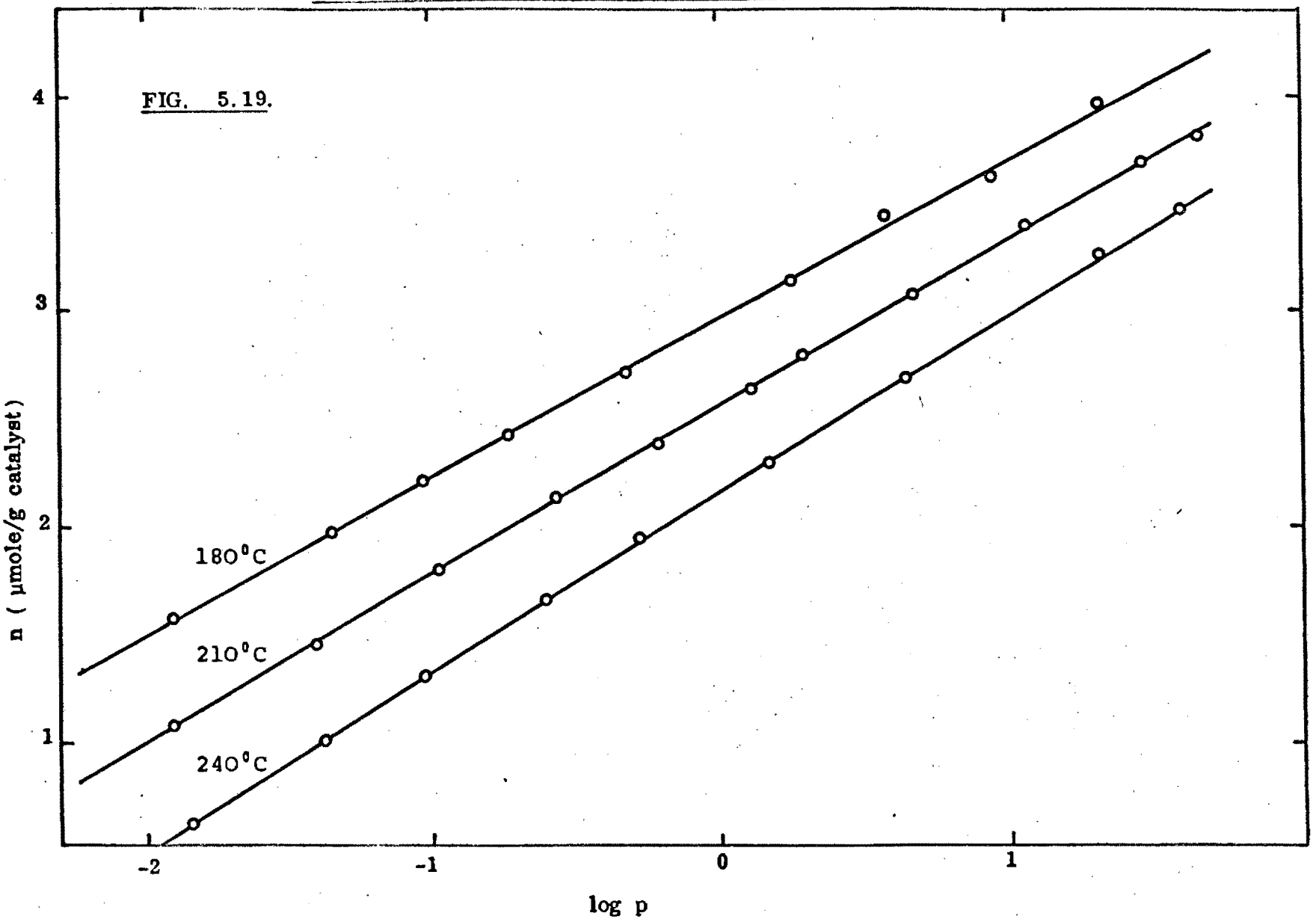

HYDROGEN ISOTHERMS

0.25% NICKEL ON GROUND SILICA CATALYST (BATCH A, SINTERED)

FIG. 5.20.

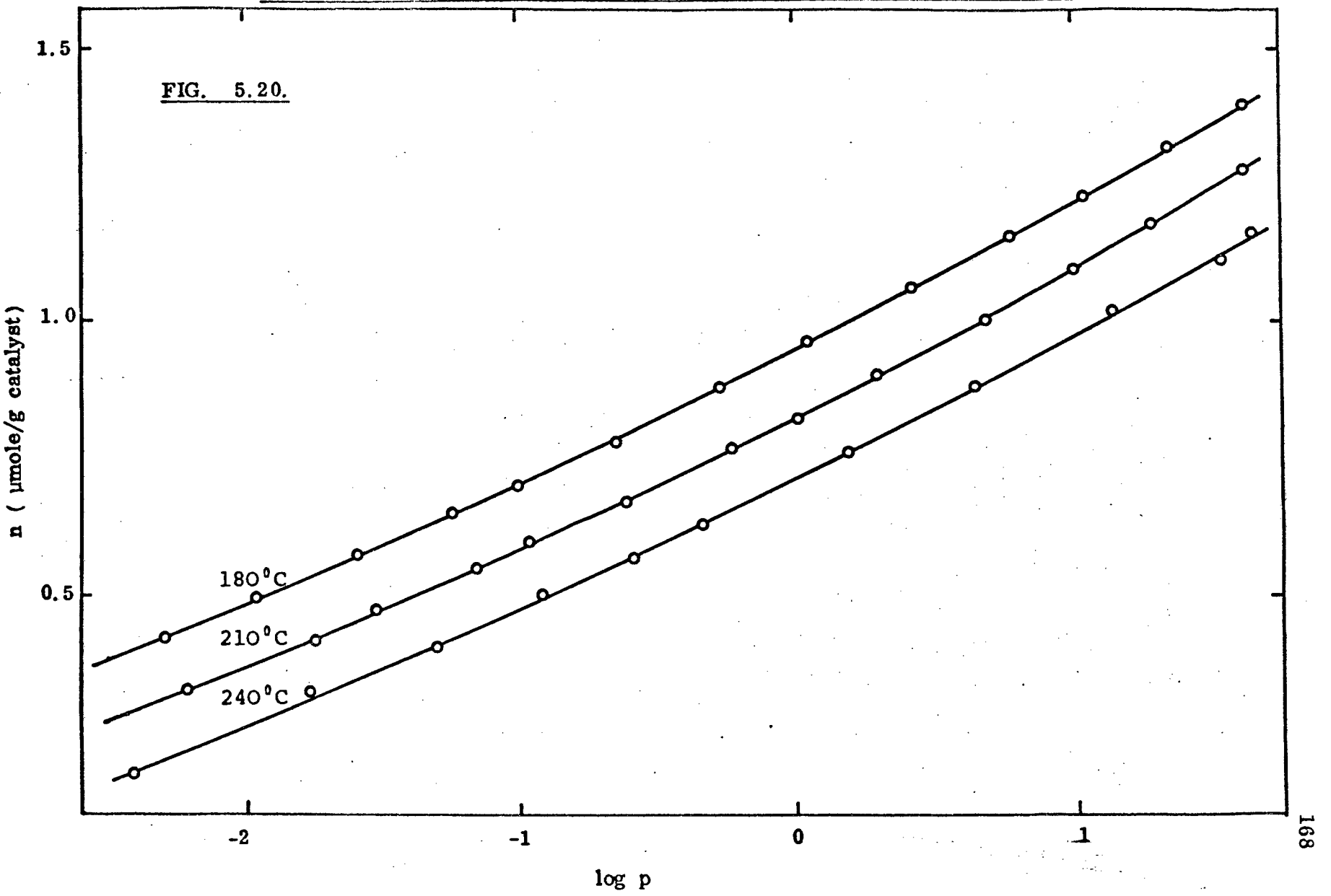

HYDROGEN ISOTHERMS

0.51% NICKEL ON GROUND SILICA CATALYST (BATCH A, SINTERED)

FIG. 5.21.

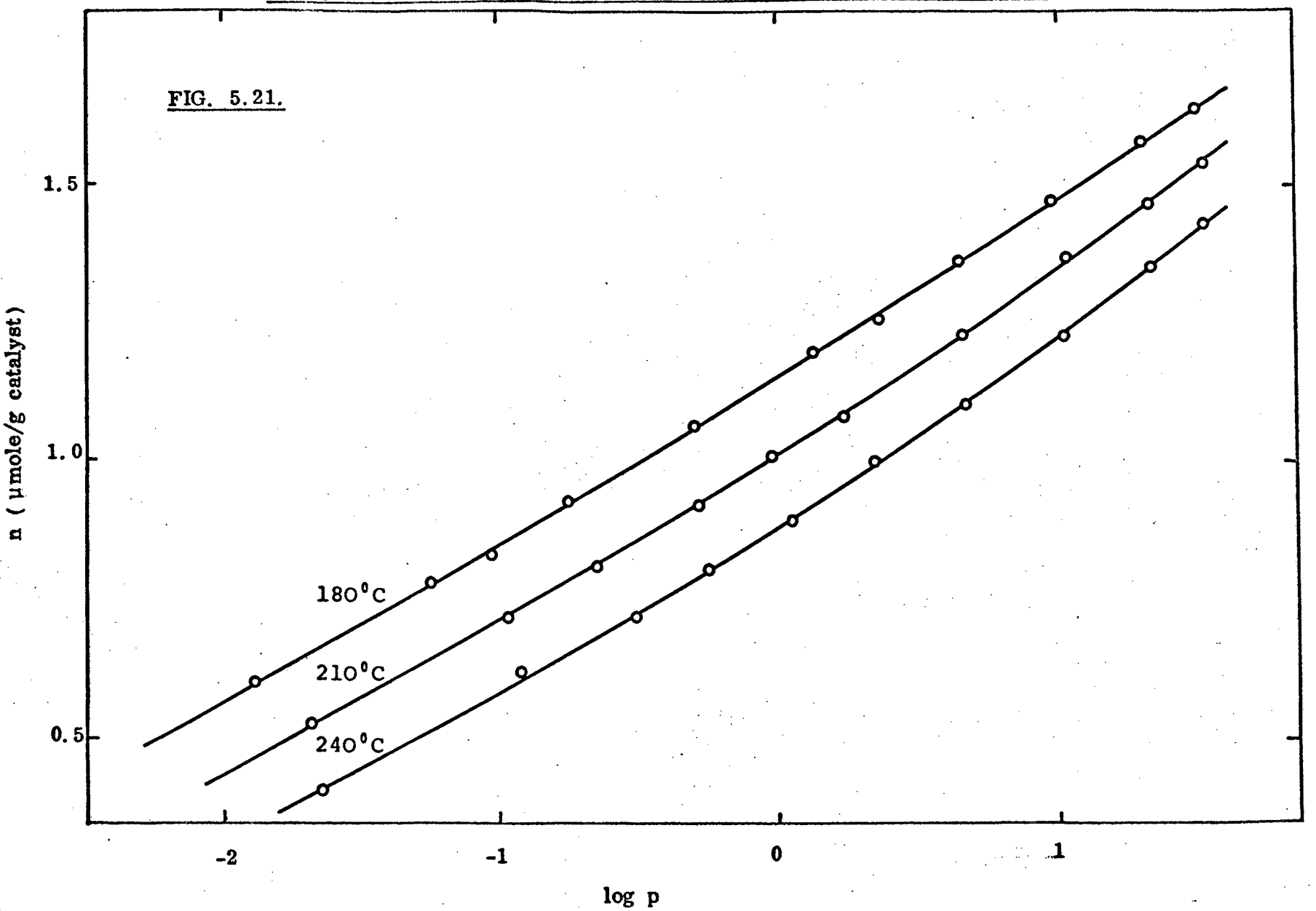

HYDROGEN ISOTHERMS

2.20% NICKEL ON GROUND SILICA CATALYST (BATCH A, SINTERED)

FIG. 5.22.

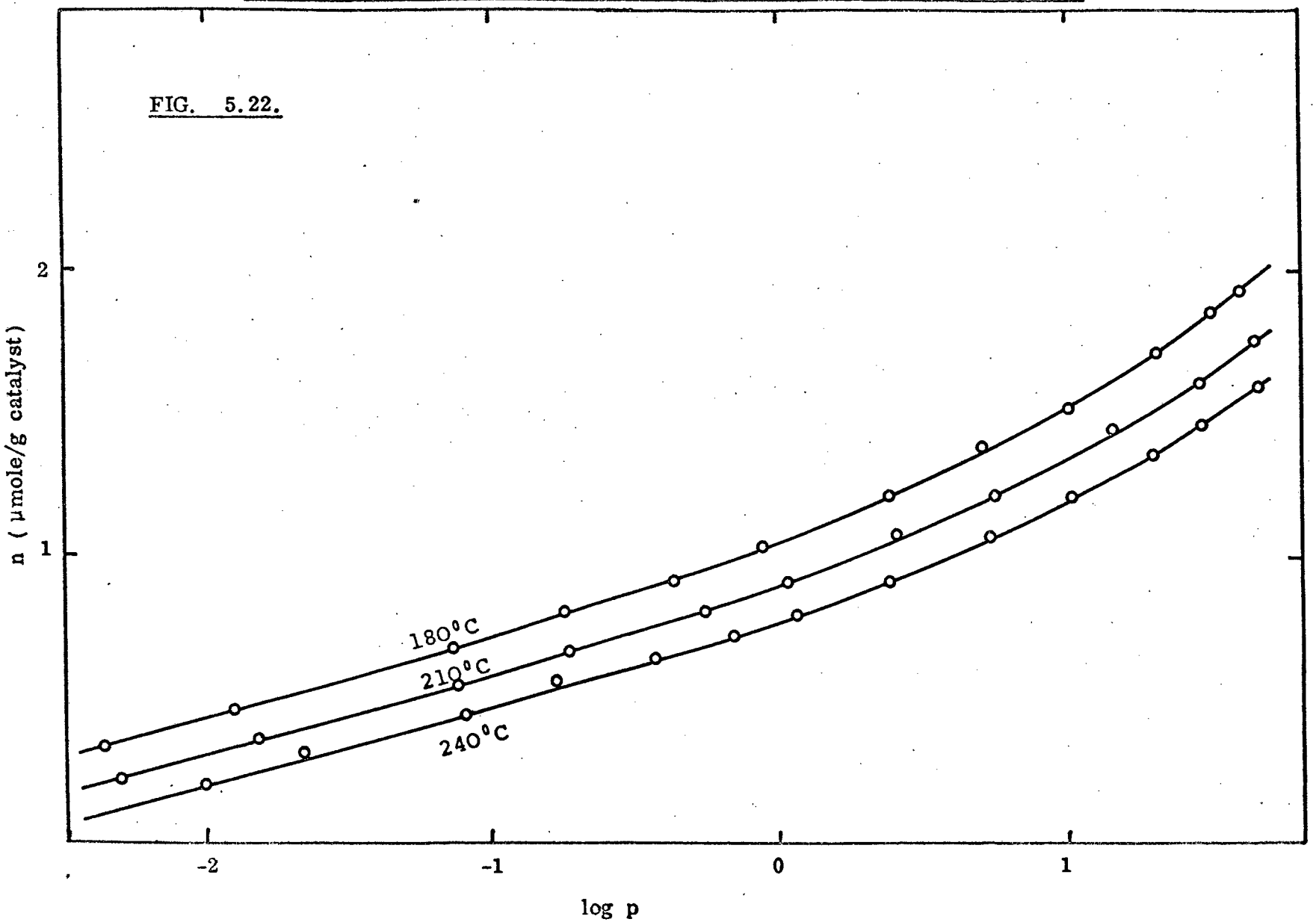

HYDROGEN ISOTHERMS

5.0% NICKEL ON GROUND SILICA CATALYST

FIG. 5.23.

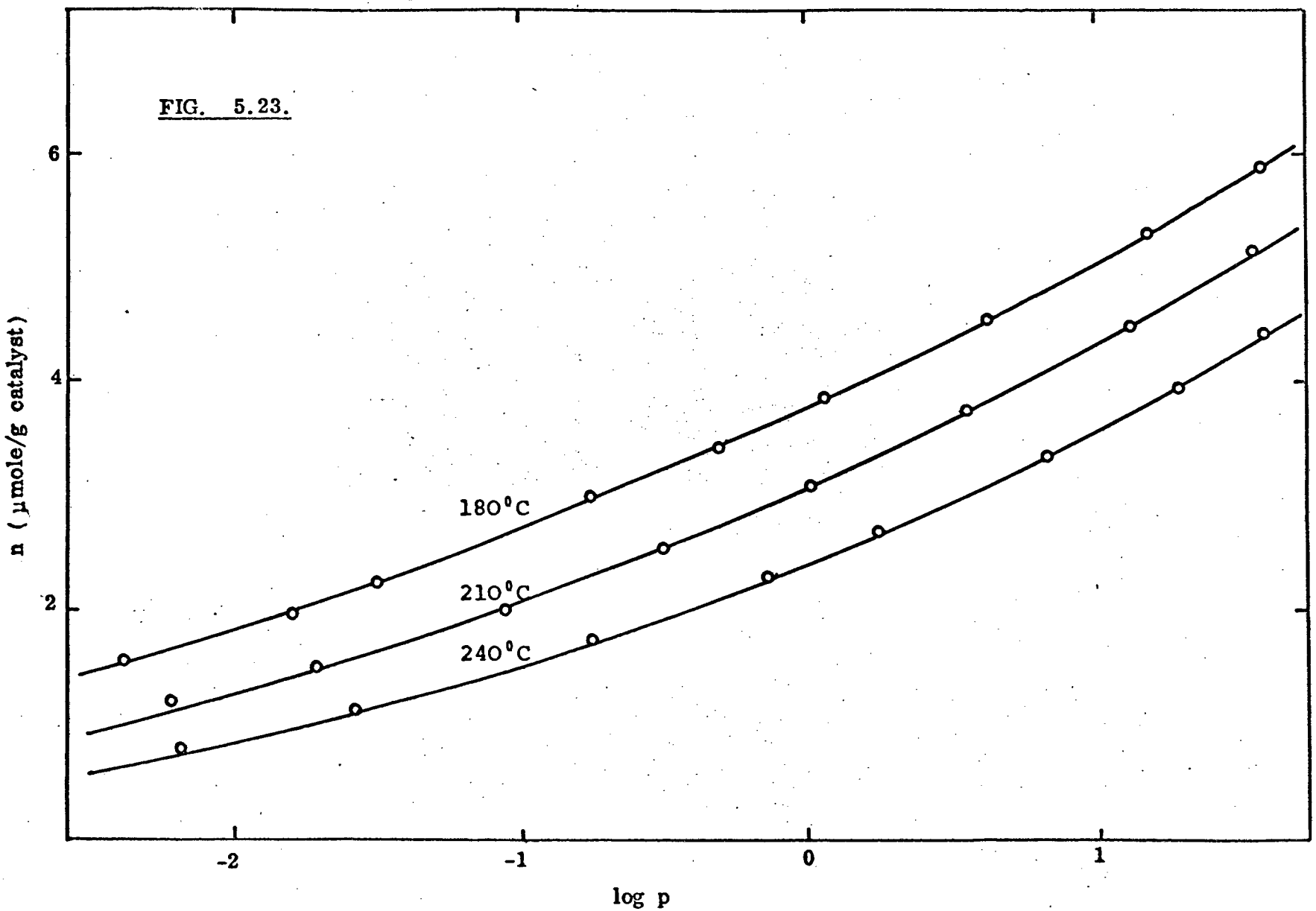

HYDROGEN ISOTHERMS
20.0% NICKEL ON GROUND SILICA CATALYST

FIG. 5.24.

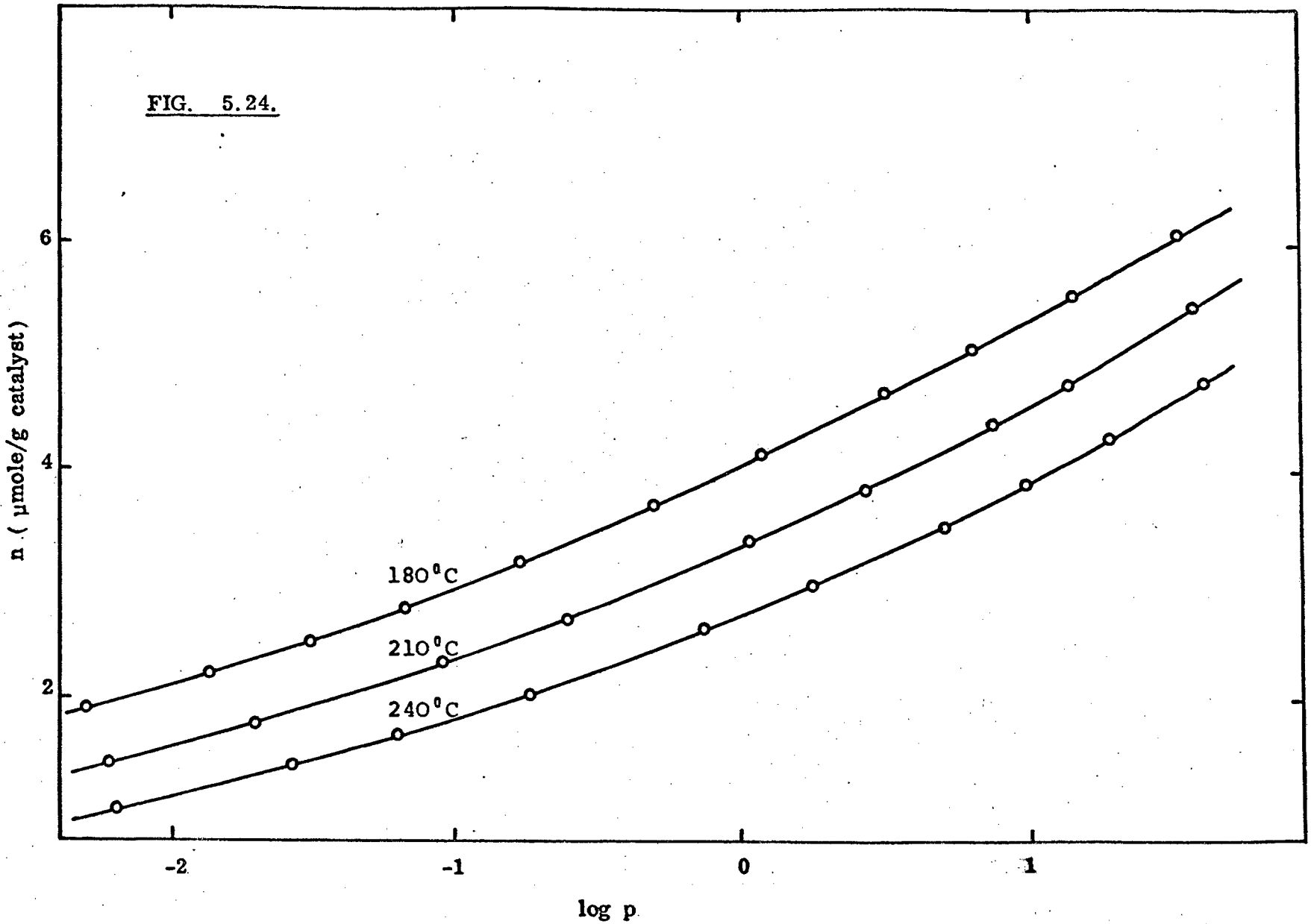

HYDROGEN ISOTHERMS

1.9% NICKEL ON CABOSIL CATALYST

FIG. 5.25.

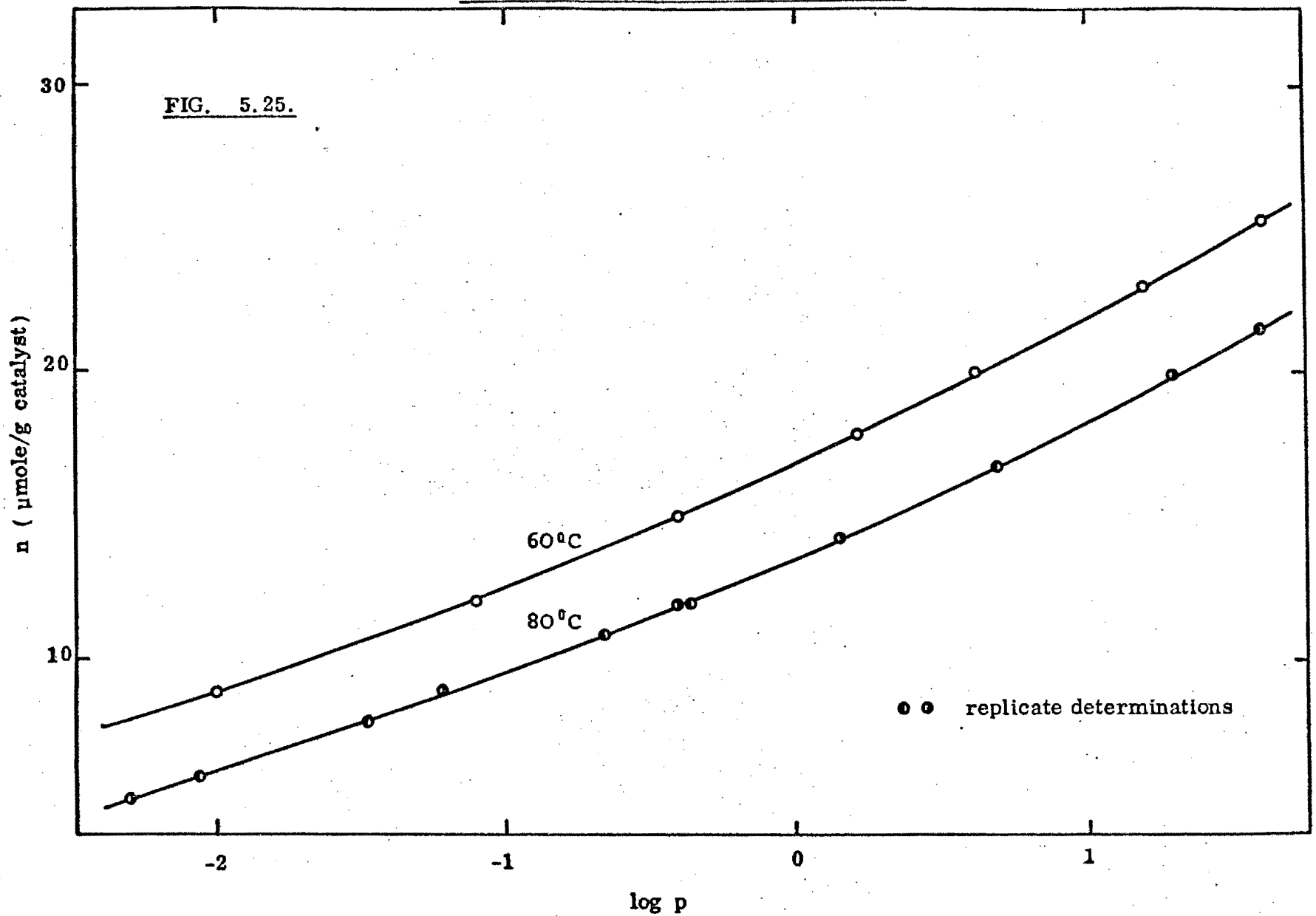

HYDROGEN ISOTHERMS

5.5% NICKEL ON CABOSIL CATALYST

FIG. 5.26.

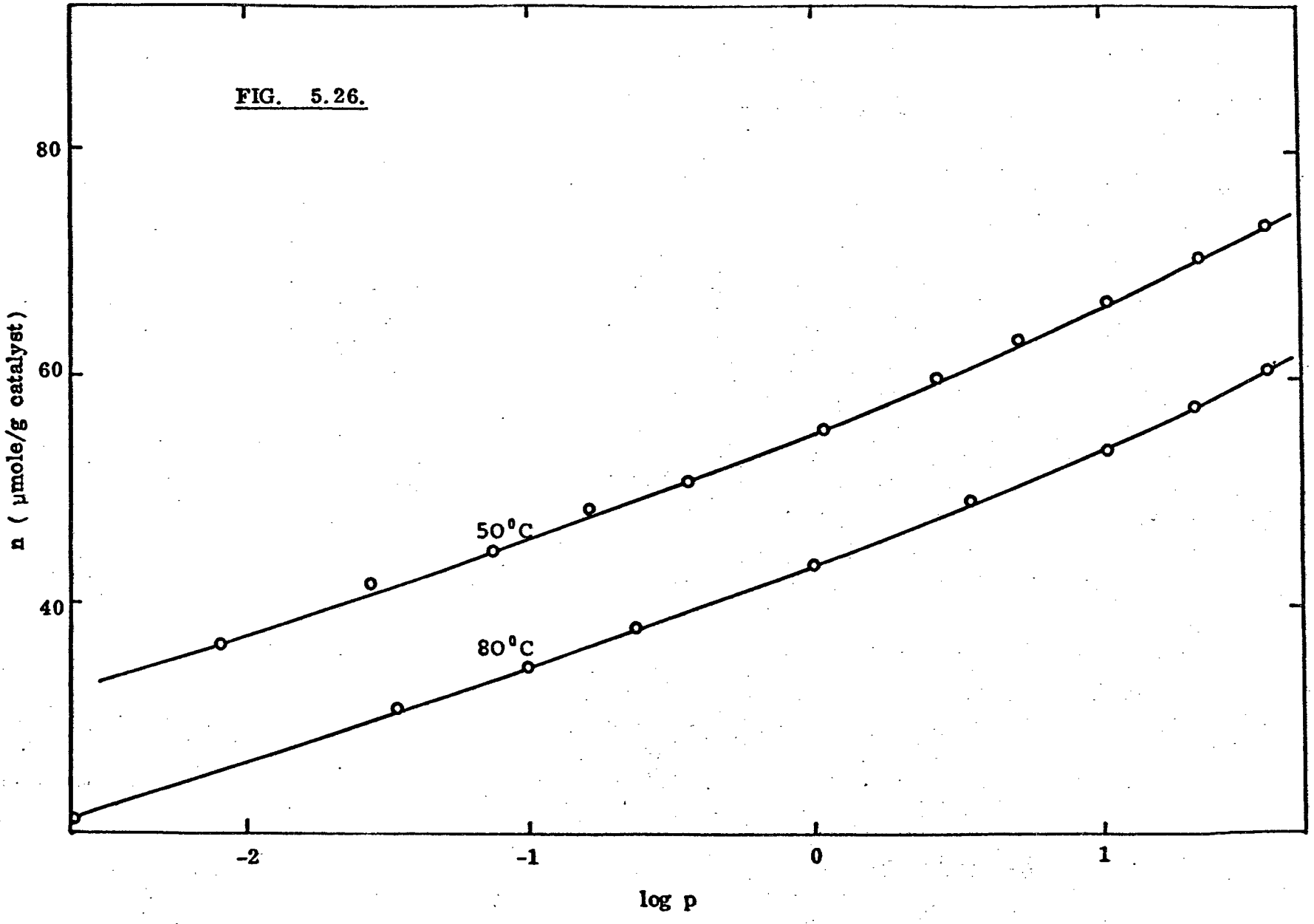

NICKEL CRYSTALLITE SIZE DISTRIBUTION

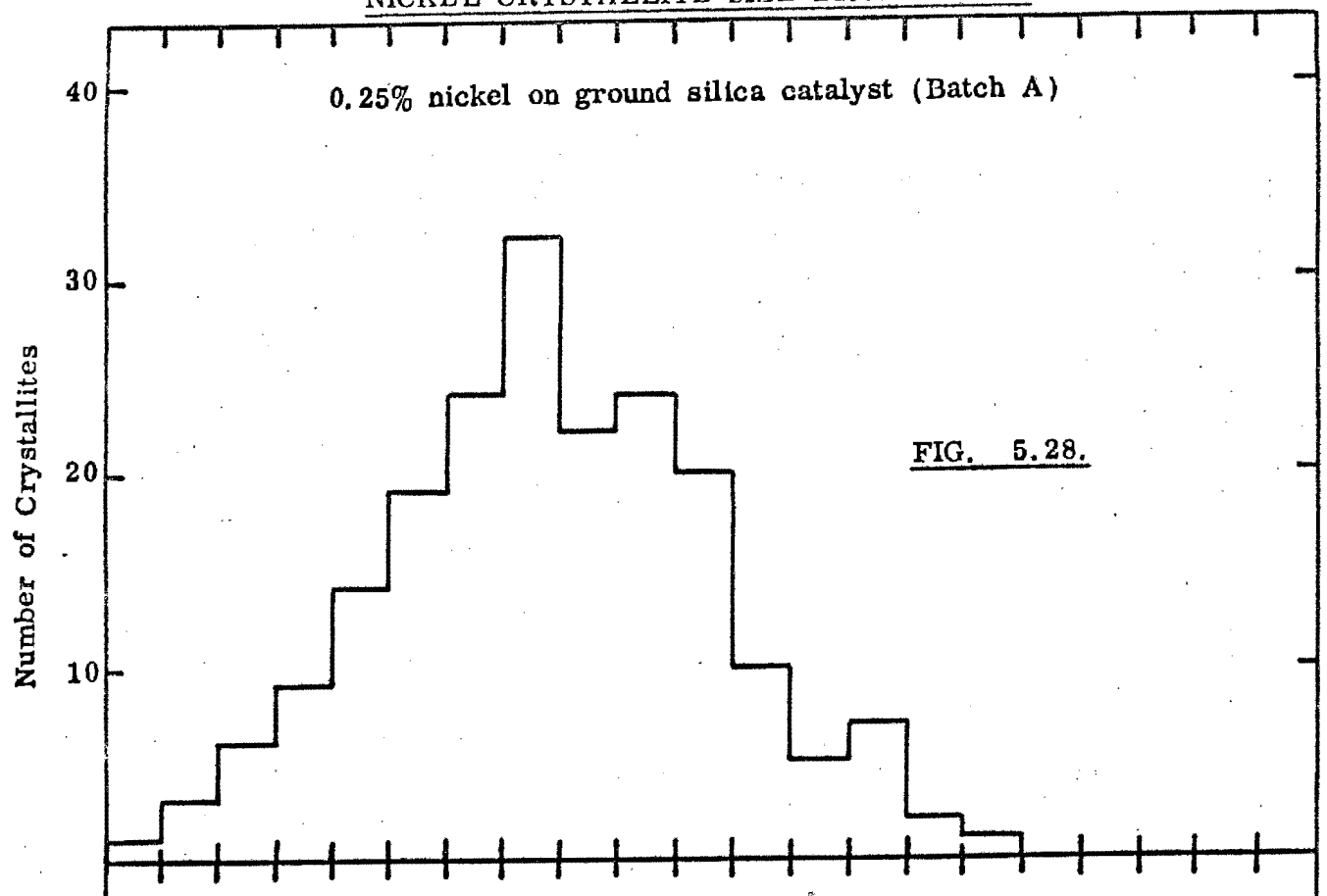

FIG. 5.28.

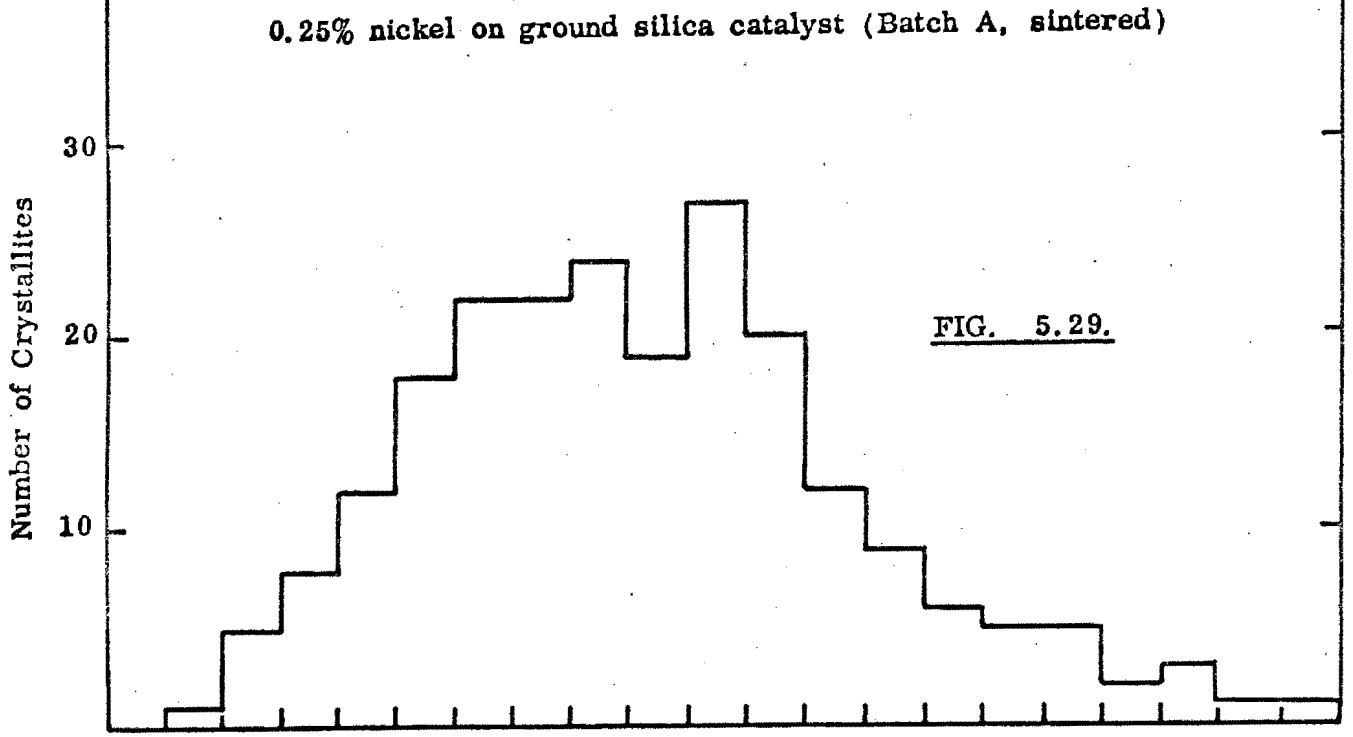

FIG. 5.29.

NICKEL CRYSTALLITE SIZE DISTRIBUTION

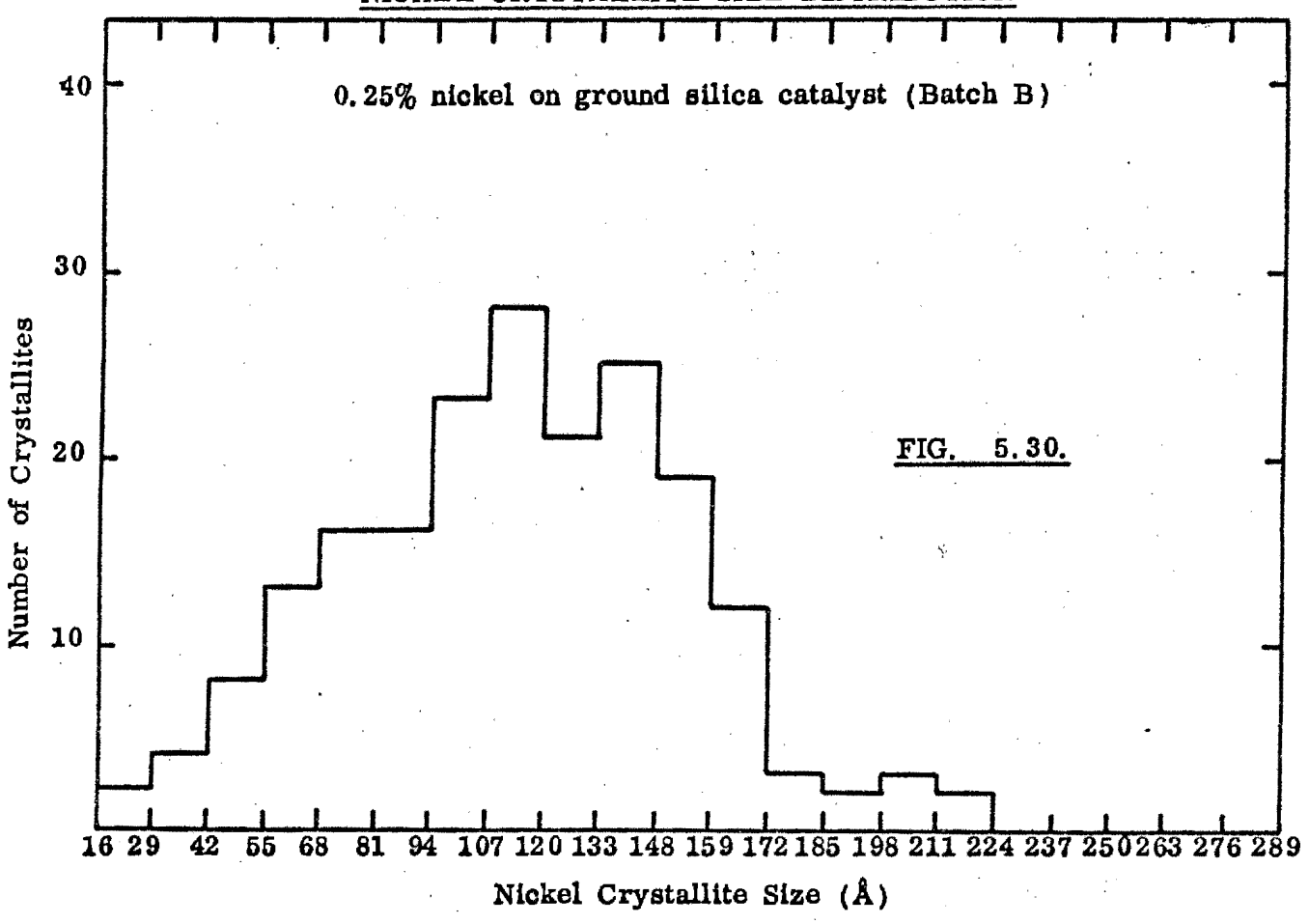

FIG. 5.30.

NICKEL CRYSTALLITE SIZE DISTRIBUTION

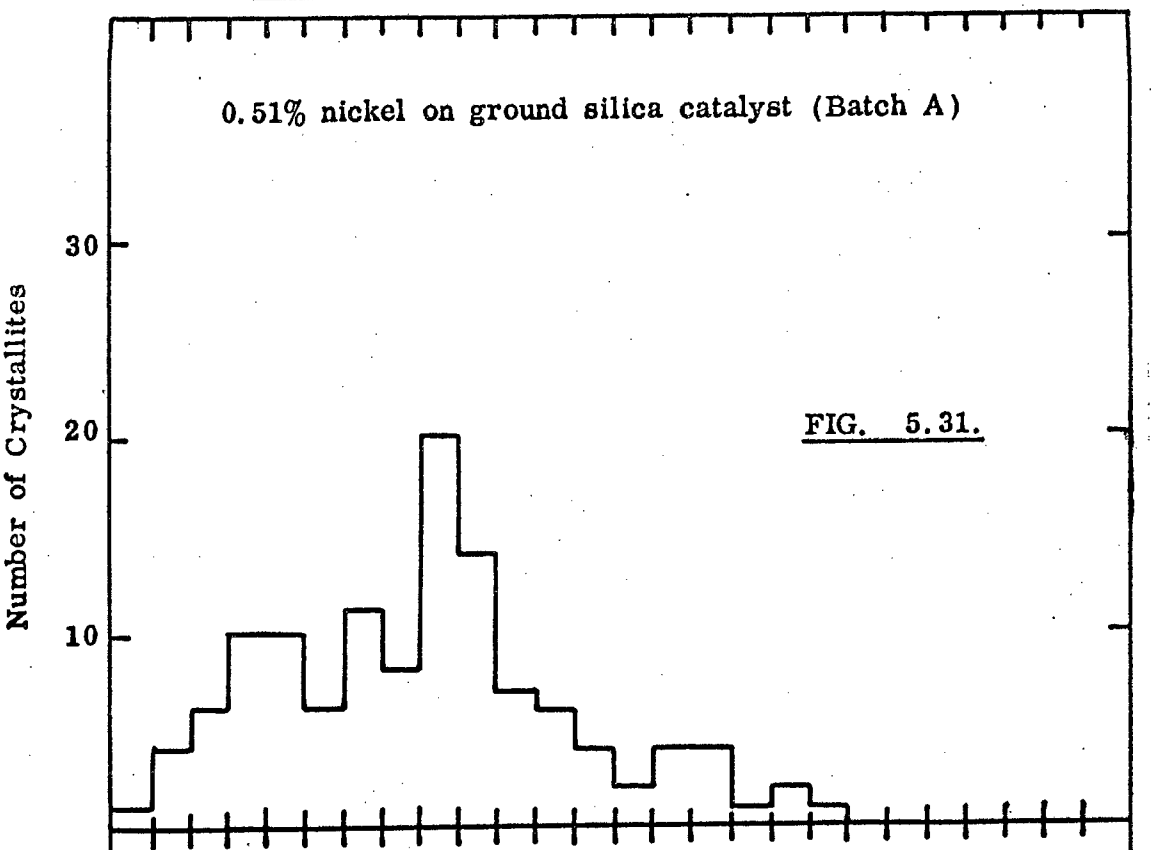

FIG. 5.31.

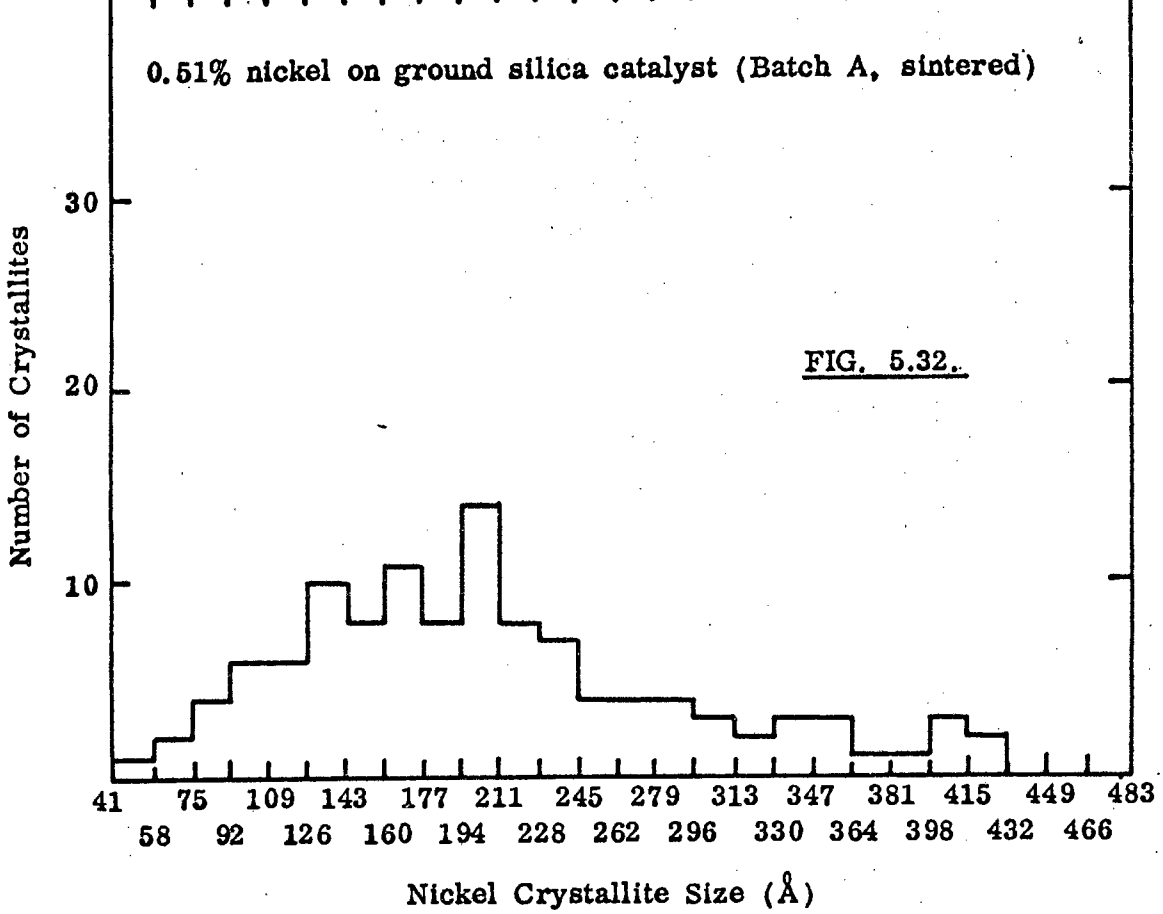

FIG. 5.32.

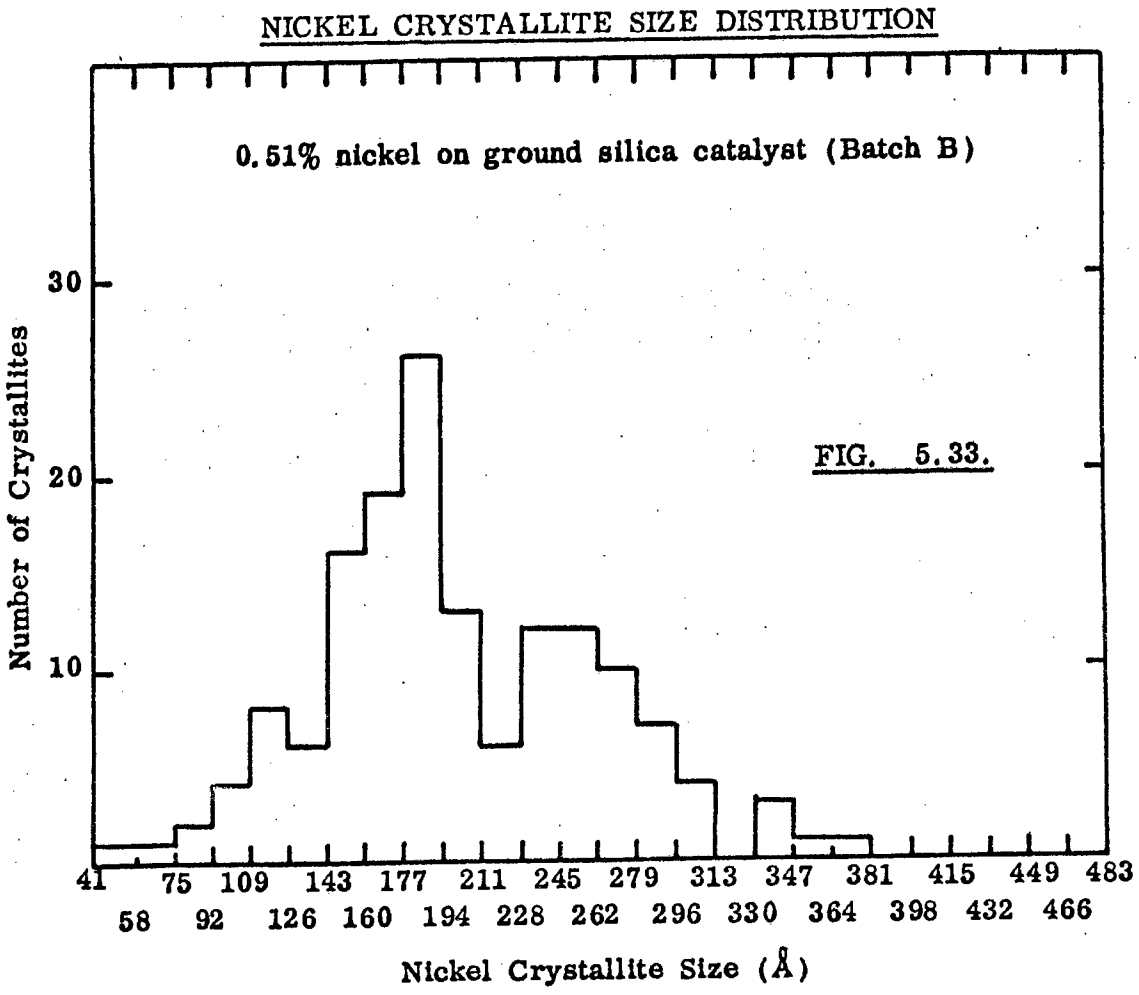
NICKEL CRYSTALLITE SIZE DISTRIBUTION
0.51% nickel on ground silica catalyst (Batch B)
Number of Crystallites
30
20
10
41 75 109 143 177 211 245 279 313 347 381 415 449 483
58 92 126 160 194 228 262 296 330 364 398 432 466
Nickel Crystallite Size (Å)

FIG. 5.33.

NICKEL CRYSTALLITE SIZE DISTRIBUTION

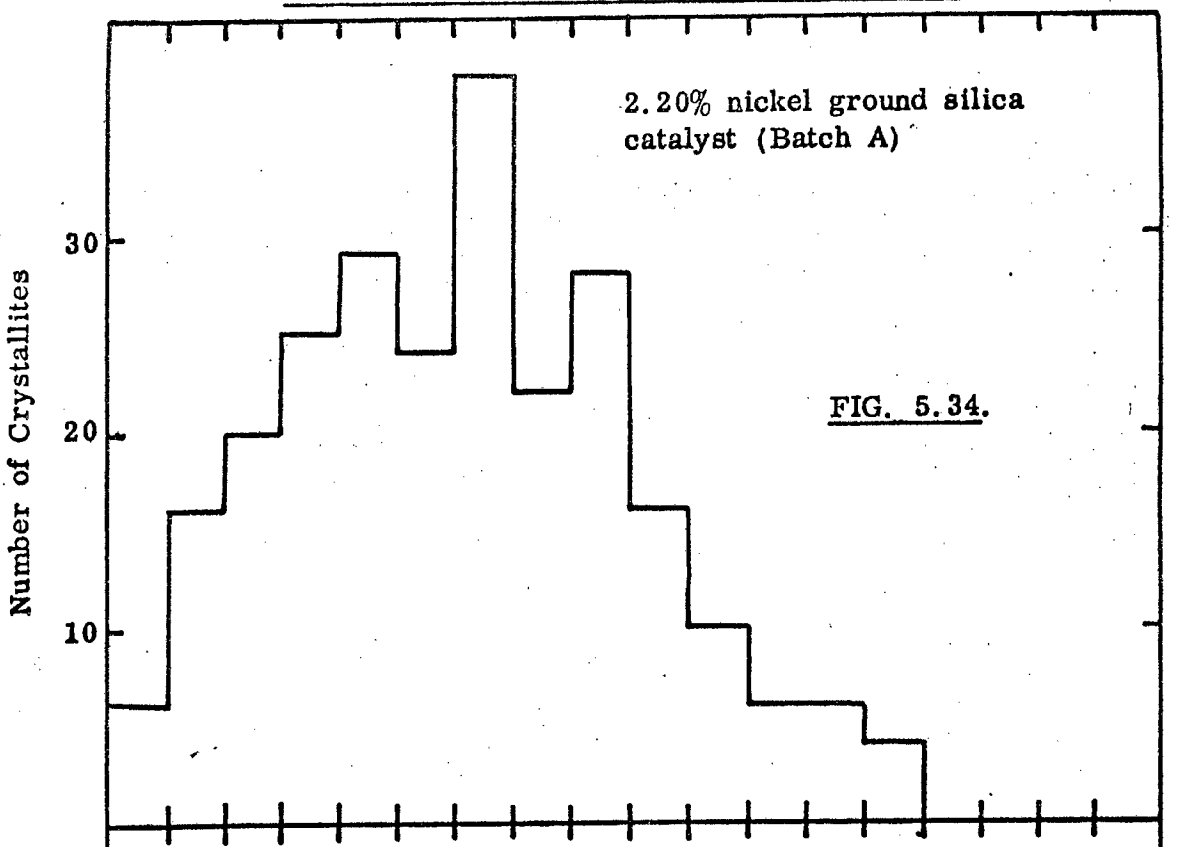

FIG. 5.34.

2.20% nickel on ground silica catalyst (Batch A, sintered)

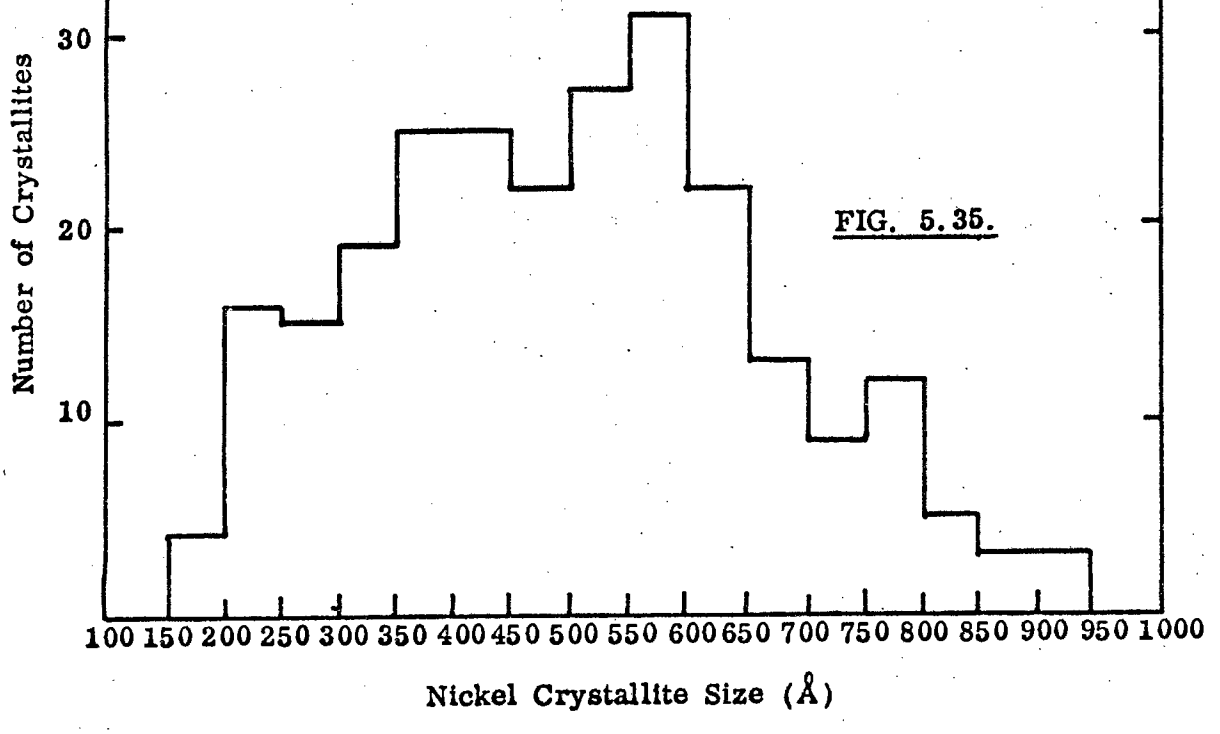

FIG. 5.35.

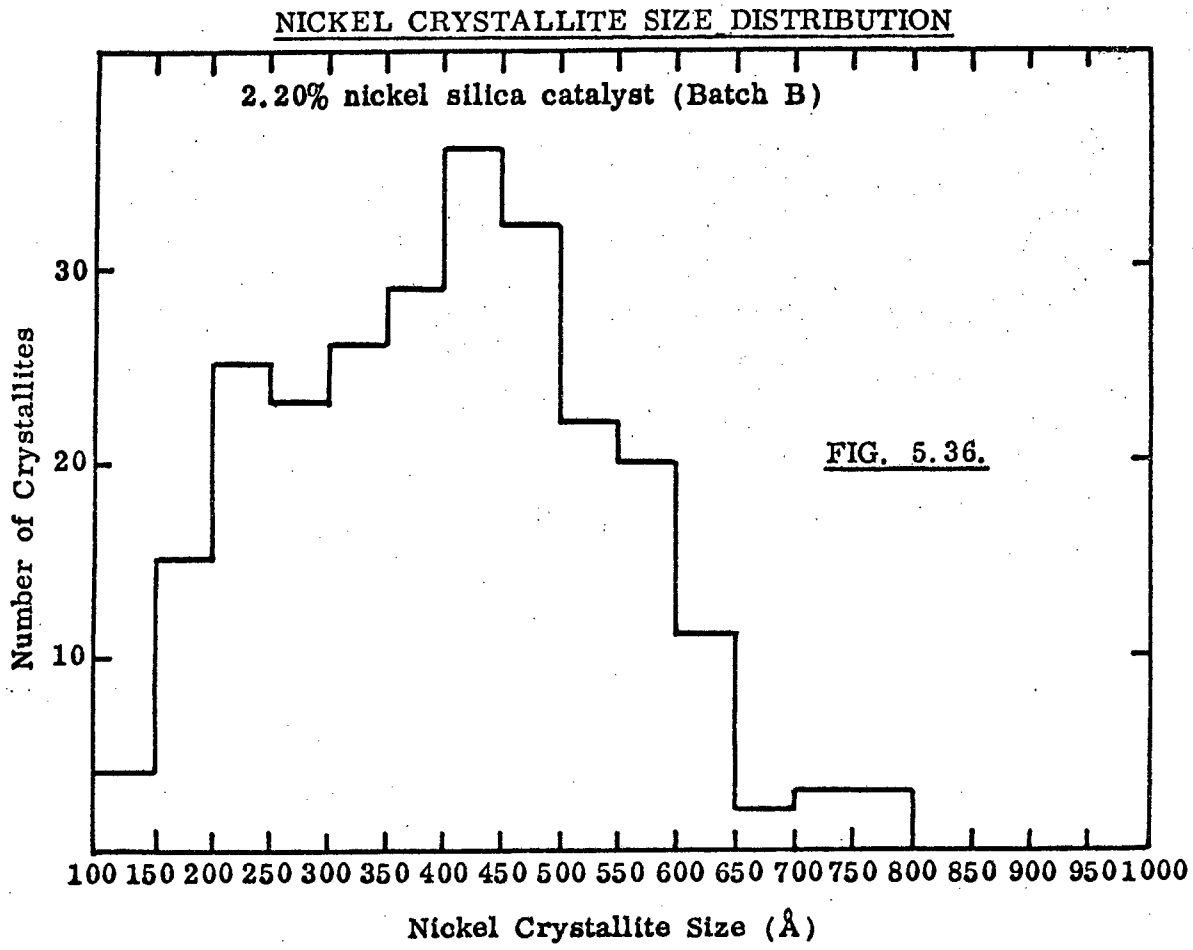
NICKEL CRYSTALLITE SIZE DISTRIBUTION
2.20% nickel silica catalyst (Batch B)
Number of Crystallites
30
20
10
100 150 200 250 300 350 400 450 500 550 600 650 700 750 800 850 900 950 1000
Nickel Crystallite Size (Å)

FIG. 5.36.

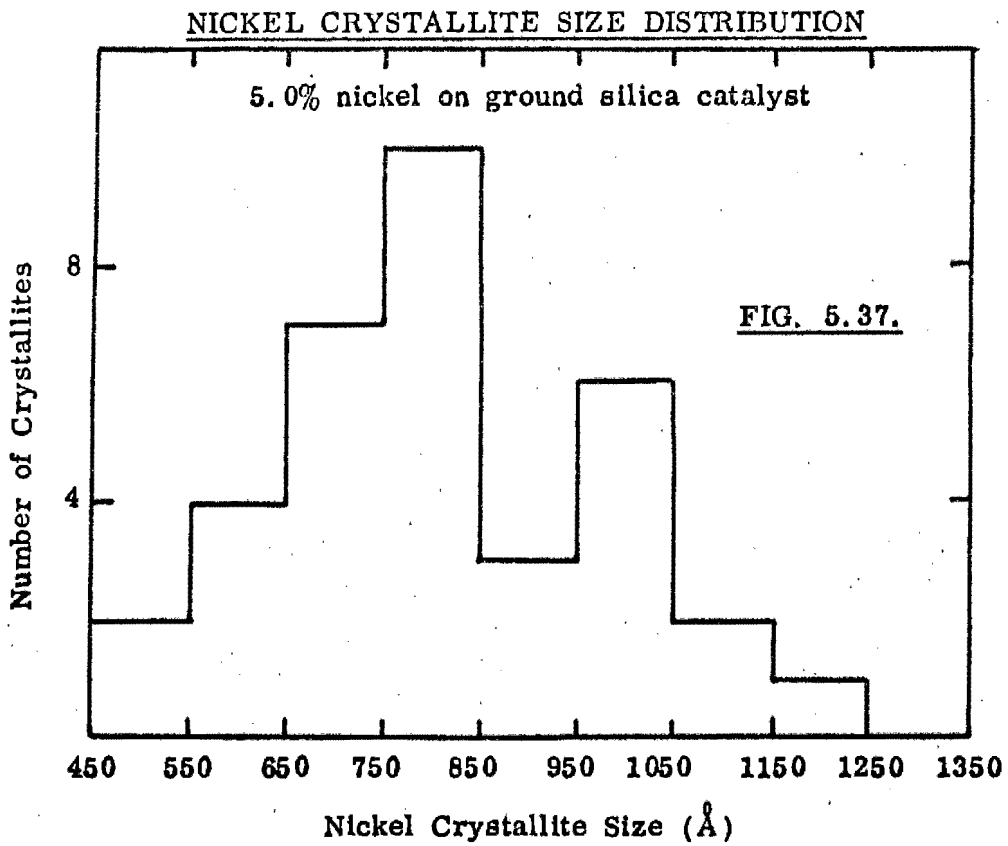

FIG. 5.37.

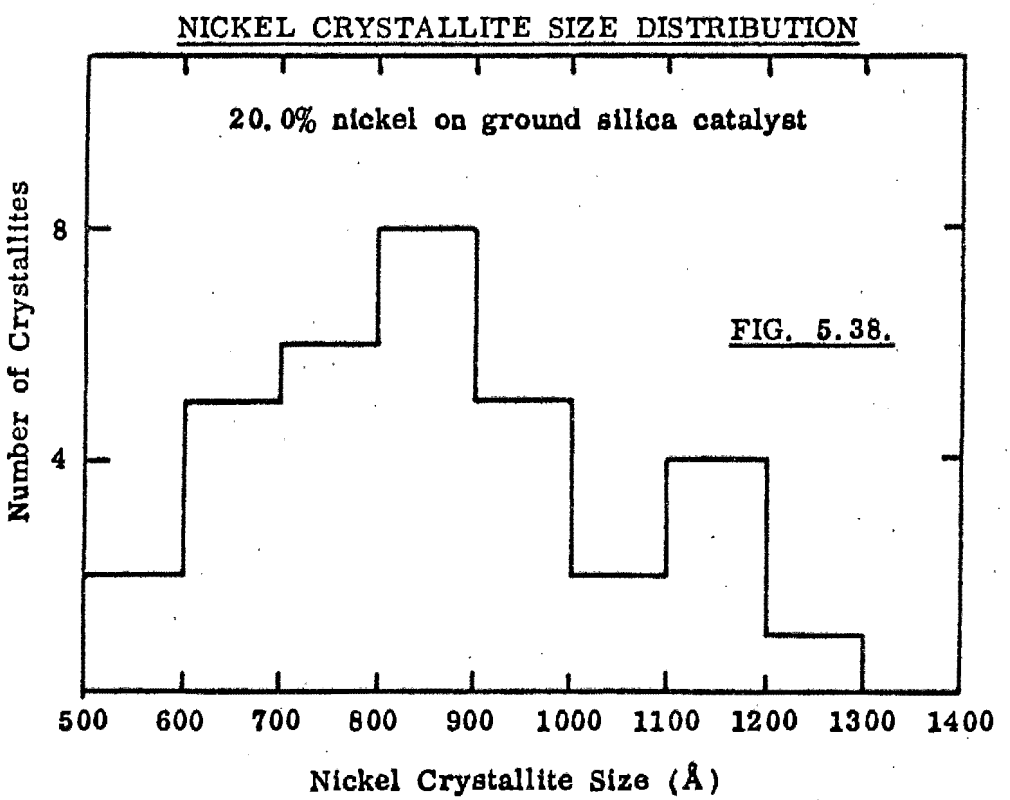

FIG. 5.38.

CHAPTER 6

GENERAL DISCUSSION

The first objective of the research project on which this thesis is based was to determine whether or not a support-metal interaction in a supported metal catalyst could be detected using heats of adsorption of hydrogen per unit metal area. As discussed in the introduction, the heat of adsorption per unit metal area is in effect a measure of the strength of the chemisorption bond between an adsorbate atom and a surface metal atom. If no support-metal interaction existed, one would not expect any change in this bond strength as the metal concentration in a supported metal catalyst was varied.

From figure 5.13, a plot of the isosteric heat of adsorption of hydrogen per unit metal area, Q_{st}, against coverage for a series of ground silica-supported nickel catalysts of different metal concentrations, it can be seen that detectable differences in Q_{st}, well outside the estimated experimental error (appendix 3), were found between the 0.25%, 0.51%, 2.20% and 5.00% nickel catalysts over the coverage range studied, namely $0.1 < \theta < 0.6$. Moreover this range of coverage of the surface of the catalysts is likely to be very much greater than those able to be investigated in kinetic studies.

The next objective was to investigate some of the factors involved in the support-metal interaction. From a plot of Q_{st} (at $\theta = 0.2$) against metal concentration (figure 6.1, page 191) for the unsintered catalysts, it can be seen that as the metal concentration is increased the magnitude of Q_{st} decreases rapidly until, at about 5% metal concentration, Q_{st} becomes independent of metal concentration. The onset of the independence of Q_{st} above a certain metal concentration may be explained in terms of the nickel crystallite sizes of

the catalysts. The two techniques used to measure the average crystallite size of the nickel are discussed in sections 4.3, 4.4 and 5.13. Figures 6.2 and 6.3 (pages 192 and 193) show curves of Q_{st} at $\theta = 0.2$ against average nickel crystallite size obtained from electron micrographic and X-ray diffraction line broadening measurements, respectively. From the curves it can be seen that as the nickel crystallite size increases, the magnitude of Q_{st} decreases. At an average metal crystallite size of about 500 Å, Q_{st} becomes independent of crystallite size.

On the basis of the information found in the literature, the hypothesis is presented in section 1.2 of this thesis that a particular crystallite size of the metal in a supported metal catalyst can be associated with maximum catalytic activity. It has been shown that if the average metal crystallite size is altered in either direction catalytic activity declines (Yates and Sinfelt, 1967). The catalytic activity of a catalyst depends on the strength with which the reactants are bound to the surface of the catalyst. If the bond is too strong, desorption will not occur easily and the catalyst surface will effectively be poisoned by the adsorbed species. On the other hand, if the bond is too weak, insufficient activation of the reactants will occur. The results of the current work fit this hypothesis, for the strength of the hydrogen chemisorption bond was shown to be a function of the average nickel crystallite size of the catalysts.

Aliquots of the 0.25%, 0.51% and 2.20% ground silica-supported catalysts were sintered at 500°C for 4 hours prior to reduction (section 3.3) in order to try to increase the average nickel crystallite size and to alter the nickel crystallite size distribution of the catalysts. On the basis of the dependence of

Q_{st} on the average nickel crystallite size found for unsintered catalysts, it was expected that an increase in the crystallite size would result in the lowering, at a particular coverage, of Q_{st} with respect to the value of Q_{st} for an unsintered catalyst of the same metal concentration. Average nickel crystallite sizes of the sintered catalysts were found, by X-ray diffraction line broadening, to be larger than those of the corresponding unsintered catalysts. The modes of the electron micrograph histograms obtained from the sintered catalysts were found to occur in a higher class interval than on the corresponding unsintered catalysts. However, contrary to expectations, no significant differences in the heats of adsorption per unit metal area were found for sintered and unsintered catalysts of the same metal concentration (figure 5.13). From the curves of Q_{st} plotted against average metal crystallite sizes (figure 6.2, curve b and figure 6.3) it can be seen that points corresponding to measurements made on sintered catalysts are anomalous in that they do not fall on the curve drawn through the points representing measurements made on the unsintered catalysts. However, if the curve of Q_{st} against the median of the electron micrograph histograms is plotted (figure 6.2, curve a), it is found that the points for the sintered and unsintered catalysts fall on a single curve. Symmetrical nickel crystallite size distributions were obtained for the unsintered catalysts, but in the case of the sintered catalysts the distributions were found to be slightly asymmetrical with the median slightly lower in value than the mode.

An understanding of why the points representing sintered catalysts in figures 6.3 and 6.2, curve b, are anomalous can be obtained as follows. The percentage of the total metal surface area of a catalyst given by metal crystallites

assumption is made that the most active sites on the catalyst surface are to be found on the surfaces of the smallest metal crystallites. If this is the case, the first amounts of hydrogen admitted to the catalyst would be expected to be adsorbed on these sites. Because of the relatively high activity of such sites, the bond strength of the resulting bond between the adsorbate atom and the metal atom will be large, thus giving rise to a high value of the heat of adsorption per unit metal area. As the catalyst concentration is increased, so the distribution of metal crystallite sizes changes to relatively larger sizes, the influence of the support is less strongly felt at the surface of the larger crystallites, and hence the surface sites on the metal may be less active. Above metal concentrations of about 5%, even the smallest metal crystallites are so large, that the support is unable to influence the activity of the metal atoms in the surface of the metal crystallites. Thus a constant heat of adsorption per unit metal area is obtained for catalysts in which the metal concentration exceeds about 5%. On the assumption that adsorption occurs on the smaller crystallites first, a more or less common heat of adsorption per unit metal area can be expected at high coverages. At such coverages adsorption on large metal crystallites will be taking place, and under these circumstances, since no influence of the support on the activity of the surface metal atoms can be felt, a common value of the heat is expected. This argument explains the convergence of the heat curves in figure 5.13.

Reverting to the problem of the anomalies displayed by the sintered catalysts, if the hypothesis that adsorption occurs on the smaller metal crystallites in the first instance is valid, then at a surface coverage correspond-

ing to a situation where all crystallites of size below the size represented by the class interval in which the median crystallite size falls, the fraction of the total metal surface covered by adsorbate atoms in both sintered and unsintered catalysts is the same (table 6.1). It is not unreasonable to expect therefore that the heat of adsorption per unit metal area corresponding to this coverage will have the same value for both sintered and unsintered catalysts. Thus although sintering did result in a decrease in the metal surface areas of the catalysts, no change in the heat of adsorption per unit metal area could be detected.

Isosteric heats of adsorption of hydrogen per unit metal area were also determined for two Cabosil-supported nickel catalysts of 1.9% and 5.5% metal concentrations. These determinations were made in order to find out whether the convergence of the heat curves as θ tends to 1 (figure 5.13) was a phenomenon confined only to ground silica-supported nickel catalysts or whether it was displayed by catalysts containing other forms of silica as support. No electron micrographs of the catalysts were obtained but average nickel crystallite sizes were determined using X-ray line broadening.

Although on extrapolation the heat curves did intersect, the intersection did not occur at $\theta = 1$ but at about $\theta = 1.4$. Two possible explanations for this phenomenon can be put forward. Since no investigation of whether the criteria for maximum hydrogen coverage discussed in section 5.7 were valid for the Cabosil-supported nickel catalysts, it is possible that if pressures in excess of 40 torr were used, more hydrogen would have been adsorbed by the

catalysts. In such a case the estimate made of full surface coverage would in fact correspond to a coverage of less than $\theta = 1$. Hence the abscissa of the point at which the heat curves do intersect may well represent full coverage of the metal surface. On the other hand, since Cabosil has an extremely large surface area (340 m^2/g), at the relatively low metal concentrations used, it is likely that very little, if any of the metal is present in crystallites of size greater than 500 Å. (This was approximately the crystallite size above which no differences in the hydrogen chemisorption bond strength could be detected using the ground silica-supported catalysts). Thus when the metal surface is almost completely covered, even if further adsorption occurs on the largest crystallites, the interaction between the metal and the support will still influence the bond strength. Different crystallite size distributions on the two Cabosil-supported catalysts may thus result in different values of Q_{st} even at $\theta = 1$.

From figure 6.3 it can be seen that points representing the two Cabosil catalysts on the graph of Q_{st} against average metal crystallite size as determined by X-ray line broadening fall very far off the curve connecting the points representing the unsintered ground silica-supported catalysts. The only explanation the author can put forward to account for this large discrepancy is that in the case of the Cabosil-supported nickel catalysts an unknown factor may have an influence on the effect the metal crystallite size has on the interaction between the metal and the support in the Cabosil-supported catalysts. Further studies on the Cabosil catalysts may prove rewarding in elucidating the nature of this factor.

In the case of the ground silica-supported catalysts discussed in this thesis, all the nickel was found to be in the metallic state (section 4.5). Thus the presence of metal ions combined with the support appears not to be a factor which influences the nature or extent of the interaction between the support and the nickel in the ground silica-supported nickel catalysts. The work of Peri (1966) pointed to the existence of incompletely coordinated metal ions in Cabosil-supported nickel catalysts. However, as Peri himself pointed out, spectroscopic data (from which he drew his conclusions) are difficult to interpret unambiguously, and the evidence obtained using the nickel carbonyl formation technique leads one to the conclusion that when silica is used as a support, only very small fraction (less than 1%), if any, of the nickel is chemically associated with the support in the form of nickel ions. The absence of such ions need not necessarily rule out the existence of an interaction between the metal and the support. Some sites on the silica surface may be more active than others and nickel impregnated on such sites might conceivably have an enhanced activity, the effect manifesting itself most strongly when the metal crystallite size of the catalyst is small.

In the case of catalysts containing alumina in the support, appreciable fractions of metal ions have been found (Swift et al, 1965; 1966). The presence of these ions could be expected to influence the interaction between the metal and the support. The current research project could be usefully extended by determining heats of adsorption per unit metal area on alumina- and silica-alumina-supported nickel catalysts which had been characterised by the techniques discussed in chapter 4 of this thesis. Such a study may well shed more light on the factors which influence the interaction between a metal and its support in a supported

metal catalyst.

Further research work which may have helped to support the conclusions drawn in this thesis could have included the determination of the isosteric heats of adsorption of hydrogen per unit metal area on sintered ground silica-supported nickel catalysts of 5% and 20% metal concentrations. No differences between the heats on the sintered and unsintered catalysts would be expected since the unsintered catalysts have an average nickel crystallite size well in excess of 500 Å (table 5.2), the value above which no support-metal interaction was detectable. Sintered catalysts of these concentrations would have even larger average nickel crystallite sizes and hence an unchanged heat would be expected.

In conclusion it may be stated that the data obtained in the current research project indicate that in ground silica-supported nickel catalysts an interaction between the metal and its support exists. The results fit the hypothesis that the crystallite size of the metal affects this interaction and the hypothesis that maximum catalytic activity can be associated with a particular metal crystallite size. Any possible confounding of the metal crystallite size effect because of the porous structure of the support was eliminated by use of a non-porous support.

It is felt that the current research project may be usefully extended by determining isosteric heats of adsorption of hydrogen per unit metal area on well-characterised alumina- and silica-alumina-supported nickel catalysts as well as Cabosil-supported nickel catalysts.

A suggested modification to the high vacuum apparatus is described in appendix 4.

ISOSTERIC HEAT OF ADSORPTION OF HYDROGEN PER UNIT METAL AREA AS A FUNCTION OF METAL CONCENTRATION

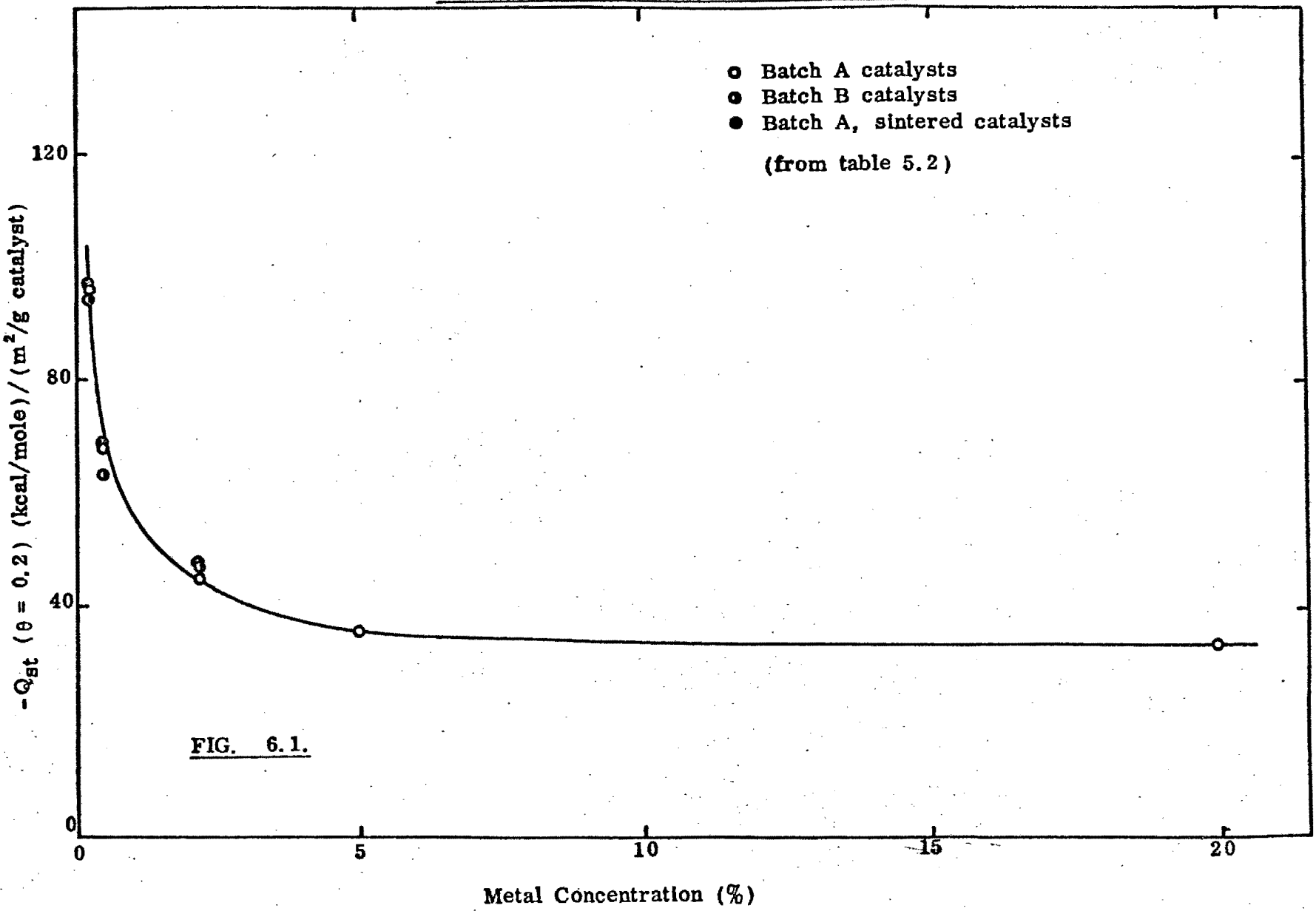

FIG. 6.1.

ISOSTERIC HEAT OF ADSORPTION OF HYDROGEN PER UNIT METAL AREA AS A FUNCTION OF NICKEL CRYSTALLITE SIZE (ELECTRON MICROSCOPY)

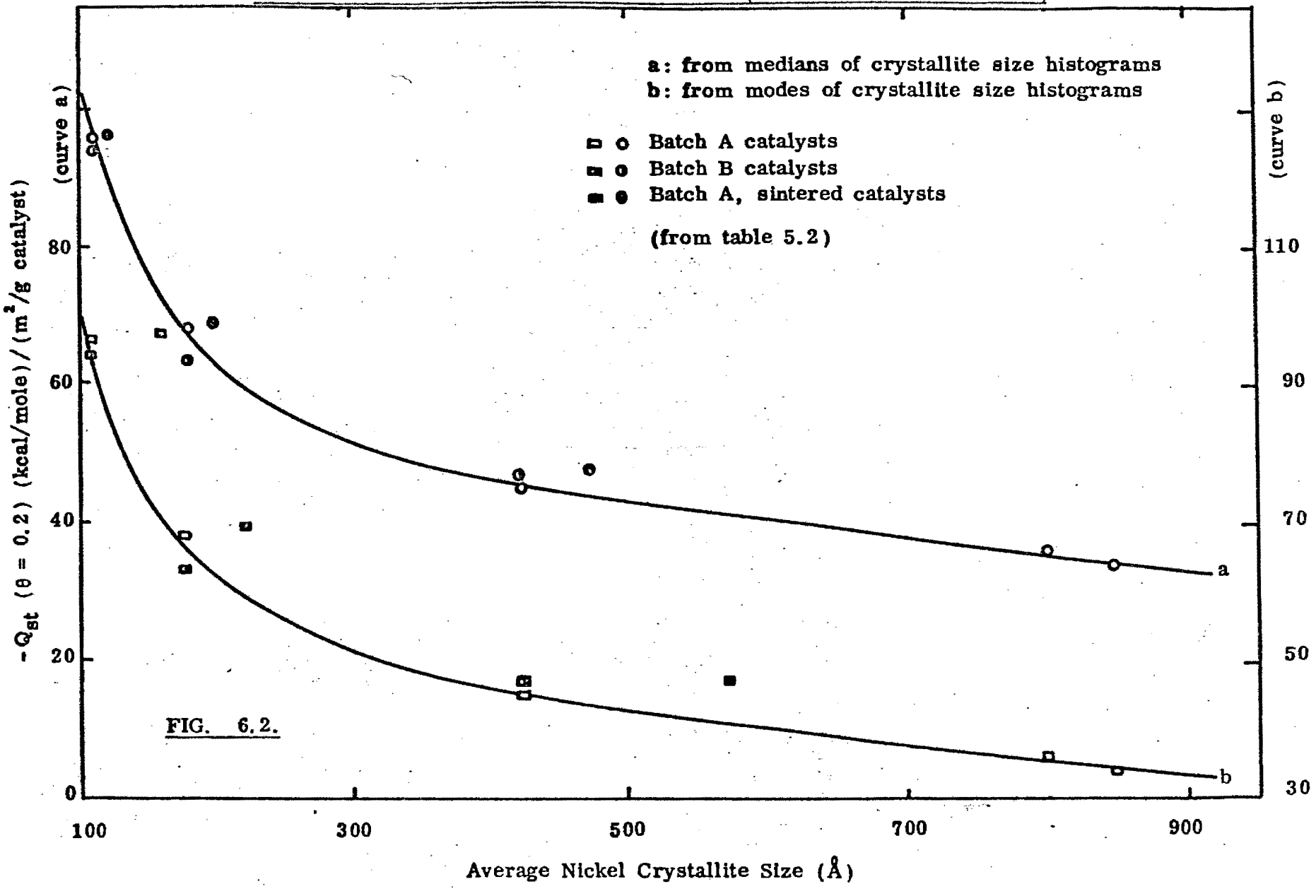

FIG. 6.2.

ISOSTERIC HEAT OF ADSORPTION OF HYDROGEN PER UNIT METAL AREA AS A FUNCTION OF NICKEL CRYSTALLITE SIZE (X-RAY LINE BROADENING)

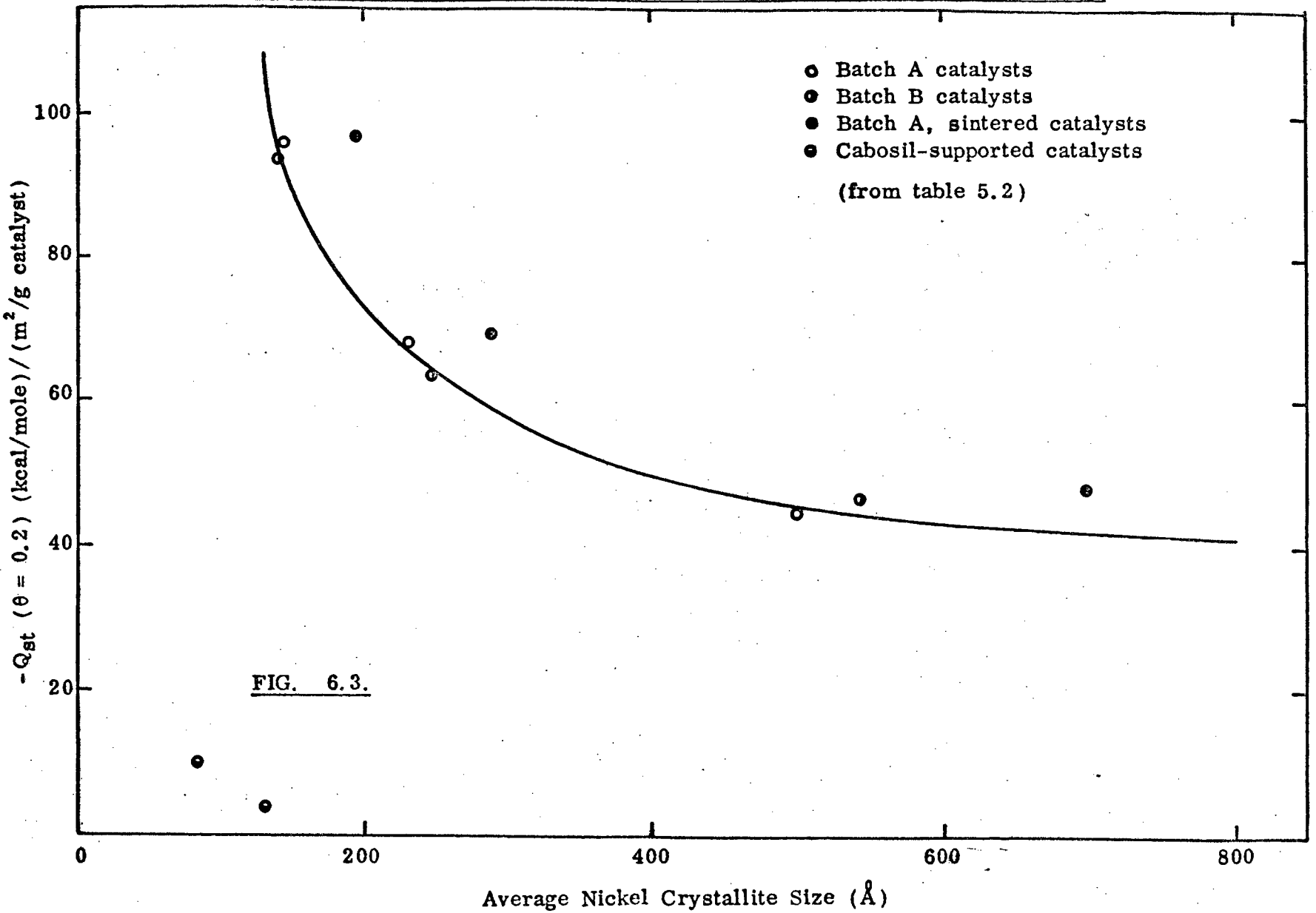

FIG. 6.3.

NICKEL CRYSTALLITE SIZE DISTRIBUTION

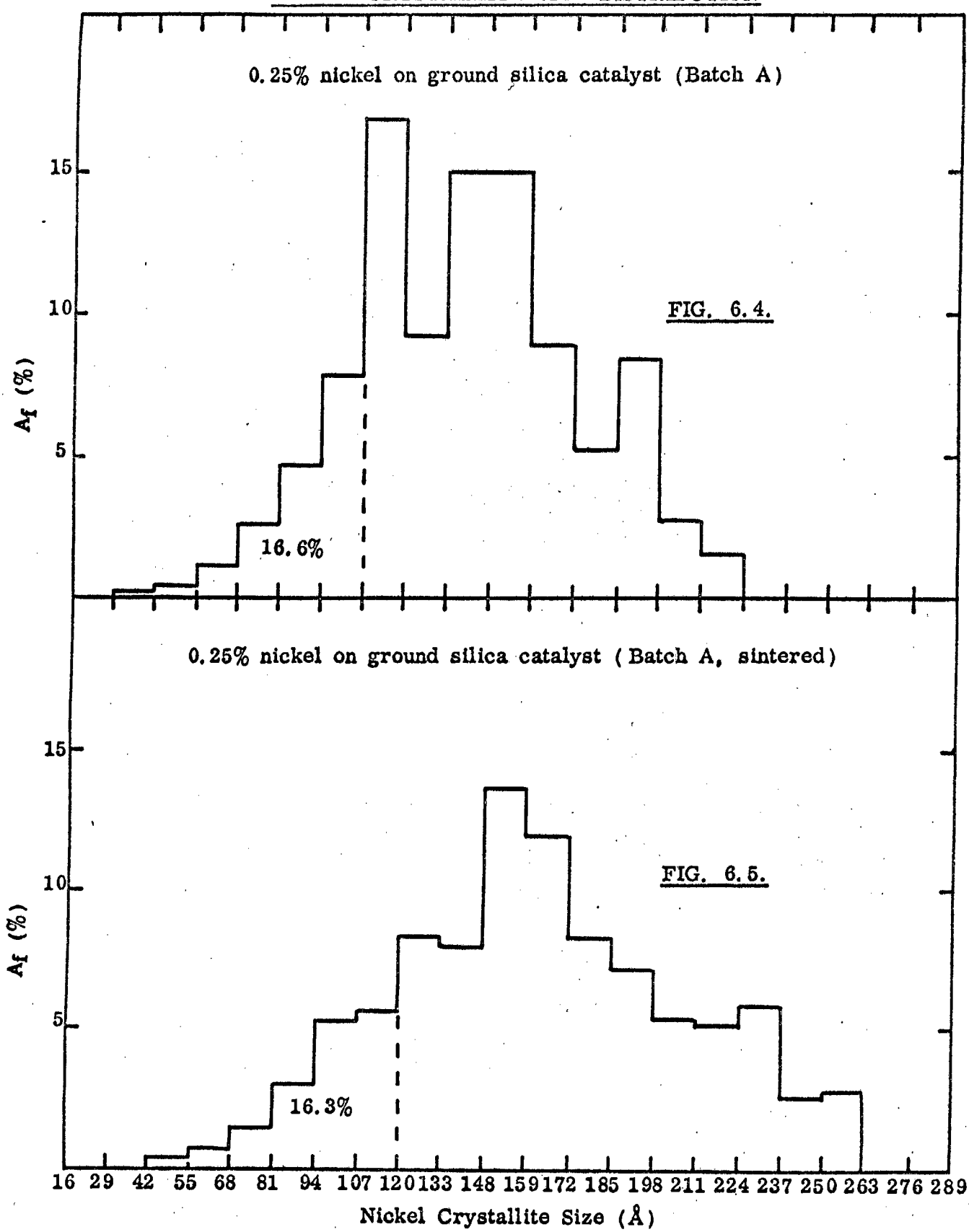

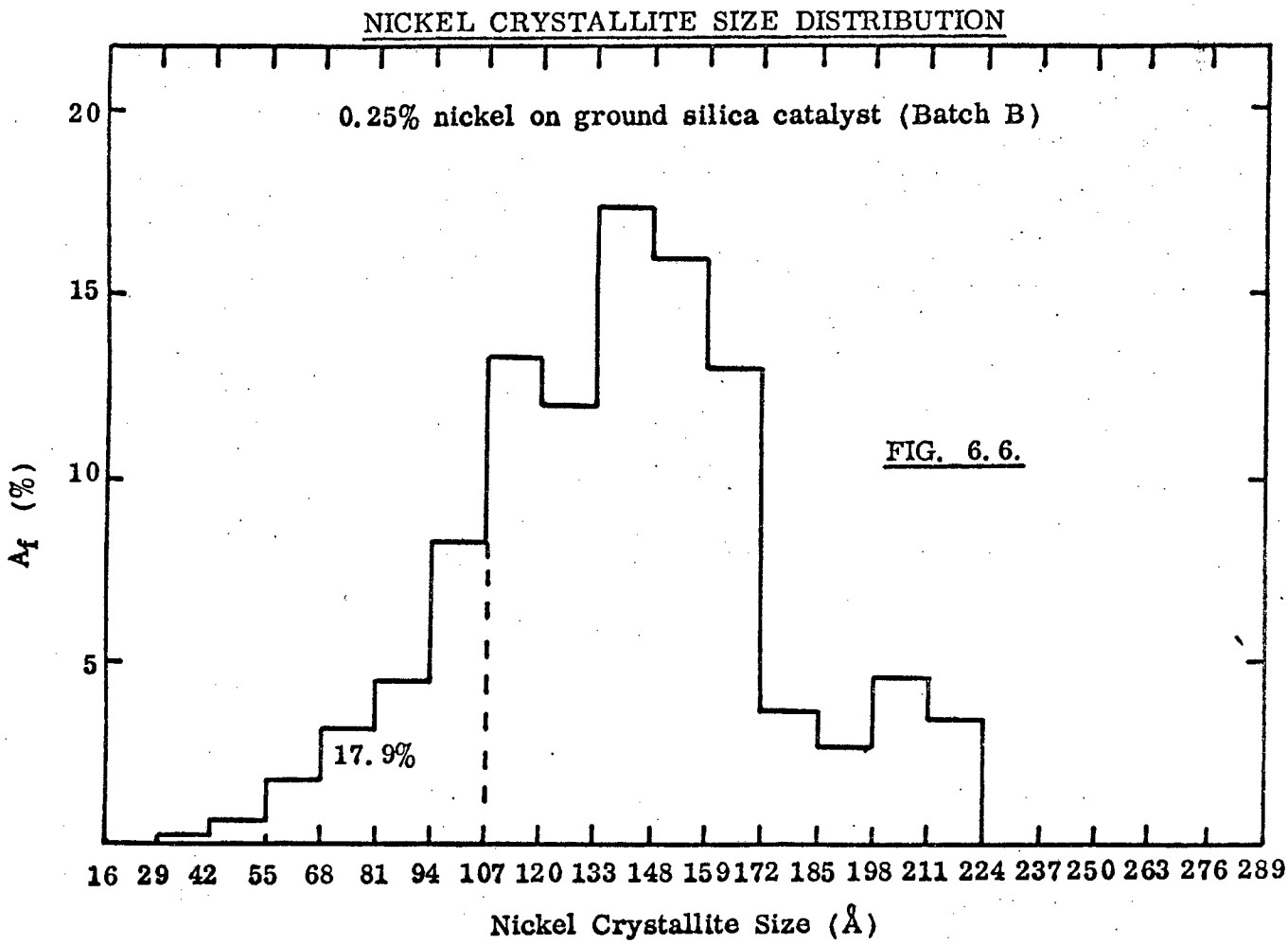
NICKEL CRYSTALLITE SIZE DISTRIBUTION
0.25% nickel on ground silica catalyst (Batch B)
20
15
10
5
A_f (%)
17.9%
16 29 42 55 68 81 94 107 120 133 148 159 172 185 198 211 224 237 250 263 276 289
Nickel Crystallite Size (Å)

FIG. 6.6.

NICKEL CRYSTALLITE SIZE DISTRIBUTION

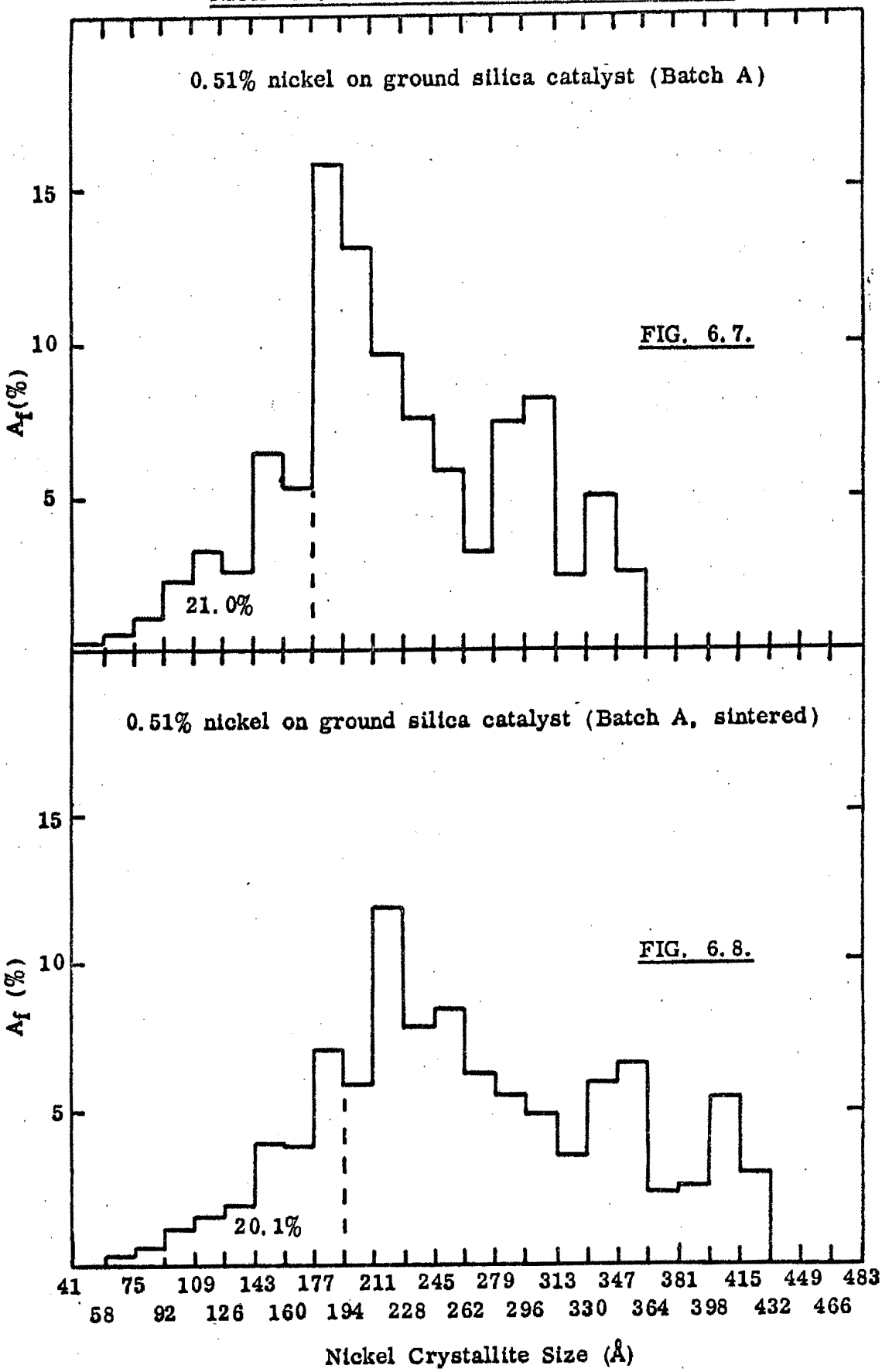

FIG. 6.7.

FIG. 6.8.

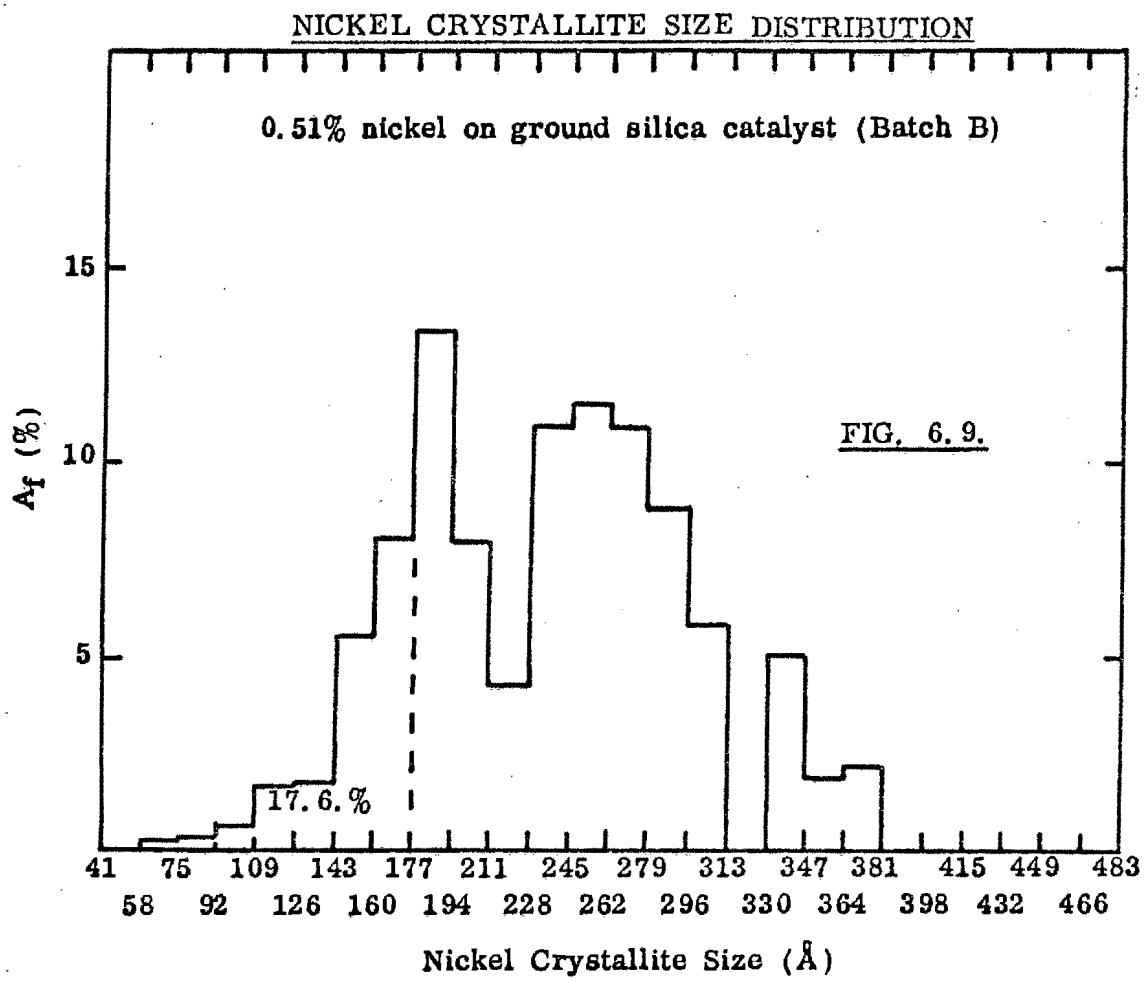
NICKEL CRYSTALLITE SIZE DISTRIBUTION
0.51% nickel on ground silica catalyst (Batch B)
15
10
5
A_f (%)
17.6.%
41 75 109 143 177 211 245 279 313 347 381 415 449 483
58 92 126 160 194 228 262 296 330 364 398 432 466
Nickel Crystallite Size (Å)

FIG. 6.9.

NICKEL CRYSTALLITE SIZE DISTRIBUTION

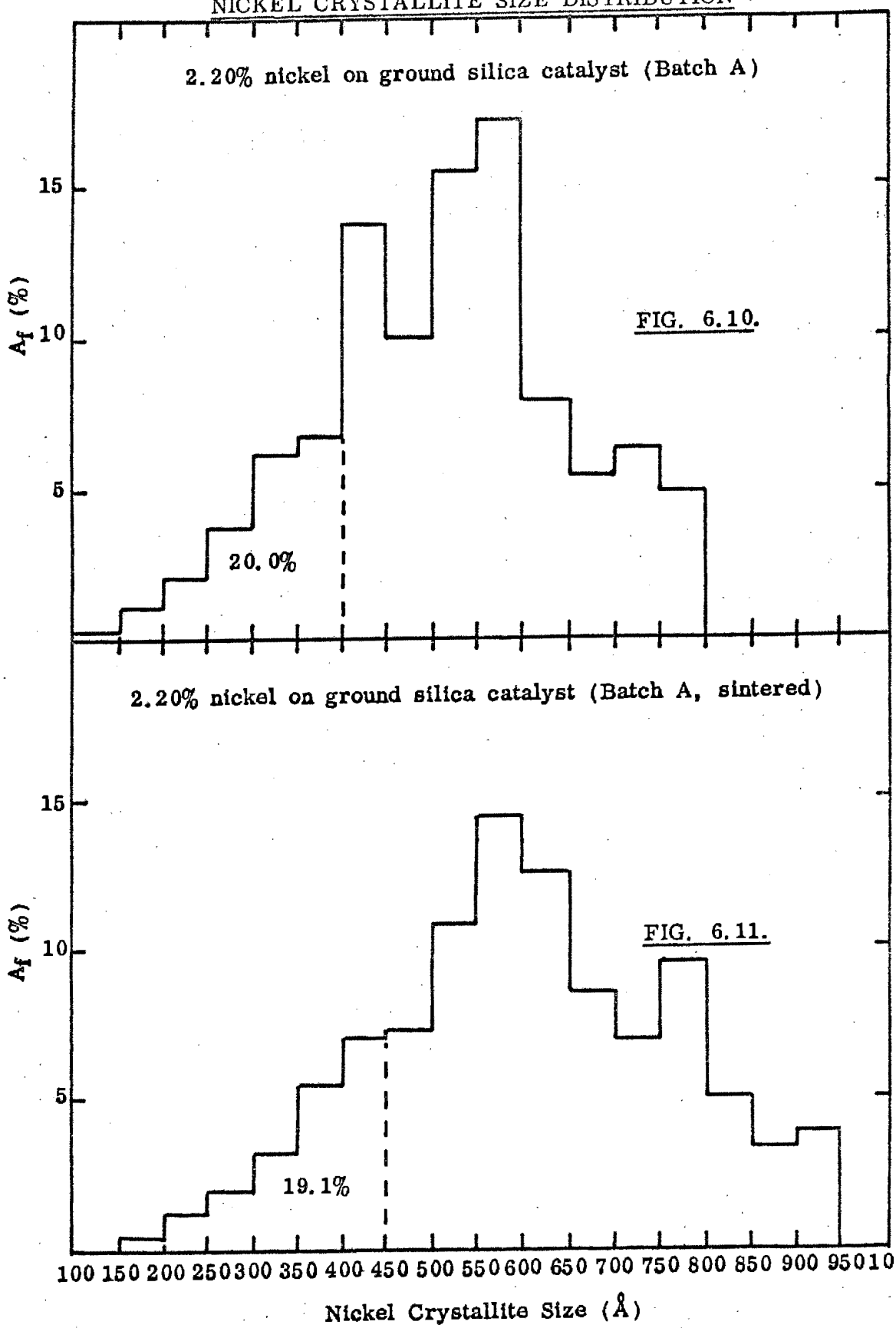

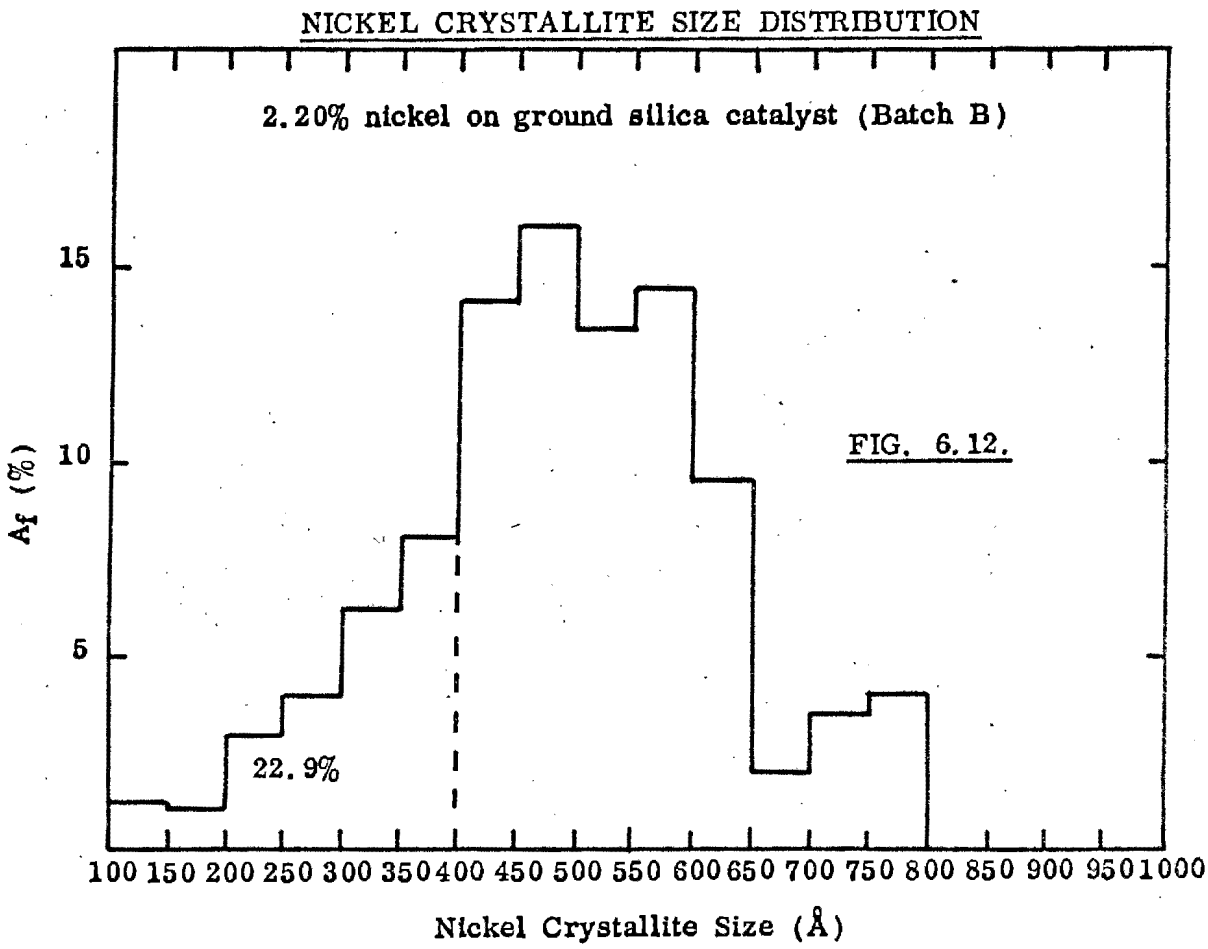
NICKEL CRYSTALLITE SIZE DISTRIBUTION
2.20% nickel on ground silica catalyst (Batch B)
15
10
5
A_f (%)
22.9%
100 150 200 250 300 350 400 450 500 550 600 650 700 750 800 850 900 950 1000
Nickel Crystallite Size (Å)

FIG. 6.12.

APPENDIX 1

THE NATURE OF THE CARBON MONOXIDE TO METAL BOND IN SUPPORTED METAL CATALYSTS

Eischens, Pliskin and Francis (1954) observed two distinct bands in the infra-red spectrum of carbon monoxide adsorbed on silica-supported nickel, palladium, and platinium catalysts. These bands are due to the C=O bond. The higher the frequency of the band, the stronger is the C=O bond and, correspondingly, the weaker the metal to carbon bond. By analogy with the well defined spectra of the metal carbonyls, Eischens et al attributed the bands to two distinct types of bonding between carbon monoxide molecules and the metal surface. They suggested that the one band, occurring at about 2100 cm^{-1} (designated band A), was due to an adsorbate molecule bound to one metal atom ("linear" form) and that the other band, occurring at about 1900 cm^{-1} (designated band B), was due to carbon monoxide molecules being bound to two metal atoms ("bridged" form). This postulate was supported by O'Neill and Yates' work (1961a) as well as by that of Yates and Garland (1961). In contrast to Eischens, Pliskin and Francis (1954), however, Blyholder (1964) considered the chemisorption of carbon monoxide on metals in the light of Hückel molecular orbitals for the metal-carbon-oxygen bonds. This model is claimed to explain qualitatively the existence of two spectral bands, both of which are attributed to linear carbon monoxide molecules. According to this molecular orbital view, the band A is due to carbon monoxide adsorbed on regular crystal faces where the adsorbent metal atoms have a high coordination number, whilst band B represents carbon monoxide adsorption on sites where the metal atoms have a somewhat lower coordination number, for example at edges of planes, corners and at dislocations.

The occurrence of several overlapping bands in both regions was observed by Yates and Garland (1961), who interpreted the bands as representing differing adsorption bond strengths of both linear and bridged carbon monoxide. On the other hand Blyholder (1964) explained the existence of the multiplicity of overlapping bands in both regions by postulating that they are the result of there being a number of different types of sites corresponding to both regions. Eischens and Pliskin (1958) reported that band B was more intense and band A was broader on alumina as compared to silica-supported platinum. Blyholder (1964) claimed that these results can be interpreted on the basis of the crystallinity of the metal. Because of the reported greater difficulty in reducing the alumina-supported metal, he supposed the alumina-supported platinum to be a little less crystalline than the silica-supported platinum so that "the ligand platinum atoms are less effective in competing for electrons in these samples, with the result that the C=O frequency is lower".

Yang and Garland (1957) observed that when alumina-supported rhodium was sintered, the low frequency band (B), assigned by Eischens, Pliskin and Francis (1954) to bridged adsorbate molecules, decreased in intensity. Blyholder explained this by arguing that sintering increases the degree of crystallinity of the metal, thereby decreasing the number of metal sites of low coordination number. Thus fewer bonds between such metal atoms and carbon monoxide molecules can exist under the particular set of experimental conditions, which therefore results in a decrease in the intensity of the band due to carbon monoxide bound in this fashion.

Ferreira and Leisegang (1969) refuted Blyholder's suggestion that the lower frequency bands can be assigned to strongly held linear ligands adsorbed on edges, corners or dislocations. They presented the following evidence in support of their objection. Band B appeared first at very low coverage and persisted tenaciously on evacuation of the cell, conditions which are optimum for sharing of metal sites by one ligand without competition from other ligands. As the pressure of carbon monoxide was increased above about 0.5 torr, the intensity of B diminished with pressure, indicating that bidentate ligands were being displaced by terminal ligands. On evacuation, this was reversible. Addition of ammonia during preparation of the catalysts was claimed by Ferreira and Leisegang to yield less crystalline samples. With these samples, band B was shifted to lower frequencies, consistent with a larger M-C-M bond angle as shown empirically by Halford (1956) for ketones. Sintering of the samples resulted in a shift of band B toward higher frequencies, in agreement with the expected smaller bond angles.

Further refutation of the Blyholder theory comes from a study by Cormack and Moss (1969). They studied the desorption of carbon monoxide from silica-supported platinum catalysts of varying metal concentrations. Carbon monoxide labelled with carbon-14 was used and the desorption followed with the aid of a Geiger-Müller tube. Their results confirmed the work of Eischens and Pliskin (1958) on supported palladium and Yates and Garland (1961) on supported nickel, in that they found that carbon monoxide could be bound to the metal surface in two distinct ways on the basis of

strengths of bonding. They found that the weaker mode decreased in extent as the crystallite size of metal increased. Thus the Blyholder theory and the results of Cormack and Moss as well as those of Eischens and Pliskin (1958) and Yates and Garland (1961) appear to be in conflict. This problem was resolved by Cormack and Moss who supposed that linear bonding was indeed stronger on atoms of low coordination number than on atoms of high coordination number, but that on crystal faces, because of neighbouring metal atoms, the linear species gives way to a bridge-bonded species which is even more strongly held.

On the basis of the evidence presented above, it appears quite reasonable to accept the postulate of the existence on a catalyst surface of both linear and bridged carbon monoxide molecules.

APPENDIX 2

THERMAL TRANSPIRATION

When a pressure measuring gauge is at a different temperature from that of another portion of a vacuum apparatus, gas tends to pass from the cooler to the warmer region. A steady state is reached when the pressure difference between the two regions is sufficient to balance this thermal transpiration (Ross and Olivier, 1964). Thus in the determination of an adsorption isotherm, thermal transpiration causes the measured equilibrium pressure, p_r, to be greater or lower than the true value, p_t, depending on whether the temperature of the adsorbent is lower or higher than that of the pressure gauge.

Knudsen (1910) has shown that when the mean free path of the gas molecules is very much greater than the diameter of the connecting tubing that is subject to the temperature gradient, the following relationship holds:

$$\frac{p_t}{p_r} = \left(\frac{T_t}{T_r}\right)^{\frac{1}{2}} \qquad \text{A. 2. 1.}$$

Increasing the pressure results in a decrease in the mean free path of the gas molecules and equation A. 2. 1 becomes invalid. Similarly if the diameter of the connecting tubing is increased, equation A. 2. 1 may again become invalid. In general, failure of equation A. 2. 1 occurs when the mean free path is less than about 20 times the diameter of the tube. For hydrogen gas, if the connecting tubing has a diameter of 0. 3 cm, equation A. 2. 1 only holds for pressures below about 10^{-3} torr. Above pressures of about 10 torr, no correction to the measured pressures need be applied (Podgurski and Davis, 1961). In the intermediate pressure range, Bennett and Tompkins

(1957) recommend the use of the following version of the equation of Liang (1955).

$$R_t = \frac{p_t}{p_r} = \frac{\alpha_{He}(f\phi_g p_r d_t)^2 + \beta_{He}(f\phi_g p_r d_t) + R_m}{\alpha_{He}(f\phi_g p_r d_t)^2 + \beta_{He}(f\phi_g p_r d_t) + 1} \qquad \text{A. 2. 2.}$$

Bennett and Tompkins (1957) give the following equations for α_{He} and β_{He}

$$\alpha_{He} = 3.70\left[1.70 - 2.6 \times 10^{-3}\ (T_r - T_t)\right]^{-2} \qquad \text{A. 2. 3.}$$

$$\beta_{He} = 7.88(1 - R_m) \qquad \text{A. 2. 4.}$$

Because $R_m \leqslant 1$, equation A. 2. 2 is suitable for use when $T_t \leqslant T_r$. Accordingly, equation A. 2. 2 was used in the work of this thesis to correct equilibrium pressures of krypton in krypton adsorption isotherms (section 3. 4. 2).

Podgurski and Davis (1961) published an empirical curve ($p_r d_t$ against p_r/p_t) for thermal transpiration corrections for hydrogen gas at T_t 478°K and T_r 299°K. With a knowledge of p_r and d_t, direct interpolation of the ratio p_r/p_t is possible. For the hydrogen adsorption isotherms in this thesis (section 3. 4. 1) measured at temperatures in the range 453°K to 513°K, corrections for thermal transpiration were applied using the curve of Podgurski and Davis. In the isotherms measured at 453°K and 513°K this procedure resulted in an estimated error of the order of 2% in p_t, since the curve of Podgurski and Davis was determined at 478°K.

APPENDIX 3

ESTIMATION OF ERRORS IN THE EXPERIMENTAL HEATS OF ADSORPTION

A.3.1.

General Considerations:

In order to be able to decide whether two experimentally determined values of a variable are significantly different or not, it is essential to make an estimate of the experimental error incurred in determining such values. In particular, in this thesis it was necessary to have an estimate of the experimental error incurred in determining heats of adsorption in order to decide whether or not heats of adsorption obtained for the various catalysts studied were significantly different.

The method used to estimate the error in the heat of adsorption is that of the propagation of errors, in which the errors in all measured quantities are supposed to be independently variable. This assumption is usually valid in most physical and chemical work. Using the concept of the propagation of error, Pantony (1961) derived the following equations which can be applied to most propagated error.

If the results of say three measurements, x, y, and z, are combined in a formula to give an overall figure, Q, by an equation of the form,

$$Q = \pm x \pm y \pm z \qquad \text{A.3.1.}$$

then the absolute error in Q can be represented by the equation,

$$e_Q = \pm \sqrt{e_x^2 + e_y^2 + e_z^2} \qquad \text{A.3.2.}$$

If the computed quantity Q is related to the measurements x, y and z by an equation of the form,

$$Q = x^{X}.y^{Y}.z^{Z}, \qquad A.3.3.$$

in which the indices may be either positive or negative, then the relative error in Q can be represented by the equation,

$$E_Q = \pm\sqrt{X^2E_x^2 + Y^2E_y^2 + Z^2E_z^2} \qquad A.3.4.$$

e_Q and E_Q are related by the equation,

$$e_Q = QE_Q \qquad A.3.5.$$

In order to estimate the error in the heat of adsorption, it is first necessary to estimate the errors in determining pressures using the McLeod gauges. Thereafter an estimate can be made of the error in the amount of gas adsorbed by a catalyst, and from this error, the error in the heat of adsorption is estimated.

A.3.2.

Estimates of Error in Determining Pressures using the McLeod Gauges:

A.3.2.1.

The Low Pressure McLeod Gauge:

The expression,

$$p = \frac{\pi r^2 \ell \Delta\ell}{V_\ell} \qquad 3.2.3,$$

(section 3.2.6) is used to calculate the pressure from McLeod gauge readings. In order to simplify the calculation, it is assumed that $\ell = \Delta\ell$. Thus equation 3.2.3. becomes

$$p = \frac{\pi r^2 \ell^2}{V_\ell} \qquad \text{A.3.6.}$$

It follows from equations A.3.4 and A.3.6 that the relative error in a pressure measurement is given by the expression,

$$E_p = \pm \sqrt{(E_{V_\ell})^2 + (2E_r)^2 + (2E_\ell)^2} \qquad \text{A.3.7.}$$

Using equation A.3.6, the estimated error in a pressure reading of 0.1 torr is now calculated. This value of the pressure, corresponding to a value of ℓ of 65.1 mm, is in the central region of the working range of the gauge, and it was felt that a typical value of the error for the gauge would be obtained using this pressure. In order to calculate E_p, it is necessary to have estimates of the errors in V_ℓ, r and ℓ, as well as their magnitudes. It may be seen from section 3.2.7 that V_ℓ has a value of 133.1 ± 0.2 ml. The radius of the McLeod gauge capillary is 1.000 ± 0.005 mm (section 3.2.7). The estimated error in reading ℓ by means of a cathetometer is ± 0.1 mm. By substituting these respective values in equation A.3.7, it follows that the relative error in a pressure reading of 0.1 torr is given by

$$E_p = \pm 0.008.$$

Substituting this value for E_p and the value of 0.1 torr for the pressure in equation A.3.5, the absolute error in the pressure is found to be ± 0.001 torr.

A.3.2.2.

The High Pressure McLeod Gauge:

The estimation of the error in determining pressure using the high

pressure McLeod gauge is analogous to the estimation of the error using the low pressure McLeod gauge. The relative error in a pressure measurement is given by the expression,

$$E_p = \pm\sqrt{(E_{V_h})^2 + (2E_r)^2 + (2E_\ell)^2} \qquad \text{A.3.8.}$$

As stated in section 3.2.7, V_h has a value of 5.12 ± 0.01 ml. The radius of the capillary is 1.000 ± 0.005 mm. A pressure reading of 6.14 torr, corresponding to a value of ℓ of 100.0 mm, was chosen as a typical value in the working pressure range of the high pressure McLeod. By substitution of the respective values in equation A.3.8, it follows that the relative error in pressure reading of 6.14 torr is given by

$$E_p = \pm 0.0055.$$

Substituting this value of E_p and the value of 6.14 torr for the pressure in equation A.3.5, the absolute error in the pressure is found to be $\pm$ 0.03 torr.

These estimates show the relative error in the measurement of pressure using the low pressure McLeod gauge to be of the order of 1% and the relative error using the high pressure McLeod gauge to be of the order of 0.5%. The higher relative error, namely that incurred when using the low pressure McLeod gauge, is used in the next step of the estimation of errors in heats of adsorption, the estimate of errors in the amount of gas adsorbed by the catalysts.

A.3.3.

Estimate of the Error in the Amount of Gas Adsorbed by the Catalysts.

The amount of gas adsorbed by a catalyst sample is calculated by subtracting the amount of gas in the volume V_L, and the amount of gas in the dead space of the adsorption cell from the total amount of gas introduced into the measuring system at the start of the experiment. This is represented by the equation,

$$n_a = n_t - n_g - n_s \qquad \text{A.3.9.}$$

A.3.3.1.

Estimate of Error in $n_t - n_g$:

The first step in the estimation is to estimate the experimental errors in n_t and n_g. n_g is given by the expression,

$$n_g = \frac{10^{-3} p V_L}{760 RT} \qquad \text{A.3.10.}$$

It follows from equations A.3.10 and A.3.4 that the relative error in n_g is given by

$$E_{n_g} = \pm \sqrt{(E_p)^2 + (E_{V_L})^2 + (E_T)^2} \qquad \text{A.3.11.}$$

In section 3.2, it is shown that the relative error in a pressure reading is ± 0.008. The estimated error in the temperature, T, of the gas is $\pm 0.5^0$ K. In section 3.2.7, V_L is shown to have a value of 233.9 ± 1.0 ml. By substitution of the respective values in equation A.3.10, it follows that the

relative error in n_g is given by

$$E_{n_g} = \pm 0.009.$$

At a typical gas temperature of 290^{0}K and a pressure of 0.1 torr, the pressure at which the relative error in pressure was estimated (section A.3.2.1), 1.31 μmole of gas are present in V_L. Substituting the value of ±0.009 for E_{n_g} and the value of 1.31 μmole for n_g into equation A.3.5, the absolute error in the value, 1.31 μmole, of n_g is found to be ±0.012 μmole.

The total amount of gas in the measuring section of the apparatus on completion of an isotherm is calculated as the sum of a number of additions of gas. Each additional amount of gas is measured by subtracting the amount of gas previously present in the volume V_L from the new amount of gas present (section 3.5.1). Assuming that 20 such additions are made during the course of an isotherm, each addition being subject to 2 errors equivalent to e_{n_g}, then it follows from equation A.3.2. that

$$e_{n_t} = \pm\sqrt{40\,(e_{n_g})^2} \qquad \text{A.3.12.}$$

By substituting the value obtained above for e_{n_g}, namely ± 0.012 μmole, in equation A.3.12, it follows that e_{n_t} has a value ±0.072 μmole. Hence it follows from equation A.3.2 that the absolute error in $n_t - n_g$ is given by

$$e_{(n_t - n_g)} = \pm\sqrt{(e_{n_t})^2 + (e_{n_g})^2} \qquad \text{A.3.13.}$$

Substituting values estimated above for e_{n_t} and e_{n_g} in equation A.3.13, it follows that $e_{(n_t - n_g)}$ has the value ± 0.073 μmole.

A.3.3.2.

Estimate of Error in n_s:

The amount of gas in the dead space of the adsorption cell, n_s, is obtained by multiplying the equilibrium pressure by the slope, w, of a calibration curve (section 3.2.9). In order to obtain the calibration curve, aliquots of helium are introduced into the adsorption cell. After each aliquot is added, the equilibrium pressure in the adsorption cell is measured. A graph of the total amount of gas added to the adsorption cell, Σn_c, where

$$n_c = \frac{10^{-3} p_1 V_L}{760RT} - \frac{10^{-3} p_2 V_L}{760RT} \qquad 3.2.4,$$

against the equilibrium pressure is plotted. The resulting straight line is the calibration curve.

The error in n_s can be propagated according to equation A.3.4, by the expression,

$$E_{n_s} = \pm\sqrt{(E_p)^2 + (E_w)^2} \qquad A.3.14.$$

The estimated relative error, E_p, in the equilibrium pressure is given in section A.3.2.2. The relative error in the slope of the calibration curve was estimated as follows. Each of the terms on the right hand side of equation 3.2.4 has the same form as the right hand side of equation A.3.10.

Therefore it may be assumed that the errors in the former two terms are both equal to e_{n_g}. Use of this assumption combined with equation A.3,2 yields the following expression for the absolute error in n_c,

$$e_{n_c} = \pm\sqrt{2(e_{n_g})^2} \qquad \text{A.3,15.}$$

Since the ordinate of the jth set of coordinates on the calibration curve is the sum of the j aliquots of helium introduced into the adsorption cell, it follows from equation A.3.2 that $e_{\sum_j n_c}$ is given by the expression

$$e_{\sum_j n_c} = \pm\sqrt{j(e_{n_c})^2} \qquad \text{A.3.16.}$$

The errors in the successive pressure readings are not propagated, however, and so the error in the equilibrium pressure after addition of the jth aliquot of helium has the same value as the error in the equilibrium pressure after addition of the first aliquot. The error in the slope of the calibration curve is represented graphically in figure A.3.1. This figure is drawn on the basis of the criteria concerning the errors in p and n_c discussed above. The arrows in the figure are representative of the errors in p and n_c. The results of a typical calibration curve are used to estimate the error in the slope of the curve. The coordinates of the first point on the curve were found to be (0.327, 0.450) and the coordinates of the fifth point (1.470, 2.170). The slope of the curve was found to be 1.49 μmole/torr. Substituting the abscissae of the first and fifth points and the value of E_p given in section

FIG. A.3.1.

SCHEMATIC DIAGRAM OF THE ERROR IN THE SLOPE OF AN ADSORPTION CELL CALIBRATION CURVE

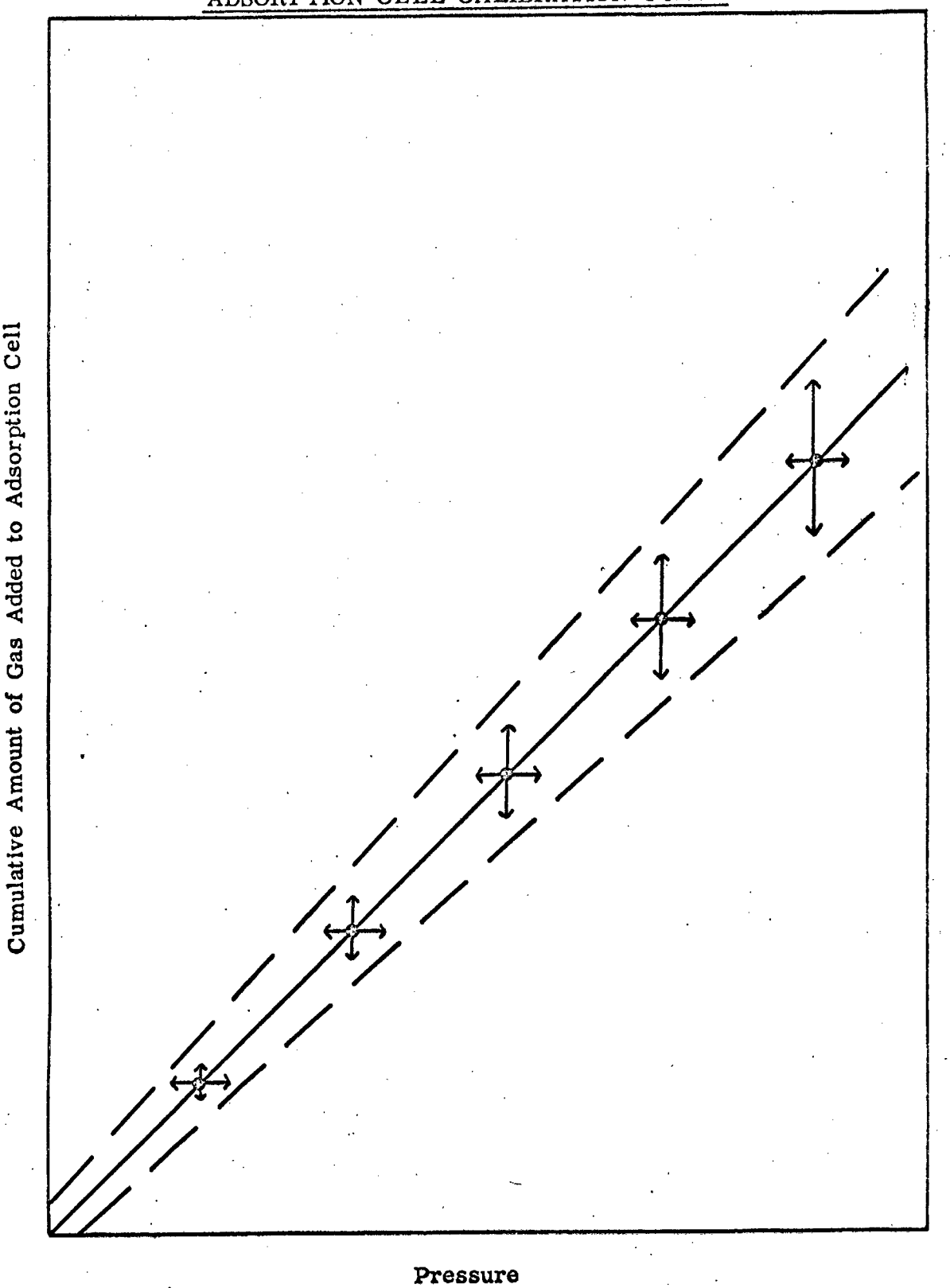

A.3.2.2 into equation A.3.5, it follows that e_p for the first point on the curve is ±0.004 torr and ±0.012 torr for the fifth point.

Errors in the amount of gas in the dead space, n_c, for the first and fifth points must now be estimated. Using equation A.3.5 and a value of E_{n_g} of ±0.009 (section A.3.3.1), e_{n_c} for the first point was estimated to be ±0.006 μmole. The fifth point will have a larger error in n_c than the first point because 5 additions of gas to the adsorption cell were made in order to determine the coordinates of this fifth point. Using equation A.3.2, the value of ±0.009 for E_{n_g} (section A.3.3.1) and equation A.3.5, the value of e_{n_c} for the fifth point was estimated to be ±0.040 μmole.

Hence the coordinates of the first point become (0.327 ± 0.004, 0.450 ±0.006) and the coordinates of the fifth point (1.470 ±0.012, 2.170 ±0.040). From the errors in these coordinates a value of ±0.025 μmole/torr for the error in the slope of the calibration curve is obtained.

Substituting the value of 1.49 μmole/torr for w and the value ±0.025 μmole/torr for e_w into equation A.3.5 gives an estimate of E_w. Substituting this value of E_w and the value of E_p of ±0.008 (section A.3.2.1) into equation A.3.14 gives a value for E_{n_s} of ±0.0186. Substituting this value of E_{n_s} and the value of n_s calculated using values of 1.49 μmole/torr for w and 0.1 torr for p into equation A.3.5, it can be shown that e_{n_s} has a value of ±0.003 μmole.

A.3.3.3.

Estimate of Error in n_a:

It follows from equations A.3.9 and A.3.4 that the absolute error in the amount of gas adsorbed by a catalyst is given by the expression,

$$e_{n_a} = \pm\sqrt{(e_{n_t - n_g})^2 + (e_{n_s})^2} \qquad \text{A.3.17.}$$

Substituting the estimated values of the errors in $(n_t - n_g)$ and n_s (section A.3.3.2) into equation A.3.17 gives a value of ± 0.073 μmole for e_{n_a}.

A.3.3.4.

Estimate of Error in n:

Since results in section 5.8 are given as the amount of gas adsorbed per gram of catalyst, n, it is necessary to estimate the absolute error in n. Typically, a 7 g mass of catalyst was used for the determination of adsorption isotherms. Thus the absolute error in n is given by

$$e_n = \frac{1}{7} e_{n_a} \qquad \text{A.3.18.}$$

Substituting the value of ± 0.073 μmole for e_{n_a} (section A.3.3.3) into equation A.3.18, it follows that e_n is approximately equal to ± 0.01 μmole/g catalyst.

In order to ensure that a realistic value for the error in the heat of adsorption is estimated, in the estimations that follow a value of e_n of twice the estimated value of ± 0.01 μmole/g catalyst is used.

A. 3. 4.

Estimate of Error in the Isosteric Heat of Adsorption:

Isosteric heats of adsorption are obtained from the slope of a plot of log p against 1/T at constant coverage (section 1. 4). In the following estimation only two values of temperature are considered in order to simplify the estimation of error. The heat of adsorption at a given coverage may, under these conditions, be obtained from the expression,

$$q_{st} = \frac{2.303 R T_1 T_2 (\log p_1 - \log p_2)}{(T_2 - T_1)} \qquad \text{A. 3. 19.}$$

It follows from equations A. 3. 4 and A. 3. 19 that the relative error in the isosteric heat of adsorption is given by the expression,

$$E_{q_{st}} = \pm \sqrt{(E_{T_1})^2 + (E_{T_2})^2 + (E_{(T_2 - T_1)})^2 + (E_{(\log p_1 - \log p_2)})^2} \qquad \text{A. 3. 20.}$$

The estimated error in the temperature at which an isotherm was determined is $\pm 2\ ^0K$. Substituting this estimated error into equation A. 3. 2, it follows that the absolute error in $(T_2 - T_1)$ is $\pm 3\ ^0K$.

From a study of the hydrogen adsorption isotherms in section 5. 8 it was found that typically the value of ± 0.02 μmole/g catalyst obtained in section A. 3. 3. 4 for e_{n_a} corresponded to an error of ± 0.08 in the value of log p on an isotherm. Using this value for log p and equation A. 3. 2, it follows that the absolute error in $(\log p_1 - \log p_2)$ is ± 0.11.

In order to estimate the relative error in q_{st} using equation A. 3. 20,

a set of results was used which pertained to a coverage of 1.2 μmole/g catalyst on a 0.51% catalyst where q_{st} had the value 17.3 kcal/mole. At the fixed coverage of 1.2 μmole/g catalyst, log p had a value of -0.51 at a temperature of 453°K and 0.32 at a temperature of 523° K. Substituting these values and the estimated values of the absolute errors in temperature, $(T_2 - T_1)$ and $(\log p_1 - \log p_2)$ into equation A.3.20, $E_{q_{st}}$ is found to have a value of ± 0.125. Substituting the above values of q_{st} and $E_{q_{st}}$ into equation A.3.5, a value of ±2 kcal/mole is obtained for the absolute error in q_{st}.

A.3.5.

Estimate of Errors in the Isosteric Heat of Adsorption per Unit Metal Area:

The isosteric heat of adsorption per unit metal area, Q_{st}, on a catalyst is obtained (section 5.8) from the expression,

$$Q_{st} = \frac{q_{st}}{\Sigma} \qquad \text{A.3.21,}$$

The specific metal surface area, Σ, of a catalyst is obtained by measuring n_m, the amount of hydrogen adsorbed by 1 g of the catalyst at a pressure of 40 torr and a temperature of -78 °C (section 5.7), and substituting this value for n_m into the equation,

$$\Sigma = N A_m n_m \times 10^{-26} \qquad \text{2.2.5.}$$

Experimental errors in Q_{st} result, therefore, from errors in q_{st} and in n_m. The error in q_{st} is estimated in section A.3.4. It is assumed that the

error in n_m has the same value as the error in n (section A.3.3.4). It follows from equations A.3.4, A.3.21 and 2.2.5 that the relative error in Q_{st} is given by the expression

$$E_{Q_{st}} = \pm\sqrt{(E_{q_{st}})^2 + (E_{n_m})^2} \qquad \text{A.3.22.}$$

It can be shown that even for the smallest value of n_m, that of a 0.25% nickel on silica catalyst sintered for 4 hours at 500°C, which would have the largest value of E_{n_m}, the estimated value of E_{n_m} is very much less than the estimated value of $E_{q_{st}}$ (section A.3.4). Equation A.3.22 therefore reduces to the expression,

$$E_{Q_{st}} = E_{q_{st}} \qquad \text{A.3.23.}$$

Substituting the value of $E_{q_{st}}$ (section A.3.4) of ± 0.125 into equation A.3.23 yields the value of $E_{Q_{st}}$ of ± 0.125. The absolute error in Q_{st} depends on the magnitude of Q_{st} (equation A.3.5). The smallest value of Q_{st} measured is -26 (kcal/mole)/(m^2/g catalyst) and the largest value -102 (kcal/mole)/(m^2/g catalyst) (figure 5.21). Substituting each of these values for Q_{st} in turn into equation A.3.5 together with the value for $E_{Q_{st}}$ of ± 0.125 estimated above, it follows that $e_{q_{st}}$ has the values ± 3.3 (kcal/mole)/(m^2/g catalyst) and ± 12.8 (kcal/mole)/(m^2/g catalyst) when Q_{st} has the above-mentioned values.

APPENDIX 4

SUGGESTED MODIFICATION TO THE ADSORPTION APPARATUS

If the apparatus were to be reconstructed, the author would make the following modification. On the diagram of the apparatus (figure 3.1) it can be seen that the gas storage bulbs, the gas purification train, the gas burette and the adsorption cell all lead off the same manifold. This meant that if, for example, catalyst was being reduced, it was not possible to fill the gas burette with the gas necessary for the isotherm about to be determined. A good deal of time would have been saved if the access to the gas burette from the storage bulbs and the tubing between gas purification train and adsorption cell were separated into two manifolds, either of which could be evacuated and isolated whilst the other was in use.

A cryostat suitable for controlling the thermostatting of the adsorption cell at temperatures between -60°C and room temperature was designed and constructed as follows. A coil of copper tubing was placed in a dewar which was filled with alcohol. The dewar surrounded the adsorption cell. One end of the copper tubing was open to the atmosphere. The other end of the tubing led from the coil almost to the bottom of a 10 litre liquid nitrogen storage dewar. The top of the storage dewar was sealed with a tight fitting rubber bung through which the copper tubing passed. A small nichrome wire heater was suspended near the bottom of the storage dewar, its electrical leads passing through the bung. A 2 cm diameter length of glass tubing and a short length of copper tubing, the latter acting as an air bleed, also passed through the bung of the storage dewar and extended about 2 cm into the dewar. The top of the glass tubing was sealed to a ground glass cone into which a ground glass stopper fitted. Onto the short length of copper tubing a threaded brass adaptor (female), which acted as a seat for a ball valve, was silver soldered. Above the adaptor a solenoid operated ball was mounted. A small heater of Nichrome wire was wound around the air bleed. Finally a -60°C to +30°C contact thermometer and a stirrer were placed in the thermostat bath. When the temperature of the thermostat bath rose above the preset value, a contact in the thermometer closed. This activated a multiple relay which closed circuits to the solenoid, (thus closing the ball valve and sealing off the air bleed), and to the heater in the storage dewar. The nitrogen boiling in the dewar set up a pressure which forced liquid nitrogen through the coil in the thermostat bath.

When the temperature of the bath fell below the set temperature, the contact thermometer contacts opened, the heater in the dewar was switched off, and the ball valve opened. The release of pressure immediately halted the flow of nitrogen through the coil, thus ensuring that the bath temperature did not fall too low. At the same time as the ball valve opened, the small heater wound around the air bleed was switched on. It was found necessary to incorporate this heater, since the air bleed tended to ice up after a few hours use. The wide bore glass tubing was used to refill the dewar when its supply of liquid nitrogen was exhausted. The cryostat was capable of maintaining the temperature in the thermostat bath to $\pm 0.2^{0}C$ for prolonged periods of time. In holding the temperature constant at $-60^{0}C$, approximately 1 litre of liquid nitrogen was consumed per hour. The cryostat was not used for maintaining temperatures below $-60^{0}C$ as no contact thermometer operative in this region was available.

When not in use as a thermostat bath, the equipment was used as a device for keeping the level of liquid nitrogen in a dewar constant. A contact thermometer was mounted so that its bulb was just above the rim of the dewar in which the level was to be kept constant. The copper tubing leading from the storage dewar was situated such that its open end was approximately 2 cm above the top of the dewar. An asbestos shield was placed between the thermometer and the copper tubing. This prevented any spray of liquid nitrogen from prematurely cooling the thermometer. As the level of liquid nitrogen in the dewar fell, the rim of the dewar warmed up, thus causing the contacts in the thermometer to close. Liquid nitrogen, by the same principle described

above, filled the dewar. As the level overflowed the top of the dewar, the bulb of the thermometer was rapidly cooled, its contacts opened and liquid nitrogen ceased flowing through the copper tubing. By this method the level of the liquid nitrogen could be kept within 2 mm of the top of the dewar.

The figures in chapter 5 representing the hydrogen adsorption isotherms were plotted in the form of log p against n. In this appendix are listed, for each catalyst, the pressures, corrected for thermal transpiration (appendix 2), and the corresponding amounts of hydrogen adsorbed per gram of catalyst at each temperature at which an isotherm was measured. The preparation of the catalysts is discussed in section 3.3.

In the tables that follow, p has the units torr and n has the units μmole/g catalyst. The temperature above each set of results refers to the temperature at which the isotherm was measured.

TABLE A.6.1.

0.25% NICKEL ON GROUND SILICA CATALYST (BATCH A).

180°C		210°C		240°C	
p	n	p	n	p	n
0.003	0.53	0.003	0.42	0.004	0.35
0.010	0.63	0.010	0.52	0.018	0.45
0.023	0.70	0.025	0.59	0.057	0.56
0.080	0.81	0.088	0.70	0.195	0.65
0.199	0.91	0.200	0.78	0.570	0.75
0.417	1.00	0.470	0.87	1.192	0.84
1.042	1.11	1.099	0.97	2.88	0.93
2.89	1.23	3.18	1.09	6.67	1.04
9.12	1.39	9.12	1.23	14.13	1.15
20.04	1.51	19.86	1.34	26.29	1.22
39.84	1.60	36.48	1.43	37.20	1.28

TABLE A.6.2.

0.25% NICKEL ON GROUND SILICA CATALYST (BATCH B).

180 °C		210 °C		240 °C	
p	n	p	n	p	n
0.002	0.45	0.003	0.29	0.004	0.20
0.009	0.60	0.008	0.41	0.012	0.31
0.022	0.70	0.017	0.50	0.032	0.42
0.046	0.81	0.046	0.62	0.082	0.52
0.183	0.98	0.089	0.70	0.181	0.62
0.541	1.14	0.190	0.81	0.337	0.69
1.53	1.32	0.465	0.93	0.643	0.79
4.06	1.45	1.021	1.05	1.540	0.94
7.94	1.56	2.46	1.18	4.15	1.10
23.28	1.71	5.02	1.30	10.03	1.24
37.45	1.87	12.65	1.43	25.19	1.42
		21.93	1.55	41.02	1.47
		43.65	1.67		

TABLE A.6.3.

0.25% NICKEL ON GROUND SILICA CATALYST (BATCH A). SINTERED AT 500 °C FOR 4 HOURS (SECTION 3.3).

180 °C		210 °C		240 °C	
p	n	p	n	p	n
0.005	0.43	0.006	0.33	0.004	0.18
0.011	0.49	0.018	0.42	0.017	0.33
0.026	0.58	0.030	0.47	0.050	0.41
0.057	0.65	0.070	0.55	0.119	0.50
0.101	0.70	0.109	0.60	0.263	0.57
0.229	0.78	0.250	0.67	0.484	0.63
0.555	0.88	0.597	0.77	1.58	0.76
1.121	0.97	1.018	0.82	4.53	0.88
2.69	1.06	2.02	0.90	13.71	1.02
6.00	1.15	4.91	1.00	33.88	1.11
10.87	1.23	9.93	1.10	44.01	1.16
22.19	1.32	18.88	1.18		
41.97	1.40	40.35	1.28		

TABLE A.6.4.

0.51% NICKEL ON GROUND SILICA CATALYST (BATCH A).

180 °C		210 °C		240 °C	
p	n	p	n	p	n
0.012	0.74	0.033	0.77	0.017	0.49
0.027	0.90	0.074	0.87	0.052	0.67
0.065	1.05	0.151	1.00	0.117	0.79
0.123	1.15	0.251	1.07	0.238	0.90
0.260	1.28	0.556	1.19	0.503	1.00
0.520	1.38	1.010	1.26	1.007	1.12
0.969	1.48	2.16	1.44	2.07	1.24
2.17	1.63	4.64	1.58	4.64	1.38
4.83	1.77	10.52	1.74	9.75	1.57
10.41	1.88	22.84	1.89	21.34	1.73
22.17	2.02	37.52	1.99	37.55	1.87

TABLE A.6.5.

0.51% NICKEL ON GROUND SILICA CATALYST (BATCH B).

180 °C		210 °C		240 °C	
p	n	p	n	p	n
0.008	0.61	0.035	0.61	0.069	0.53
0.061	0.93	0.086	0.80	0.171	0.70
0.166	1.11	0.163	0.91	0.413	0.87
0.289	1.23	0.441	1.08	0.661	0.97
0.571	1.32	0.796	1.18	1.265	1.10
1.095	1.46	1.92	1.38	2.87	1.26
2.17	1.64	4.40	1.56	5.53	1.43
10.18	1.93	9.15	1.76	11.25	1.60
17.78	2.05	22.05	1.93	19.95	1.75
		38.36	2.05		

TABLE A.6.6.

0.51% NICKEL ON GROUND SILICA CATALYST (BATCH A). SINTERED AT 500°C FOR 4 HOURS (SECTION 3.3).

180°C		210°C		240°C	
p	n	p	n	p	n
0.013	0.60	0.022	0.53	0.023	0.42
0.056	0.78	0.109	0.72	0.121	0.62
0.083	0.83	0.236	0.81	0.321	0.72
0.178	0.93	0.541	0.92	0.596	0.81
0.513	1.07	0.989	1.01	1.147	0.89
1.381	1.20	1.785	1.08	2.32	1.00
2.36	1.26	4.71	1.23	4.74	1.10
4.54	1.36	10.06	1.37	10.71	1.23
9.85	1.47	21.22	1.46	21.25	1.35
20.01	1.58	32.81	1.54	32.89	1.43
31.28	1.64				

TABLE A.6.7.

2.20% NICKEL ON GROUND SILICA CATALYST (BATCH A).

180°C		210°C		240°C	
p	n	p	n	p	n
0.009	1.86	0.007	1.46	0.006	1.19
0.025	2.08	0.015	1.61	0.010	1.29
0.065	2.35	0.030	1.83	0.016	1.39
0.122	2.54	0.048	1.93	0.031	1.56
0.536	2.92	0.097	2.10	0.074	1.75
0.834	3.02	0.173	2.23	0.161	1.92
1.200	3.15	0.254	2.30	0.278	2.04
2.28	3.33	0.441	2.50	0.528	2.21
3.88	3.48	0.889	2.69	1.070	2.41
5.82	3.62	1.66	2.89	1.84	2.55
9.58	3.82	3.47	3.11	4.10	2.81
15.37	3.88	10.51	3.44	7.98	3.08
25.58	4.14	14.39	3.58	21.24	3.37
36.66	4.20	26.30	3.74	35.18	3.52

TABLE A.6.8.

2.20% NICKEL ON GROUND SILICA CATALYST (BATCH B).

180°C		210°C		240°C	
p	n	p	n	p	n
0.013	1.58	0.013	1.08	0.014	0.66
0.046	1.98	0.040	1.46	0.042	1.02
0.095	2.21	0.105	1.80	0.094	1.33
0.191	2.42	0.276	2.14	0.259	1.67
0.495	2.75	0.631	2.38	0.533	1.94
1.800	3.16	1.327	2.64	1.560	2.28
3.90	3.45	2.00	2.80	4.56	2.70
9.89	3.67	4.80	3.08	20.89	3.24
20.94	3.98	11.75	3.40	39.81	3.46
		29.44	3.70		
		45.81	4.02		

TABLE A.6.9.

2.20% NICKEL ON GROUND SILICA CATALYST (BATCH A). SINTERED AT 500°C FOR 4 HOURS (SECTION 3.3).

180° C		210° C		240° C	
p	n	p	n	p	n
0.004	0.33	0.005	0.22	0.010	0.21
0.012	0.46	0.015	0.35	0.022	0.31
0.074	0.68	0.078	0.55	0.084	0.47
0.181	0.81	0.190	0.62	0.171	0.56
0.433	0.92	0.553	0.82	0.381	0.65
0.899	1.04	1.099	0.91	0.706	0.73
2.43	1.23	2.63	1.08	1.180	0.80
5.12	1.40	5.74	1.22	2.43	0.91
10.29	1.52	9.12	1.33	5.54	1.07
20.53	1.73	14.52	1.45	11.03	1.22
31.48	1.86	28.84	1.61	20.04	1.36
38.99	1.94	44.26	1.76	29.44	1.46
				44.46	1.60

TABLE A.6.10.

5.0% NICKEL ON SILICA CATALYST.

180°C		210°C		240°C	
p	n	p	n	p	n
0.004	1.56	0.008	1.21	0.008	0.81
0.32	2.24	0.048	1.50	0.026	1.14
0.176	3.00	0.089	2.00	0.179	1.75
0.501	3.42	0.684	2.55	0.729	2.30
1.183	3.87	1.050	3.11	1.78	2.68
4.22	4.56	3.56	3.75	6.79	3.35
15.13	5.30	13.21	4.49	18.99	3.92
38.02	5.89	34.83	5.18	37.72	4.34

TABLE A.6.11.

20.0% NICKEL ON SILICA CATALYST.

180°C		210°C		240°C	
p	n	p	n	p	n
0.005	1.91	0.006	1.44	0.006	1.01
0.014	2.22	0.020	1.79	0.028	1.41
0.032	2.50	0.091	2.31	0.063	1.69
0.069	2.79	0.251	2.70	0.187	2.04
0.174	3.20	1.096	3.38	0.755	2.61
0.513	3.73	2.75	3.85	1.82	2.99
1.230	4.16	7.59	4.39	5.24	3.55
3.30	4.71	13.50	4.77	9.98	3.91
6.59	5.09	37.15	5.40	19.05	4.32
14.55	5.56			39.81	4.79
41.78	6.10				

TABLE A.6.12.

1.9% NICKEL ON CABOSIL CATALYST.

60 °C		80 °C		80 °C (Replicate)	
p	n	p	n	p	n
0.001	6.01	0.002	3.99	0.005	5.25
0.010	8.82	0.009	6.00	0.060	8.99
0.098	12.0	0.034	7.78	0.407	11.9
0.389	14.9	0.219	10.8	1.441	14.2
1.68	17.8	0.446	12.0	39.9	21.5
4.36	19.8	5.01	16.7		
15.81	23.0	19.52	19.9		
38.96	25.3				

TABLE A.6.13.

5.5% NICKEL ON CABOSIL CATALYST.

50 °C		80 °C	
p	n	p	n
0.001	30.0	0.003	21.1
0.008	36.5	0.035	30.9
0.028	42.0	0.100	34.8
0.076	44.5	0.241	37.9
0.166	48.4	1.02	43.4
0.371	50.9	3.55	49.1
1.095	55.4	10.45	53.3
2.69	59.7	21.39	57.5
5.24	63.2	38.03	60.6
10.45	66.6		
22.42	70.5		
38.00	73.4		

APPENDIX. 7

KRYPTON ISOTHERM RESULTS

It was felt that it was unnecessary to present all the BET isotherms (section 2.2) of krypton adsorption (section 5.9) graphically. The replicate isotherms on the 0.51% nickel on ground silica catalyst (batch A) are presented in figure 5.10 as being typical. Thus in this appendix the coordinates of the BET plots of krypton adsorption on the ground silica support and on the ground silica-supported catalysts discussed in section 5.2 are listed in table A.7.1. The slopes and intercepts of these plots are listed in table A.7.2.

$\frac{p}{n(p_o - p)}$ in table A.7.1 has the units g catalyst/ μmole.

TABLE A.7.1.

Catalyst	p/p_o	$\frac{p}{n(p_o - p)}$	Catalyst	p/p_o	$\frac{p}{n(p_o - p)}$
Ground Silica Support	0.048 0.072 0.103 0.139 0.206	0.00598 0.00818 0.01096 0.01407 0.01993	0.25% Nickel on Silica (Batch B)	0.032 0.050 0.073 0.108 0.145 0.193	0.00359 0.00510 0.00697 0.00969 0.01250 0.01626
0.25% Nickel on Silica (Batch A)	0.049 0.087 0.136 0.180 0.228	0.00466 0.00746 0.01097 0.01418 0.01760	0.25% Nickel on Silica (Batch A) Sintered at 500 °C for 4 hours (section 3.3)	0.021 0.036 0.060 0.095 0.136 0.199	0.00310 0.00430 0.00621 0.00893 0.01208 0.01699
0.51% Nickel on Silica (Batch A)	0.068 0.120 0.208 0.268	0.00550 0.00907 0.01520 0.01922	0.51% Nickel on Silica (Batch A) Replicate determination	0.034 0.084 0.147 0.219 0.260	0.00317 0.00662 0.01083 0.01582 0.01870

TABLE A.7.1. (Continued).

Catalyst	p/p_o	$\frac{p}{n(p_o - p)}$	Catalyst	p/p_o	$\frac{p}{n(p_o - p)}$
0.51% Nickel on Silica (Batch B)	0.075	0.00623	0.51% Nickel on Silica (Batch A) Sintered at 500 °C for 4 hours (section 3.3)	0.035	0.00337
	0.101	0.00801		0.053	0.00465
	0.160	0.01210		0.083	0.00680
	0.209	0.01542		0.118	0.00921
	0.258	0.01878		0.159	0.01211
2.20% Nickel on Silica (Batch B)	0.036	0.00307	2.20% Nickel on Silica (Batch A)	0.028	0.00255
	0.078	0.00566		0.048	0.00376
	0.102	0.00713		0.084	0.00606
	0.166	0.01111		0.120	0.00828
	0.200	0.01320		0.143	0.00965
				0.174	0.01152
2.20% Nickel on Silica (Batch A) Sintered at 500 °C for 4 hours (section 3.3)	0.031	0.00322	5.0% Nickel on Silica	0.042	0.00267
	0.058	0.00525		0.060	0.00357
	0.104	0.00858		0.091	0.00514
	0.168	0.01306		0.135	0.00728
	0.238	0.01811		0.210	0.01111
20.0% Nickel on Silica	0.074	0.00406			
	0.109	0.00577			
	0.143	0.00740			
	0.184	0.00930			
	0.240	0.01060			

TABLE A.7.2.

Catalyst	Slope of BET Isotherm (g catalyst/μmole)	Intercept of BET Isotherm (g catalyst/μmole)
Ground Silica support	0.0881	0.0018
0.25% (A)	0.0740	0.0011
0.25% (B)	0.0770	0.0013
0.25% (Sintered)	0.0786	0.0011
0.51% (A)	0.0689	0.0008
0.51% (B)	0.0679	0.0011
0.51% (Sintered)	0.0706	0.0010
2.20% (A)	0.0610	0.0009
2.20% (B)	0.0628	0.0008
2.20% (Sintered)	0.0716	0.0010
5.0 %	0.0500	0.0006
20.0 %		

The descriptions of the catalysts in the first column refer to the percentage of nickel in a nickel on ground silica catalyst. A and B refer to the batch of catalyst and sintered refers to catalysts of batch A which were sintered for 4 hours at 500 ^{0}C (section 3.3).

A	:	Pre-exponential term in Arrhenius equation.	
A_F	:	Percentage of the total metal surface area of a supported metal catalyst given by all metal crystallites of size below the lower limit of the class interval in which the median crystallite size (as determined from an electron micrograph) was found to occur.	
A_f	:	Percentage of the total metal surface area of a supported metal catalyst given by the metal crystallites in a particular class interval on a metal crystallite size distribution histogram.	
A_m	:	Area occupied by an adsorbate atom or molecule on the surface of a solid (equation 2.2.4).	($\AA^2$)
A_s	:	Pre-exponential term in Arrhenius equation at temperature T_s.	
B	:	Breadth of an X-ray diffraction line, corrected for $K\alpha_1\alpha_2$-doublet separation, as observed under a given set of experimental conditions.	(radians)
B_o	:	Breadth of an X-ray diffraction line as observed under a given set of experimental conditions.	(radians)
C_s	:	Constant in Scherrer equation (equation 4.4.1).	(radians)
D	:	Angular separation of the $K\alpha_1\alpha_2$-doublet of nickel-filtered copper X-radiation at a particular value of 2γ.	(degrees 2γ)
E	:	Activation energy term in Arrhenius equation.	(kcal/mole)
E_j	:	Estimated relative error in a parameter j.	
ΔG_a	:	Molar integral change in Gibbs free energy of a system on adsorption (equation 2.1.1).	(kcal/mole)
ΔH_a	:	Molar integral change in enthalpy of a system on adsorption (equation 2.1.1).	(kcal/mole)
ΔH_L	:	Heat of liquefaction of an adsorbate (equation 2.2.3).	(kcal/mole)
K	:	Equilibrium constant.	

K_g	:	Volume of gas burette dead space (equation 3.2.2).	(ml)
K_h	:	High pressure McLeod gauge constant,	(mm^{-1})
K_ℓ	:	Low pressure McLeod gauge constant.	(mm^{-1})
M	:	Molecular weight of an adsorbate (equation 2.2.4).	
N	:	Avogadro's constant.	
N_i	:	Number of metal crystallites of diameter d_i (equation 6.1).	
Q	:	A dependent variable, (equation A.3.1).	
Q_{st}	:	Isosteric heat of adsorption per unit metal area.	(kcal/mole)/ (m^2/g catalyst)
R	:	Gas constant.	
R_m	:	$R_m = \left(\frac{T_t}{T_r}\right)^{\frac{1}{2}}$ (equation A.2.2).	
R_t	:	Thermal transpiration effect: $R_t = \frac{p_t}{p_r}$ (equation A.2.2).	
ΔS_a	:	Molar integral change in the entropy of a system on adsorption (equation 2.1.1).	(kcal/mole/^{0}K)
T	:	Temperature.	(^{0}K)
T_r	:	Room temperature (equation A.2.1)	(^{0}K)
T_s	:	A characteristic temperature at which the catalytic activities of all catalysts in a series are equal (figure 1.1).	(^{0}K)
T_t	:	Temperature of an adsorbent (equation A.2.1).	(^{0}K)
V	:	Volume.	(ml)
V_c	:	A precisely known volume for calibration purposes.	(ml)

V_g	:	Volume of bulb plus capillary of a McLeod gauge (equation 3.2.3)	(ml)
V_H	:	Volume of high pressure McLeod gauge plus connecting tubing up to stopcocks 2, 4 and 6 (figure 3.1).	(ml)
V_h	:	Volume of bulb plus capillary of high pressure McLeod gauge.	(ml)
V_L	:	Volume of the low pressure McLeod gauge plus connecting tubing up to stopcocks 2, 3, 5 and 6 (figure 3.1).	(ml)
V_ℓ	:	Volume of bulb plus capillary of low pressure McLeod gauge.	(ml)
V_u	:	An unknown volume.	(ml)
X, Y, Z	:	Positive or negative indices.	
b	:	Breadth of X-ray diffraction line corrected for $K\alpha_1\alpha_2$-doublet separation, produced by a material with crystallite size well in excess of 10^{-5} cm.	(radians)
b_o	:	Breadth of X-ray diffraction line produced by a material with crystallite size well in excess of 10^{-5} cm.	(radians)
c	:	Constant in BET equation (equation 2.2.2).	
c_A	:	Constant in equation 1.3.1.	
d	:	Mean crystallite size as measured by X-ray diffraction.	(Å)
d_i	:	Class mark of the ith class interval on a nickel crystallite size distribution histogram (equation 6.1).	(Å)
d_t	:	Internal diameter of tubing over which a thermal transpiration effect is occurring (equation A.2.2).	(cm)
e_j	:	Estimated absolute error in a parameter j.	(units of j)

f	:	Pressure correction factor (equation A. 2. 2).	
k	:	Constant in Langmuir isotherm (equation 2. 2. 1).	$(torr^{-1})$
ℓ	:	Height of gas in enclosed limb of McLeod gauge (equation 3. 2. 3).	(mm)
$\Delta\ell$	:	Difference in heights of mercury in the open and closed limbs of a McLeod gauge (equation 3. 2. 3).	(mm)
m	:	Constant in equation 1. 3. 1.	$(kcal/mole)^{-1}$
n	:	Amount of gas adsorbed per gram of adsorbent.	(μmole/g)
n_a	:	Amount of gas adsorbed on an adsorbent.	(μmole)
n_c	:	Amount of gas added in one dose to the adsorption cell.	(μmole)
n_g	:	Amount of gas in McLeod gauge and its connecting tubing.	(μmole)
n_m	:	Amount of gas required to form a monolayer on one gram of adsorbent.	(μmole/g)
n_s	:	Amount of gas in dead space of adsorption cell	(μmole)
n_t	:	Total amount of gas in the measuring section of the apparatus.	(μmole)
p	:	Equilibrium pressure of an adsorbate	(torr)
p_o	:	Saturated vapour pressure of an adsorbate at a particular temperature.	(torr)
p_r	:	Pressure as read on a gauge at room temperature (equation A. 2. 1).	(torr)
p_t	:	Equilibrium pressure of an adsorbate, corrected for thermal transpiration (equation A. 2. 1).	(torr)
q_{st}	:	Isosteric heat of adsorption (equation 1. 4. 2).	(kcal/mole)
r	:	Radius of capillaries of McLeod gauges (equation 3. 2. 3).	(mm)

w	:	slope of an adsorption cell calibration curve.	(μmole/torr)
x, y, z	:	Experimentally determined quantities (equation A.3.1)	
Σ	:	Specific surface area of an adsorbent or a component thereof.	(m^2/g)
β	:	Breadth of X-ray diffraction line after correction for instrumental broadening and $K\alpha_1\alpha_2$-doublet separation (equation 4.4.1).	(radians)
$\beta_{\frac{1}{2}}$	:	Breadth of X-ray diffraction line at half-maximum intensity after correction for instrumental broadening and $K\alpha_1\alpha_2$-doublet separation.	(radians)
β_I	:	Integral breadth of X-ray diffraction line after correction for instrumental broadening and $K\alpha_1\alpha_2$-doublet separation.	(radians)
γ	:	Bragg angle (equation 4.4.1).	(degrees)
θ	:	Fraction of the surface of a solid (or a component thereof) covered by an adsorbate.	
λ	:	X-ray wavelength (equation 4.4.1).	(Å)
ρ	:	Density of liquefied or solidified adsorbate (equation 2.2.4).	(g/ml)
ϕ_g	:	Pressure shifting factor (equation A.2.2) defined such that $\phi_{He} \equiv 1$.	

REFERENCES

V_g	:	Volume of bulb plus capillary of a McLeod gauge (equation 3.2.3)	(ml)
V_H	:	Volume of high pressure McLeod gauge plus connecting tubing up to stopcocks 2, 4 and 6 (figure 3.1).	(ml)
V_h	:	Volume of bulb plus capillary of high pressure McLeod gauge.	(ml)
V_L	:	Volume of the low pressure McLeod gauge plus connecting tubing up to stopcocks 2, 3, 5 and 6 (figure 3.1).	(ml)
V_ℓ	:	Volume of bulb plus capillary of low pressure McLeod gauge.	(ml)
V_u	:	An unknown volume.	(ml)
X, Y, Z	:	Positive or negative indices.	
b	:	Breadth of X-ray diffraction line corrected for $K\alpha_1\alpha_2$-doublet separation, produced by a material with crystallite size well in excess of 10^{-5} cm.	(radians)
b_o	:	Breadth of X-ray diffraction line produced by a material with crystallite size well in excess of 10^{-5} cm.	(radians)
c	:	Constant in BET equation (equation 2.2.2).	
c_A	:	Constant in equation 1.3.1.	
d	:	Mean crystallite size as measured by X-ray diffraction.	(Å)
d_i	:	Class mark of the ith class interval on a nickel crystallite size distribution histogram (equation 6.1).	(Å)
d_t	:	Internal diameter of tubing over which a thermal transpiration effect is occurring (equation A.2.2).	(cm)
e_j	:	Estimated absolute error in a parameter j.	(units of j)

f	:	Pressure correction factor (equation A. 2. 2).	
k	:	Constant in Langmuir isotherm (equation 2. 2. 1).	($torr^{-1}$)
ℓ	:	Height of gas in enclosed limb of McLeod gauge (equation 3. 2. 3).	(mm)
$\Delta\ell$	:	Difference in heights of mercury in the open and closed limbs of a McLeod gauge (equation 3. 2. 3).	(mm)
m	:	Constant in equation 1. 3. 1.	$(kcal/mole)^{-1}$
n	:	Amount of gas adsorbed per gram of adsorbent.	(μmole/g)
n_a	:	Amount of gas adsorbed on an adsorbent.	(μmole)
n_c	:	Amount of gas added in one dose to the adsorption cell.	(μmole)
n_g	:	Amount of gas in McLeod gauge and its connecting tubing.	(μmole)
n_m	:	Amount of gas required to form a monolayer on one gram of adsorbent.	(μmole/g)
n_s	:	Amount of gas in dead space of adsorption cell	(μmole)
n_t	:	Total amount of gas in the measuring section of the apparatus.	(μmole)
p	:	Equilibrium pressure of an adsorbate	(torr)
p_o	:	Saturated vapour pressure of an adsorbate at a particular temperature.	(torr)
p_r	:	Pressure as read on a gauge at room temperature (equation A. 2. 1).	(torr)
p_t	:	Equilibrium pressure of an adsorbate, corrected for thermal transpiration (equation A. 2. 1).	(torr)
q_{st}	:	Isosteric heat of adsorption (equation 1. 4. 2).	(kcal/mole)
r	:	Radius of capillaries of McLeod gauges (equation 3. 2. 3).	(mm)

w	:	slope of an adsorption cell calibration curve.	(μmole/torr)
x, y, z	:	Experimentally determined quantities (equation A.3.1)	
Σ	:	Specific surface area of an adsorbent or a component thereof.	(m^2/g)
β	:	Breadth of X-ray diffraction line after correction for instrumental broadening and $K\alpha_1\alpha_2$-doublet separation (equation 4.4.1).	(radians)
$\beta_{\frac{1}{2}}$	:	Breadth of X-ray diffraction line at half-maximum intensity after correction for instrumental broadening and $K\alpha_1\alpha_2$-doublet separation.	(radians)
β_I	:	Integral breadth of X-ray diffraction line after correction for instrumental broadening and $K\alpha_1\alpha_2$-doublet separation.	(radians)
γ	:	Bragg angle (equation 4.4.1).	(degrees)
θ	:	Fraction of the surface of a solid (or a component thereof) covered by an adsorbate.	
λ	:	X-ray wavelength (equation 4.4.1).	(Å)
ρ	:	Density of liquefied or solidified adsorbate (equation 2.2.4).	(g/ml)
ϕ_g	:	Pressure shifting factor (equation A.2.2) defined such that $\phi_{He} \equiv 1$.	

REFERENCES

Adams, C.R., Benesi, H.A., Curtis, R.M. and Meisenheimer, R.G., 1962. J. Catal. 1, 336.

Adler, S.F. and Keavney, J.J., 1960. J. Phys. Chem. 64, 208.

Anderson, R.B., 1956. "Catalysis", vol. IV, p.19, ed. Emmett, P.H, Baltimore: Waverley Press.

Anderson, R.B., Hall, W.K. and Hofer, L.J.E., 1948. J. Amer. Chem. Soc. 70, 2465.

Baladin, A.A., 1929. Z. Phys. Chem. 132, 289.

Barr, W.E. and Anhorn, V.J., 1949. "Scientific and Industrial Glass Blowing and Laboratory Techniques", chapter XII, Pittsburgh: Instruments Publishing Company.

Bandrowski, J., Bickling, C.R., Yang, K.H. and Hougen, O.A., 1962. Chem. Eng. Sci. 17, 379.

Beebe, R.A., Beckwith, J.B. and Honig, J.M., 1945. J. Amer. Chem. Soc. 67, 1554.

Beebe, R.A. and Wildner, E.L., 1934. J. Amer. Chem. Soc. 56, 642.

Beeck, O., 1950a. Adv. Catal. 2, 151.

Beeck, O., 1950b. Discuss. Faraday Soc. 8, 118.

Beeck, O., Smith, A.E. and Wheeler, A., 1941. Proc. Roy. Soc. London A177, 62.

Belcher, R. and Nutten, A.J., 1960. "Quantitative Inorganic Analysis", 2nd Edition, p.330, London: Butterworths.

Benesi, H.A., Curtis, R.M. and Studer, H.P., 1968. J. Catal. 10, 328.

Bennett, M.J. and Tompkins, F.C., 1957. Trans. Faraday Soc. 53, 185.

Benton, A.F. and Emmett, P.H., 1924. J. Amer. Chem. Soc. 46, 2728.

Benton, A.F. and White, T.A., 1930. J. Amer. Chem. Soc. 52, 2325.

Blyholder, G., 1964. J. Phys. Chem. 68, 2772.

Bond, G.C., 1962. "Catalysis by Metals", New York: Academic Press.

Boreskov, G.K. and Karnaukhov, A.P., 1952. Zhur. Fiz. Khim. 26, 1814.

Boudart, M., 1950. J. Amer. Chem. Soc. 72, 1040.

Boudart, M., Aldag, A., Benson, J.E., Dougharty, N.A. and Harkins, C.G., 1966. J. Catal. 6, 92.

Bradley, D.E., 1954. Brit. J. Appl. Phys. 5, 96.

Brennan, D., Hayward, D.O. and Trapnell, B.M.W., 1960. Proc. Roy. Soc. London A256, 81.

Brock, E.G., 1957. Adv. Catal. 9, 452.

Brooks, C.S. and Christopher, G.L.M., 1968. J. Catal. 10, 211.

Brownlie, I.C., Fryer, J.R. and Webb, G., 1969. J. Catal. 14, 263.

Brunauer, S., Emmett, P.H. and Teller, E.J., 1938. J. Amer. Chem. Soc. 60, 309.

Brunauer, S., Deming, L., Deming, W.E. and Teller, E.J., 1940. J. Amer. Chem. Soc. 62, 1723.

Bunn, C.W., 1961. "Chemical Crystallography", 2nd Edition, Oxford : Oxford University Press.

Carter, J.L., Cusumano, J.A. and Sinfelt, J.H., 1966. J. Phys. Chem. 70, 2257.

Carter, J.L. and Sinfelt, J.H., 1966. J. Phys. Chem. 70, 3003.
Carter, J.L. and Sinfelt, J.H., 1968. J. Catal. 10, 134.
Cohan, L.H., 1938. J. Amer. Chem. Soc. 60, 433.
Cohan, L.H., 1944. J. Amer. Chem. Soc. 66, 98.
Constable, F.H., 1925. Proc. Roy. Soc. London A108, 355.
Cormack, D. and Moss, R.L., 1969. J. Catal. 13, 1.
Cremer, E., 1955. Adv. Catal. 7, 75.
Cusumano, J.A., Dembinski, G.W. and Sinfelt, J.H., 1966. J. Catal. 5, 471.
Dodge, B. and Davis, H., 1927. J. Amer. Chem. Soc. 49, 610.
Dollimore, D. and Heal, G.R. 1963. Trans. Faraday Soc. 59, 2386.
D'Or, L. and Orzechowski, A., 1954. J. Chem. Phys. 51, 467.
Dorling, T.A., Eastlake, M.J. and Moss, R.L., 1969. J. Catal. 14, 23.
Dorling, T.A. and Moss, R.L., 1966. J. Catal. 5, 111.
Dorling, T.A. and Moss, R.L., 1967. J. Catal. 7, 378.
Dorling, T.A., Burlace, C.J. and Moss, R.L., 1968. J. Catal. 12, 207.
Dubinin, M.M., 1960. Chem. Rev. 60, 235.
Eischens, R.P. and Pliskin, W.A., 1958. Adv. Catal. 10, 2.
Eischens, R.P., Pliskin, W.A. and Francis, S.A. 1954. J. Chem. Phys. 22, 1786.
Eischens, R.P. and Selwood, P.W., 1947a. J. Amer. Chem. Soc. 69, 1590.
Eischens, R.P. and Selwood, P.W., 1947b. J. Amer. Chem. Soc. 69, 2698.
Eischens, R.P. and Selwood, P.W., 1948. J. Amer. Chem. Soc. 70, 2271.
Eley, D.D., 1951. J. Phys. Chem. 55, 1017.
Elkins, P.B., Shull, C.G. and Roess, L.C., 1945. Ind. Eng. Chem. 37, 327.
Emmett, P.H., 1948. Adv. Catal. 1, 79.
Emmett, P.H. and Brunauer, S., 1937a. J. Amer. Chem. Soc. 59, 310.
Emmett, P.H. and Brunauer, S., 1937b. J. Amer. Chem. Soc. 59, 1553.
Emmett, P.H. and Skau, N., 1943. J. Amer. Chem. Soc. 65, 1029.
Eucken, A., 1949. Z. Elektrochem. 53, 285.
Ferreira, L.C. and Leisegang, E.C., 1969. Paper presented to a symposium entitled "Aspects of Heterogenous Catalysis" held at African Explosives and Chemical Industries, Modderfontein, South Africa.
Foster, A.G., 1932. Trans. Faraday Soc. 28, 645.
Foster, A.G., 1948. Discuss. Faraday Soc. 3, 41.
Foster, A.G. 1951. J. Phys. Colloid Chem. 55, 638.
Garner, W.E. and Veal, F.J., 1935. J. Chem. Soc. 1436.
Geus, J.W. and Nobel, A.P.P., 1966. J. Catal. 6, 108.
Gilliland, W.L. and Blanchard, A.A., 1946. "Inorganic Syntheses", vol. II, p. 234, New York : McGraw Hill.
Gregg, S.J., 1961. "The Surface Chemistry of Solids", chapter 2, 2nd Edition, London : Chapman and Hall.
Gregg, S.J. and Jacobs, J., 1948. Trans. Faraday Soc. 44, 574.
Gruber, H.L., 1962. J. Phys. Chem. 66, 48.
Guenther, H.W., 1955. Diss. Abs. 15. 507.
Halford, J.O., 1956. J. Chem. Phys. 24, 830.
Halliday, D. and Resnick, R., 1960. "Physics for Students of Science and Engineering" part II, p. 951, New York : John Wiley and Sons.

Harkins, W.D. and Jura, G., 1943. J. Chem. Phys. 11, 430.
Harkins, W.D. and Jura, G., 1944. J. Amer. Chem. Soc. 66, 1362.
Haul, R.A.W., 1956. Angew. Chem. 68, 238.
Hayward, D.O. and Trapnell, B.M.W., 1964. "Chemisorption", London : Butterworths.
Hightower, J.W. and Kemball, C., 1965. J. Catal. 4, 363.
Hill, F.N. and Selwood, P.W., 1949. J. Amer. Chem. Soc. 71, 2522.
Homfray, I.F., 1910. Z. Phys. Chem. 74, 129.
Hughes, T.R., Houston, R.J. and Sieg, R.P., 1962. Ind. Eng. Chem. Proc. Design Develop. 1, 96.
Irving, H., 1967. Private Communication.
Jones, F.W., 1938. Proc. Roy. Soc. London A166, 16.
Keeson, W.H., Mazur, J. and Meihuizen, J.J., 1935. Physica 2, 669.
Kisliuk, P., 1959. J. Chem. Phys. 31, 1605.
Klemperer, D.F. and Stone, F.S., 1958. Proc. Roy. Soc. London A243, 375.
Klug, H.P. and Alexander, L.E., 1954. "X-ray Diffraction Procedures", chapter 9, New York : John Wiley and Sons.
Knudsen, M., 1910. Ann. Physik 31, 205.
Kubicka, H., 1966. J. Catal. 5, 39.
Kubicka, H., 1968. J. Catal. 12, 223.
Kwan, T., 1949. J. Res. Inst. Catal., Hokkaido Univ. 1, 81.
Laidler, K.J., 1954. "Catalysis", vol. I, chapter 4, ed. Emmett, P.H., New York : Reinhold.
Langmuir, I., 1915. Phys. Rev. 6, 79.
Langmuir, I., 1916. J. Amer. Chem. Soc. 38, 2267.
Langmuir, I., 1918. J. Amer. Chem. Soc. 40, 1361.
Laue, M. von, 1926. Z. Krist. 64, 115.
Liang, S.C., 1955. Canad. J. Chem. 33, 279.
Livingstone, H.K., 1949. J. Colloid Sci. 4, 447.
Margineanu, P. and Olariu, A., 1967. J. Catal. 8, 359.
Maxted, E.B. and Akhtar, S., 1960. J. Chem. Soc. 1995.
Maxted, E.B. and Ali, S.J., 1961. J. Chem. Soc. 4137.
Maxted, E.B. and Ali, S.J., 1964. J. Chem. Soc. 1127.
Maxted, E.B. and Elkins, J.S., 1961. J. Chem. Soc. 5086.
Maxted, E.B. and Ismail, S.M., 1962a. J. Chem. Soc. 2330.
Maxted, E.B. and Ismail, S.M., 1962b. J. Chem. Soc. 5293.
Meihuizen, J.J. and Crommelin, C.A., 1937. Physica IV, 1.
Nikolajenko, V., Bosacek, V. and Danes, V., 1963. J. Catal. 2, 127.
Nowak, E.J. and Koros, R.M., 1967. J. Catal. 7, 50.
O'Neill, C.E., 1961. Ph.D. Thesis, Columbia Univ.
O'Neill, C.E. and Yates, D.J.C., 1961. J. Phys. Chem. 65, 901.
Pantony, D.A., 1961. "A Chemist's Introduction to Statistics, Theory of Error and Design of Experiment" Roy. Inst. Chem., Lecture Series 1961, number 2.
Patterson, A.L., 1939. Phys. Rev. 56, 978.
Peri, J.B., 1966. Discuss. Faraday Soc. 41, 121.

Podgurski, H.H. and Davis, F.N., 1961. J. Phys. Chem. 65, 1343.
Poltorak, O.M. and Boronin, V.S., 1965. Russ. J. Phys. Chem. 39, 781.
Porter, A.S., 1950. Discuss. Faraday Soc. 41, 121.
Reinen, D. and Selwood, P.W., 1963. J. Catal. 2, 109.
Rideal, E.K. and Sweet, F., 1960. Proc. Roy. Soc. London. A257, 291.
Roberts J.K., 1935. Proc. Roy. Soc. London. A152, 445.
Roberts, M.W. and Sykes, K.W., 1958. Trans. Faraday Soc. 54, 548.
Ross, S. and Olivier, J.P., 1964. "On Physical Adsorption", New York: Interscience.
Rostrup-Nielson, J.R., 1968. J. Catal. 11, 220.
Russell, A.S. and Stokes, J.J., 1947. J. Amer. Chem. Soc. 69, 1316.
Sadek, H. and Taylor, H.S., 1950. J. Amer. Chem. Soc. 72, 1168.
Scherrer, P., 1918. Göttinger Nachrichten 2, 98.
Schuit, G.C.A. and de Boer, N.H., 1953. Rec. Trav. Chim. 72, 909.
Schuit, G.C.A. and van Reijen, L.L., 1958. Adv. Catal. 10, 243.
Schwab, G.M. and Schwab-Agallidis, E., 1943. Naturwissenschaften 31, 322.
Sears, G.W. and Hudson, J.B., 1963. J. Chem. Phys. 39, 2380.
Selwood, P.W., 1948. J. Amer. Chem. Soc. 70, 883.
Selwood, P.W., Adler, S. and Phillips, T.R., 1955. J. Amer. Chem. Soc. 77, 1462.
Selwood, P.W. and Dallas, N.S., 1948. J. Amer. Chem. Soc. 70, 2145.
Selwood, P.W., Ellis, M. and Wethington, K., 1949. J. Amer. Chem. Soc. 71, 2181.
Selwood, P.W., Hill, F.N. and Boardman, H., 1946. J. Amer. Chem Soc. 68, 2055.
Selwood, P.W., Moore, T.E., Ellis, M. and Wethington, K., 1949. J. Amer. Chem. Soc. 71, 693.
Shield, L.S. and Russell, W.W., 1960. J. Phys. Chem. 64, 1592.
Shillaber, C.P., 1944. "Photomicrography", p.67, New York : John Wiley and Sons.
Sinfelt, J.H., 1964. J. Phys. Chem. 68, 344.
Sinfelt, J.H., Taylor, W.F. and Yates, D.J.C., 1965. J. Phys. Chem. 69, 95.
Sing, K.S.W. and Swallow, D., 1960. J. Appl. Chem. 10, 171.
Sing, K.S.W. and Swallow, D., 1965. Proc. British Ceram.Soc. No. 5.
Snell, F.D. and Snell, C.T., 1959. "Colorimetric Methods of Analysis", vol. IIA, p.263, Princeton, N.J. : van Nostrand.
Stokes, A.R., 1948. Proc. Phys. Soc. 61, 382.
Stokes, A.R. and Wilson, A.J.C., 1942. Proc. Cambridge Phil. Soc. 38, 313.
Swift, H.E., Lutinski, F.E. and Kehl, W.L.J., 1965. J. Phys. Chem. 69, 3268.
Swift, H.E., Lutinski, F.E. and Tobin, H.H., 1966. J. Catal. 5, 285.
Taylor, G.F. Thompson, S.J, and Webb, G., 1968. J. Catal. 12, 191.
Taylor, H.S., 1925. Proc. Roy. Soc. London A108, 105.
Taylor, W.F., 1967. Sc. D. Thesis, Stevens Inst. of Technology.
Taylor, W.F., Sinfelt, J.H. and Yates, D.J.C., 1965. J. Phys. Chem. 69, 3857.

Taylor, W.F. and Staffin, H.K., 1967. Trans. Faraday Soc. 63, 2309.
Taylor, W.F., Yates, D.J.C. and Sinfelt, J.H., 1964. J. Phys. Chem. 68, 2962.
Taylor, W.F., Yates, D.J.C. and Sinfelt, J.H. 1965, J. Catal. 4, 374.
Trout, W.E., 1937. J. Chem. Ed. 14, 575.
Thomas, J.M., and Thomas, W.J., 1967. "Introduction to the Principles of Heterogenous Catalysis", chapter 3, New York : Academic Press.
Uchida, H. and Imai, H., 1962. Bull. Chem. Soc. Japan 35, 989, 995.
Wahba, M. and Kemball, C., 1953. Trans. Faraday Soc. 49, 1351.
Ward, A.F.H. 1931. Proc. Roy. Soc. London A133, 506.
Warren, B.E., 1941. J. Appl. Phys. 12, 375.
Wheatley, K., 1959. J. Appl. Chem. 9, 159.
Wilson, C.L. and Wilson, D.W., 1962. "Comprehensive Analytical Chemistry", vol. Ic, p. 676, Princeton, N.J. : van Nostrand.
Yang, A.C. and Garland, C.W., 1957. J. Phys. Chem. 61, 1504.
Yates, D.J.C. and Sinfelt, J.H. 1967. J. Catal. 8, 348.
Yates, D.J.C., Sinfelt, J.H. and Taylor, W.F., 1965. Trans. Faraday Soc. 61, 2044.
Yates, D.J.C., Taylor, W.F. and Sinfelt, J.H., 1964. J. Amer. Chem. Soc. 86, 2996.
Yates, J.T. Jr. and Garland, C.W. 1961. J. Phys. Chem. 65, 617.
Yoshimoti, S., Morita, Y. and Yamomoto, K., 1963. Bull. Japan Petroleum Inst. 5, 27.
Young, D.M. and Crowell, A.D., 1962. "Physical Adsorption of Gases", p. 227, London : Butterworths.